Perturbation of critical metabolic processes associated with 3-hydroxynorvaline induced teratogenesis.

R Louw (B.Sc. Honns.)

Thesis submitted for the degree Philosophiae Doctor in Biochemistry in the School for Chemistry and Biochemistry at the Potchefstroom University for Christian Higher Education.

Promotor: Prof. H.C. Potgieter

Co-promotor: Dr. F.H. van der Westhuizen

Potchefstroom

2004

CONTENTS

SUMMARY

Neural tube defects (NTD) are a group of folate-responsive congenital defects that occur relatively frequently in humans. NTD display a multi-factorial aetiology, resulting from a complex interplay of genetic and environmental factors (i.e. dietary folate and/or vitamin B_{12} deficiency, teratogenic xenobiotics, etc.). β-Hydroxy-norvaline (HNV) is a proven toxic, non-protein amino acid (xenobiotic agent), structurally related to L-threonine and L-serine and able to substitute L-threonine in the primary structure of proteins. The main objectives of this study were to investigate the teratogenic potential of HNV in the chicken embryo and Hanover NMRI mouse embryo models and to elucidate some of the molecular mechanisms involved in the aetiology of NTD.

HNV was dosed to chicken embryos (*in ovo*), 24 h post incubation (p.i.) at 37.8 °C ± 0.5 °C. Controls received a sterile saline solution. Chicken embryos were removed 12 days p.i., weighed, fixed in Allen's solution and investigated stereomicroscopically to assess the incidence and nature of dysmorphogenic events (i.e. NTD). Body, toe and beak lengths of the chicken embryos were measured. Chicken embryo fibroblasts were cultured and used to measure the effect of HNV on the biosynthesis of DNA in fibroblasts.

Pregnant Hannover NMRI female mice were dosed with HNV or a saline solution (*per os*) on days 7-9 *post coitus* (p.c.). Following the last dose of HNV on day 9, the pregnant mice were placed in metabolic cages for 24 h to collect urine samples. Urinary organic acids (GC-MS), acylcarnitines and amino acids (ESI-MS-MS) were quantitatively and qualitatively determined to assess the catabolic breakdown of HNV and its effects on vital metabolic processes, such as amino acid catabolism and the β-oxidation of fatty acids.

Control and HNV exposed mouse embryos were removed on days 10 or 18 *post coitus* (*p.c.*). Embryos, removed from each individual mother on day 10 were pooled and either immediately used to assess the catalytic activity of the glycine

cleavage system (GCS), or stored at -75 °C until the catalytic activities of cytosolic (cSHMT), mitochondrial serine hydroxymethyltransferase (mSHMT) and citrate synthase (CS) could be assayed. Mouse embryos removed on day 18 *p.c.*, weighed and stereomicroscopically investigated to assess the incidence and nature of dysmorphogenic events. Bio-indicators of the effect of HNV on the flow of one-carbon units through the folate and remethylation cycles (i.e. [^{3}H]-thymidine incorporation, DNA methylation and synthesis, polyamine synthesis, carnitine synthesis, etc.) were determined in the liver tissues of pregnant females and in pooled batches of whole embryos.

HNV proved to be embryotoxic and displayed the capacity to induce a variety of congenital defects, including NTD, in both the chicken and mouse embryo models. The incidence of NTD in both models proved to be dose-dependent. Selected stereoisomers of HNV were rapidly catabolised and the main HNV derived metabolite in the urines of HNV treated pregnant mice, was identified as 2,3-dihydroxypentanoic acid (DHPA; GC-MS). The structure of DHPA was confirmed by chemical synthesis and subsequent GC-MS, NMR (^{13}C-NMR, ^{1}H-NMR, HETCOR and COSY) spectroscopy and IR spectrometry.

HNV altered the flow of one-carbon units through the folate and remethylation cycles, causing a decrease in DNA synthesis, DNA methylation, polyamine biosynthesis, carnitine and trimethyllysine synthesis. Free carnitine stores in HNV treated pregnant mice appeared to be depleted, probably due to a combined effect of the detoxification of vast amounts of accumulated metabolites, generated as a result of HNV toxicosis and decreased carnitine biosynthesis. HNV also appeared to have altered serine/glycine interconversion, due to an inhibition of cSHMT and to a lesser degree the inhibition of GCS. Organic acid profiles of urine samples, collected from HNV treated pregnant mice, suggested that HNV had induced a general ketothiolase defect in pregnant females by inhibiting the β-oxidation of fatty acids, isoleucine catabolism and ketone body utilisation.

HNV affected the homocysteine to cysteine transulffuration by acting as a substrate for CBS, culminating in the biosynthesis of 3-ethylcysteine (GC-MS). The presence of 3-ethylcysteine in the urines of HNV treated pregnant mice was

confirmed by GC-MS, following its *in vitro* synthesis, employing a reaction system containing mouse liver homogenate, homocysteine, HNV and pyridoxal-5-phosphate.

In conclusion, HNV can apparently cause multiple metabolic perturbations in pregnant mice and their developing embryos. One-carbon flux, energy metabolism and a number of other vital biochemical processes can be adversely affected, resulting in a disturbance of normal embryonic development (i.e. proper closure of the neural tube) and subsequent dysmorphogenesis in developing embryos.

OPSOMMING

Neuraalbuisdefekte (NTD) is 'n groep folaatresponsiewe, kongenitale defekte wat gereeld by mense voorkom. NTD vertoon 'n multifaktoriale etiologie wat die gevolg is van 'n komplekse interaksie tussen genetiese en omgewingsfaktore (bv. folaat in die diëet en/of vitamien B_{12}-tekort, teratogeniese xenobiotika, ens.). β-Hydroksienorvalien (HNV) is `n bekende nie-proteïenaminosuur (xenobiotiese verbinding), struktureel verwant aan L-threonine en L-serien en kan in die plek van L-threonien in die primêre struktuur van proteïene ingebou word. The belangrikste oogmerke van hierdie studie was om die teratogeniese potensiaal van HNV te ondersoek in die kuikenembrio- en Hannover NMRI-muismodelle en om sommige van die molekulêre meganismes in die etiologie van NTD toe te lig.

Kuikenembrios is 24 uur post-inkubasie (p.i.) (37.8 °C ± 0.5 °C) met 'n oplossing van HNV gedoseer (*in ovo*). Kontroles is met 'n steriele fisiologiese soutoplossing gedoseer. Die kuikenembrios is op 12 dae p.i. uit die eiers verwyder, geweeg, in Allen se oplossing gefikseer en daarna stereomikroskopies ondersoek om die insidensie en aard van die dismorfogenetiese gevalle (o.a. NTD, ens.) te bepaal. Lyf-, toon- en beklengte van die kuikenembrio's is gemeet. Kuikenfibroblastkulture is gekweek en gebruik om die effek van HNV op die biosintese van DNA *in vitro* te meet.

Dragtige Hannover NMRI-muise is met HNV of 'n fisiologiese soutoplossing op dae 7-9 *post coitus* (*p.c.*) gedoseer. Na die laaste dosering (dag 9 *p.c.*) is die dragtige wyfies in metaboliese hokke geplaas vir 24 uur, waartydens urienmonsters versamel is. Urinêre organiese sure (GC-MS), asielkarnitiene en aminosure (ESI-MS-MS) is kwantitatief en kwalitatief bepaal om die kataboliese afbraak van HNV en sy effek op lewensbelangrike metaboliese prosesse, soos aminosuurkatabolisme en β-oksidasie van vetsure te bepaal. Kontrole en HNV behandelde muisembrios is op dag 10 of 18 *p.c.* verwyder. Die 10 dae-oue embrios van elke individuele ma is gepoel. Die glisiensplytingskompleks se

katalitiese aktiwiteit is dadelik bepaal en die res van die weefsel is gevries by -70 °C. Die gevieste weefsel is later gebruik om die katalitiese aktiwiteit van sitosoliese (cSHMT) en mitochondriale serienhidroksiemetieltransferase (mSHMT), asook sitraat sintetase (CS) te bepaal. Muis embrios wat op dag 18 *p.c.* verwyder is, is geweeg en stereomikroskopies ondersoek om die insidensie en die aard van dismorfogenese te evalueer. Bio-indikators van die effek van HNV op die vloei van een-koolstof eenhede deur die folaat- en hermetileringsiklusse (o.a. [^{3}H]-timidine inkorporasie, DNA metilering en -sintese, poliamien biosintese, karnitien sintese, ens.) is gemeet in die lewers van dragtige wyfies en die gepoelde embrio monsters. HNV was embriotoksies en het verskeidenheid van kongenitale defekte, insluitende NTD, in beide kuiken- en muisembriomodelle te induseer. Die insidensie van NTD in beide modelle was dosis-afhanklik. Spesifieke stereoisomere van HNV is vinnig gekataboliseer en die belangrikste HNV-metaboliet in die uriene van HNV-behandelde, dragtige muise, is as 2,3-dihidroksiepentanoësuur (DHPA) geïdentifiseer (GC-MS). Die struktuur van DHPA is met behulp van chemiese sintese en opvolgende GC-MS, NMR (^{13}C NMR, ^{1}H NMR, HETCOR en COSY) spektroskopie en IR-spektrometrie bevestig. HNV het die vloei van een-koolstof eenhede deur die folaat en hermetileringsikluse beinvloed. Die gevolg was 'n afname in DNA-sintese, DNA-metilering, poliamienbiosintese, asook karnitien- en trimetiellisienbiosintese. Vrye karnitien in HNV-behandelde muise is uitgeput, waarskynlik as gevolg van 'n gekombineerde effek van die detoksifisering van geweldige groot hoeveelhede opgehoopte metaboliete (gegenereer a.g.v. HNV-toksisiteit) en verlaagde karnitienbiosintese. HNV het ook die serine/glisien interskakeling beinvloed, moontlik a.g.v. die inhibisie van cSHMT en tot 'n mindere mate GCS. Organiese suurprofiele van HNV-behandelde muise dui daarop dat HNV 'n algemene ketotiolasedefek induseer in die dragtige muise deur die inhibisie van β-oksidasie van vetsure, isoleusien katabolisme asook die verbruik van ketoon-ligaampies.

HNV het die homosisteïen na sisteïen transsulfurasie beïnvloed deur op te tree as 'n substraat vir CBS, met die gevolglike vorming van 3-etielsisteïen (GC-MS). The teenwoordigheid van 3-etielsisteïen in die uriene van HNV-behandelde muise is bevestig met GC-MS nadat dit *in vitro* gesintetiseer is. Muislewerhomogenaat, homosisteïen, HNV en piridoksaal-5-fosfaat is gebruik vir die sintese.

Om saam te vat, HNV kan moontik meervuldige metaboliese versteurings veroorsaak in dragtige muis wyfies en hul embrios. Een-koolstof vloei en energie metabolisme, asook 'n groot hoeveelheid ander metaboliese weë kan moontik beïnvloed word. Dit kan die normale ontwikkeling van die embrio belemmer (bv. neuraalbuissluiting) en kan aanleiding gee tot dismorfogenese in die ontwikkelende embrios.

CHAPTER 1

INTRODUCTION

Neural tube defects (NTD) are a constellation of folate-responsive congenital defects that occur, relatively frequently, in humans (Lemire, 1988; Leech, 1991; Sulik, 1993). This condition displays a multi-factorial aetiology and may result from a complex, but as yet unknown, interplay of genetic and environmental factors (Lemire, 1988; Leech, 1991). The global incidence of NTD lies between 0.6 to 3.7 cases per 1000 live births (Leech, 1991) and some of the highest incidences have been reported for Ireland, Mexico and China (Moore, 1997; Hendricks, 1999; McDonnell, 1999). In comparison, some rural communities in the Republic of South Africa (RSA) display some of the highest incidences of NTD in the world (i.e. the Limpopo Province and the Transkei region of the Eastern Cape Province, displaying 3.55 and 6.12 cases per 1000 live births, respectively). The incidence of NTD in these rural communities is also much higher than in some of the urban communities (0.99 to 1.39 cases/1000 live births) of the RSA (Ncayiyna, 1986; Christensen, 1995; Venter, 1995).

Although NTD appear to be prevalent in all populations over a fairly wide socioeconomic divide, the highest incidences of this debilitating condition are still reported among the poorest sector, of mostly rural populations, all over the world (Wasserman, 1998; Kloeblen, 1999). The lack of access to a healthy, well balanced diet, containing sufficient proteins, vitamins and micronutrients and probably also the exposure to hazardous environmental agents, may be the result of the socioeconomic status of the family into which a baby is born (Tew, 1974; Nevin, 1981). Whatever the real cause of the condition, the psychological, social and economic impact of the occurrence of NTD in any family, but especially in socially disenfranchised families, as well as the burden of lifelong disability to the child and his family, can be devastating (Athreya, 1987). As with any other

disease, the only way to eradicate the burden of NTD is to learn to understand the causes and mechanisms of this condition and to employ that knowledge in designing prophylactic measures to eradicate the problem of NTD.

Folic acid has been positively linked to NTD. A dietetic or metabolically induced folic acid deficiency, coinciding with the process of neural tube closure, may be important factors that can impact on the incidence of NTD (Eskes, 2000). The British Medical Council and the Budapest trials also conclusively proved that a woman's risk for an NTD-affected pregnancy is reduced substantially by taking folic acid periconceptionally (Medical Research Council [MRC] Vitamin Study Group, 1991; Czeizel, 1992).

Recent studies on a group of Venda women in the north-eastern part of the Limpopo Province indicated that plasma and red cell folate levels of women, who previously gave birth to babies with NTD, were within the normal reference ranges (Ubbink, 1998). The general nutritional status of these women also appeared to be normal. These results suggest that the incidence of NTD in humans can be high, in spite of a relative abundance of folic acid and other B-group vitamins in the diet and an apparently healthy nutritional status. Other informational sources however indicate that protein nutrition of the general population in this region may be inappropriate, both in terms of quantity and quality (Alberts, 2004; Modjadji, 2004). These findings indicate that some other cause or causes (i.e. dietetic, environmental, genetic etc.) than just a folate deficiency may play a role in the high incidence of NTD in these populations.

The aetiology of NTD in the Transkei region of the Eastern Cape Province, however, appears to have a different aetiological profile than that occurring in the Limpopo Province. Previous investigations have indicated that the rural population in this region display signs of B-vitamin and other micronutrient deficiencies (Gelderblom, 1988). There is also a growing suspicion that mycotoxins (i.e. fumonisin B1, etc.) may be involved in the development of NTD in this region (Marasas, 2004). The population also display the highest global prevalence rate of esophagal cancer, which somehow appears to be linked to the presence of high levels of the mycotoxin, fumonisin B_1, in maize consumed in this region

(Sydenham, 1990; Makaula, 1995). It is a known fact that fumonisin B1 occurs in maize all over the world, but especially in regions known to have a high incidence of NTD (i.e. Transkei region in the Eastern Cape, China, Mexico) (Somdyala, 2003). It therefore makes a lot of sense that the probable relationship between mycotoxins and other xenobiotic agents with teratogenic potential should be rigorously investigated.

Research on the aetiology of NTD is currently entering a rapid phase, due to significant advances made in experimental embryology and genetics. Clinical epidemiology can provide a number of feasible and testable hypotheses on the aetiology and pathogenesis of NTD, which can then be investigated empirically. To this end animals models (i.e. rat, mouse, chicken) have contributed enormously to a deeper understanding of the basic mechanisms underlying the embryological development of NTD (Campbell, 1986). Studies on humans will unfortunately always be retrospective in nature and can, at best, only provide a very limited insight into the complex causes of NTD.

The current research program on the role of environmental teratogens in the high incidence of neural tube defects in rural populations of the RSA focuses on selected aetiological factors (i.e. nutritional deficiencies, xenobiotic agents, etc.) that may be associated with the high incidence of NTD in certain rural areas of the RSA. This research programme was divided into two subprograms (a) a subprogram focusing entirely on the epidemiological relationships between nutritional and environmental factors that may be associated with the high incidence of NTD in these populations and (b) a subprogram aiming at studying the effects of selected xenobiotic agents (i.e. mycotoxins, non-protein amino acids, organic acids) with teratogenic potential on one carbon metabolism in particular and intermediary metabolism in general. This thesis forms part of the latter subprogram.

CHAPTER 2

LITERATURE REVIEW

2.1 NEURAL TUBE DEFECTS

The neural tube plays a vital role in the development of the embryo. This dorsal structure runs the entire length of the embryo and gives rise to all the neurons and most of the glia of the central nervous system. Its derivative, the neural crest, contributes to the peripheral nervous system and to a variety of other organ and body systems including the craniofacial skeleton, thymus, thyroid, parathyroid and important cardiac structures. The neural tube is of critical importance as an inducer of the formation of other organ systems, i.e. the mesodermally derived vertebrae and the ectodermally derived inner-ear primordium (Copp, 1997)

Defects of the central nervous system arise when the processes of normal neural tube development become disturbed, particularly during the embryonic and fetal periods. These abnormalities may be structural, as when the neural tube fails to close during the third and fourth weeks of human development, leading to malformations such as anencephaly and spina bifida. Defects like these are of major clinical importance, both as a cause of death around the time of birth and of disability in children and adults. Disturbances during later nervous system development yield functional rather than gross structural defects, leading to conditions such as epilepsy, mental retardation or behavioural disturbances (Copp, 1997).

2.1.1 Development of the central nervous system

The nervous system, including the brain and spinal cord, is one of the first parts of the human embryo to develop. On the nineteenth day after conception, when the embryo is only 1.4 mm long, the skin along the midline of the back thickens to form a neural plate that is the forerunner of the brain and spinal cord (Figure 2.1a). During the third week of pregnancy it folds along its length, to form the open neural groove (Figure 2.1b). During the fourth week the folds on the two sides of this groove fuse along its length to complete the formation of the neural tube (Figure 2.1d) (Op't Hoff, 1985).

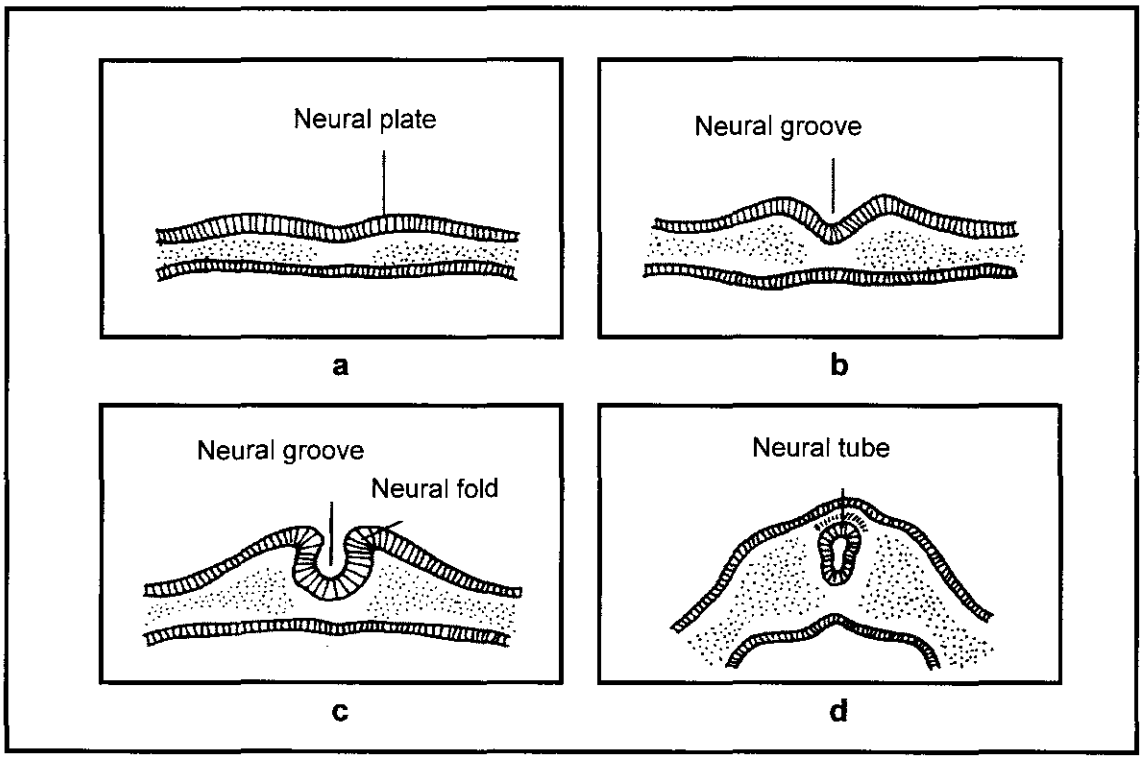

Figure 2.1 **Formation and closure of the neural tube.** (a) Formation of the neural plate; (b) neural groove formation; (c) neural fold formation; (d) closure of the neural tube. Modified from Op't Hoff (1985).

Closure of the neural groove is initiated in the centre of the groove and proceeds towards the anterior and posterior ends, leaving temporary openings known as the neuropores (Sweeney, 1998). Closure of the anterior neuropore occurs approximately on day 25 of the development of the human embryo and the posterior end closes on day 27 (Langman, 1975). The anterior end enlarges and

develops into the highly specialised structures of the brain, while the rest of the neural tube have a small diameter and give rise to the spinal meninges and spinal cord (Singh, 1978; Dodds, 1947). Just before the neural groove closes to form the neural plate, a group of cells known as the neural crest forms where the neural plate touches the surface of the ectoderm. The neural crest cells later give rise to most of the components of the peripheral nervous system (Sweeney, 1998).

2.1.2 Congenital defects

Abnormal central nervous system development results in a diverse group of abnormalities ranging from major abnormalities that are incompatible with postnatal life, to disabilities that only slightly affect the physical or mental function of the individual. Failure of the neural tube to close completely will give rise to what is generally referred to as neural tube defects (NTD). If the neural tube does not close completely at the anterior end, anencephaly or exencephaly will result. It is not yet clear whether anencephaly represents a defect in the primary closure of the neural tube, or whether the anterior neuropore closes prematurely, with a subsequent defect in differentiation, followed by degeneration (World Health Organization, 1970). Incomplete closure at the posterior end of the neural tube will result in some form of spina bifida (Sweeney, 1998).

2.1.2.1 Anencephaly and Exencephaly

Anencephaly is one of the most severe congenital defects, although it does not contribute greatly to infant mortality (Warkany, 1971), due to its low incidence. Absence of the vault of the skull is characteristic in anencephaly. A mass of disorganised vascular and often haemorrhaging neural tissue, covered by a transparent membrane, forms the top of the head. The eyes are usually protruding and the ears are often deformed (World Health Organization, 1970). Anencephaly is characterised by a partial or complete absence of the brain and the affected neonates are either stillborn or pass away within hours after birth.

Exencephaly differs from anencephaly in that a fully developed brain is present, although it is protruding through an opening in the skull (Warkany, 1971).

The primary cause of anencephaly and exencephaly is usually failure of the neural tube to close at the anterior end. The neural tissues do not differentiate properly, resulting in the formation of an abnormal or incomplete skull around it (Sweeney, 1998). This developmental defect is generally not compatible with life and the life expectancy of an affected infant is seldom more than a few hours (Warkany, 1971).

2.1.2.2 Spina bifida

Spina bifida refers to a spectrum of defects where the left and right sides of one of the vertebrae did not fuse properly, resulting in the spine and meninges being exposed (Sweeney, 1998). Different types of spina bifida defects are found and differ from one another by the degree of disability (Beck, 1973) imposed on the affected infant.

Spina bifida occulta

This is a relatively common form of spina bifida and seldom causes any serious disability of the affected individual. It is caused when one or more of the arches of the vertebrae have not fused, but there is no protrusion of either the spinal cord or of its membranes (Figure 2.2b). The defect is usually visible as a slight swelling, a dimple in the skin, or a tuft of hair. Sometimes there are no external signs of the defect and the condition can only be detected by X-ray (Op't Hoff, 1985).

Spina bifida cystica

In this "open" form of spina bifida, some of the spinal cord tissue protrudes to form a sac–like cyst, which is covered by a thin layer of skin. Two subtypes of spina bifida cystica are distinguished:

Meningocele is the less severe form of the two subtypes and occurs only in 4% of all spina bifida cystica cases. The cyst contains only cerebrospinal fluid and

some of the membranes that normally cover the spinal cord (Figure 2.2c). The spinal cord is normal, there is seldom paralysis, and usually little or no disability.

Myelomeningocele is the more severe of the two subtypes and occurs in 96% of all spina bifida cystica cases. The cyst not only contains membranes and cerebrospinal fluid, but also nerves and a section of the spinal cord, which may be improperly formed or damaged (Figure 2.2d). As a result there is always some degree of paralysis from the damaged vertebrae downwards and this type of spina bifida is often associated with hydrocephalus.

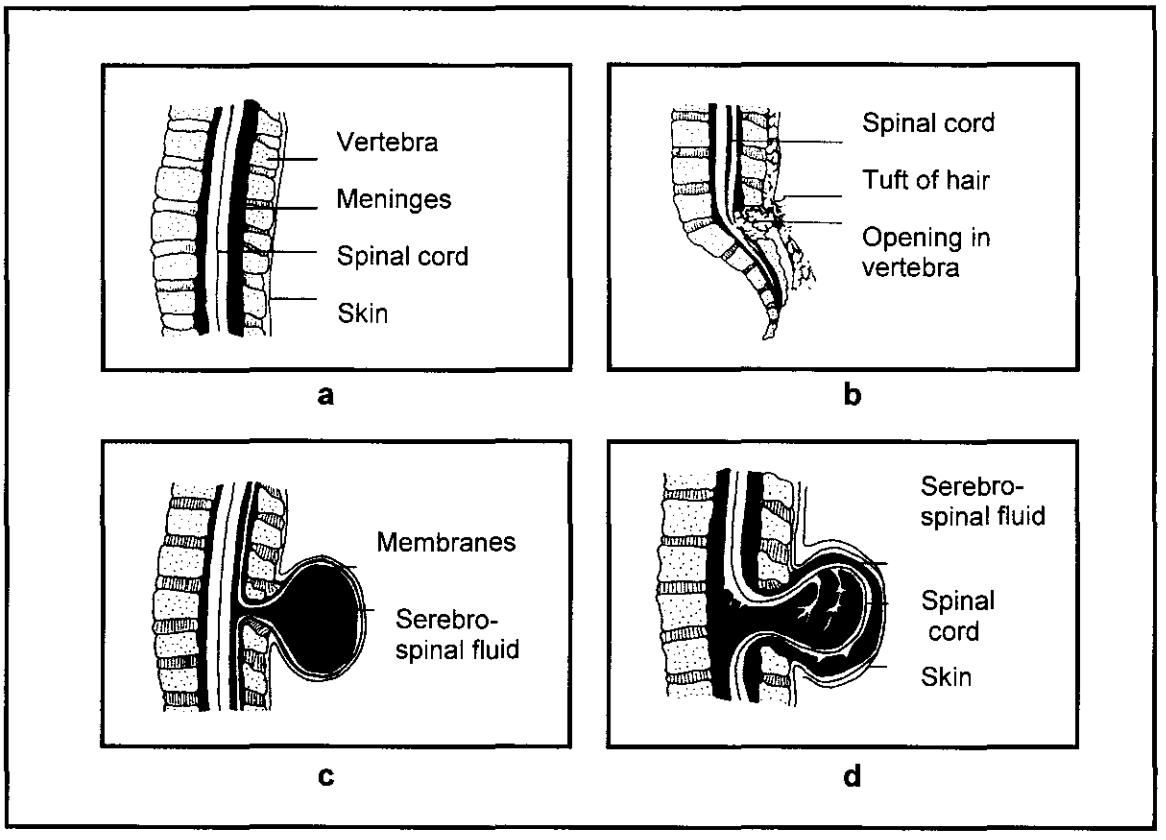

Figure 2.2 **Diagram showing section through the spine** (a) Normal spine; (b) Spina bifida occulta; (c) Spina bifida cystica – meningocele; (d) Spina bifida cystica – myelomeningocele. Modified from Op't Hoff (1985).

2.1.3 Incidence of neural tube defects

Spina bifida is one of the most common congenital defects (Op't Hoff, 1985). Studies in Europe and other parts of the world indicate an incidence of between 0.2 and 1.0 cases of NTD per 1000 live births (Leck, 1977). Some of the highest

recorded frequencies (> 5 NTD cases per 1000 live births) have been reported for cities in Northern Ireland and the Republic of Ireland (World Health Organization, 1970; Warkany, 1971), as well as the northern provinces of China (> 6 cases per 1000 live births; Moore, 1997). In South Africa, a study performed on black neonates, born at the Kalafong Academic Hospital, over a three-year period revealed an incidence of 0.99 per 1000 live births (Delport, 1995). Studies in the rural areas of South Africa showed that the incidence of NTDs in black neonates, from the former Transkei, was 6.13 per 1000 live births (Ncayiyana, 1986) and 3.55 per 1000 live births in the Limpopo or Northern Province (Venter, 1995). The reasons why urbanisation is associated with such a dramatic decline in the NTD incidence in South Africa remain, as yet, unexplained.

2.1.4 Aetiology of neural tube defects

Neural tube defects in general and spina bifida in particular, display a multi-factorial aetiology and may result from a complex interplay of genetic and environmental factors (Lemire, 1988; Leech, 1991). Genes from both parents, as well as a number of environmental factors, appear to be involved (Op't Hoff, 1985). Demeler (as quoted by Warkany, 1971) reported on a family in which the first child was born with anencephaly and thoracic spina bifida, the second with hydrocephaly, thoracic spina bifida, cleft lip and palate and the third with anencephaly and thoracic spina bifida. All three of these infants were females and were stillborn. The fourth child, also female, displayed no developmental anomalies. Two subsequent miscarriages were followed up by the birth of a living infant with lumbosacral spina bifida. After this baby was born, the mother had one more miscarriage. This unfortunate case study strongly suggests that genetic factors are involved in the aetiology of NTD. There are, however, also some observations that suggest that some cases of spina bifida may be caused by environmental influences. Morison (as quoted by Warkany, 1971) reported on a pair of identical twins, where the one sibling was normally developed, while the other was affected with spina bifida, Arnold-Chiari malformation, encephalocele and other malformations.

Maternal hyperhomocysteinaemia appears to be a major risk factor for neural tube defects. This condition is accompanied with an approximate 3-fold relative risk increase for an NTD-affected pregnancy (Harmon, 1996). Elevated homocysteine levels have been reported in women with NTD affected offspring (Steegers-Theunissen, 1994; Mills, 1995). Mild hyperhomocysteinaemia can be caused by deficiencies of folate, vitamin B_6, vitamin B_{12} or by a metabolic abnormality in one or more of the three enzymes involved in homocysteine metabolism: 5,10-methylenetetrahydrofolate reductase (MTHFR), cystathionine-β-synthase (CBS) or methionine synthase (MS).

MTHFR defects in certain population groups are currently regarded as well-established risk factors for neural tube defects. Kang *et al.* (1991) were the first to report the presence of a C677T, heat-sensitive mutant form of this enzyme in Caucasians. Van der Put *et al.* (1996a) later confirmed the presence of this relatively common mutation in the MTHFR gene as a risk factor for spina bifida offspring in the Dutch population. Ou *et al.* (1996) studied NTD affected fetuses against a control group and established that the thermolabile MTHFR gene is associated with a 7.2 fold increased risk for NTD. This phenomenon demonstrates that a single nucleotide substitution in the coding region of MTHFR, resulting in reduced activity of the enzyme, can impair homocysteine and folate metabolism and as a result generate an increased genetic risk for the occurrence of spina bifida (van der Put, 1996b). In a recent South African study, no homozygotes for the C677T mutation in the MTHFR gene were found in mothers with NTD affected offspring or controls (Ubbink *et al.*, 1998). The presence of heterozygotes for this mutation was, however, detected in both the black and Caucasian sample groups, employed in the investigation, confirming that the C677T mutation does occur in the South African population. Although relatively small samples of subjects were used in this investigation, the results suggested that the incidence of the C677T mutation is very rare in the black population, while the Caucasian population in South Africa displays incidence characteristics, similar to that of the Dutch population.

Several studies have focused on the relationship between mutations in CBS and NTD. Ramsbottom *et al.* (1997) compared individuals with NTD to a control

group in regard to relatively common mutations in CBS. Neither the severely dysfunctional G307S CBS-allele, nor the 68-bp insertion I278T allele was observed at increased frequency in the cases relative to the controls. Steegers-Theunissen *et al.* (1994) studied CBS activity in fibroblasts from women who previously gave birth to NTD affected infants. CBS activities within the normal range were observed. The authors could therefore not make any positive link between a defective CBS and an increased risk for NTD.

A number of studies have addressed the possible role of methionine synthase (MS) in the aetiology of NTD. Although a mutation in MS was reported, it apparently did not contribute to an increased risk for pregnancies affected by NTD (van der Put, 1997). Heil *et al.* (2001) recently investigated the involvement of serine hydroxymethyltransferase (SHMT) in NTD. Both isoforms (cSHMT and mSHMT) were studied and several mutations and polymorphisms were found in the two genes. These mutations led to elevated homocysteine levels but no positive connection could be made to a group of spina bifida patients or their parents. Several other enzymes and protein factors have also been implicated as probable risk factors for NTD (Matsuda, 1994; Zittoun, 1995; Chen, 2003).

In experimental animal models, numerous chemicals have been used to induce NTD. The anti-epileptic drug valproic acid (VPA) proved to be a potent inducing agent of NTD in numerous studies executed on animal models (Naruse, 1988; Wegner, 1992; Alonso-Aperte, 1999). VPA apparently interferes with fetal folate metabolism, which may contribute to its mechanism of teratogenesis (Elmazar *at al.*, 1995). A study on the mouse model for NTD also revealed that valproic acid may alter the expression of several genes in the folate pathway (Finnell, 1997).

A high incidence of pregnancies affected by NTD in Hispanic women has been associated with chronic exposure of the mothers to relatively high levels of fumonisin B1, present in maize products which make up their staple diet (Stack, 1998; Hendricks, 1999). Biochemical investigations seem to indicate that the function of the GPI-anchored folate receptor may be compromised by fumonisin B1, a sphingolipid analogue and inhibitor of ceramide synthesis (Stevens, 1997).

More recently, Sadler *et al.* (2002) proved that folate could prevent the development of fumonisin B1-induced NTD in an *in vitro* mouse model.

Several other xenobiotic chemicals have been identified as probable aetiological factors involved in the epidemiology of NTD, i.e. anti-epileptics (i.e. valproic acid), hypoglycin-A, diazepam, concanavalin-A, ethanol, retinoic acid, vitamin A, methotrexate, nitric oxide, short-chain carboxylic acids and many more (Persaud, 1970; Coakley, 1986; Elmazar, 1995; Vorster, 1995; Inagaki, 1996; Yerby, 2003; Finnell, 2003; Lewis, 1998). It therefore makes a lot of sense that the probable relationship between mycotoxins and other xenobiotic agents with teratogenic potential should be rigorously investigated.

2.1.5 Occurrence and recurrence studies – the value of folate supplementation

The British Medical Council and the Budapest trials conclusively demonstrated that a woman's risk for an NTD-affected pregnancy is reduced substantially by taking folic acid periconceptionally. The British Medical Research Council trial was a randomised double-blind prevention study, carried out in 33 centres (Medical Research Council [MRC] Vitamin Study Group, 1991). This investigation included 1817 women at risk of having a pregnancy, complicated with NTD, following a previously affected pregnancy. The carefully selected study subjects were allocated to one of four groups; the first group received 4 mg of folic acid per day, the second group received the same but additionally a multivitamin preparation, the third group received only the multivitamin preparation (without the folic acid), while the fourth group received a placebo, containing only minerals. The subjects were instructed to take the supplements from at least 1 month, prior to conception and to continue with supplementation until the 12th week of their pregnancies. The recurrence of NTD was found to be reduced by 72 %, following periconceptionally folic acid supplementation, relative to the placebo group. Vitamins and minerals without folic acid therefore proved to be ineffective in preventing the recurrence of NTD.

Czeizel *et al.* (1992) investigated the extent to which vitamin supplementation could reduce the first occurrence of NTD. Women planning their first pregnancy were randomly assigned to receive a daily vitamin supplement (containing 12 vitamins, including 0.8 mg folic acid, 4 minerals and 3 trace elements), or a trace element supplementation only. Pregnancy was confirmed in 4753 women. Six cases of NTD occurred in the trace element group compared to none in the vitamin group. The authors concluded that periconceptional vitamin use decreases the risk of a first occurrence of NTD.

During 1991, the Centre for Disease Control (CDC) issued a public health statement in the United States of America recommending folic acid supplementation for "high-risk" women with a previous affected NTD pregnancy. Investigators now firmly believe that folate supplementation does not only correct a simple nutritional deficiency, but rather overcomes an underlying, genetically predetermined metabolic block (Mills, 1996; Lucock, 1998).

2.2 FOLATE

Folic acid was first recognised during 1930 as a factor present in the yeast preparation Marmite, which was able to cure megaloblastic anaemia occurring in Hindu women, particularly during pregnancy. Following the isolation of folate from spinach leaves in 1941, the term folic acid was introduced, derived from the Latin word folium, or "leaf". The synthetic form, folic acid, was successfully synthesised in 1946 (Rowe, 1983; Steegers-Teunissen, 1995). The common feature of all folates is a *p*-aminobenzoic acid (PABA) moiety, bound to a pteridine ring and one or more L-glutamic acid molecules, linked to the carboxyl end of the PABA moiety, via peptide bonds (Figure 2.3).

Although folate acts as a cofactor/co substrate in numerous enzymatic reactions, humans are not able to synthesise folate and are therefore entirely dependent on exogenous dietary sources of this vitamin (i.e. green leafy vegetables, liver, kidney, citrus fruit, whole wheat bread, etc.). Synthetic folic acid is produced in the monoglutamate form, although natural folates occur as polyglutamates, with the glutamate moieties linked via the γ-carboxyl peptide bonds. Only

monoglutamates and to a small extent oligoglutamate derivatives, can be absorbed by the intestines and the polyglutamates therefore need to be specifically hydrolysed, prior to or during uptake. Two forms of human pteroylpolyglutamate hydrolase ("conjugase") occur in the intestine and are involved in the hydrolysis of polyglutamates to monoglutamates. The absorption process comprises active as well as passive transport of the monoglutamate molecules into the mucosal cells. Once absorbed, the monoglutamates are fully reduced to tetrahydrofolate (THF) by dihydrofolate reductase, followed by methylation to 5-methyltetrahydrofolate (5-MeTHF), before it is rapidly transported to the tissues.

Once the monoglutamates enters the cells, they are metabolised to polyglutamates by the enzyme folylpolyglutamate synthetase (FPGS). FPGS adds L-glutamate molecules, one at a time, to the folate by catalysing the formation of a peptide bond between the γ-carboxyl of the glutamate already present on the folate and the α-amino group of the incoming L-glutamate molecule. Up to eleven L-glutamate molecules can be bound to one folate molecule via this ATP dependent reaction:

$$H_4PteGlu_n + ATP + \text{L-Glutamate} \rightarrow H_4PteGlu_{n+1} + ADP$$

To accurately describe the number of glutamate residues, the nomenclature system is related to tetrahydropteroate (H_4Pte), which has no glutamate residues. Tetrahydrofolate containing a single glutamate residue is known as $H_4PteGlu$, while the hexaglutamate form would be denoted as $H_4PteGlu_6$. In addition to the different chain lengths of the glutamate residues, six different derivatives of $H_4PteGlu_n$ can be distinguished, with the one carbon group in a variety of oxidation states. The major forms present in cells are 5-methyl-, 5-formyl-, 5,10-methylene-, and 10-formyl-$PteGlu_n$. Two other forms also exist (5,10-methenyl- and 5-formimino-$PteGlu_n$) but do not greatly contribute to the total cellular concentration of folates, although they are important metabolites in the interconversion of the various forms of folate contributing to one-carbon metabolism (Figure 2.3; van der Put, 1997).

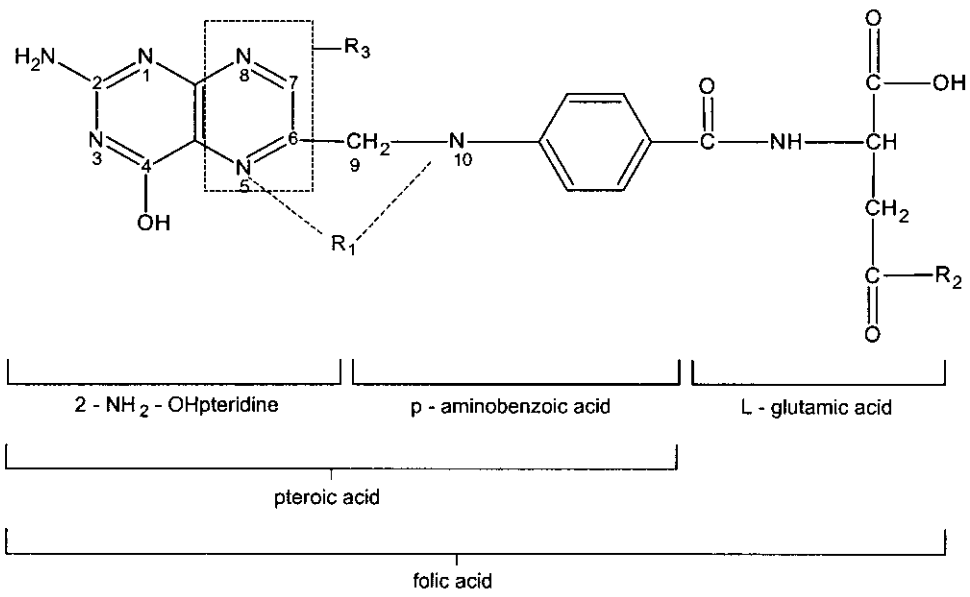

R1	— CH_3 at N^5, — H at N^{10} (5-methyl) — CHO at N^5, — H at N^{10} (5-formyl) — CHNH at N^5, — H at N^{10} (5-formimino) =CH= at N^5, N^{10} (5,10-methenyl) —CH_2— at N^5, N^{10} (5,10-methylene) —CHO at N^{10} (10-formyl)
R2	poly (γ - glutamyl)$_n$ glutamic acids — OH
R3	Unreduced pteridine ring 7, 8 Dihydro (H_2 Folate) 5, 6, 7, 8 Tetrahydrofolate (H_4 Folate)

Figure 2.3. Folic a cid structure and its derivatives. Modified form Rowe, 1983.

Human cells need a critical concentration of folates to allow normal activity of folate-dependant enzymes. Because the highly negatively charged polyglutamates are poorly transported across cell membranes, the metabolism of monoglutamates to polyglutamates allows the cell to maintain folate levels much higher than the external medium. Folate is thus trapped inside the cell by poly-glutamation and this process contributes to the metabolic control of intracellular and extracellular folate dependent biochemical reactions. The chain length of the glutamate also plays a huge role on the affinity of the folate-dependant enzyme for the substrate. Polyglutamate folates of appropriate chain lengths have much lower K_m values for some of the folate-dependant reactions than the monoglutamate forms and this allows folate metabolism to progress at the normal concentrations of folates in the cell (Rosenblatt, 1995; Atkinson, 1997).

2.2.1 Folate and one-carbon metabolism

Folate is an essential coenzyme/co substrate and vital for cell division and homeostasis. In mammals, the major reactions constitute a series of interconnected biochemical reactions in which folic acid is partially reduced to dihydrofolate (DHF), followed by reduction to tetrahyrofolate (THF). THF is subsequently metabolised to a number of one-carbon derivatives, with the carbon in various oxidation states that are involved in purine biosynthesis (Section 2.2.1.5), thymidine biosynthesis (Section 2.2.1.6), methionine synthesis *via* the remethylation of homocysteine (Section 2.2.1.2), serine/glycine interconversion (Section 2.2.1.4), and the metabolism of histidine and formate. Because folate is involved in the formation of methionine, it is indirectly involved in many methylation reactions *via* S-adenosylmethionine (SAM). SAM is the most important biomethylating agent and involved in DNA methylation and gene regulation (Section 2.3.1), carnitine biosynthesis (Section 4.2.4.3), polyamine biosynthesis (Section 4.2.4.2), the synthesis of cysteine and glutathione via the transsulfuration route (Section 2.2.1.3) and numerous other methylation reactions (Figure 2.4; Heby, 1981; Selhub, 1992; Bailey, 1999; Avila, 2002; Herbig, 2002; Mattson, 2003).

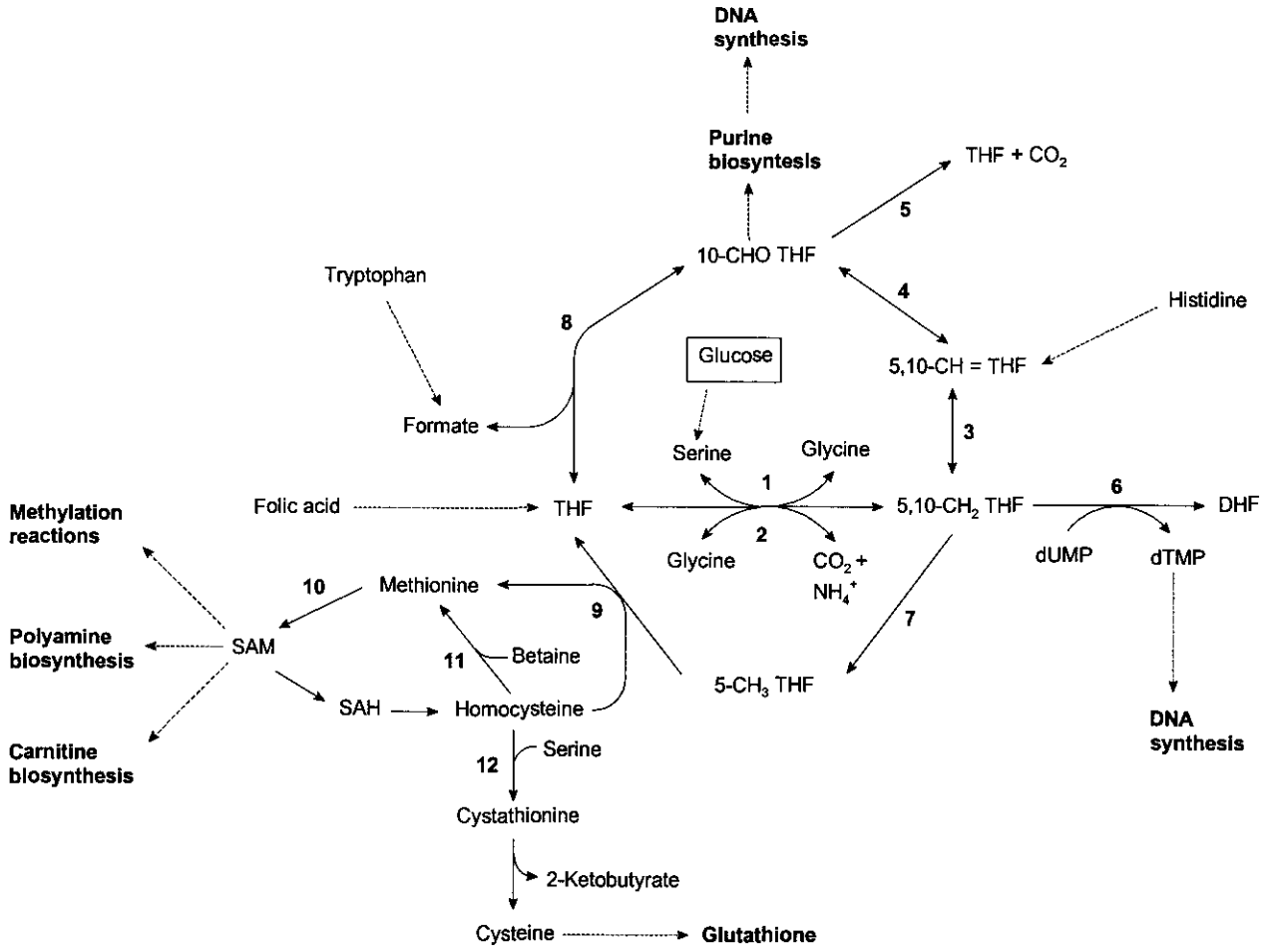

Figure 2.4. **Overview of one-carbon metabolism.** 1) Serine hydroxymethyltransferase, 2) Glycine cleavage system, 3) Methylene THF dehydrogenase, 4) Methenyl THF cyclohydrolase, 5) Formyl THF dehydrogenase, 6) Thymidylate synthase, 7) Methylene THF reductase, 8) Formyl THF synthase, 9) Methionine synthase, 10) Adenosyl transferase, 11) Betaine homocysteine methyltransferase, 12) Cystathionine-β-synthase.

2.2.1.1 The folate cycle

The folic acid absorbed from the diet must be fully reduced to tetrahydrofolate (THF) before it can enter the folic acid cycle. This reduction is catalysed by dihydrofolate reductase (EC 1.5.1.3) (Figure 2.4). Folic acid is reduced to DHF and in a second reaction to THF, both reactions being NADPH dependant. These are the first reactions in the one-carbon metabolism and therefore an attractive target for anti-cancer therapeutic agents, i.e. methotrexate, a potent dihydrofolate reductase inhibitor. By inhibiting these reactions in the one-carbon metabolism, DNA synthesis is inhibited, especially in rapidly dividing tumor cells with a huge need of DNA precursors for the *de novo* synthesis of DNA (Salway, 1994).

Folate enters the folic acid cycle as tetrahydrofolate. Because serine and glycine are the major donors of one-carbon units, entry to the active one-carbon pool of intermediates occurs *via* 5,10-methylene THF. The latter can be formed by a pyridoxal-5'-phosphate (PLP)-dependent reaction catalysed by serine hydroxy-methyltransferase (SHMT; EC 2.1.2.1), present in both cytoplasma and mitochondria (Section 2.2.1.4). This conversion of THF to 5,10-methylene THF is a crucial first step in the cycle, utilising the carbon-3 atom of serine as a major one-carbon source (Rosenblatt, 1995; Bailey, 1999). Tetrahydrofolate can also be converted to 5,10-methylene THF by the action of the glycine cleavage system (GCS; EC 2.1.2.10). This NADH-coupled reaction use glycine as a one-carbon source, while CO_2 and HN_4^+ (Section 2.2.1.4) are formed as by-products.

5,10-Methylene THF can be directly used in the synthesis of thymidine, reduced to 5-methyl THF for the biosynthesis of methionine or oxidised to 10-formyl THF for purine synthesis (Rosenblatt, 1995). The oxidation of 5,10-methylene THF to 5,10-methenyl THF is catalysed by 5,10-methylene THF dehydrogenase (MTHFR; EC 1.5.1.5) in a reversible reaction. 10-Formyl THF is formed form 5,10-methenyl THF and used in the *de novo* synthesis of purine nucleotides. 10-Formyl THF can also be derived from the essential amino acids histidine and tryptophan, although the major sources of one-carbon units are serine and glycine (Rosenblatt, 1995; Girgis, 1997; Herbig, 2002). 5,10-Methylene THF is reduced to 5-methyl THF by MTHFR in an NADPH dependent reaction. Although

this reaction is bi-directional *in vitro,* it is unidirectional in the formation of 5-methyl THF in cells (van der Put, 1999; Herbig, 2002). The formed 5-methyl THF acts as one-carbon donor for the remethylation of homocysteine to methionine, where it interconnects the folic acid and remethylation cycles.

2.2.1.2 The remethylation cycle

The one-carbon group enters the remethylation cycle when it is transferred from 5-methyl THF to L-homocysteine (Hcy) to form the essential amino acid L-methionine and THF in a ATP dependent reaction catalysed by methionine synthase (MS, EC 2.1.1.13). This enzyme is probably present in all mammalian tissues and requires cobalamin (vitamin B_{12}) as cofactor. Methionine synthase is the only enzyme that can use 5-methyl THF as a substrate and it is critical for channelling one-carbon groups derived from histidine, tryptophan, glycine and serine into the remethylation cycle. MS is also essential for maintaining adequate intracellular methionine and tetrahydrofolate levels, as well as for ensuring that homocysteine concentrations does not reach toxic levels (Selhub, 1992; van der Put, 1997).

Homocysteine can also be remethylated to methionine by betaine-homocysteine methyltransferase (BHMT; EC 2.1.1.5), using betaine as a methyl source. During this reaction, betaine (trimethylglycine) is converted to dimethylglycine and homocysteine is methylated to methionine. The betaine used in this reaction is derived from the catabolism of choline. Fisher *et al.* (2002) studied choline metabolism in the mouse embryo and found that betaine-homocysteine methyltransferase was not yet expressed in 10 day-old embryos. Closure of the neural tube is almost complete at day 10 *p.c.* and it therefore seems unlikely that BHMT will play any role in providing one-carbon units during closure of the neural tube in the developing mouse embryo.

L-Methionine is used for protein synthesis or can be converted to S-adenosyl-L-methionine (SAM) in a reaction catalysed by L-methionine-S-adenosyltransferase (MAT; 2.1.1.14). In this unusual reaction, the adenosyl moiety of ATP is

transferred to methionine, forming a sulfonium bond between the 5'-carbon atom of the ribose and the sulphur atom of the amino acid. The tripolyphosphate that results from this transfer remains bound to the enzyme, which then cleaves the tripolyphosphate to form inorganic phosphate and pyrophosphate in a second catalytic step. Removal of the tripolyphosphate assists in making the synthesis of SAM essentially irreversible under physiological conditions (Mudd, 1995). The intracellular concentration of L-methionine appears to be the rate-limiting factor for SAM biosynthesis.

As the most important cellular biomethylating agent, SAM is responsible for more than a hundred known methylation reactions, including the methylation of proteins, phospholipids, hormones, neurotransmitters, RNA and DNA (Heby, 1981; Selhub, 1992; Bailey, 1999; Herbig, 2002). During these methylation reactions, the methyl group is transferred from SAM to the methyl-acceptor and the by-product S-adenosylhomocysteine (SAH) is produced. Adenosyl homocysteinase (SAHase; EC 3.3.1.1) converts SAH back to homocysteine, and the latter can then participate in yet another one-carbon transfer reaction (Salway, 1994). The SAM:SAH ratio is termed the methylation ratio and when this ratio falls below a certain value, methylation reactions are inhibited, leading to hypomethylation of DNA. Such a fall in the ratio can be caused by a rise in the concentration of SAH, a decrease of SAM, or both (Weir, 1995). An increase in the concentration of SAH, due to high homocysteine concentrations, has been hypothesised to be the first step in the embryotoxic mechanism of L-homocysteine (van Aerts, 1994).

2.2.1.3 The transsulfuration route

Homocysteine (Hcy) is metabolically positioned at an important branch point. It may be either remethylated to form methionine and thus completing the sulphur conservation cycle or it may be catabolised *via* the transsulfuration route. The catabolic conversion of Hcy is initiated when it condenses with serine to form L-cystathionine in an irreversible chemical reaction, catalysed by cystathionine-β-synthase (CBS; EC 4.2.1.21), a pyridoxal-5'-phosphate (PLP)-containing enzyme

(Selhub, 1992; Mudd, 1995; Kluijtmans, 1996). L-Cystathionine is subsequently hydrolysed by a second PLP-containing enzyme, cystathionine γ-lyase (CGL; EC 4.4.1.1), with the resultant formation the non-essential amino acid, L-cysteine and the ketoacid, α-ketobutyrate. L-Cysteine can be used in protein synthesis or in the synthesis of the tripeptide glutathionine, essential for numerous detoxification, transport and metabolic processes (Salway, 1994). Excess cysteine is oxidised to taurine and eventually to inorganic sulfates. Thus, in addition to the synthesis of cysteine, the transsulfuration route effectively catabolises the potentially toxic homocysteine, not required for methyl transfer (Selhub, 1992).

2.2.1.4 Serine/Glycine interconversion

Results from several metabolic studies suggest that serine and glycine occupy a unique metabolic position in the fetus (Cetin, 1991; Cetin, 1992; Narkewicz, 1996b). The fetus relies to a large extent on the endogenous synthesis of serine and glycine. Changes in the regulation of serine and glycine biosynthesis and their utilisation appear to be the only mechanisms available through which the fetus can modulate the supply of these two amino acids. Serine also appears to function as a semi-essential amino acid in the fetal liver and is therefore important in the regulation of fetal growth (Narkewicz, 1996b). The serine/glycine interconversion is catalysed by the cytosolic (cSHMT) and mitochondrial (mSHMT) isoforms of serine hydroxymethyltransferase, as well as the glycine cleavage system (GCS). This interconversion is especially important when there is a need for one-carbon tetrahydrofolate coenzymes (co substrates) or when either one of these amino acids are used or supplied (Xue, 1999).

Serine hydroxymethyltransferase (SHMT; EC 2.1.2.1) catalyses the reversible transfer of a methyl group from serine to tetrahydrofolate (THF) to form 5,10-methylene THF and glycine (Schirch, 1982). The cytosolic (cSHMT) and mitochondrial (mSHMT) isoforms are encoded by separate genes (Narkewicz, 1996). Setoyama *et al.* (1990) showed that the cytosolic and mitochondrial isoforms of SHMT do not share common promoter elements and that the two

genes are separately regulated. Although cSHMT and mSHMT catalyse the same chemical reaction, they play different roles in one-carbon metabolism (Figure 2.5). Tissue culture studies proved that loss of mSHMT activity could not be rescued by the cSHMT isoenzyme (Herbig, 2002).

The glycine cleavage system (GCS) plays a major role in the catabolic breakdown of both serine and glycine. The GCS, is a hetero-tetrameric complex located in the inner membrane of mitochondria in cells of the liver, the kidney, the brain and the placenta. This enzyme-complex converts tetrahydrofolate and glycine to CO_2 and HN_4^+ in a reversible, NADH-coupled reaction. In contrast to SHMT, which is already expressed at high levels in the cells of neonate rats, the GCS is not yet fully active in the newborn rat. The GCS activity in 2-day old rat neonates was apparently only 29 % of the levels normally expressed in the adult rat. The specific activity of the GCS, however, steadily increases with the age of the young rat (Hamosh, 1995).

A study of the literature published on serine/glycine interconversion revealed that different schools of thought exist on this matter. The precise role of cSHMT, mSHMT and the GCS in this interconvertion still remains unresolved. However, intracellular compartmentation of the serine/glycine interconversion ensures proper metabolic control of the serine/glycine flux (Narkewicz, 1996b). Mitochondrial SHMT and the GCS are involved in the conversion of serine to glycine and formate (a one-carbon unit). Glycine and formate are apparently the ultimate products of one-carbon metabolism in the mitochondria and formate is transported to the cytoplasm. Cytoplasmic SHMT uses the mitochondrial-derived formate for the synthesis of purines (i.e. supplies carbon atoms 2 and 8 of the purine ring), thymidine (conversion of dUMP to dTMP) and methionine from homocysteine (Girgis, 1997; Gregory, 2000; Herbig, 2002; Figure 2.5).

Narkewicz *et al.* (1996a) illustrated that mSHMT is responsible for 87 % of the glycine synthesis and virtually all of the synthesis of glycine from serine in Chinese hamster ovary cells (CHO). Up to 90 % of the one-carbon units in mammalian cells are derived from formate, generated *via* serine metabolism in the mitochondria (Herbig, 2002). Narkewicz *et al.* (1996b) also reported that

50 % of serine biosynthesis occurs as a result of the activities of the GCS and mSHMT. Approximately 20 % of the serine is derived from the transamination of glutamine, glutamate and alanine, and the rest is provided *via* the catabolic breakdown of proteins and glucose.

Cytosolic SHMT mediates competition between the biosynthesis of deoxyribonucleotides and S-adenosylmethionine. According to Herbig *et al.* (2002), cSHMT can act as a metabolic switch under certain conditions to increase DNA synthesis at the expense of homocysteine remethylation. This is accomplished in one or both of 2 mechanisms: deoxyribonucleotide synthesis can be enhanced by providing 5,10-methylene THF to thymidylate synthase for thymidine synthesis, at the same time increasing the cytoplasmic THF pool for conversion of the 5,10-methylene THF to 10-formyl THF, which is needed for purine biosynthesis. Simultaneously, cSHMT can inhibit homocysteine remethylation by decreasing the availability of 5,10-methylene THF to MTHFR (at elevated glycine levels) and by binding 5-methyl THF and depleting cellular SAM levels.

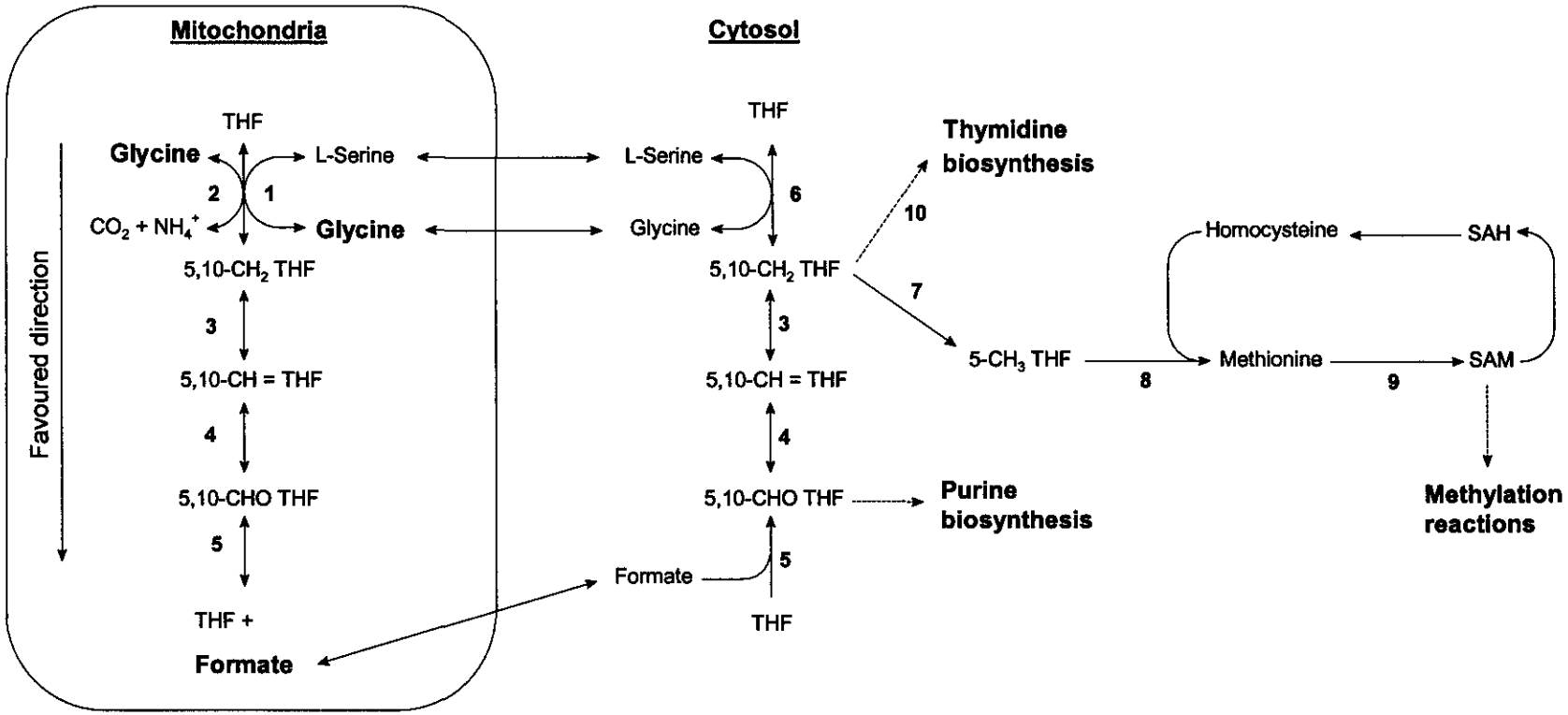

Figure 2.5. **Compartmentation in one-carbon metabolism between cytosol and mitochondria.** 1) Mitochondrial serine hydroxymethyltransferase (mSHMT), 2) Glycine cleavage system (GCS), 3) Methylene THF dehydrogenase (MTHFD), 4) Methenyl THF cyclohydrolase. 5) Formyl THF synthetase, 6) Cytosolic serine hydroxymethyltransferase (cSHMT), 7) Methylene THF reductase (MTHFR), 8) Methionine synthase (MS), 9) Adenosyl transferase (MAT), 10) Thymidylate synthase. Modified form Gregory, 2000.

2.2.1.5 Purine biosynthesis

Purine nucleotides can be synthesised *de novo*, or they can be reclaimed from the existing nucleoside pools by the salvage pathways. For the *de novo* synthesis of purine nucleotides, 10-formyl THF is required. This THF derivative can be synthesised from the essential amino acids, histidine and tryptophan, or from serine *via* the action of serine hydroxymethyltransferase (SHMT, EC 2.1.2.1) (Fig. 2.4).

During histidine catabolism, 5-formimino THF and glutamate is formed. 5-Formimino THF is converted to 5,10-methenyl THF by N^5-formimino THF cyclodeaminase (THF-CD; EC 4.3.1.4). The resultant 5,10-methenyl THF can be converted to 5,10-methylene THF by an NADPH dependant reaction, or it can be converted to 10-formyl THF, following the addition of H_2O through the action of a cyclohydrolase. THF can, however, also be directly converted to 10-formyl THF in an ATP dependent reaction, catalysed by 10-formyl THF synthetase (F-THF-S, EC 6.3.4.3), which transfers a formate moiety, derived from tryptophan catabolism, directly to THF. However, the main source of one-carbon units for the synthesis of 10-formyl THF and ultimately the purine nucleotides is not these essential amino acids, but the non-essential amino acid, serine (Rosenblatt, 1995; Girgis, 1997; Stover, 1997; van der Put, 1999; Herbig, 2002). THF and serine is metabolised to 5,10-methylene THF and glycine by SHMT, generally regarded as a key enzyme in one-carbon metabolism. Methylene THF can then be converted to all the other forms of THF derivatives, including 10-formyl THF (Figure 2.4).

Ribose-5-phosphate, generated *via* the pentose monophosphate pathway, is an important precursor for the *de novo* synthesis of inosine monophosphate (IMP), an intermediate product in purine biosynthesis. A series of enzyme reactions are involved in the synthesis of IMP and includes the addition of 2 molecules of 10-formyl THF (derived from histidine, tryptophan or serine). IMP is also used for the *de novo* synthesis of deoxyguanosine triphosphate (dGTP) en deoxyadenosine triphosphate (dATP). These two metabolites are important building blocks in the synthesis of DNA by DNA polymerase (EC 2.7.7.7). IMP is also metabolised to

guanosine triphosphate (GTP) and adenosine triphosphate (ATP), building blocks in the synthesis of RNA by RNA polymerase (Salway, 1994).

2.2.1.6 Thymidine biosynthesis

Thymidine can be synthesised *de novo* or can be recovered *via* the nucleotide salvage pathway, the latter requiring far less ATP than the *de novo* synthesis. For the synthesis of thymidine, folate is essential. Thymidine biosynthesis starts with ribose-5-phosphate, derived from the pentose monophosphate pathway. Ribose-5-phosphate is metabolised to orotidine monophosphate (OMP) and then decarboxylated to render uridine monophosphate (UMP). UMP is converted to uridine diphosphate (UDP) and uridine triphosphate (UTP), following two ATP requiring steps. The resultant UTP can be utilised for the synthesis of RNA, but it is also used for the synthesis of cytosine triphosphate (CTP) by the enzyme cytosine triphosphate synthetase (CTPS, EC 6.3.4.2). CTP is also required for RNA synthesis, but part of this compound is converted to deoxyuridine monophosphate (dUMP), the immediate precursor of thymidine.

For the conversion of dUMP to deoxythymidine monophosphate (dTMP), folate is essential. This reaction is catalysed by thymidylate synthase (TS, EC 2.1.1.45), and involves the ultimate addition of a methyl group to the 5-position of dUMP (Figure 2.6). This one-carbon group is derived from 5,10-methylene THF, formed by the action of cytoplasmic serine hydroxymethyltransferase (cSHMT), where the 5,10-methylene THF is oxidised to dihydrofolate (DHF) in the process. Oppenheim *et al.* (2001) found that the activity of cSHMT is rate-limiting for the *de novo* biosynthesis of thymidine. DHF is reduced to THF by dihydrofolate reductase (DHFR, EC 1.5.1.3) before it can enter the folate cycle again and participate in one-carbon transfer reactions. The dTMP is first phosphorylated by dTMP kinase (TK, EC 2.7.4.9) and then by nucleoside diphosphate kinase (NDPK, EC 2.7.4.6) to produce deoxythymidine triphosphate (dTTP), needed by DNA polymerase for DNA synthesis and DNA repair (Salway, 1994). The synthesis of deoxyribonucleotides, which is mediated by thymidylate synthase and ribonucleotide reductase (RNR, EC 1.17.4.1), is considered to be the rate-limiting step in DNA synthesis (van der Put, 1997).

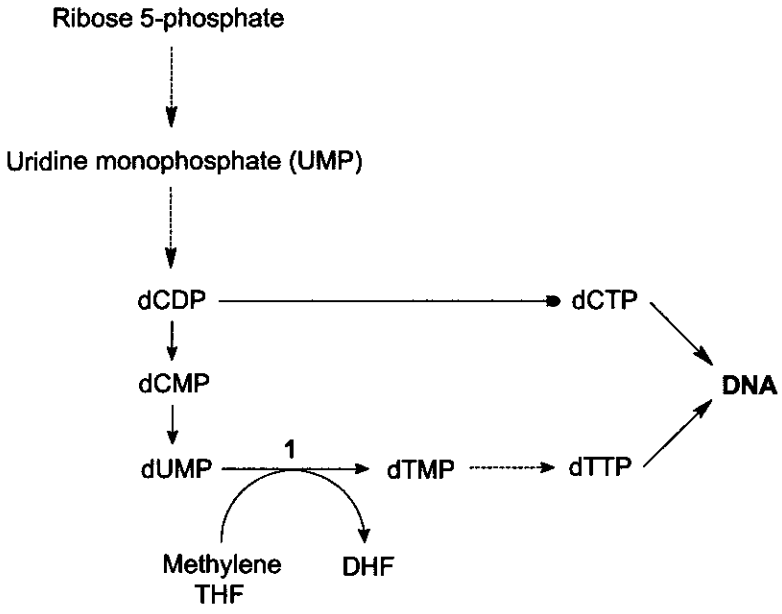

Figure 2.6 **Simplified thymidine biosynthesis, indicating the role of 5,10-methylene THF.** 1) Thymidylate synthase. Modified from Salway, 1994.

2.2.2 Regulation of one-carbon metabolism

Folate one-carbon metabolism is highly complex and regulated *via* several mechanisms. The first regulation point is the number of glutamate residues in the functional folate molecule. The number of glutamate residues also plays a crucial role in the affinity of a folate-dependant enzyme for its substrate. Polyglutamate folates with the appropriate number of glutamate residues, linked in a polyglutamate chain, have much lower K_m values for some of the folate-dependant reactions than the monoglutamate forms. This phenomenon makes it possible for folate metabolism to operate at the normally low intracellular concentrations of participating folate species in the cell (Rosenblatt, 1995; Atkinson, 1997).

Compartmentation provides a useful mechanism for regulation of one-carbon metabolism. Because the highly negatively charged polyglutamates are poorly transported across cell membranes, the conversion of monoglutamates to polyglutamates allows the cell to maintain intracellular folates at much higher levels than in the external medium. Polyglutamates are also very poorly transported across inner- and outer mitochondrial membranes. Folate can

therefore not move freely between the cytosol and mitochondria, creating well separated cytosolic and mitochondrial folate pools. Three of the folate-dependent enzymes, including the GCS, only occur in the mitochondria.

SHMT catalyses the very first reaction in a metabolic pathway, involved in providing one-carbon groups for the synthesis of purines, thymidilate and methionine. The activity of SHMT is therefore highly regulated in the cell. 5-Methyl THF and 5-formyl THF bind with equal affinity to the folate-binding site of SHMT, compared to the THF and methylene THF. Both 5-methyl THF and 5-formyl THF can be considered to be effective physiological inhibitors, since their concentrations in the cell exceed that of THF (Schirch, 1982).

Some studies have indicated that folate metabolism is regulated to the extent that SAM biosynthesis has metabolic priority over thymidine biosynthesis. Herbig *et al.* (2002) reported that, under certain conditions, cSHMT may act as a metabolic switch to increase DNA synthesis at the expense of homocysteine remethylation. This is achieved by providing more 5,10-methylene THF to thymidine synthase (TS) for thymidine synthesis and by increasing the cytoplasmic availability of THF for the biosynthesis of 10-formyl THF, which is needed for purine synthesis. cSHMT can simultaneously, inhibit homocysteine remethylation by decreasing the availability of 5,10-methylene THF to MTHFR and/or by sequestering 5-methyl THF and depleting cellular SAM levels (Herbig, 2002).

The concentrations of SAM and S-adenosylhomocysteine (SAH) are critical parameters in numerous allosteric regulatory mechanisms. SAM can act as an allosteric regulator of homocysteine flux through the remethylation or transsulfuration routes. When the concentration of SAM exceeds a certain critical intracellular level, it can inhibit MTHFR. The purpose of this step is to protect the cell against a folate "methyl trap", ensuring that one-carbon units are spared for DNA precursor biosynthesis (Herbig, 2002). SAM can also act as an allosteric activator of cystathionine-β-synthase (CBS), stimulating the irreversible conversion of homocysteine to cystathionine in the transsulfuration pathway (Kluijtmans, 1996). Many SAM-dependent reactions are strongly inhibited by

SAH, therefore a SAM:SAH ratio of 1:4 have been found to decrease the activity of a variety of methyltransferases up to 60 % (van der Put, 1999). It is apparently essential that a high intracellular SAH:SAH ratio must be maintained to ensure the progression of normal one-carbon metabolism.

2.3 S-ADENOSYLMETHIONINE

S-Adenosylmethionine (SAM) is responsible for more than a hundred known biomethylation reactions, including the methylation of proteins, phospholipids, hormones, neurotransmitters, RNA and DNA (Heby, 1981; Selhub, 1992; Bailey, 1999; Herbig, 2002). During these methylation reactions, the methyl group is transferred from SAM to the methyl-acceptor and the by-product S-adenosylhomocysteine (SAH) is formed. Adenosyl homocysteinase converts SAH back to homocysteine and free adenosine, and homocysteine can then participate in another one-carbon transfer reaction (Salway, 1994). SAM is also involved in the biosynthesis of polyamines (Section 4.2.4.2) and carnitines (Section 4.2.4.3).

2.3.1 DNA methylation

The adenine and cytosine residues of DNA may be methylated in a species-specific pattern, to form N^6-methyladenine, N^4-methylcytosine, and N^5-methyl-cytosine residues, respectively (Voet, 1995). In higher order eukaryotes, DNA is methylated mostly (but not exclusively) on cytosine bases located 5' to guanosine in a CpG dinucleotide, although not all cytosines in this dinucleotide are methylated (Adams, 1990; Meehan, 2003). Following DNA synthesis, N^5-methylcytosine methyltransferase (m^5C-Mtase, EC 2.1.1.73) methylate cytosine residues on the newly synthesised strand, in positions symmetric to those on the template strand (Ushijima, 1997). This method of maintaining the methylation status of DNA would permit the stable "inheritance" of a methylation pattern. In vertebrates, 3 – 6 % of cytosine residues in DNA are methylated, but this value decreases along the evolutionary scale so that in many insects and single-cell eukaryotes there is no detectable 5-methylcytosine (Adams, 1990).

The DNA methyltransferases responsible for the methylation of cytosine residues in DNA employ SAM as co-substrate, and the process involves the transfer of a one-carbon unit, in the form of a methyl group, from SAM to cytosine (methyl acceptor) to form 5-methylcytosine and SAH. The latter is subsequently hydrolysed by S-adenosylhomocysteine hydrolase (SAHase) to adenosine and L-homocysteine. L-homcysteine is eventually recycled through the remethylation cycle to produce a replenished pool of SAM (Section 2.2.1.2).

In the genome, the upstream promoter region of many genes possesses CpG rich areas, referred to as CpG-islands. Methylation of these CpG-islands is involved in gene regulation through a number of direct and indirect mechanisms (Adams, 1990; Herman, 1996). CpG methylation can effect gene expression directly by altering the recognition sites of transcription factors. Indirectly, CpG methylation can alter DNA structure at secondary and tertiary levels and these alterations may produce distinct structural patterns that are recognised by a range of methyl-CpG-binding proteins (MeCPs). The CpG pairs act as ligands for MeCPs which, in turn can target repressor complexes that contain histone deaminases, leading to the formation of deacetylated and repressed chromatin structure that is refractory to the transcription machinery (Meehan, 2003).

DNA methylation is also involved in mismatch repair of newly synthesised DNA. When a normal, but incorrect, base is introduced into DNA during replication, it is usually removed by a proof-reading mechanism before the next nucleotide is added. When this mechanism fails, the product is a duplex of DNA molecule with a mismatch. A repair system that can correct the mismatch needs to discriminate between the two normal bases, one of which is incorrect. The mismatch repair system use the lack of methylation on the newly synthesised (incorrect) strand to determine which strand should be repaired (Adams, 1990).

DNA methylation is necessary for embryonic development in vertebrate. Massive alterations in the methylation pattern may occur frequently in embryonic cell types, an integral part of the early developmental program (Cedar, 1990). Mutant mice embryos, deficient in DNA methyltransferase 1 (*Dnmt1*) activity, fail to develop properly and die at mid-gestation, displaying a complex phenotype

which includes mesodermal defects and abnormally high levels of cellular apoptosis. The dysmorphic embryos also display a distorted neural tube and lack visible somites. Somatic cell inactivation of *Dnmt1* in primary mouse fibroblasts also leads to hypomethylation of DNA and p53-dependent apoptosis (Meehan, 2003).

2.4 ANIMAL MODELS

In order to understand the aetiology and pathology of congenital neural tube defects, it is important to comprehend the mechanisms of the processes invoked during closure of the neural tube. Understanding the molecular basis for cellular, genetic and metabolic events that play a role in the development of the neural tube may eventually facilitate the design of novel therapeutic strategies that may help to prevent NTD. Nearly all research on epidemiology, pathology and therapeutic interventions, relating to NTD in humans are retrospective in nature. Prospective and mechanistic studies are necessary to resolve the numerous questions relating to NTD. Ethical principles, however, exclude the use of humans and human embryos to obtain species-specific information, so urgently needed to understand the aetiology and development of NTD in man.

Numerous animal models have been developed to study neural tube defects, including the rhesus monkey, rat, rabbit, mouse and chicken models (Naruse, 1988). The chicken and mouse embryos proved to be the best models for research on the aetiology and pathology of NTD, due to interspecies similarities in neurulation (George, 1995). However, species differences do occur and extrapolation from animal models to man still poses numerous problems. Spina bifida aperta (a defect of the posterior end of the neural tube) is the predominant congenital malformation observed in human neonates, as a result of valproate induced NTD. However, valproate predominantly induces exencephaly (a defect of the anterior portion of the neural tube) in mouse embryos.

Species also differ in their sensitivity to certain teratogens. Hypoglycin-A, a leucine analogue, is teratogenic to rat, but not chicken embryos. Persaud *et al.*

(1970) ascribed this apparent anomaly to the following aspects: mammalian (i.e. rat, etc.) embryos develop *in utero*, where they are continuously exposed to potential teratogens (i.e. hypoglycine-A, etc.) and the resultant teratogen metabolites produced by the mother. The teratogen and/or its metabolites may compromise the nutrition of the developing embryos during a period when adequate nutrition is essential for normal morphogenesis. The chicken embryo, on the other hand, develops in an egg that is "pre-loaded" with a balanced supply of nutrients needed for development. The teratogen therefore competes with a large pool of nutrients accessible to the chicken embryo, while the mammalian embryo is absolutely dependent on a continuous nutrient supply from the mother which is contaminated with the teratogen and teratogen metabolites, produced by the mother.

Different strains of the same species of animal may display differences in the degree of their responses to the same teratogen (Naruse, 1988; Finnell, 1997). By treating different mouse strains with 600 mg/kg valproic acid, Finnell *et al.* (1988) induced exencephaly in 35 % of SWV mice, 20 % in LM/Bc mice and none in C57BL/6J and DBA/2J mice. By using an *in vitro* mouse embryo model, Naruse *et al.* (1988) found that SWV embryos are 1.5 – 3 times more sensitive to the embryo lethal and teratogenic effects of valproic acid than C57BL embryos. Therefore, the choice of an animal species and strain appears to be of great importance in NTD studies.

Although animal studies have proved to be valuable, experimental results are difficult to extrapolate to the human situation. This problem can be ascribed to species associated differences in developmental sensitivities to teratogens and the pharmacokinetics of various teratogens, as well as the fact that no experimental model system may be able to reproduce the conditions that exist for the human embryo *in utero* (Wegner, 1992; Locksmith, 1998).

2.5 β- HYDROXYNORVALINE

β-Hydroxynorvaline (HNV), a threonine analogue, was first synthesised by Sunko *et al.* (1955) from copper sulphate and glycine under alkaline conditions. Potgieter *et al.* (1976) obtained a near 100% yield of stereospecific HNV (2S,3R-2-amino-3-hydroxypentanoic acid, following catalytic hydrogenation of the toxic non-protein amino acid, 2S,3R-2-amino-3-hydroxypent-4-ynoic acid (rolfsin) from the fungus *Sclerotium rolfsii (Sacc.)*. More recently, the presence of HNV was demonstrated in living organisms (i.e. thermophilic bacteria and archaea).

Reddy *et al* (1992) identified two novel nucleosides in unfractionated transfer RNA, prepared from thermophilic bacteria (*Thermodesulfobacterium commune*, *Thermotoga maritima*), hyperthermophilic archaea (i.e. *Pyrobaculum islandicum*, *Pyrococcus furiosus*, *Thermococcus sp.*, etc.) and mesophilic archaea (*Methanococcus vannielii*, *Methanolobus tindarius*), containing a residue of HNV in their structures. The structural identity of the nucleosides were resolved by mass spectrometry. They were subsequently identified as 3-hydroxy-N[[(9-β-D-ribofuranosyl-9H-purin-6-yl)amino]carbonyl]-norvaline and 3-hydroxy-N-[[9-β-D-ribofuranosyl-9H-2-methylthiopurin-6-yl)-amino]carbonyl]norvaline. The HNV residue was released from the nucleosides, following alkaline hydrolysis. After trimethylsilylation of the hydrolysates, the amino acid residue was identified as 3-hydroxynorvaline (HNV) by gas chromatography-mass spectrometry.

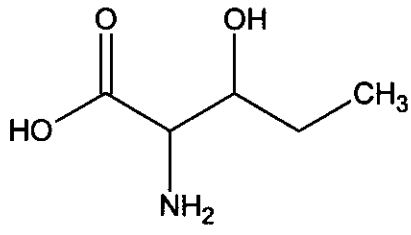

Figure 2.10. Structure of β-hydroxynorvaline, a threonine analogue.

In the past three decades, HNV has been studied by numerous investigators and found to exhibit many toxic effects. HNV inhibits herpes virus DNA replication *in vitro.* Treatment of Green monkey kidney cells (GMK), infected with the Herpes simplex virus (HSV-1), with HNV resulted in reduced herpes virus DNA replication: both the rate and the total DNA synthesis were reduced (Massare, 1987). Infection with HSV-1 results in the synthesis of > 50 proteins, including viral encoded thymidine kinase (TK) and a DNA-dependent DNA polymerase (DP). The activity of both these enzymes was drastically reduced in the HNV treated cells. The authors concluded that the inhibitory effect could be due to one and/or more of the following reasons: 1) the incorporation of HNV into the enzyme, forming mutant enzymes with altered activity; 2) HNV inhibited the formation of regulatory viral polypeptides and/or altered its acivity; 3) HNV caused the production of altered viral polypeptides that were more labile to proteolytic cleavage; 4) HNV produced alterations in the regulatory genes of the DNA polymerase which modified the TK. Due to the presence of a at least one Threonine (Thr) residue within the ATP-binding site of the TK molecule and three Thr residues directly adjacent to the ATP-binding site, the authors concluded that the incorporation of HNV into proteins could be the main reason for the altered enzyme activity.

Glycosylation of proteins is inhibited by HNV. Proteins destined for excretion, incorporation into membranes, or localisation inside membranous organelles contain carbohydrates and are therefore classified as glycoproteins. N-Linked glycosylation of proteins occur on the HN_2 group of an asparagine (Asn) residue on a growing polypeptide (Voet, 1995). HNV inhibited the addition of asparagines-linked oligosaccharides to nascent murine leukaemia virus (MuLV)-encoded membrane glycoproteins, specifically at Asn-X-Thr glycosylations sites (Polonoff, 1982). This inhibition was due to the incorporation of HNV instead of Thr. HNV has also been reported to inhibit O-glycosylation of proteins (Blough, 1986). O-Linked glycosylation of proteins occur on the serine (Ser) or Thr residues in proteins. The inhibitory effect exhibited by HNV is therefore possibly due to HNV being incorporated into proteins instead of Ser and/or Thr.

Numerous other toxic effects of HNV have been described. HNV caused increased intracellular degradation of collagen in human fetal lung fibroblasts by interfering with the association of pro-alpha chains (Barile, 1989). In chicken embryo fibroblasts, HNV inhibited the assembly and secretion of procollagen (Christner, 1975). Green *et al.* (1991) reported an inhibition of steroidogenesis in rat adrenal cortex cells by HNV. Most, if not all, of these toxic effects relate to the fact that HNV is structurally related to L-threonine and possibly incorporated into proteins. This proved to be possible, since HNV could apparently be activated by the same aminoacyl-tRNA-synthase involved in the activation of L-threonine, prior to incorporation into peptides/proteins (Christner, 1975).

The transport mechanism of HNV into mammalian systems remains unresolved. A gene has been identified in *Escherichia coli* that encode a product responsible for the active transport of HNV (Zakataeva, 1999). This protein belongs to a group of proteins (*rht B*) known as the amino-acid-efflux proteins. These proteins play an important role in resistance to toxic substrates, in the maintenance of an optimum intracellular concentration of metabolites and in the excretion of some regulatory metabolites. Amplification of the *rht B* gene in *E. coli* provided resistance to HNV.

2.6 SUMMARY

Neural tube defects (NTD) are among the most common and distressing of all human congenital malformations. The prevalence at birth varies among countries and socioeconomic and ethnic groups. In certain rural areas of South Africa, the incidence of NTD varies between 4 - 6 cases per 1000 live births, compared to a global mean incidence of between 0.2 and 1 per 1000 live births. The precise molecular mechanism of NTD remains unclear. Both the British Medical Research Council and the Budapest folate supplementation trails proved beyond doubt that folic acid can prevent a relatively large proportion of NTDs. These results confirmed previous notions that folate metabolism is critically important for normal embryogenesis and that disturbances in folate metabolism may lie at the heart of the NTD problem. Most researchers agree that folate does not only

correct a simple nutritional deficiency, but rather overcomes an underlying metabolic block.

Normal, uncompromised one-carbon metabolism is important for the synthesis of DNA precursors and the remethylation of homocysteine to methionine. Mild hyperhomocysteinaemia increasingly appears to be a major risk factor in the aetiology of neural tube defects. Elevated homocysteine levels can be caused by several factors: a reduced flow of one-carbon units through the folic acid cycle and the remethylation cycle, but also because of defects in the transsulfuration of homocysteine to cysteine and a decrease in S-adenosylmethionine levels (SAM). SAM is responsible for more than a hundred known biomethylation reactions, including the methylation of proteins, phospholipids, hormones, neurotransmitters, RNA and DNA. The methylation of DNA is especially important in the developing embryo, due to its involvement in gene regulation. SAM is also needed for the synthesis of carnitines (involved in energy metabolism and detoxification) and polyamines (critical for cell differentiation and proliferation). This puts a great demand on one-carbon folic acid metabolism, especially during embryonic development.

2.7 AIMS AND OBJECTIVES OF THIS STUDY

An understanding of the molecular basis for cellular, genetic and metabolic events that play a role in the aetiology and development of neural tube defects is absolutely imperative to study the mechanisms of dysmorphogenesis on the molecular level. Nearly all research on the epidemiology and pathology of NTD are retrospective in nature. However, prospective and mechanistic studies are necessary to resolve the numerous questions relating to NTD. Ethical principles, however, exclude the use of humans and human embryos to obtain species-specific information on these events that are so urgently needed to understand the aetiology and development of NTD in man. The main aim of this investigating was therefore to employ the chicken and mouse embryos models in an effort to gain insight into some of the molecular events involved in the aetiology of NTD.

The specific objectives of the project can be summarised as follows:

(i). Investigation of the teratogenic and toxicological properties of HNV in the chicken and mouse embryos.

- Attempted induction of NTD in chicken and mouse embryos.
- Investigation of general embryotoxic effects of HNV.

(ii). An investigation of the effects of HNV on selected aspects of one carbon metabolism in pregnant female mice and their fetuses.

- The influence of HNV on the flow of one-carbon units in mouse embryos employing the [^{3}H]-thymidine incorporation test.
- Investigation of the *in vitro* effect of HNV on the catalytic activity of serine hydroxymethyltransferase (SHMT) and cystathionine-β-synthase (CBS).
- The effect of HNV on DNA methylation status of mouse embryos.
- Effects of HNV on polyamine biosynthesis.
- Effects of HNV on carnitine biosynthesis.
- The effect of HNV on the catalytic activity of cytosolic serine hydroxymethyltransferase (cSHMT), mitochondrial serine hydroxymethyltransferase (mSHMT) and the glycine cleavage system (GCS).
- The effect of HNV on the transsulfuration route.

(iii). The catabolic fate of HNV and the metabolic implications for selected aspects of intermediate metabolism.

- Investigation into the catabolic breakdown of HNV.
- The effect of HNV metabolites on selected intermediary metabolic pathways.

CHAPTER 3

INDUCTION OF NEURAL TUBE DEFECTS IN ANIMAL MODELS WITH β-HYDROXYNORVALINE

3.1 INTRODUCTION

In order to understand the pathology involved in the occurrence of neural tube defects, it is important to have an insight into the mechanisms underlying the development of the neural tube during embryogenesis. Knowledge of the cellular and molecular events responsible for dysmorphogenesis of the neural tube could ultimately facilitate the development of novel therapeutic strategies to prevent NTD. Numerous animal models have been developed to study neural tube defects. These include the rhesus monkey, rat, rabbit, mouse and chicken model (Naruse, 1988). Chicken and mouse embryos proved to be the most suitable models because of interspecies similarities in the process of neurulation, as observed in man (George, 1995).

In order to develop reliable experimental models to study the molecular processes underlying dysmorphogenic events, caused by teratogenic xenobiotics, the correct biological event window needs to be selected accurately. Closure of the neural tube occurs very early in the development of the chicken embryo (Hamburger, 1951). The anterior neuropore already starts to close during the 13-somite stage (40 – 45 h of development), while closure of the posterior neuropore occurs during the 16-somite stage (45 – 49 h of development). To ensure that NTD will be induced, it is therefore critical that chicken embryos must be exposed to the potential teratogenic xenobiotic, just before the anterior neuropore starts to close.

The mouse embryo neural tube starts to close at about the 7-somite stage (8.25 days p.c.), at the level of the fourth and fifth somite (Hogan, 1986). Closure then

proceeds in a zipper-like manner in both the anterior and posterior directions. Closure of the anterior neuropore is completed by the 15- to 20-somite stage (9 days p.c.), while the posterior neuropore closes some time later (32-somite stage, 10 days p.c.). Neural tube defects can be induced in mouse embryos by a single treatment with a variety of teratogens on day 9 of gestation (Elmazar, 1995; Finnell, 1997) or by treatment once a day on days 7, 8 and 9 of gestation.

While studying the potential osteolathyrogenic properties of β-hydroxynorvaline (HNV) in the chicken embryo, Potgieter *et al.* (unpublished results) observed that HNV caused NTD (i.e. encephalocoele, spina bifida, etc.) in the chicken embryo. This model was initially selected to investigate the teratogenic properties of HNV. Practical issues concerning poor control over the xenobiotic levels that the embryos are exposed to and the relevance of the model to the human situation eventually swayed the choice of an animal model in the direction of the mouse model.

Like in humans the murine fetus develops in the closed confines of the uterus, essentially in an environment created by the physiological and metabolic characteristics of the mother. This model was therefore regarded to have significantly more relevance for investigations focused on the effects of a variety of potential teratogenic xenobiotics (i.e. β-hydroxynorvaline, etc.) on embryonic development (i.e. neural tube closure, etc.). Since urine and/or blood samples could also be collected in the course of experiments, the added advantage of the mouse model was that it enabled us to investigate metabolic perturbations that may have been induced by the chemicals (i.e. HNV, etc.) during the selected biological event window.

3.2 MATERIALS AND METHODS

3.2.1 Fixatives used

Allen's fluid (fixative)

- Formaldehyde solution (40 %) 250 ml
- Saturated picric acid solution 750 ml
- Acetic acid 50 ml
- Urea 20 g

Todd's fixative (Todd, 1986)

- Glutaraldehyde solution (25 %) 10 ml
- Paraformaldehyde in sodium cacodylate buffer (6.25 %) 20 ml
- $CaCl_2$ in sodium cacodylate buffer (0.3 %) 10 ml
- Picric acid in sodium cacodylate buffer (0.3 %) 10 ml
- Sodium cacodylate buffer (pH 7.4) 50 ml

3.2.2 Induction of NTD in the chicken embryo model

The Ethics Committee of the University of Pretoria originally approved this study since the experimental work was performed at the Department of Anatomy of the Medical Faculty of the University of Pretoria.

White Leghorn eggs (>80% fertility) were obtained from the Department of Virology, Onderstepoort Veterinary Institute, Pretoria. Eggs were collected overnight and kept at 12 °C to prevent embryonic development. The eggs were then divided into experimental and control groups, properly labelled and placed in egg racks of an egg incubator (Buckeye Model 20), with the sharper apex of the egg facing downwards. All eggs were simultaneously incubated at 37.8 °C to initiate synchronous embryonic development. Incubator temperature and humidity were well controlled (37.8 ± 0.5 °C, 65 ± 5 % relative humidity). Egg trays were automatically tilted through 90° every 50 minutes.

After 40 hours of development (stage 11 of development, approximately 13 somites; Hamburger, 1951), the blunt end of the egg was sterilised with 70 % ethanol solution and a small hole was drilled through the shell in the centre of the air chamber with a dental drill. Care was taken not to rupture the membrane at the bottom of the air chamber. Fifty microlitres of a sterilised solution (0.22 µm filter) of stereoisomeric HNV (synthesised, APPENDIX M) were injected through the drilled hole into the air sac and the toxin containing droplets allowed to settle on the inner shell membrane on the bottom of the air sac. Three experimental subgroups received aliquots of the HNV solutions, containing three different concentrations of HNV (75 mM, 150 and 300 mM; estimated final concentrations are 75, 150 and 300 µM, respectively). Controls were treated with 50µl of a sterile saline solution

(0.9% NaCl). All the eggs were subsequently resealed with hot paraffin wax and returned to the incubator.

Embryos were removed on the 10th day of development, during stage 36 of normal development (Hamburger, 1951). The eggs were opened, the embryos removed, examined for mortality and thoroughly scrutinised under a stereomicroscope to detect any gross abnormalities. Unfertilised eggs were identified and tallied. Following examination, all embryos were fixed in Allen's solution, blotted dry and weighed. Total body length was measured from the tip of the beak to the tip of the tail, over the dorsal circumference of the body. The toe and beak lengths of the embryos were also measured. Beak length was measured from the anterior angle of the nostril to the tip of the bill, (Hamburger, 1951).

3.2.3 Induction of NTD in the mouse embryo model

Hanover-NMRI mice were used since they are highly sensitive to teratogen induced NTD (Wegner, 1992; Elmazar, 1995) and was available to this study. The mice were kept at the Animal Testing Facility of the Potchefstroom University for CHE. They were pathogen free and healthy. Approval for the study was obtained from the Ethics Committee of the Potchefstroom University for CHE (Approval number: 01D02).

Animals were kept under controlled conditions at ambient temperature (21 ± 1 °C), relative humidity of 55 ± 5 %, and a 12 hour light:dark cycle (with changes at 06h00 and 18h00). Air changes were kept constant (the total volume of air in the room was replaced 15 – 20 times per hour) and a light intensity of 350 – 400 lux was maintained 1 meter above floor level. Animals were fed a standard laboratory diet (Rainbow Farms (Pty) Ltd) and had free access to food and water.

Virgin females, 40 – 60 days old, were mated overnight with experienced males (from 16h00 to 09h00 the following morning). The presence of vaginal plugs confirmed that copulation took place and these females were regarded as potentially pregnant. The following 24 hours was designated as the first day of gestation.

β-Hydroxynorvaline (HNV, Sigma Chemical Company) was dissolved in a saline solution and sterilised by filtration (0.22 μm filter). The HNV containing and the control saline solutions were administered orally, once daily on days 7, 8 and 9 of gestation. Experimental animals were treated with 300, 450 or 600 mg/kg HNV, respectively, while the control group received only saline (0.2 ml). Animals were sacrificed by decapitation on day 18 of gestation. Embryos were removed, dried on filter paper and weighed. They were examined for mortality and examined under a stereomicroscope to detect gross abnormalities. Embryos were subsequently fixed in Todd's fixative for photographic purposes.

All embryos were considered independent of each other, even in a single litter. This was used in the statistical analysis of the mouse embryo data, with respect to the induction of neural tube defects, the toxicity of HNV and the effect of HNV on the growth and general development of the embryos.

3.2.4 Statistical analysis

The same statistical approach and methods were used for both the chicken- and mouse embryo studies. Results were expressed as the mean ± standard error of the mean (SEM). The Levene test for homogeneity of variances and the Shapiro-Wilk W-test were used to determine if the data was normally distributed. Because of the relatively small samples employed in the study and since the data proved not be normally distributed (See Figures 3.3, 3.5, 3.7, 3.9), statistically significant differences were further assayed by the Kruskal-Wallis non-parametric test. Fisher's exact test was used to analyse the relationship between concentration and death rates as well as the rates for the induction of neural tube defects.

3.3 RESULTS

3.3.1 β-Hydroxynorvaline induction of NTD in the chicken embryo model

The first objective was to determine if HNV could induce NTD in the chicken embryo model. The control group consisted of 75 eggs and the experimental group of 150 eggs. After 40 hours of development, experimental embryos were treated with 50 µl of a 300 mM HNV-solution (estimated final concentration of 300 µM), while the controls received saline. On the 10th day of incubation, there were 62 embryos in the control group and 131 in the HNV-treated group.

Table 3.1. Defects observed in chicken embryos exposed to 300 µM HNV.

Type of defect	Number of embryos	Percentage embryos	One-sided p-value
Encephalocele	1	0.8	0.2461
Spina bifida	2	1.5	0.1668
Incomplete closure of skull roofs	5	3.8	0.0608
Abnormal tail buds	3	2.3	0.1151
Total neural tube defects	**11**	**8.4**	**0.0099**
Omphalocele	2	1.5	0.1668
Total Congenital defects	**13**	**9.9**	**0.0055**
Non-specific defects	34	26.0	<0.0001
TOTAL DEFECTS	**47**	**35.9**	**<0.0001**
Toxic mortality	**20**	**15.9**	**0.0024**

Embryos of the control group had no gross deformities or abnormalities. The embryos of the experimental group had numerous abnormalities (Table 3.1). In this group, 8.4 % of the embryos had neural tube defects, i.e. significantly more ($p = 0.01$) than the control group (see Figure 3.14 for photographs).

Two cases of omphalocele were found, where the intestines were protruding through an opening. Non-specific defects were most common and included growth

retardation, subcutaneous haemorrhage and focumelias. Twenty mortalities occurred in the experimental group and none in the control group.

3.3.1.1 Dose-response effects observed in the induction of NTD in chicken embryos with HNV

The dose-dependent effect of the induction of NTD in the chicken embryo model, with HNV, was subsequently investigated. One hundred and twenty eggs were divided into 4 different groups (30 eggs per group). Experimental eggs received 50 µl of a 75, 150 and 300 mM sterile HNV solution, respectively, while control eggs were dosed with 50 µl sterile saline. The estimated final concentrations of HNV were calculated to be a thousand times lower (75, 150, 300 µM). The calculation was based on the assumptions that the mean volume of the eggs was approximately 50 ml and that HNV would be evenly distributed throughout the contents of each egg. The eggs were incubated as described previously. Embryos were harvested on day 10 of development and investigated for the occurrence of neural tube defects.

Table 3.2. Contingency table for the induction of NTD in chicken embryos with HNV.

Effect	Number of Embryos				
	0 µM	**75 µM**	**150 µM**	**300 µM**	**TOTAL**
Normal	30	22	26	22	100
NTD	0	3	4	5	12
TOTAL	**30**	**25**	**30**	**27**	**112**

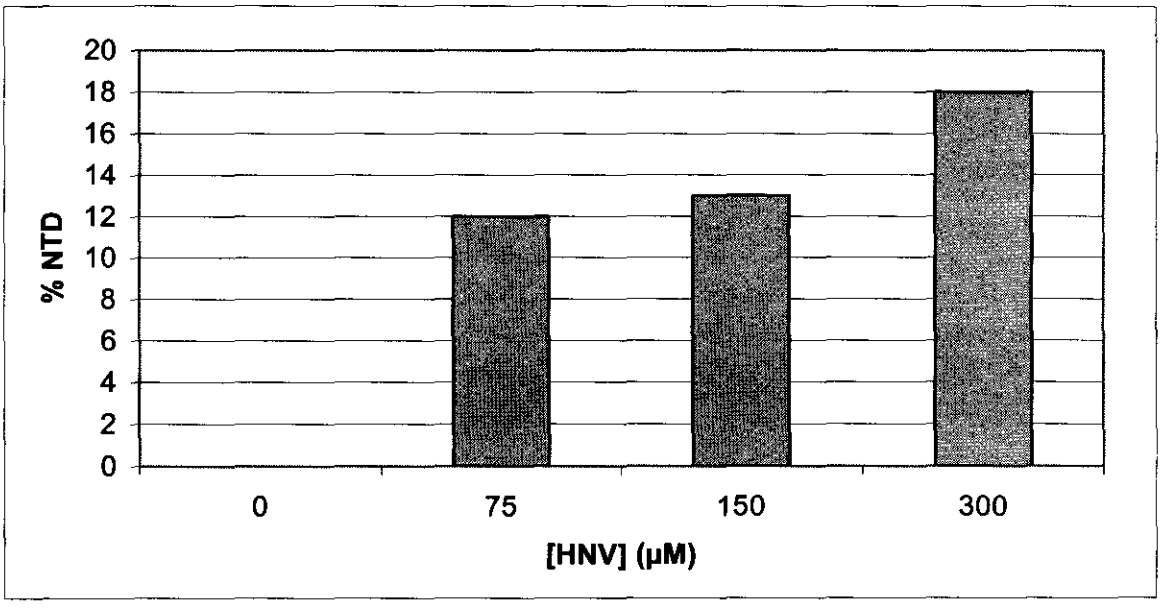

Figure 3.1. Dose dependent induction of neural tube defects in the chicken embryo model.

3.3.1.2 Statistical significance of the observed dose-response effect of HNV on the induction of NTD in the chicken embryo model

Fisher's exact probability test was executed on the data reported in Table 3.2. A definite tendency was observed in the incidence of NTD as a function of the concentration of HNV. However, the dose-response effect did not appear to be statistically significant at the 95% confidence interval ($p = 0.076$; Fisher's exact probability test). The observed effect proved to be statistically significant at the 90% confidence interval. Logistic regression analysis was used (Equation 3.1) to calculate a probable Tg_{50} (concentration of teratogen that will induce 50 % NTD in exposed embryos):

$$\log\left(\frac{p}{1-p}\right) = \alpha + \beta x \qquad \textit{(3.1)}$$

Where: p = proportion of the embryos with neural tube defects

x = HNV concentration.

The estimated Tg_{50} value was 528 µM (95 % confidence interval) and the values ranged from 343 µM to 7858 µM. One must bear in mind that the relatively small number of observations on which the estimation is based renders it impossible to draw too many conclusions with regard to Tg_{50}.

3.3.1.3 Effect of HNV on the growth and development of the chicken embryo

The effect of increasing β-hydroxynorvaline concentration on the growth and general development of chick embryos was investigated. Eighty eggs were randomly divided into 4 different groups, 20 eggs per group. After 40 hours of development, the control group received 50 µl saline and the other groups received 50 µl of a 75, 150 and 300 mM HNV solution in saline, respectively. Embryos were harvested on day 10 of development and fixed in Allen's fluid. The mass, length, beak length and toe length of each embryo was measured, a standard method to monitor/measure embryonic growth (Hamburger, 1951).

3.3.1.3.1 Effect of HNV on the body mass of the chicken embryos

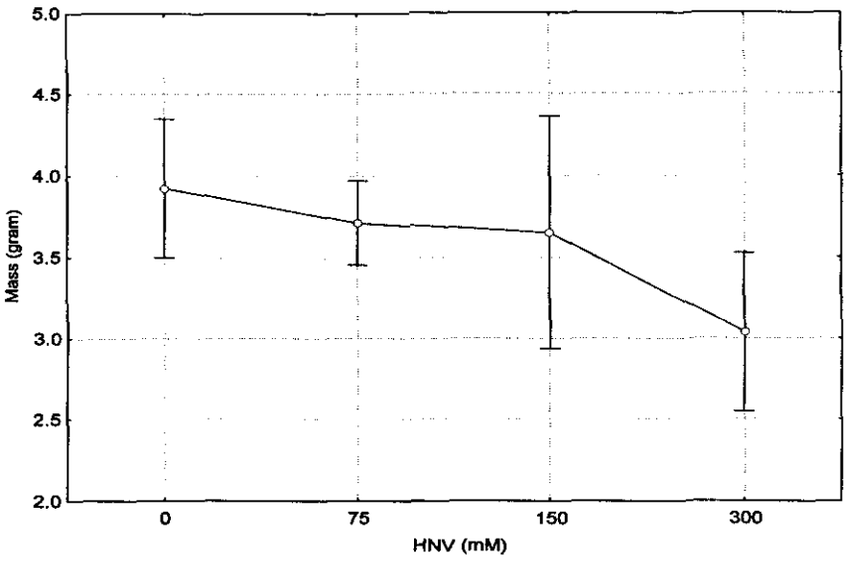

Figure 3.2. The effect of HNV on the body mass of chicken embryos.

The effect of HNV on embryo body mass is clearly depicted in Figure 3.2. The mean body mass of the control group was 3.93 ± 0.73 grams. In comparison the mean embryo body mass decreased by up to 23 % to 3.04 ± 0.95 grams in the 300 µM HNV group. The data (Figure 3.3) were tested for normal distribution, using the Levene test for homogeneity of variances ($p < 0.05$) and the Shapiro-Wilk test ($p < 0.01$). Since the data was not normally distributed, we tested for statistical significance between the groups, using the Kruskal-Wallis non-parametric test (Table 3.3).

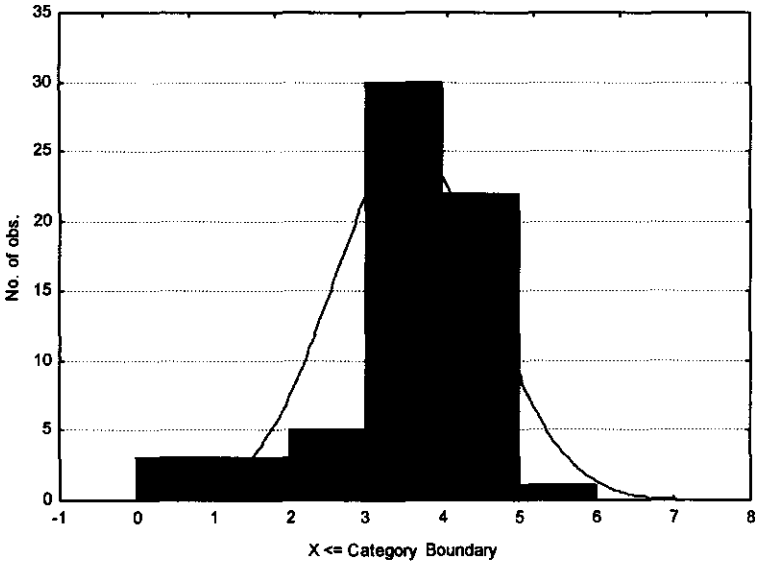

Figure 3.3. Frequency distribution of the body mass of chicken embryos.

Table 3.3. Kruskal-Wallis non-parametric test on the median mass of chicken embryos

	Multiple Comparisons p values (2-tailed); Mass (Mass of embryos) Independent (grouping) variable: Concentration Kruskal-Wallis test: H (3, N= 64) =9.940141 p =.0191			
Depend.: Mass	0 R:38.500	75 R:33.063	150 R:38.647	300 R:20.882
0		1.000000	1.000000	0.052480
75	1.000000		1.000000	0.362186
150	1.000000	1.000000		0.032444
300	0.052480	0.362186	0.032444	

The median mass of embryos decreased with increasing concentrations of HNV ($p = 0.019$; Kruskal-Wallis ANOVA). Multiple comparisons show that the 150 and 300 µM groups significantly differ from each other ($p = 0.032$) at the 95% confidence interval.

3.3.1.3.2 Effect of HNV on the body length of chicken embryos

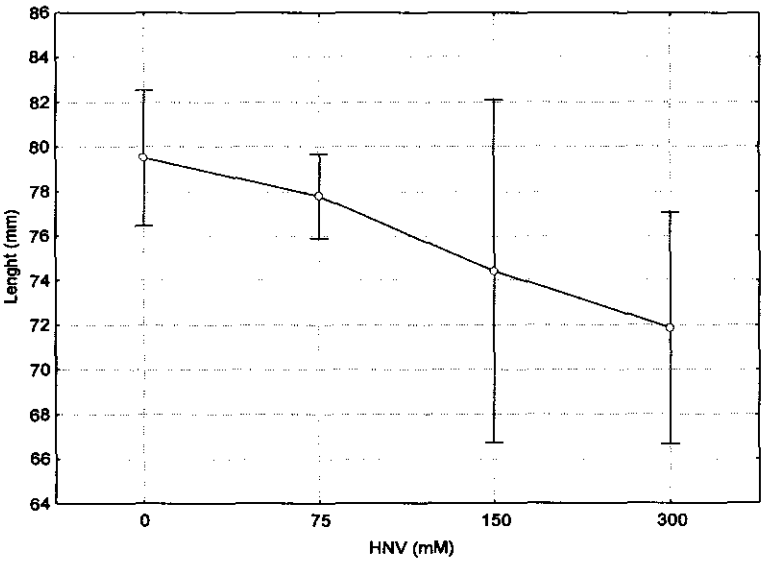

Figure 3.4. Effect of HNV on the total body length of chicken embryos.

The effect of HNV on body length of chicken embryos is summarised in Figure 3.4. The mean body length of the embryos in the control group was 79.5 ± 5.3 mm while that of embryos exposed to an estimated final dose of 300 µM HNV was 71.9 ± 10.1 mm, i.e. a mean decrease of 9.6 %. A Levene test for homogeneity of variances ($p = 0.03$) and the Shapiro-Wilk test ($p < 0.01$) on the data (Figure 3.5) indicated a non-normal distribution. Therefore, the Kruskal-Wallis non-parametric test was executed on the data set (Table 3.4).

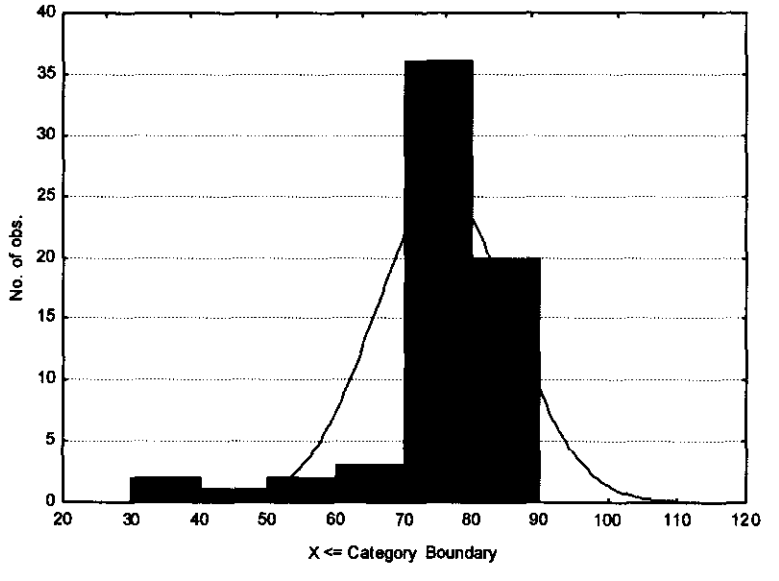

Figure 3.5. Frequency distribution of the body length of chicken embryos.

Table 3.4. Kruskal-Wallis non-parametric test on the median length of chicken embryos.

	Multiple Comparisons p values (2-tailed); Length (Length of embryos) Independent (grouping) variable: Concentration Kruskal-Wallis test: H (3, N= 64) =6.906626 p =.0749			
Depend.: Length	0 R:40.179	75 R:32.656	150 R:35.235	300 R:23.294
0		1.000000	1.000000	0.071889
75	1.000000		1.000000	0.893113
150	1.000000	1.000000		0.369050
300	0.071889	0.893113	0.369050	

A definite tendency was observed in the concentration dependent effect of HNV on the mean body length of the chicken embryos. However, the dose-response effect did not appear to be statistically significant at the 95% confidence limit. No statistically significant difference was found in the mean body length of the embryos between the four different concentration groups (p = 0.075; Kruskal-Wallis ANOVA). The sample size may have been too small to indicate a statistically significant effect.

3.3.1.3.3 Effect of HNV on the beak length of the chicken embryos

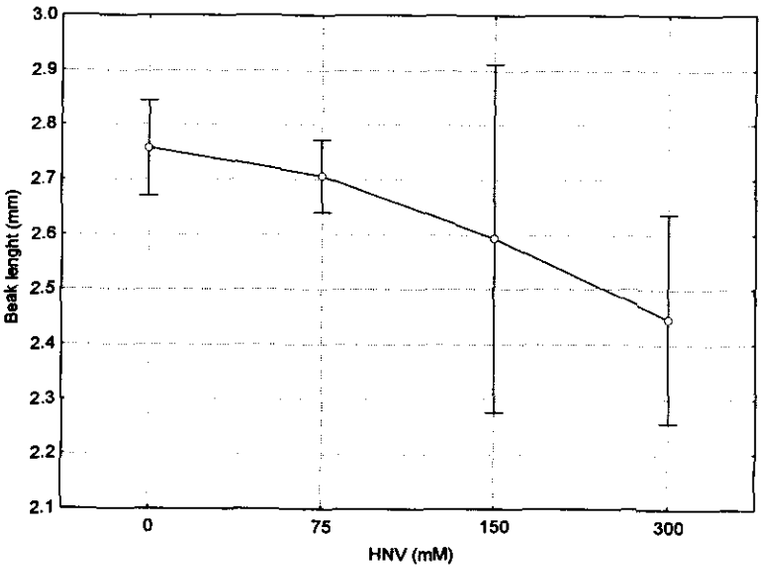

Figure 3.6. Effect of HNV on the beak length of chicken embryos.

The concentration dependent effect of HNV on the mean beak length of chicken embryos is depicted in Figure 3.6. Mean beak length of the control group was 2.76 ± 0.15 mm, while that of the 75, 150 and 300 µM groups decreased to 2.71 ± 0.12, 2.59 ± 0.62 and 2.45 ± 0.37, respectively. The 300 µM group showed an 11.2 % decrease, with respect to the control group. Data were tested for normal distribution (Figure 3.7), using the Levene test for homogeneity of variances ($p < 0.01$) and the Shapiro-Wilk test ($p < 0.01$). Since the data was not normally distributed, the Kruskal-Wallis non-parametric test (Table 3.5) was applied to test for significance between groups.

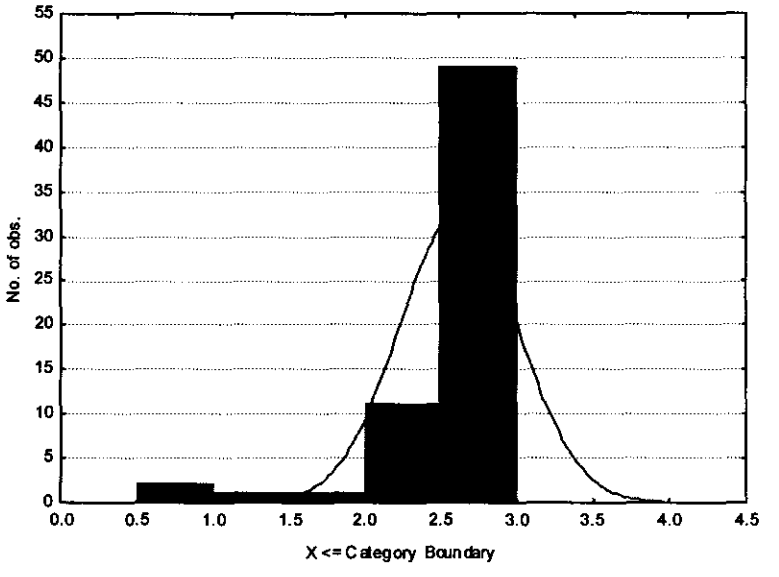

Figure 3.7. Frequency distribution of the beak length of chick embryos.

Table 3.5. Kruskal-Wallis non-parametric test on the median beak length of chicken embryos.

	Multiple Comparisons p values (2-tailed); Beaklength (Beak length of embryos) Independent (grouping) variable: Concentration Kruskal-Wallis test: H (3, N= 64) =12.90859 p =.0048			
Depend.: Beaklength	0 R:39.464	75 R:32.688	150 R:39.500	300 R:19.588
0		1.000000	1.000000	0.018585
75	1.000000		1.000000	0.260396
150	1.000000	1.000000		0.010928
300	0.018585	0.260396	0.010928	

Beak length appeared to be significantly ($p = 0.048$) affected by increasing HNV concentrations within the 95% confidence interval. Multiple inter-group comparisons indicated significant differences between the 300 µM and the control ($p = 0.019$) groups and between the 300 µM and 150 µM groups ($p = 0.01$).

3.3.1.3.4 Effect of HNV on the toe length of chicken embryos

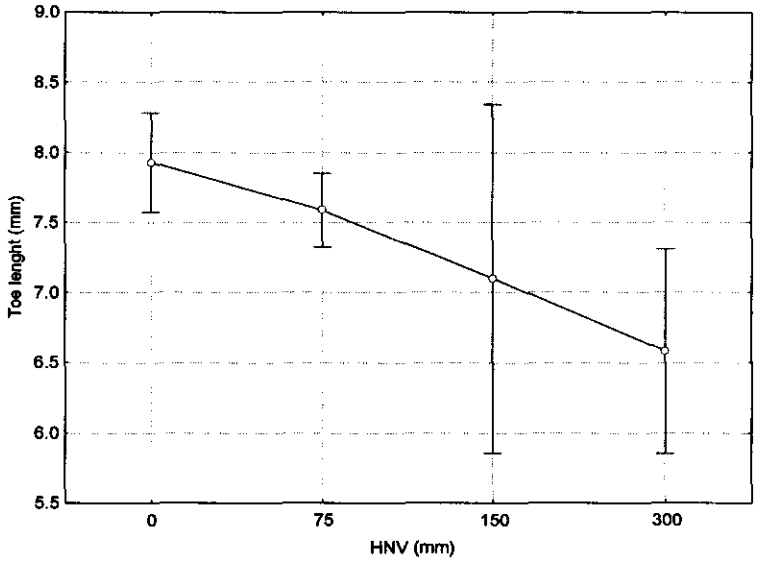

Figure 3.8. Effect of HNV on the toe length of chicken embryos.

Results on the effect of HNV on the toe length of chicken embryos are summarised in Figure 3.8. The mean toe length of the control group was 7.93 ± 0.62 mm and this decreased to 6.58 ± 1.42 mm in the 300 µM group, a 17.0 % decrease. The data were tested for normal distribution (Figure 3.9), using the Levene test for homogeneity of variances ($p < 0.01$) and the Shapiro-Wilk test ($p < 0.01$). The Kruskal-Wallis non-parametric test (Table 3.6) was applied to test for statistically significant differences between groups.

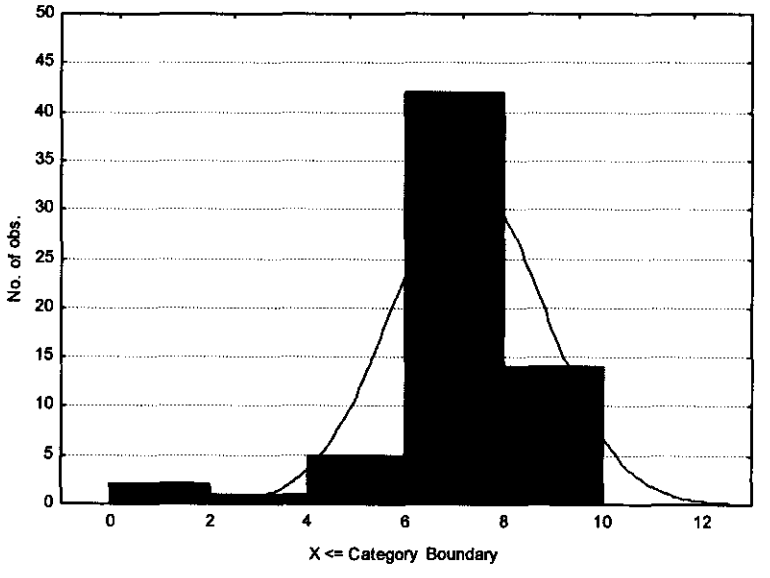

Figure 3.9. Frequency distribution of the toe length of chicken embryos.

Table 3.6. Kruskal-Wallis non-parametric test on the median toe length of chicken embryos.

	Multiple Comparisons p values (2-tailed); Toelength (Toe length of embryos) Independent (grouping) variable: Concentration Kruskal-Wallis test: H (3, N= 64) =15.57820 p =.0014			
Depend.: Toelength	0 R:42.321	75 R:33.406	150 R:37.941	300 R:18.118
0		1.000000	1.000000	0.001895
75	1.000000		1.000000	0.110411
150	1.000000	1.000000		0.011452
300	0.001895	0.110411	0.011452	

Toe length was significantly (p = 0.014) affected by increasing HNV concentrations. Multiple comparisons indicate a significant difference between the control group and the 300 µM group (p = 0.001). The 150 µM and 300 µM groups also differed significantly (p = 0.011). No difference between the control group and the lower concentration groups (75 and 150 µM) could be clearly demonstrated, although the inhibitory tendency of the effect of the HNV was quite obvious. This might be due to the relative small sample sizes in these groups.

3.3.2 β-Hydroxynorvaline induced NTD in the mouse embryo model

Pregnant female Hanover NMRI mice were divided into a control group and three experimental groups and dosed (per os) on three consecutive days (days 8, 9 and 10 *p.c.*). The four groups respectively received filter sterilised doses of 0 (control group), 300, 450 and 600 mg/kg HNV, dissolved in saline. Animals were sacrificed (decapitation) on the 18th day of gestation. Embryos were examined for dysmorphogenic effects (i.e. neural tube defects, etc.) under a stereomicroscope (Section 3.3.2.1). All embryos were blotted dry and weighed to determine if HNV had an effect on their growth and general development (Section 3.3.2.5). The number of dead embryos was tallied to assess the toxicity of HNV (Section 3.3.2.3). Embryos with defects were fixed in Todd's fixative for photographic purposes.

3.3.2.1 Dose-response effects observed in the induction of NTD in mouse embryos with HNV

Neural tube defects induced in mouse embryos included exencephaly and anencephaly. No spina bifida was observed. One embryo suffered from a limb reduction defect (amelia). See Figure 3.15 for photographs.

Table 3.7. Contingency table for the induction of neural tube defects in mouse embryos.

Effect	Number of Embryos				
	0 mg/kg	300 mg/kg	450 mg/kg	600 mg/kg	TOTAL
Normal	112	36	89	34	271
Defect	0	2	10	7	19
TOTAL	**112**	**38**	**99**	**41**	**290**

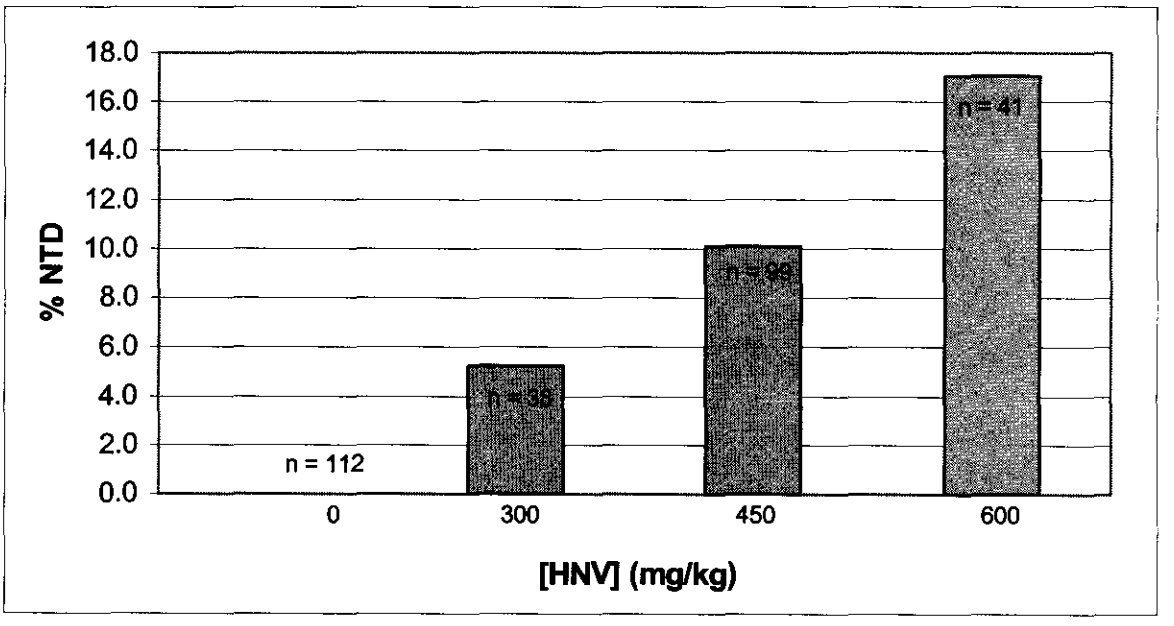

Figure 3.10. Concentration dependent induction of neural tube defects in the mouse embryo model.

3.3.2.2 Statistical significance of the observed dose-response effect of HNV on the induction of NTD in the mouse embryo model

Increasing HNV concentrations caused increased numbers of NTD ($p < 0.001$; Fisher's exact probability test). Logistic regression analysis was used to calculate a possible Tg_{50} (Equation 3.2):

$$\log\left(\frac{p}{1-p}\right) = \alpha + \beta x \qquad \textit{(3.2)}$$

Where: p = proportion of the embryos with neural tube defects

x = HNV concentration.

The estimated Tg_{50} value for the mouse embryos was 818 mg/kg, with values ranging from 680 to 1290 mg/kg (95 % confidence interval). The wide range of estimated values indicated that the Tg_{50} value may not be very accurate and this may have been caused by performing logistic regression analysis on a data set with a small number of defects in each of the groups. By increasing the sample size, it might be possible to obtain a more accurate estimation of the Tg_{50}.

3.3.2.3 Toxic effects of HNV on mouse embryos

Table 3.8. Contingency table for the toxicity of HNV in the mouse embryo model.

Effect	Number of Embryos				
	0 mg/kg	300 mg/kg	450 mg/kg	600 mg/kg	TOTAL
Alive	112	34	99	41	286
Dead	1	4	14	21	40
TOTAL	**113**	**38**	**113**	**62**	**326**

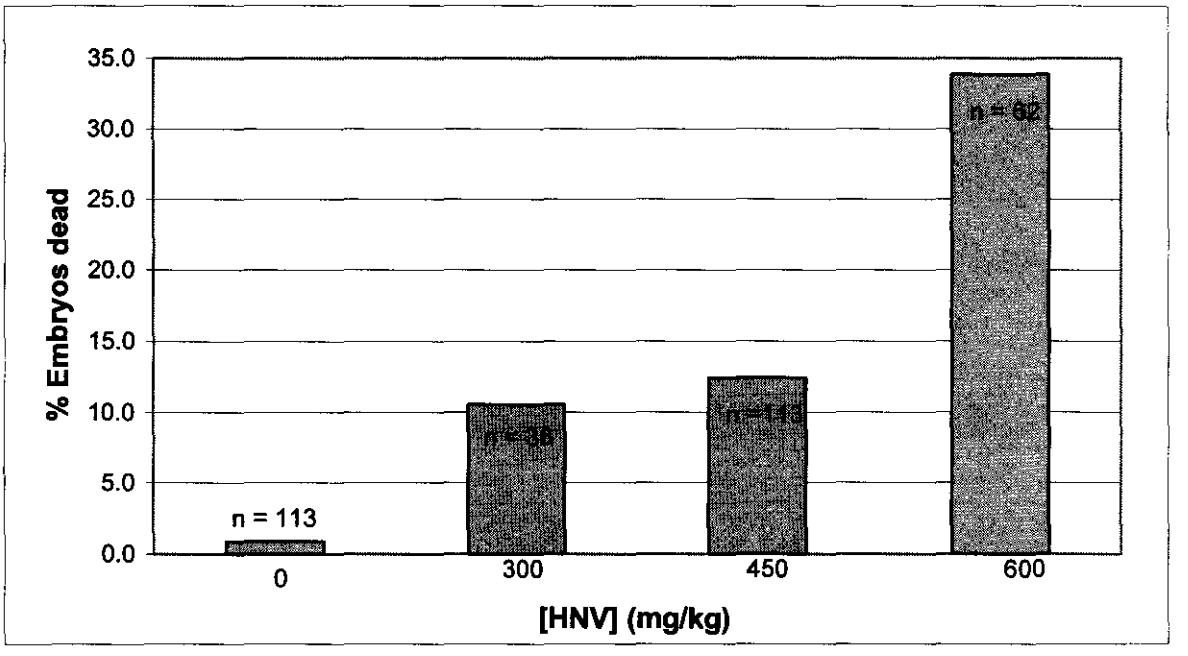

Figure 3.11. Concentration dependent toxicity of HNV in the mouse embryo model.

Fisher's exact probability test on the data set indicated that HNV had a statistically significant ($p < 0.001$) toxic effect on the mouse embryos.

Table 3.9. The Odds Ratio Estimates on the toxicity of HNV.

Effect	Point Estimate	95 % Confidence Interval
Dose of 300 vs 0 mg/kg	13.170	[1.424 ; 121.772]
Dose of 450 vs 0 mg/kg	15.830	[2.046 ; 122.505]
Dose of 600 vs 0 mg/kg	57.337	[7.476 ; 439.751]

Odds-ratio calculations indicated that the probability that an embryo will die because of exposure to HNV escalated significantly with increasing HNV concentration. Exposure to HNV raised the probability of death from 13 to 57 times greater than that of an embryo in the control group. Due to the wide variation observed in the 95 % confidence intervals, the point estimates may only be regarded as an indication of the increased risk of an embryo in the experimental groups to die of exposure to HNV, in comparison to the control group (zero exposure).

3.3.2.4 Estimated LD_{50} of HNV in the mouse embryo model

The LD_{50} of β-hydroxynorvaline could not be determined experimentally, due to restrictions in the rules of the Ethnical Committee of the Potchefstroom University for CHE. Fisher's exact probability test was executed on the data set and logistic regression analysis implemented to calculate the probable LD_{50} for HNV in the mouse embryo model (Equation 3.3).

$$\log\left(\frac{p}{1-p}\right)=\alpha+\beta x \qquad \textit{(3.3)}$$

Where: p = proportion of the embryos with neural tube defects
x = HNV concentration.

The estimated LD_{50} value for HNV was calculated to be 719 mg/kg (range: 637 to 901 mg/kg; 95 % confidence interval). A relatively narrow concentration range for the LD_{50} value was observed (95 % confidence interval). The estimated LD_{50} may therefore be more accurate than the calculated Tg_{50}, because the incidence of mortality was higher in all the groups, relative to embryos with NTD.

3.3.2.5 The effect of HNV on growth in the mouse embryo model

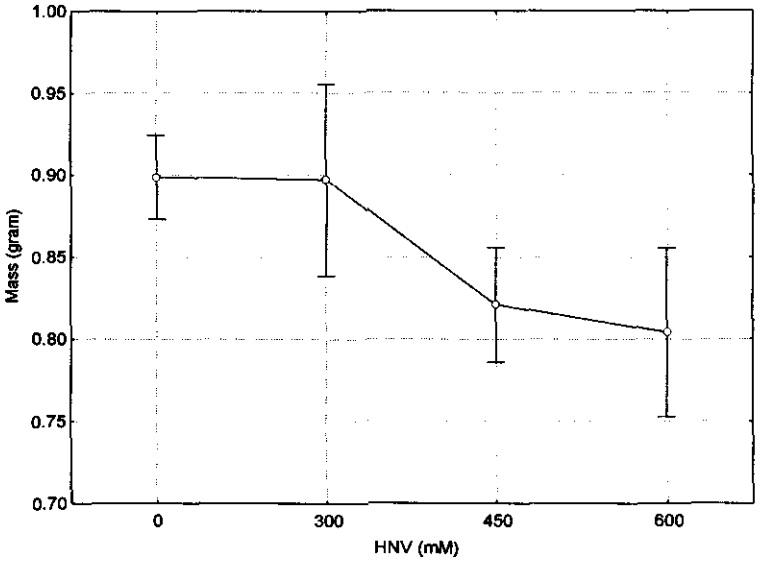

Figure 3.12. Effect of HNV on growth (body mass) of mouse embryos.

Results on the effect of HNV on the growth (body mass) of mouse embryos are depicted in Figure 3.12. The mean body mass of the embryos in the control group was 0.899 ± 0.113 grams, compared to 0.804 ± 0.124 grams in the 600 mg / kg group (10.6 % decrease). The data were tested for normal distribution (Figure 3.13), using the Levene test for homogeneity of variances ($p < 0.01$) and the Shapiro-Wilk test ($p < 0.01$). The Kruskal-Wallis non-parametric test was used to test for statistical significance between groups.

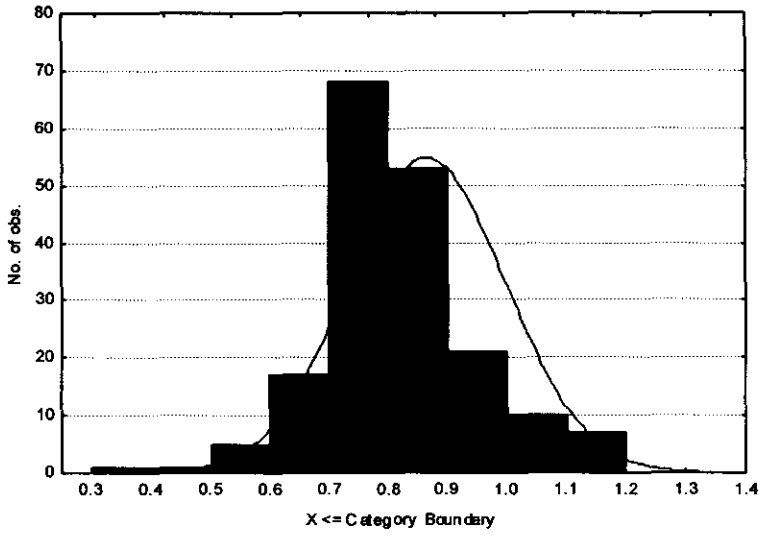

Figure 3.13. Frequency distribution of the mass of mouse embryos.

Table 3.10. Kruskal-Wallis non-parametric test on the median body mass of mouse embryos.

	Multiple Comparisons p values (2-tailed); Mass (Mass of mouse embryos) Independent (grouping) variable: Concentration Kruskal-Wallis test: H (3, N= 183) =20.94066 p =.0001			
Depend.: Mass	0 R:109.80	300 R:95.456	450 R:72.479	600 R:70.660
0		1.000000	0.000795	0.008105
300	1.000000		0.317888	0.453685
450	0.000795	0.317888		1.000000
600	0.008105	0.453685	1.000000	

The median mass of embryos proved to be indirectly proportional to the concentration of HNV ($p = 0.001$; Kruskal-Wallis ANOVA). Multiple comparisons show a statistically significant difference between the control group and the 450 mg/kg dosage group ($p < 0.001$), as well as between the controls and the 600 mg/kg group ($p = 0.008$). The data clearly exhibited a dose-dependent relationship for the growth inhibitory effect of HNV on mouse embryos. The mean body mass

of the embryos that received the lowest concentration of HNV group (300 mg/kg) did not differ significantly from the controls. It may be inferred that this dose was probably below the critical toxic level, where serious growth inhibition occurred.

3.4 DISCUSSION

The chicken and mouse embryo models have been used extensively for experimental investigations into the aetiology and mechanisms associated with neural tube defects. These two models also proved to be the best animal models for these studies due to similarities in the process of neurulation observed in human embryos (George, 1995).

The chicken embryo model appears to be useful in applied teratological studies, due to the sensitivity of the embryos to a variety of drugs (Gebhardt, 1972). This investigation indicated that HNV was clearly teratogenic in chicken embryos, inducing a relatively high incidence of NTD. This phenomenon proved to be concentration dependent, with the highest concentration (final estimated concentration of 300 µM) being responsible for inducing NTD in 18.5 % of the embryos, compared to zero NTD in saline treated controls. An estimated Tg_{50} was calculated from these results (528 µM) and the effect on the growth of the embryos assessed (*in ovo*). Various indicators of growth inhibition were measured (i.e. body mass, body length, beak length and toe length) and appear to exhibit statistically significant dose-dependent effects for HNV.

Probably the greatest disadvantage of the *in ovo* chicken embryo model experienced in this study, is the large variations observed in the outcomes of consecutive experiments. This observation may be due the fact that not all the embryos were exposed to the same concentrations of HNV. During dosage of the eggs, 50 µl of the HNV solution was injected into the air sack and came to rest on the inner membrane at the bottom of the air sac. The position of the embryo on this membrane may differ considerably from egg to egg. HNV must diffuse through the membrane into the egg contents (i.e. egg yolk, etc.) to come into contact with the developing embryo and be absorbed. Due to the different positions of the embryos on the membrane, individual embryos were probably not all exposed to the same *in ovo* concentrations of HNV. Another factor that may have contributed

to the potentially large variability in HNV concentrations could be the large variation in the sizes and therefore the volumes of individual eggs, used in the investigation (intra- and interbatch).

Exposure of chicken embryos to different concentration of HNV (due to the position of the embryo and the size and volume of the eggs) might explain the huge differences seen within groups of embryos receiving similar dosage levels of HNV. Another interesting observation that may, in part, corroborate this inference was the fact that the standard deviation within all the control groups appeared to be smaller than that of the groups receiving HNV (specifically the 150 and 300 µM groups). In the latter groups some embryos displayed body masses similar to the controls, but at the same time there were embryos exhibiting a dramatic reduction in their body mass. This phenomenon may be due to different genetic predispositions in the individual embryos and/or due to the fact that the embryos may have been exposed to different concentrations of HNV.

Difficulties with the chicken embryo model led to the implementation of the mouse embryo model in this study. This model closely resembles the exposure of the human embryo/fetus to variations in the physiological, biochemical and metabolic characteristics of the mother's uterus. Pregnant females were dosed with HNV, relative to their body mass and one could argue that the final HNV concentration in all the mice were similar and/or displayed much smaller variations, compared to what occurred in the chicken embryo model. HNV also proved to be teratogenic in mouse embryos, inducing NTD in up to 17.1 % of the mouse embryos in the 600 mg/kg treatment group.

The mouse embryo model proved to be a better model to use for this type of investigation. The concentrations of HNV, and subsequently its metabolic derivatives to which individual embryos were exposed to at the various dosage levels, probably displayed smaller variations than what occurred in the chicken embryo model. The more pronounced dose-response effect observed in the mouse embryo model may have been the result of the higher quality teratological data that can be generated with this model.

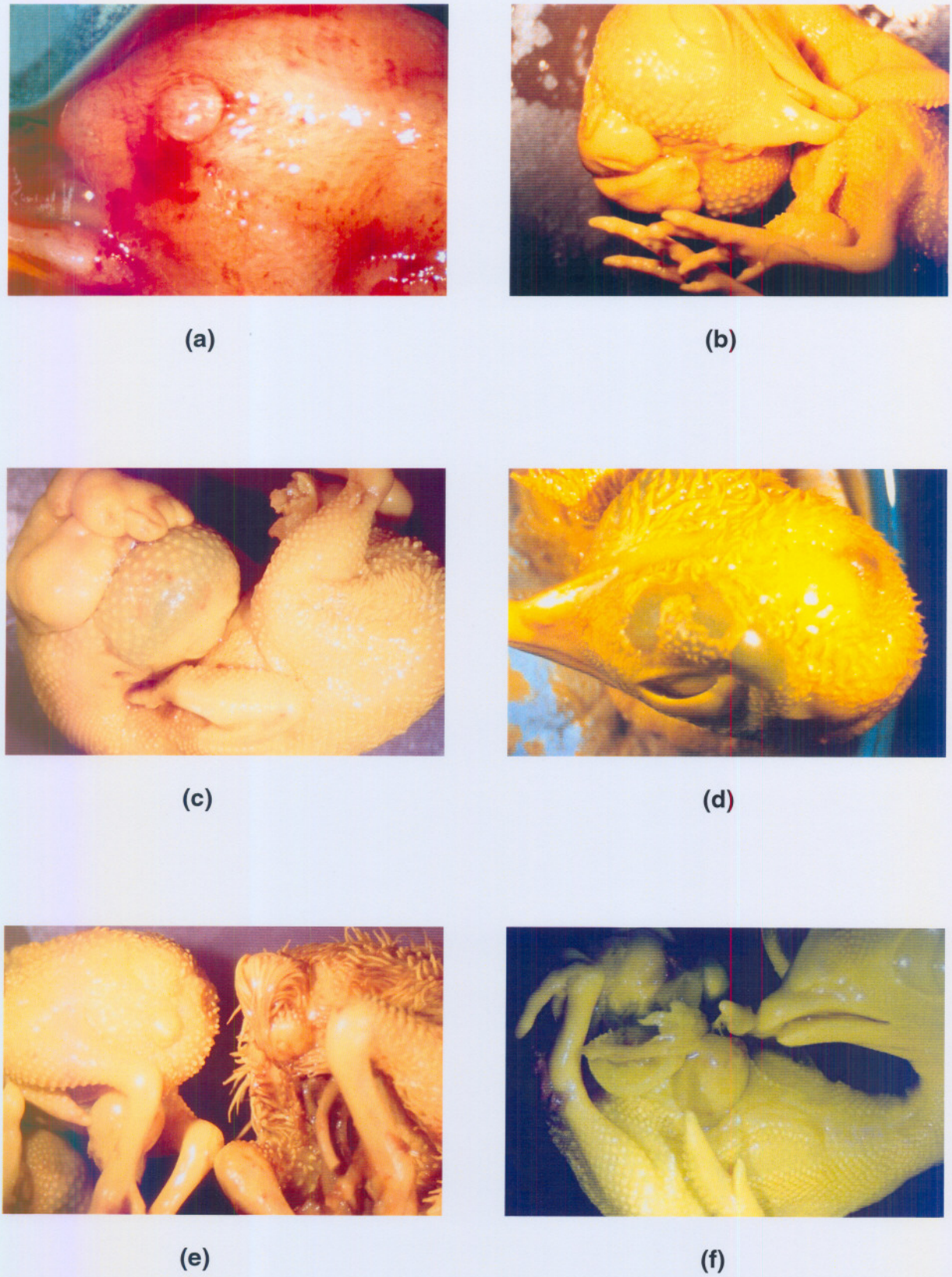

Figure 3.14. **Induction of neural tube defects in chicken embryos with β-hydroxynorvaline.** (a) Spina Bifida; (b) Exencephaly; (c) Exencephaly; (d) Anencephaly; (e) Normal vs. abnormal tail buds; (f) Omphalocele.

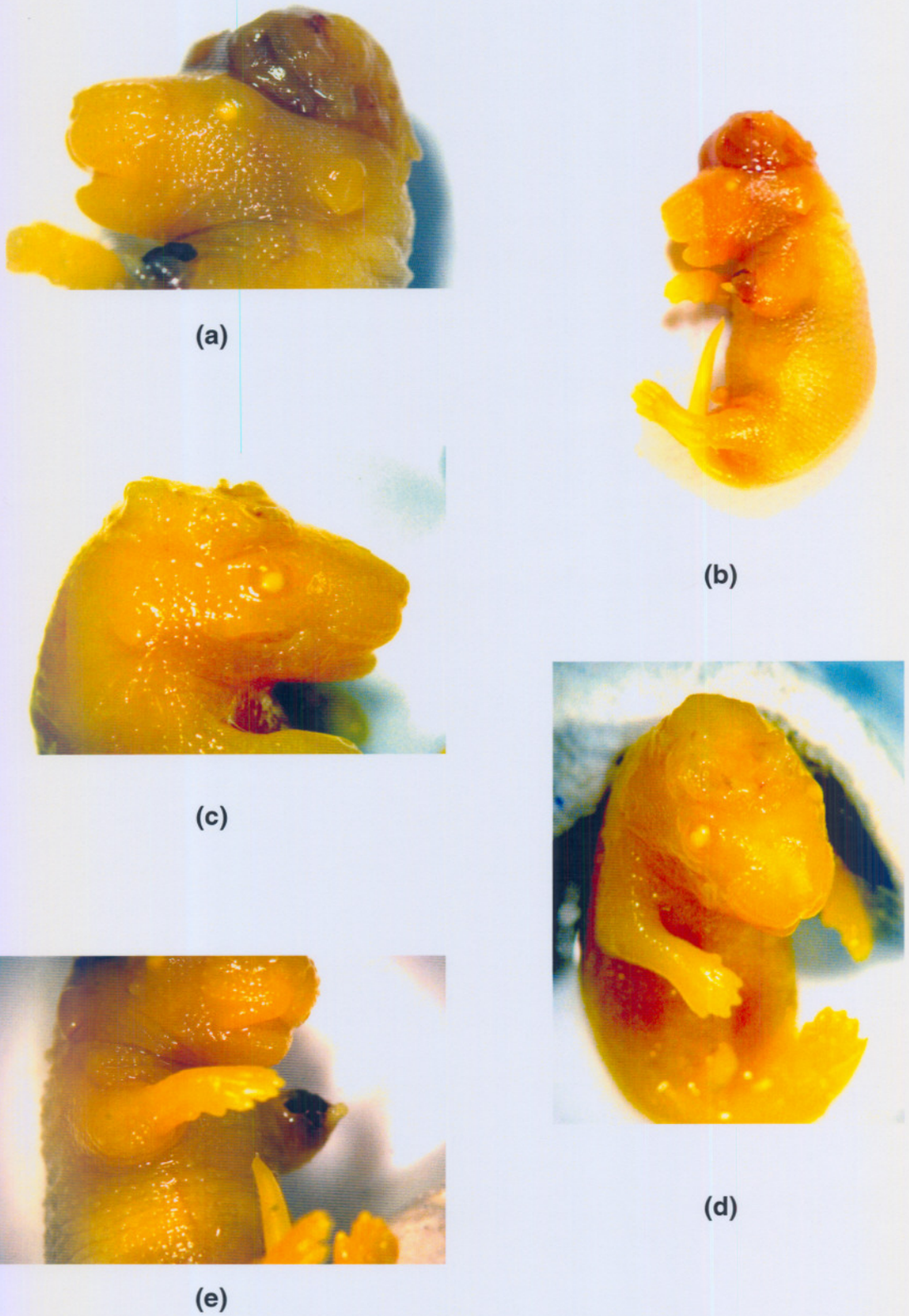

Figure 3.15. Induction of neural tube defects in mouse embryos with β-hydroxynorvaline. (a) Exencephaly; (b) Embryo with Exencephaly and Amelia; (c) Anencephaly; (d) Anencephaly; (e) Limb reduction defect (Amelia).

The toxic action of HNV may, however, also be attributed to its structural resemblance to L-serine (Figure 4.1). Several other possible scenarios of the toxic potential of HNV then become clear. Besides being an important building block for proteins, L-serine is a precursor for the biosynthesis of some important biomolecules (i.e. sphingolipids, glycolipids, etc.). At the same time, L-serine is a substrate for key enzymes in the folate cycle (Section 2.2.1.1) and the transsulfuration route (Section 2.2.1.3). The activity of these enzymes can theoretically be compromised on either or both of two different levels: (a) the production of mutant forms of i.e. SHMT and CBS and/or (b) the inhibition of their catalytic activity.

Folate metabolism is interconnected to a number of important biochemical pathways (Figure 4.2). THF is metabolically converted to various one-carbon derivatives, with the carbon atom in various oxidation states. The one-carbon derivatives of THF subsequently participate in the interconversion of serine and glycine (Section 2.2.1.4), the metabolism of histidine and formate (Figure 2.4), the biosynthesis of purines (Section 2.2.1.5), synthesis of thymidine (Section 2.2.1.6), and the remethylation of homocysteine to methionine (Section 2.2.1.2). Methionine serves as a co-substrate with ATP in the biosynthesis of S-adenosylmethionine (SAM) by methionine adenosyltransferase (MAT; EC 2.5.1.6). SAM is probably the most important biomethylating agent in mammalians and serves as a methyl donor in the biosynthesis of carnitine (Section 4.2.4.3), polyamines (Section 4.2.4.2), glutathione (Section 2.2.1.3), neurotransmitters, as well as for numerous other biomolecules (Figure 2.4; Heby, 1981; Selhub, 1992; Bailey, 1999; Avila, 2002; Herbig, 2002; Mattson, 2003). Most importantly, SAM is responsible for DNA methylation and hence contribute to gene regulation (Section 2.3.1).

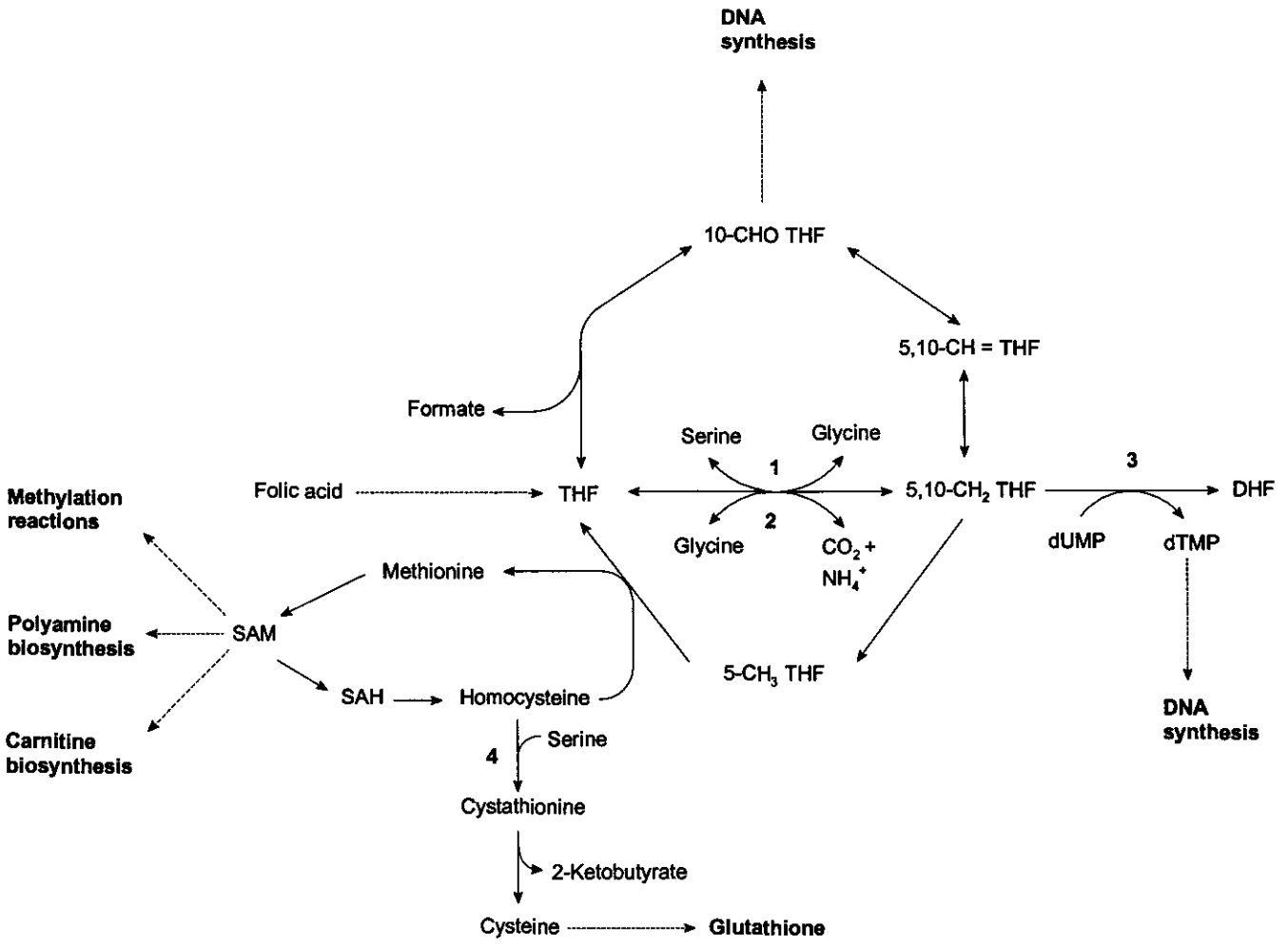

Figure 4.2. **Overview of one-carbon metabolism.** 1) Serine hydroxymethyltransferase, 2) Glycine cleavage system, 3) Thymidylate synthase, 4) Cystathionine-β-synthase.

4.2. β-HYDROXYNORVALINE AND ONE-CARBON METABOLISM: HYPOTHESES AND APPROACH

4.2.1 Potential effects of HNV on DNA synthesis in animal models

De novo synthesis of thymidine is critical for the synthesis of DNA. Ribose-5-phosphate is converted through a series of reactions to ultimately form deoxyuridine monophosphate (dUMP), the direct precursor of thymidine. This reaction is catalysed by thymidylate synthase (EC 2.1.1.45) and involves the transfer of a methyl group to dUMP, derived from 5,10-methylene tetrahydrofolate (5,10-CH_2-THF), with the resultant formation of thymidine. The 5,10- CH_2-THF is formed *via* the action of serine hydroxymethyltransferase (SHMT, EC 2.1.2.1). Reduced availability of one-carbon units in the form of 5,10-CH_2-THF will result in reduced thymidine biosynthesis. In the presence of [^{3}H]-thymidine, a reduced flow of one-carbon units will result in increased radio-labelled thymidine being incorporated into DNA.

Variations in the natural rate of the incorporation of ^{3}H-thymidine into DNA can be used as a potential marker for any alterations in the rates of the folate or remethylation cycles (Greene, 2003). Increased [^{3}H]-thymidine incorporation into DNA may therefore be interpreted to signify a decreased flux of one-carbon units through the folic acid cycle (Fell, 1990).

4.2.2 Potential effects of an inhibition of SHMT by HNV in animal models

SHMT catalyses the first step in a metabolic pathway involved in providing one-carbon groups for the biosynthesis of a number of important biomolecules. It is responsible for the initial step in the transfer of one-carbon units from serine to tetrahydrofolate and produces glycine and 5,10-CH_2-THF. More than 80% of all one-carbon units are derived from L-serine, *via* this enzyme reaction (Herbig, 2002). Methylene tetrahydrofolate is essential for the synthesis of thymidine, an essential building block of DNA during replication and DNA repair (Fell, 1990). The

activity of cytoplasmic serine hydroxymethyltransferase (cSHMT) is considered to be the rate-limiting step for the *de novo* synthesis of thymidine (Oppenheim, 2001).

SHMT can catalyse more than ten different chemical reactions, displaying a rather broad spectrum of substrate specificity (Schirch, 1982). This property of SHMT may, at the same time, render SHMT vulnerable to numerous potential inhibitors. It is therefore not surprising that this enzyme is an important target in the development of cytotoxic drugs for the treatment of cancer, especially drugs that would affect the rate of DNA synthesis in rapidly growing cells (Rao, 1991).

Because of its structural similarity to L-serine and L-threonine, β-hydoxynorvaline is a potential competitive inhibitor for SHMT. The *in vitro* inhibition of SHMT with HNV was subsequently investigated.

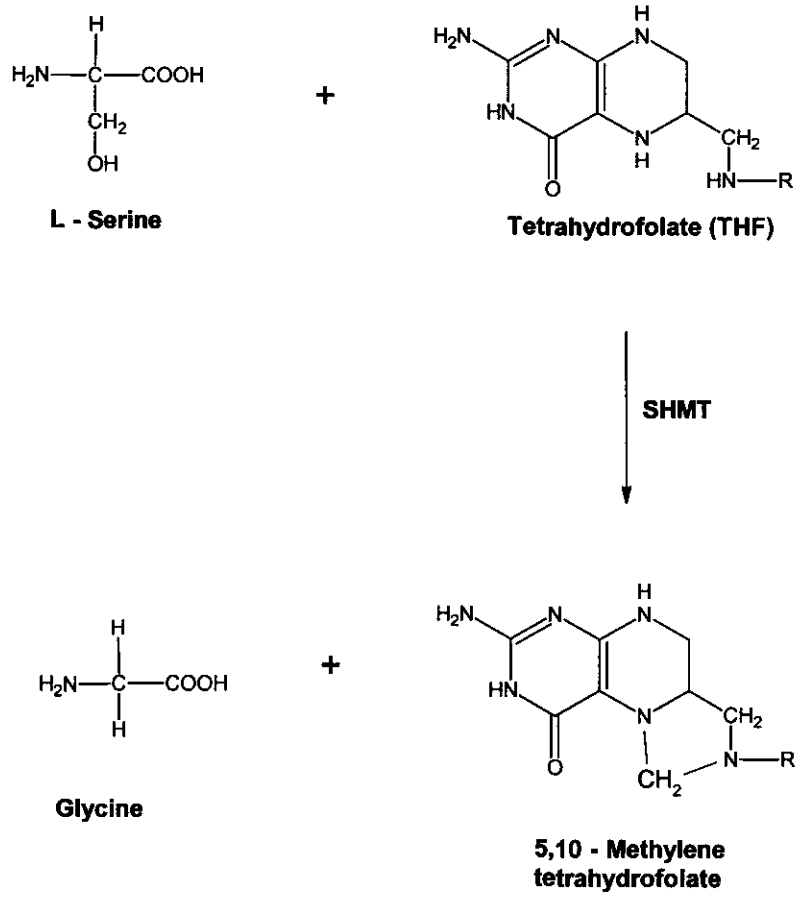

Figure 4.3. Conversion of serine and THF to glycine and 5,10-methylene THF by serine hydroxymethyltransferase.

4.2.3 Potential effects of the inhibition of CBS by HNV in animal models

Because of its structural resemblance to L-serine, β-hydroxynorvaline can potentially act as a substrate (competitive inhibitor) for cystathionine-β-synthase (CBS), compromising the activity of this important enzyme. Condensation of HNV with homocysteine can result in decreasing levels of cystathionine, the formation of 3-ethylcystathionine and the resultant intracellular accumulation of homocysteine. This potential effect of HNV may influence the normal activity of the enzyme since CBS will most probably display different affinities for its natural substrate, serine and the potential competitive inhibitor, HNV.

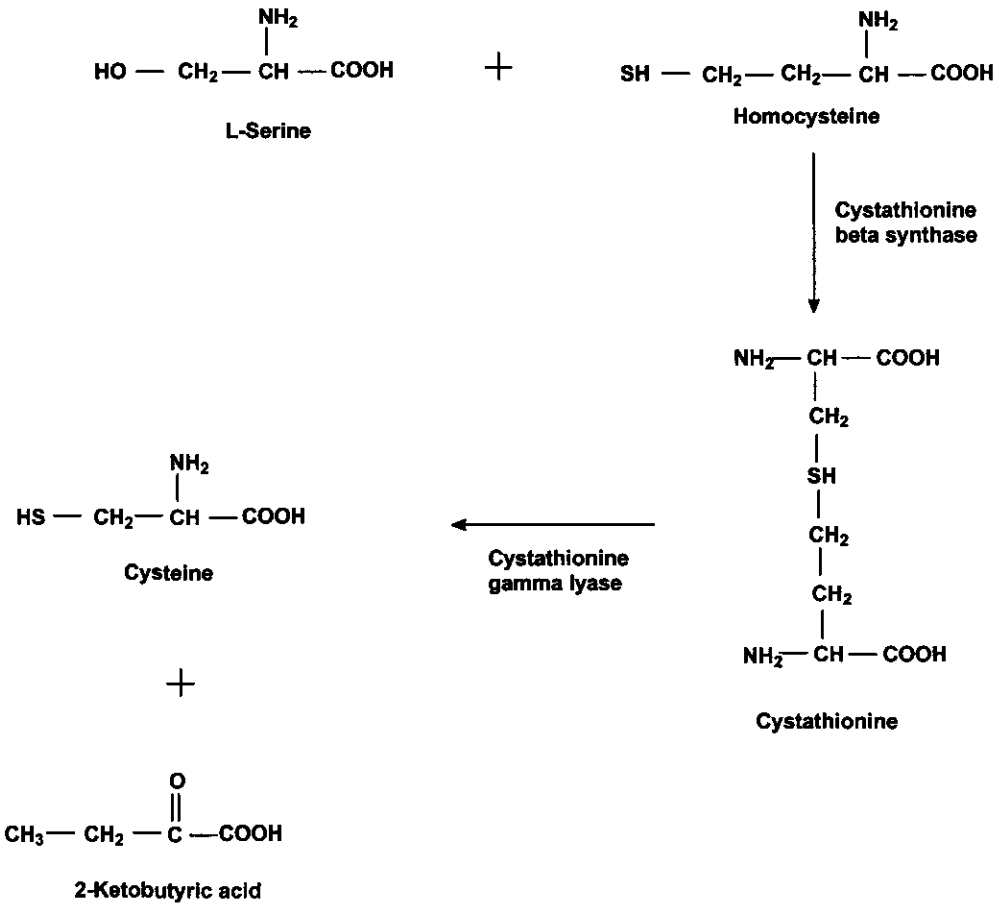

Figure 4.4. Probable conversion of serine and homocysteine to cystathionine by cystathionine-β-synthase in the transsulfuration route.

4.2.4 Potential effects of the inhibition of S-adenosylmethionine biosynthesis in animal models

An inhibition of the flow of one-carbon units through the folic acid and remethylation cycles will ultimately lead to reduced S-adenosylmethionine (SAM) and increased S-adenosylhomocysteine (SAH) levels. Since SAM is a universal biomethylation reagent, responsible for more than 100 different methylation reactions, reduced SAM levels will have a resounding effect on intermediary metabolism on a much broader scale.

4.2.4.1 Potential effects of HNV on DNA methylation

Methylation of DNA at the C5 position of cytosine residues plays an important role in the regulation of gene expression in vertebrates and is essential for mammalian development (Lei, 1996). Tissue-specific methylation patterns are established during embryonic development and involve *de novo* methylation and demethylation. Demethylation occurs throughout the mouse genome during the preimplantation stage of embryonic development, resulting in hypomethylation of the genome at the blastula stage. After implantation, methylation of specific cytosine residues occurs, resulting in a rapid increase in the methylation status of the DNA (Monk, 1987; Kafri, 1992) and hence alterations in gene expression.

DNA methyltransferases (DNA MTase) are responsible for the methylation of cytosine residues in DNA. The reaction uses SAM as a co-substrate, and involves the transfer of a one-carbon unit from SAM to cytosine. SAH and 5-methylcytosine are formed in the process. Mutant alleles of the DNA MTase gene (*Dnmt*) have been reported (Li 1993; Lei, 1996). Mice heterozygous for either the mutant $Dnmt^s$ or the $Dnmt^c$ allele showed no discernable abnormalities and were fertile. Embryos homozygous for either mutation displayed a distorted neural tube at 9.5 days p.c. The DNA of these embryos was highly demethylated (Lei, 1996).

A transgenic mouse with a knockout of the *Mthfr* gene was constructed (Chen, 2001). This gene encodes for methylene tetrahydrofolate reductase, responsible for the conversion of methylene tetrahydrofolate to 5-methyl tetrahydrofolate. The

latter is involved in the conversion of homocysteine to methionine and eventually to SAM, a universal biomethylation agent. Both heterozygous and homozygous knockouts showed increased homocysteine and SAH levels, reduced SAM levels and global DNA hypomethylation.

The C677T mutation in the MTHFR gene is the first identified genetic risk factor for spina bifida in man (van der Put, 1995). Following a study of the prevalence of this mutation in children affected with spina bifida, van der Put *et al.* (1996a) concluded that DNA methylation might be involved. The authors argued that a MTHFR mutation would lead to reduced SAM levels and ultimately to DNA hypomethylation. A disruption of the regulation of genes, involved in closure of the neural tube during embryonic development, may be a possible underlying mechanism through which a deficient MTHFR could provoke the formation neural tube defects.

If β-hydroxynorvaline is indeed able to inhibit the flow of one-carbon units through the folate and remethylation pathways, reduced SAM levels may be the result. Since SAM is directly responsible for DNA methylation, this effect may eventually result in the hypomethylation of the DNA in developing embryos, causing disturbances in gene expression and the programmed development of the embryo.

4.2.4.2 Potential effects of HNV on polyamine biosynthesis

The term "polyamines" is a generic name for a group of basic molecules that are ubiquitously present in all living organisms. Prokaryotic cells contain only putrescine (Put) and spermidine (Spd), however, nucleated eukaryotic cells additionally contain spermine (Spm). These aliphatic polyamines, Put, Spd and Spm are normal cell constituents that seem to play critical roles in cell proliferation and differentiation (Goyns, 1982; Haukanes, 1990; Pillai, 1997; Khuhawar, 2001).

All eukaryotic cells synthesise Put, Spd and Spm. The synthesis of Put starts with the catabolism of L-arginine to urea and L-ornithine in the urea cycle. This reaction is catalysed by arginase (L-arginine amidino hydrolase). Put is formed by direct

decarboxylation of L-ornithine by ornithine decarboxylation (ODC). This may be the rate-limiting step in polyamine synthesis in non-proliferating cells. However, in rapidly dividing cells (e.g., embryonic cells, tumor cells), ODC activity is usually vastly increased and not considered to be the rate-limiting parameter (Khuhawar, 2001) in polyamine synthesis. A dramatic increase in ODC activity, up to 1000 times, occurs during the early phase of cellular response to a variety of hormones and other agents that stimulate cell growth and division, suggesting a functional coupling between polyamine synthesis and early growth-related events (Heby, 1981).

The synthesis of the higher polyamines, Spd and Spm requires two aminopropyl-moieties (decarboxylated S-adenosylmethionine residues). These moieties are ultimately derived from L-methionine, which is converted to S-adenosylmethionine (SAM) by L-methionine-S-adenosyltransferase (Figure 2.4). SAM is decarboxylated to form an aminopropyl-moiety (decarboxylated SAM), catalysed by S-adenosylmethionine decarboxylase (SAM-DC). The concentration of decarboxylated SAM is usually very low in mammalian cells and the enzyme responsible for its formation, SAM-DC, is activated by Put. This enzyme reaction is considered a key step in polyamine synthesis (Khuhawar, 2001). The synthesis of spermidine is catalysed by spermidine synthase (putrescine aminopropyl-transferase), and utilises Put and one molecule decarboxylated SAM to form spermidine and 5-methylthioadenosine. Spermidine is converted to Spm and 5-methylthioadenosine by spermine synthase (spermidine aminopropyltransferase), using an additional molecule of decarboxylated SAM.

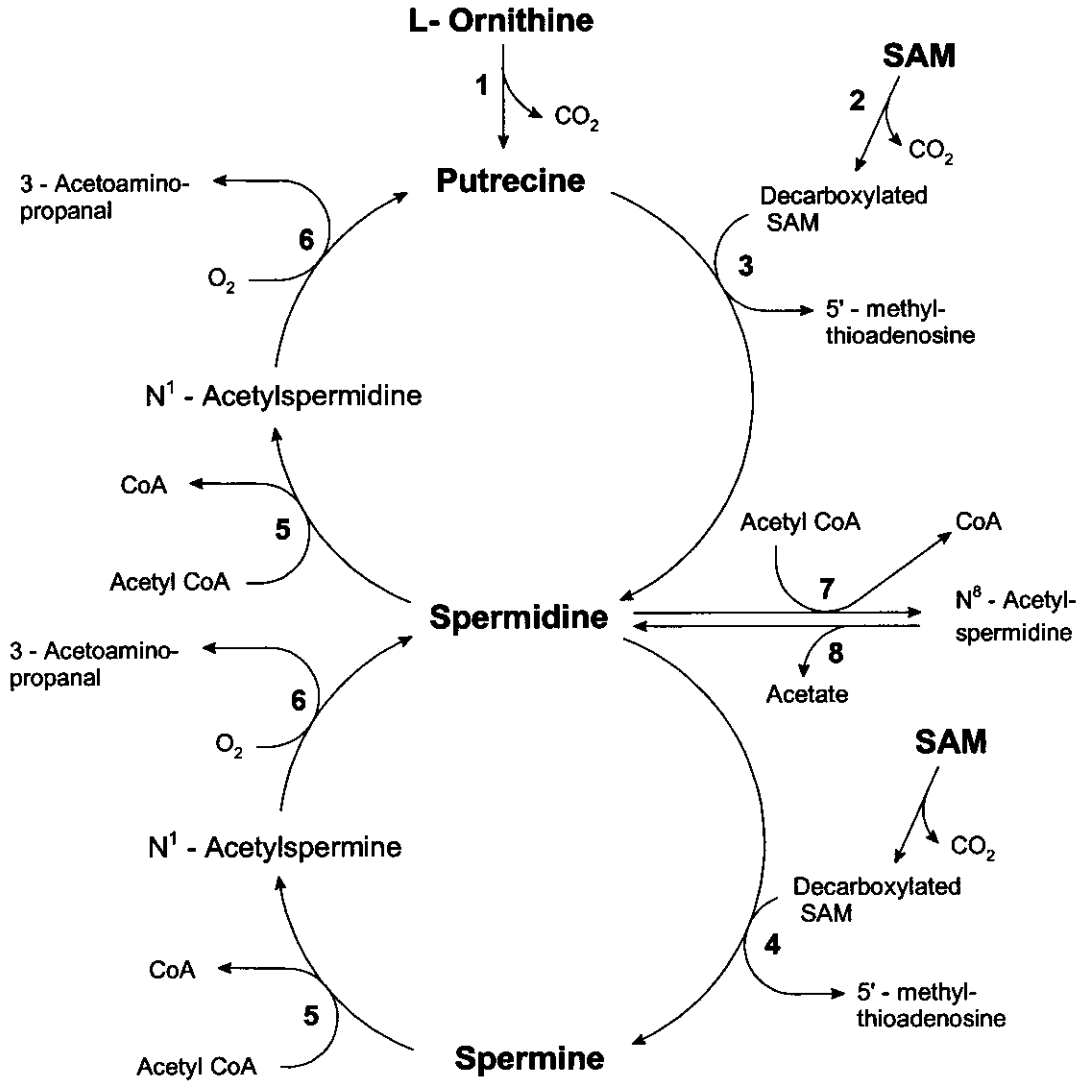

Figure 4.5. **Reactions involved in the synthesis of polyamines.** (1) Ornithine decarboxylase (ODC), (2) S-adenosyl-L-methionine decarboxylase (SAM-DC), (3) Spermine synthase, (4) Spermidine synthase, (5) Spermine/spermidine N^1-acetyltransferase, (6) Polyamine oxidase (PAO), (7) Spermidine N^8-acetyltransferase, (8) N^8-Acetylspermidine acetylhydrolase. SAM: S-Adenosyl-methionine. Modified from Seiler, 1987.

Polyamines are catabolised and degraded back to Put by the actions of polyamine oxidase (PAO) and spermidine/spermine acetyltransferase. The latter enzyme converts Spm and Spd to N^1-acetylspermine (N^1-Acspm) and N^1-acetylspermidine (N^1-Acspd), which are rapidly degraded by PAO after splitting of 3-acetoaminopropanal. The activity of the acetyltransferase is normally low and may be the rate limiting reaction in the catabolism of polyamines. The

acetyltransferase/oxidase system may constitute a regulatory response mechanism that serves to reduce excessive levels of cellular polyamine concentration. Put can eventually be degraded by diamine oxidase (Khuhawar, 2001) and excreted in the urine.

Polyamines are apparently only acetylated on their primary amino group(s). Natural polyamines bearing an acetyl moiety on the secondary amino group have not yet been identified in cells (Seiler, 1987). Acetyltransferases, which acetylate polyamines with acetyl-CoA as co-substrate, have been demonstrated in the cytosol and nucleus of various rat tissues. The substrates for the nuclear N-acetyltransferases are histones and numerous polyamines including putrescine, cadaverine and spermidine (leading predominantly to the formation of N^8-acetylspermidine). The cytosolic enzyme uses Spd and Spm as substrates (leading to the N^1-acetyl conjugates). Putrescine, cadaverine and histones are not substrates for the latter enzyme. The ratio of acetylated to free polyamines is considerably lower in tissues than in urine. This is probably due to the rapid excretion of acetylated polyamines by cells, speedy clearance from blood, intracellular deacetylation to free polyamines by deacetylases and polyamine oxidases and their rapid intracellular oxidative deamination (Van der Berg, 1987). Rodents excrete a large portion of their polyamines in the unconjugated form, thereby demonstrating that acetylation is not an absolute requirement for polyamine excretion (Seiler, 1987).

The exact roles that polyamines play in the support of normal cellular functions are not well understood. A number of studies suggested interactions between polyamines and DNA/RNA (Goyns, 1982; Seiler, 1987; Haukanes, 1990; Khuhawar, 2001). *In vitro* studies indicated that polyamines and their acetyl derivatives can stabilise DNA and nucleosomes against thermal and X-ray induced denaturation, enzymatic cleavage and induce the aggregation of DNA. An increasing conversion of B-DNA to Z-DNA has also been observed.

Polyamines are also known to affect the activity of enzymes involved in nucleic acid metabolism, i.e. DNA polymerases, DNA ligases, apurinic/apyrimidinic endonucleases, polynucleotide kinase, UV-endonuclease, 3-methyladenine-DNA

glycosylases, as well as prokaryotic and eukaryotic topoisomerases (Haukanes, 1990; Pillai, 1997). Several models have been proposed for the interaction between polyamines and DNA, although conflicting results have been reported. Liquiri *et al.* (1967) proposed that the secondary- and N^1-amino group of spermidine interact with the same, single polynucleotide chain when the N^8-amino group interacts with the opposite polynucleotide chain. Thus the secondary- and N^1-amino group of spermidine might have a larger influence on the phosphodiester bond cleavage than the N^8-amino group because they interact on the same polynucleotide chain and will therefore form a more stable complex with this chain. This implies that the polyamines might act like clamps, holding together two distinct parts of the same molecule or different molecules (Seiler, 1987).

The use of specific inhibitors of enzymes of polyamine biosynthesis has partially elucidated the role of polyamines in mammalian cells and embryonic development. When tissue culture cells were deprived of polyamines by DL-α-difluoromethylornithine (DFMO), a specific inhibitor of ornithine decarboxylase, they cease to proliferate (Metcalf, 1978). Administration of bis-cyclohexylammonium sulfate (BCHS, a spermidine synthase inhibitor) to cultured chicken embryo fibroblasts caused a decrease in Spm levels, an increase in Put and Spd levels, and an inhibition of cell proliferation and DNA synthesis (Caruso, 1992). Löwkvist *et al.* (1985) reported that stimulation of polyamine synthesis is necessary for early development of the chicken embryo. If stimulation of polyamine synthesis does not occur, the development is blocked at the end of gastrulation. Heby (1981) also concluded that polyamines play a fundamental role during gastrulation.

The synthesis of spermidine and spermine is also critical at an early stage of mouse embryo development. Zwierzchowski *et al.* (1986) found that treatment of pregnant mice with methylglyoxal-*bis*-(guanylhydrazone) (MGBG), a spermine/spermidine synthase inhibitor, resulted in a strong inhibition of DNA synthesis and subsequent arrest of embryonic development at the 8-cell or morula stage. The group also found that DFMO had no effect on embryos cultured for 1 or 2 day, but on the 3rd day, DNA synthesis was significantly inhibited. Although the precise mechanism of polyamines on the molecular level remains unsolved, it is

clear that polyamines play a critical role in cell differentiation and proliferation, especially during embryonic development.

Inhibition of one-carbon metabolism by β-hydroxynorvaline might influence polyamine synthesis. Since polyamines are essential in cell development and differentiation, especially during embryonic development, inhibition of polyamine synthesis might contribute to the induction of neural tube defects in embryos exposed to HNV.

4.2.4.3 Potential effects of HNV on carnitine biosynthesis

Carnitine (L-3-hydroxy-4-*N,N,N*-trimethylaminobutyrate) is an equally ubiquitous, but essential metabolite with a number of indispensable roles in intermediary metabolism, including energy metabolism and detoxification. It is probably present in all animal species and in numerous micro-organisms and plants. In mammals, carnitine homeostasis is maintained by endogenous biosynthesis, absorption from dietary sources and efficient tubular re-absorption by the kidney. The major sources of carnitine in the human diet are meat, fish and dairy products. In non-vegetarian humans, approximately a third of the daily carnitine needs are provided by *de novo* synthesis (Krähenbühl, 1996; Vaz, 2002).

Carnitine is ultimately synthesised from the amino acids methionine and lysine. In mammals, certain proteins contain N^6-trimethyllysine (TML) residues. N-methylation of lysine residues occurs as a post-translational event in proteins such as myosin, actin, cytochrome *c*, calmodulin and histones (Vaz, 2002). The *N*-methylation reaction is catalysed by specific methyltransferases and use S-adenosylmethionine (SAM) as a methyl donor, where three molecules of SAM are needed for the generation of one molecule of TML. Lysosomal hydrolysis of these trimethyllysine-containing proteins generates TML. The peptide-linked lysine methylation is considered the rate-limiting step in carnitine biosynthesis (Rebouche, 1986), in conjunction with the hydrolysis of protein to yield TML (Krähenbühl, 1996).

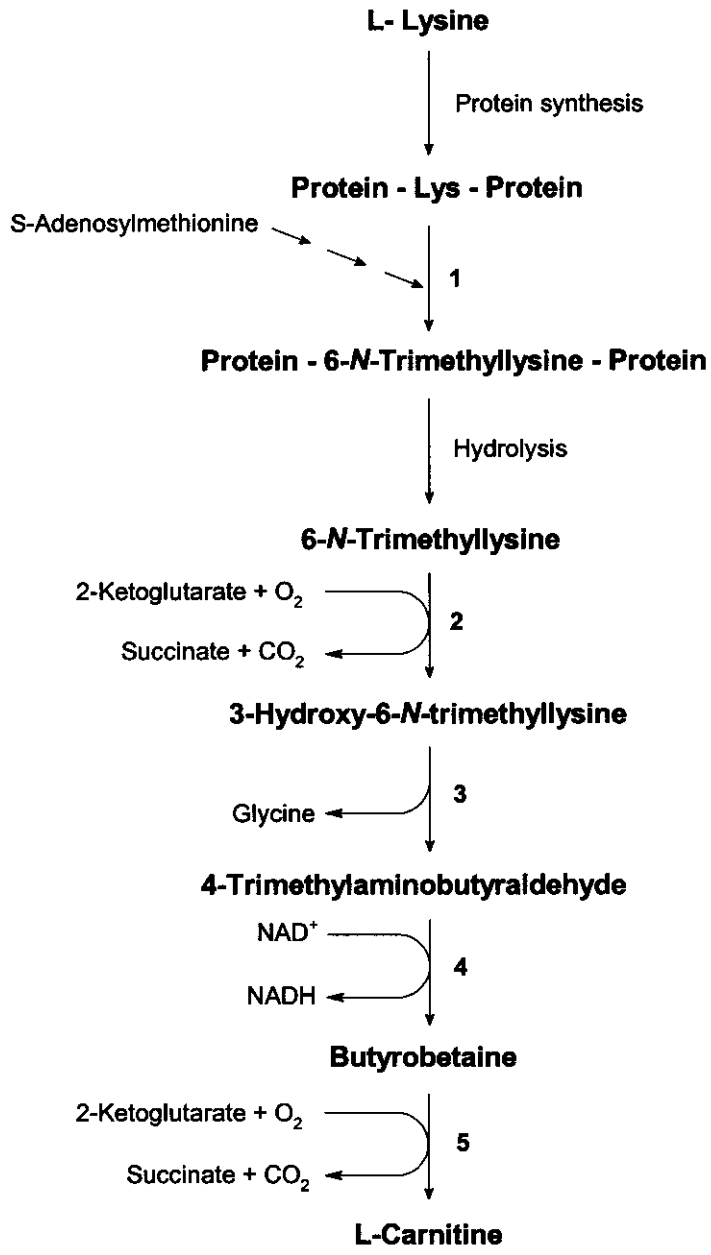

Figure 4.6. **Reactions involved in the synthesis of carnitine.** (1) Methyltransferases, (2) Trimethyllysine hydroxylase (TMLH), (3) 3-Hydroxytrimethyl aldolase (HTMLA)/Serine hydroxymethyl-transferase (SHMT), (4) 4-Trimethylaminobutyraldehyde dehydrogenase (TMABA-DH), (5) Butyrobetaine-3-hydroxylase. Modified from Krähenbühl, 1996.

Trimethyllysine, released from protein, is first hydroxylated in the 3-position by trimethyllysine hydroxylase (TMLH, EC 1.14.11.8) to yield 3-hydroxy-trimethyllysine (HTML). In both the human and rat, this enzyme is present in liver,

skeletal muscle, heart and brain. The aldolytic cleavage of HTML is catalysed by HTML aldolase (HTMLA) to yield 4-trimethylaminobutyraldehyde (TMABA) and glycine. Very little is known about this enzyme, responsible for the synthesis of carnitine and some researchers suggested that HTMLA may be similar, or perhaps even identical to SHMT (Henderson, 1982; Vas, 2002). The next step in the biosynthesis of carnitine is the dehydrogenation of TMABA to yield butyrobetaine in an NAD^+ dependent reaction, catalysed by TMABA dehydrogenase (TMABA-DH). The last step entails the stereo-specific hydroxylation of butyrobetaine to form L-carnitine, and is catalysed by butyrobetaine-3-hydroxylase (Vaz, 2002).

Carnitine is absolutely essential for the transport of long-chain fatty acids in energy metabolism. Long-chain fatty acids cannot enter the mitochondrial matrix from the cytosol as free acids and have to be bound by carnitine in the form of long-chain acylcarnitines. These acylcarnitines can then successfully cross the outer- and innermembranes of the mitochondria to enter the mitochondrial matrix. Once inside the mitochondrial matrix, the long-chain fatty acid is released from carnitine, *via* a transacylation reaction and the resulting long chain fatty acyl-CoA molecules catabolised through β-oxidation. Carnitine is also involved in the transport of peroxisomal β-oxidation products, including acetyl-CoA, into the mitochondrial matrix for oxidation to H_2O and CO_2 *via* the Krebs cycle. Carnitine is also involved in the modulation of the intramitochondrial acyl-CoA/CoA ratio, storage of energy as acetylcarnitines and detoxification of poorly metabolised acyl groups by excreting them as carnitine esters (Vaz, 2002).

HNV induced reduction of SAM levels, due to an inhibition of the flux of one-carbon units, will ultimately affect carnitine biosynthesis. If SHMT is indeed involved in carnitine synthesis and this enzyme is inhibited by HNV, the resultant decrease in carnitine levels may have detrimental effects on the energy metabolism and carnitine related detoxification in HNV-treated animals. These effects may collectively contribute to the high incidence of neural tube defects induced in mouse embryos by HNV.

4.2.5 A brief summary of hypotheses to be investigated

(i) β-Hydroxynorvaline influences the flow of one-carbon units in mouse embryos.

(ii) HNV is an *in vitro* inhibitor of SHMT and CBS.

(iii) DNA methylation status is altered in mice and their embryos by HNV.

(iv) Polyamine synthesis is compromised in mother and fetus by HNV.

(v) HNV inhibits carnitine biosynthesis.

(vi) The activity of cSHMT, mSHMT and GCS is affected by HNV in mothers and embryos.

(vii) HNV will affect the transsulfuration route by acting as a substrate for CBS and hence forming 3-ethylcysteine.

4.3 METHODS AND MATERIALS

4.3.1 Experimental animals

Hanover-NMRI mice were used to study HNV catabolism and the effects of this compound and its metabolic derivatives on one-carbon metabolism (Chapter 4), and intermediary metabolism in general (Chapter5). Since we were able to induce neural tube defects in experimental animals with HNV (Chapter 3), the same conditions were used to treat the animals used for the biochemical investigation. These conditions were described in detail in Section 3.2.3.

Virgin females, 40 – 60 days old, were mated overnight with experienced males (from 16h00 to 09h00 the following morning). The presence of vaginal plugs confirmed that copulation took place and these females were regarded as potentially pregnant. The following 24 hours was designated as the first day of gestation.

The effect of HNV on DNA synthesis and the flow of one-carbon units in mouse embryos was investigated using the [^{3}H]-thymidine incorporation test. Pregnant female mice were divided in 2 groups. The control group consisted of 5 mice and the experimental group of 4. HNV (Sigma Chemical Company) was dissolved in saline and sterilised (0.22 μm filter). Oral administration of saline and HNV solutions was executed once a day on days 7, 8 and 9 of gestation. Experimental animals were treated with 450 mg/kg HNV, while the control group received only saline (0.2 ml). All animals were injected with [^{3}H]-thymidine on day 9 of gestation. Animals were sacrificed by decapitation on day 10 of gestation, the embryos removed and immediately frozen at -20 °C for later use.

The direct and indirect effects of HNV on one-carbon metabolism were investigated in a separate experiment. Pregnant female mice were randomly divided into 2 groups. The control group consisted of 8 mice, while the experimental group contained 10 mice. Oral administration of saline and HNV solutions was executed once a day on days 7, 8 and 9 of gestation. Experimental animals were treated with 450 mg/kg HNV, while the control group received only

saline (0.2 ml). On day nine of gestation, animals were put in metabolic cages with free access to water but no food. These metabolic cages were specifically designed to collect urine samples without any faecal contamination (faeces were collected in a separate tube). The urine was collected in customised urine collection tubes containing thymol as a bacteriocide to inhibit any microbial growth in the urine over the 24-hour collection period.

Animals were sacrificed by decapitation on day 10 of gestation. Firstly the liver of the mother was removed and stored on ice for later use. The embryos were then removed, pooled and preserved on ice. Preliminary studies revealed that the amount of mitochondria, isolated form a single embryo, were not sufficient to execute all the relevant analyses (i.e. mSHMT, CBS and CS). All the embryos from a single mother therefore had to be pooled and was subsequently treated as a single sample. This step ensured that sufficient amounts of mitochondria could be generated so that all the relevant analyses could be executed on each of the samples generated in the course of the investigation. Urine samples were frozen and stored at –20 °C for later use.

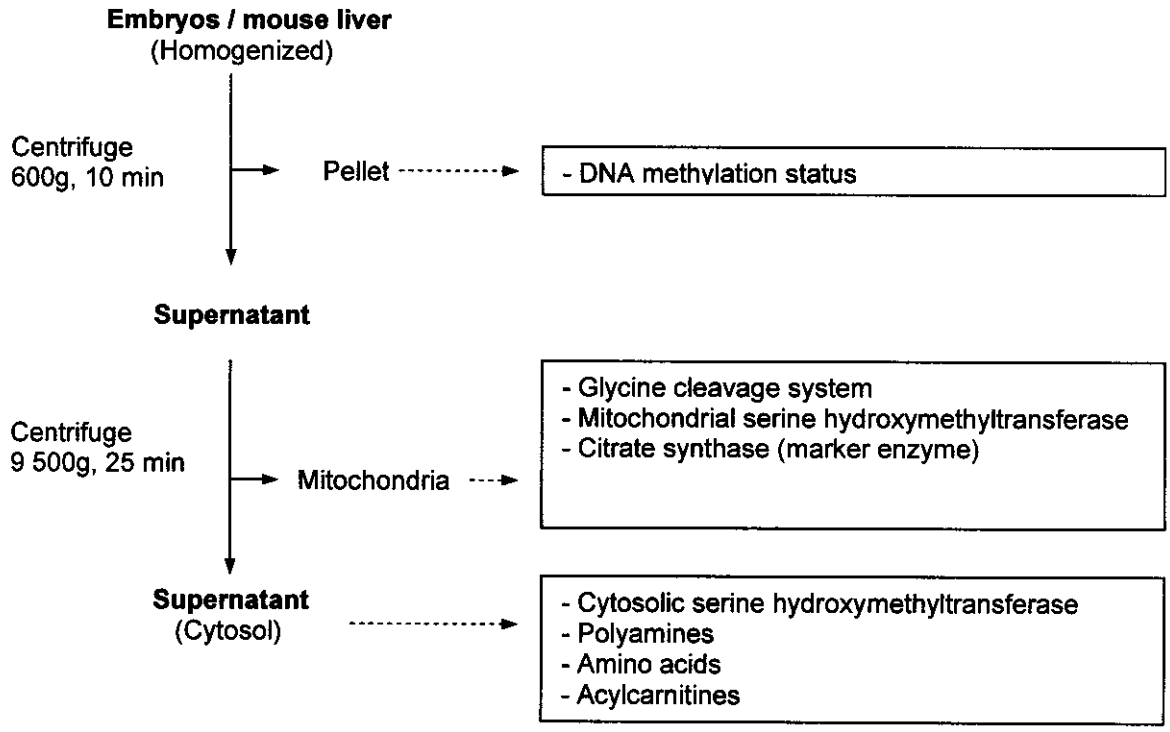

Figure 4.7. Simplified schematic diagram of the isolation of mitochondria and the analyses performed on each fraction obtained from the isolation.

Mitochondria were isolated from the liver and embryo samples as soon as possible (APPENDIX C). Freshly isolated mitochondria were immediately employed in the analysis of the highly labile glycine cleavage system (GCS) analyses, since these analyses could only be performed on fresh mitochondria (Kalbag, 1990). The 600 x *g* pellet, 9500 x *g* supernatant and the enriched fraction of mitochondria were frozen for the analysis of non-labile entities (i.e. mSHMT, CS, cSHMT, polyamines, amino acids, acylcarnitines) at a later stage (Figure 4.7).

4.3.2 Analytical methods employed in this investigation

Variations in the levels of radioactively labelled thymidine (^{3}H-thymidine) incorporated into DNA, can be used to measure changes in the flux of one-carbon units through the folate and/or remethylation cycles (Greene, 2003). Increased [^{3}H]-thymidine incorporation into DNA may be the result of decreased flow of one-carbon units through the folic acid cycle.

The effect of HNV on DNA synthesis and the flow of one-carbon units in mouse embryos was investigated using the [^{3}H]-thymidine incorporation test. DNA was isolated from the 10-day-old mouse embryos and the [^{3}H]-thymidine content of the DNA determined (APPENDIX A).

The effect of HNV on DNA synthesis in the animal model was also investigated by using chicken embryo fibroblast cultures (CEF). CEF were cultured in the presence of a concentration range of β-hydroxynorvaline (0 – 315 μM). The DNA content of cells was measured, using a fluorescent dye (Hoechst 33258), while the MTT assay was used to demonstrate cell viability (APPENDIX B).

The DNA methylation status of the mother and unborn offspring was measured by electrospray ionisation tandem mass spectrometry (ESI-MS-MS). DNA was isolated from the 600 x *g* pellet (Figure 4.1) and hydrolysed to its corresponding bases with formic acid. The bases were quantified by ESI-MS-MS using a stable isotope procedure (APPENDIX D).

Polyamines in the 600 x *g* supernatant fraction were quantified, using high performance liquid chromatography (HPLC), APPENDIX E. The employed method was a modified version of a method described by Marcé *et al.* (1995).

The glycine cleavage system was measured in freshly isolated mitochondria with a radiometric method (APPENDIX G). This assay is based on the cleavage of 1-^{14}C-glycine in the presence of β-nicotinamide adenine dinucleotide (NAD^+) as a coenzyme, to liberate $^{14}CO_2$, NH_4^+ and reduced β-nicotinamide adenine dinucleotide (NADH). In the process, tetrahydrofolic acid (THF) is converted to unlabelled N^5, N^{10}-methylene THF, while the released $^{14}CO_2$ is trapped in a KOH solution and subsequently quantified by means of liquid scintillation counting.

Serine hydroxymethyltransferase activity was also assayed with a radiometric method (APPENDIX F). The principle of the assay is based on selectively isolating [^{3}H]-methylene tetrahydrofolate with the aid of a solid phase anion extraction matrix (DEAE-cellulose paper). During the enzyme reaction, the methylene group, originating from the hydroxymethyl group (i.e. the C3 atom) of 3-[^{3}H]-L-serine, is transferred to tetrahydrofolate (THF) by SHMT to form radiolabelled N^5,N^{10}-methylene tetrahydrofolate (CH_2-THF) and unlabeled glycine. The labelled THF-derivative is then quantified by streaking out an aliquot of the assay mixture onto DEAE-cellulose ion-exchange paper and washing the paper with copious amounts of distilled water to remove unreacted, 3-[^{3}H]-L-serine. The amount of radiolabelled CH_2-THF, produced in the enzyme reaction, is assessed by measuring the radioactivity remaining on the DEAE-cellulose paper. Cytosolic serine hydroxymethyltransferase (cSHMT) was measured in the 9 500 x *g* supernatant while mitochondrial serine hydroxymethyltransferase (mSHMT) was measured in isolated mitochondria. Protein content was determined with the bicinchoninic acid (BCA) method (Smith, 1985).

Amino acids and carnitines were quantified with electrospray ionisation tandem mass spectrometry (ESI-MS-MS). Since numerous problems were encountered following direct injection of unfractionated, derivatised urine samples into the tandem mass spectrometer, it was decided to employ chromatographic fractionation of the metabolites, prior to quantification (APPENDIX K) with the

instrument. Prior to derivitisation, all samples were spiked with a number of stable-isotope standards, to assist with the accurate quantification of amino acids and carnitine metabolites.

S-Adenosylmethionine (SAM) and S-adenosylhomocysteine (SAH), as well as homocystine were quantified with electrospray ionisation tandem mass spectrometry (ESI-MS-MS). The methods are described in detail in APPENDIX P and APPENDIX Q, respectively.

4.3.3 Statistical methods employed in the analysis of results

Results were expressed as the mean ± standard error of the mean (SEM). The Levene test for homogeneity of variances and the Shapiro-Wilk W-test were used to determine if the data were normally distributed. If the data were normally distributed, statistically significant differences were further assessed with the student's T-test. The Kruskal-Wallis non-parametric test was used to test for the statistically significance of results in data sets that were not normally distributed or skewed. A confidence interval of 95% was used in all statistical assessments and results exhibiting a $p < 0.05$ were considered to be statistically significant.

4.4 RESULTS

4.4.1 Inhibition of one-carbon flow by β-hydroxynorvaline and the effect on DNA synthesis

Data on the incorporation of [^{3}H]-thymidine into DNA in 10-day-old embryos were not normally distributed ($p = 0.0001$; Shapiro-Wilk). β-Hydroxynorvaline appeared to exhibit a statistically significant effect on the incorporation of [^{3}H]-thymidine into the DNA of 10-day-old embryos ($p < 0.001$; Mann-Whitney U test). The mean [^{3}H]-thymidine incorporation into control embryos was 1.11 ± 0.23 dpm/mg DNA, while that of the HNV-treated embryos was 1.51 ± 0.38 dpm/mg DNA, representing a 36 % increase.

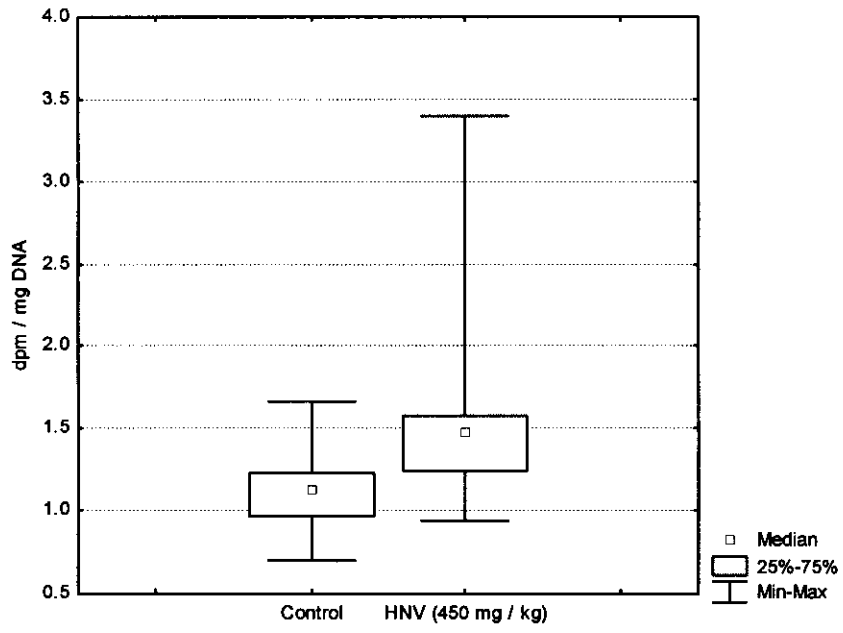

Figure 4.8. Box and Whisker plot of the [^{3}H]-Thymidine-incorporation into DNA of 10-day-old mouse embryos.

Increased incorporation of [^{3}H]-thymidine into DNA can be due to one of two reasons, or perhaps both:

(a) A greater amount of radio-labelled thymidine incorporation into DNA could represent an increased rate of DNA synthesis (Zwierzchowski, 1986; Botero-Ruiz, 1997; Fleming, 1998). The dTMP-pool is labelled with radio-active thymidine to

form [^{3}H]-dTMP and ultimately [^{3}H]-dTTP. The latter is incorporated into DNA during the replication of DNA as the cells undergo mitosis in the course of embryonic development. An increased rate of DNA synthesis will result in more of the [^{3}H]-dTTP being incorporated into DNA within 24 hours and hence demonstrate an increase in the rate of DNA synthesis in experimental embryos.

(b) An increased incorporation of [^{3}H]-thymidine into DNA can be due to decreased deoxythymidine synthesis (Figure 3.3). This decreased synthesis can be the result of an inhibition of thymidylate synthase and/or a shortage in the supply of 5,10-methylene THF. In control embryos, dTMP is synthesised from dUMP. This dilutes the pools of [^{3}H]-dTMP and [^{3}H]-dTTP, arising from exogenous [^{3}H]-thymidine (Pelliniemi, 1980; Lertratanangkoon, 1997). When deoxythymidine synthesis decreases in the presence of an inhibitor (i.e. HNV, etc.), the [^{3}H]-dTMP and [^{3}H]-dTTP pools are not diluted to the same extend as in the control embryos. Because more dTTP is radio-labelled in the experimental animals than in the controls, more [^{3}H]-dTTP will be incorporated into DNA in 24 hours. The increased incorporation of [^{3}H]-thymidine in experimental embryos (Figure 4.8) can thus be due to an increased rate of DNA synthesis or due to a decrease in the synthesis of deoxythymidine.

Another possibility for the increased incorporation of [^{3}H]-thymidine could be unscheduled DNA synthesis due to DNA damage, normally associated with mutagens (Sega, 1974). HNV has not yet been proven to be mutagenic. This compound does not appear to display the typical characteristics of a mutagen and therefore this possibility was regarded as remote and less likely to be the real cause of the increased incorporation of [^{3}H]-thymidine.

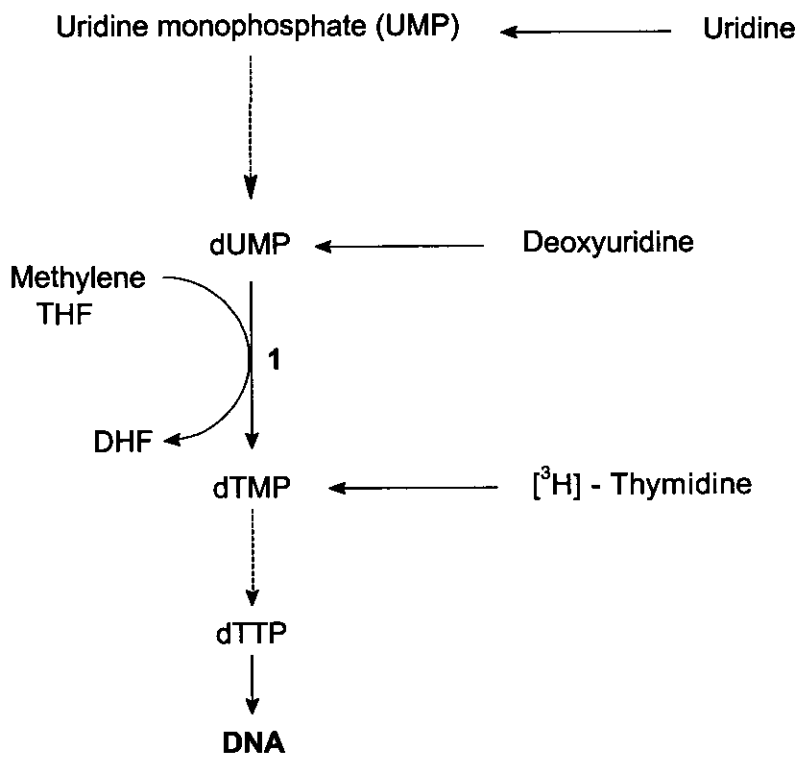

Figure 4.9. Diagram showing the incorporation of [^{3}H] thymidine into DNA. (1) Thymidylate synthase

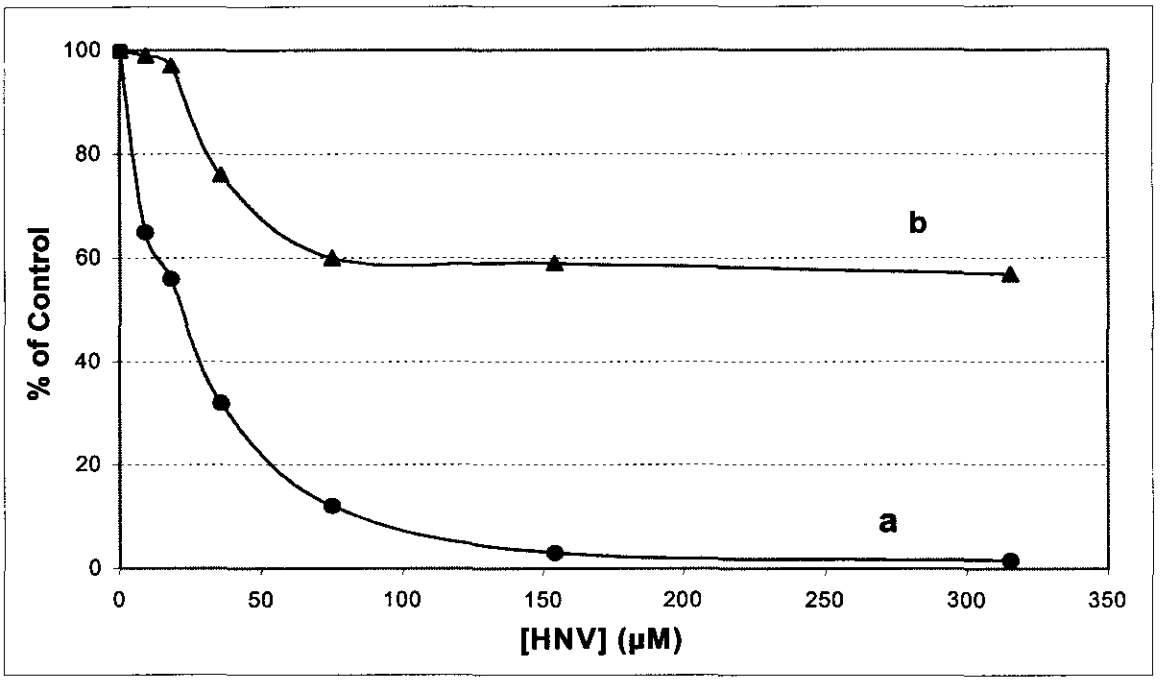

Figure 4.10. Effect of HNV on DNA Synthesis in Chicken Embryo Fibroblast Cultures. (a) DNA synthesis measured by a fluorescence method; (b) Cell viability as measured with the MTT assay.

The effect of HNV on the rate of DNA synthesis was investigated in chicken embryo fibroblasts (CEF). At relatively low HNV concentrations, the cell viability appeared to be high (> 97 %) compared to controls (~100%). DNA synthesis was however significantly decreased by 45 % at these concentrations compared to the controls. This is an indication that HNV effectively inhibited DNA synthesis, even at very low concentrations.

[^{3}H]-Thymidine incorporation was greatly increased by HNV in mouse embryos. This indicates that HNV increased the rate of DNA synthesis in experimental embryos, or decreased deoxythymidine synthesis, or both. In CEF cultures, HNV appeared to inhibit DNA synthesis even at low HNV concentrations while the cells remain viable. This is an indication that HNV do not stimulate the rate of DNA synthesis in mouse embryos, but rather decreases the synthesis of dTMP. A decrease in dTMP could be due to inhibition of thymidine synthase or reduced 5,10-methylene THF. Lower methylene-THF levels could be explained if HNV have an influence on the folate metabolism.

A possible extrapolation of the ramifications of the decreased dTMP synthesis may be an abnormal increase in the indirect induction of cellular apoptosis. Low dTTP concentrations may lead to dUTP being incorporated into DNA, causing DNA damage. This will be followed by excision-repair reactions, DNA strand breaks, cell cycle arrest and ultimately apoptosis (Zetterberg, 2004).

A more direct answer to this problem could be obtained by employing the deoxyuridine suppression test (Metz, 1968). In this test, incorporation of [^{3}H]-thymidine into dTMP, and hence into DNA, is suppressed by exogenous dUMP (Figure 4.8). Suppression occurs when folate metabolism is unimpaired, whereas [^{3}H]-thymidine incorporation is suppressed less by dUMP when folate cycling is compromised (Fleming, 1998). By challenging the incorporation of [^{3}H]-thymidine in developing mouse embryos with dUMP, one could get a direct answer to the effect of β-hydroxynorvaline on the folate cycle of these animals.

4.4.2 The *in vitro* effect of HNV on the catalytic activity of SHMT

β-Hydroxynorvaline can potentially inhibit the catalytic activity of SHMT. Due to structural similarities to L-serine and L-threonine, the natural substrates of SHMT, HNV can potentially be a competitive inhibitor of the enzyme (Section 4.2.2). This possibility was investigated *in vitro*. Freshly prepared mouse liver homogenate (600 x *g* supernatant) was used for this investigation since it contains both cSHMT and mSHMT. The assay conditions are described in detail in APPENDIX F.

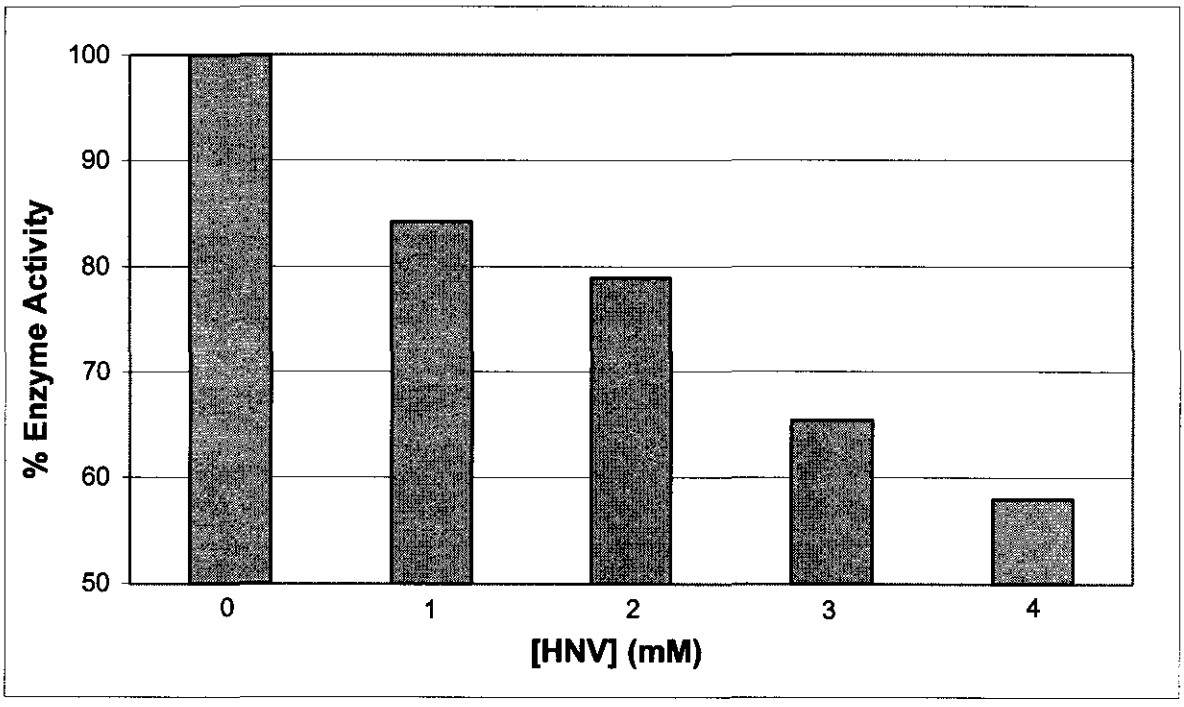

Figure 4.11. Concentration dependent inhibition of serine hydroxymethyl-transferase (SHMT) activity HNV.

HNV appeared to exhibit a concentration-dependent inhibitory effect on the catalytic activity of SHMT (Figure 4.11). Kinetic studies on the liver homogenate confirmed that HNV was in fact a competitive inhibitor of SHMT (Figure 4.12). The apparent K_i was 0.426 mM (calculated from Figure 4.12 with the assumption that HNV is a competitive inhibitor). Since a crude liver homogenate was used for this investigation, the calculated inhibitor constant (K_i) is therefore only an indication of the potency of HNV as an inhibitor of SHMT. The absolute K_i value will be calculated, as soon as a pure SHMT preparation becomes available.

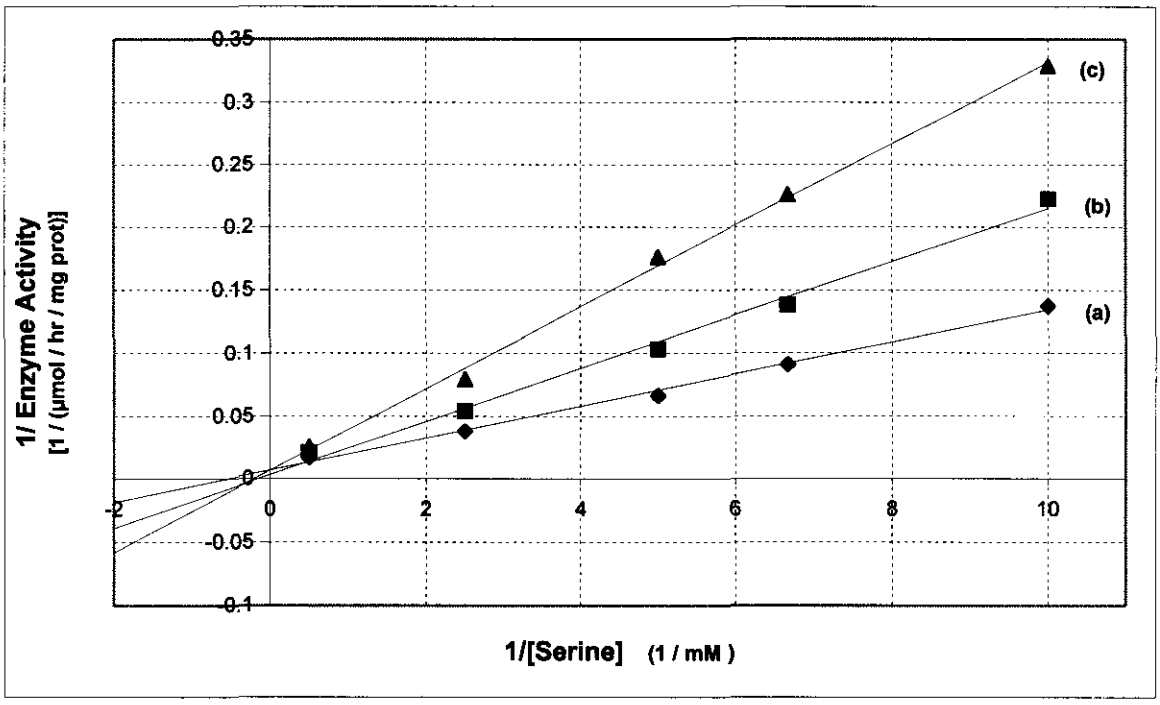

Figure 4.12. Lineweaver-Burk plot showing the effect of increasing HNV concentrations on serine hydroxymethyl-transferase (SHMT) activity. (a) 0 mm HNV; (b) 2 mM HNV; (c) 3 mM HNV (apparent Ki = 0.426 mM).

4.4.3 *In vitro* inhibition of cystathionine-β-synthase by β-hydroxynorvaline

β-Hydroxynorvaline can potentially act as a substrate (competitive inhibitor) for cystathionine-β-synthase (CBS) because of its structural resemblance to L-serine, the natural substrate of the enzyme. This potential effect of HNV may influence the normal activity of the enzyme since CBS will most probably display different affinities for its natural substrate, L-serine and the potential competitive inhibitor, HNV. This possibility was investigated *in vitro* using a freshly prepared mouse liver homogenate. The assay used is described in detail in APPENDIX O, except that L-serine was used as substrate instead of HNV. HNV was added in increasing concentrations as an inhibitor of the reaction.

HNV displayed a concentration dependent effect on the catalytic activity of CBS (Figure 4.13), but our results indicated that it is a poor inhibitor of this enzyme. Even at 14 mM HNV, the reaction was only inhibited by 45 %. No kinetic studies

(Lineweaver-Burk) were performed on the homogenate although this may have shed some light on the inhibitory properties of HNV on CBS.

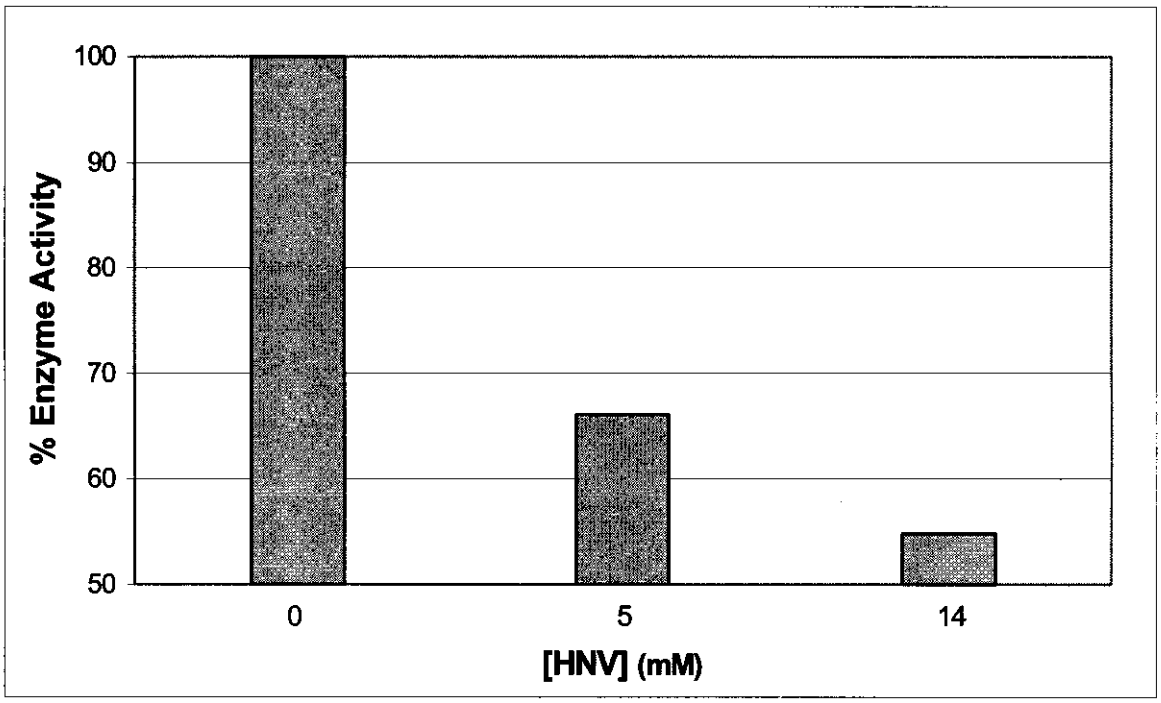

Figure 4.13. Concentration dependent inhibition of cystathionine-β-synthase by β-hydroxynorvaline.

4.4.4 The effect of HNV on the one-carbon metabolism of pregnant female mice and their fetuses

HNV influences the flow of one-carbon units through the folic acid cycle and/or the remethylation cycle (Section 4.4.1) and also inhibits the activity of SHMT and CBS (*in vitro*). The effect of this reduced flow was studied in pregnant female mice and their fetuses. Parameters that could potentially be influenced by a reduced flow of one-carbon units were measured (DNA methylation, polyamine synthesis and carnitine biosynthesis). Enzyme activities were also measured (cSHMT, mSHMT and GCS) that could be responsible for the reduced flow of one-carbon units.

S-adenosylmethionine (SAM) and S-adenosylhomocysteine (SAH) levels could not be succsessfully measured in the livers of pregnant female mice and their embryos. Problems were experienced with the sensitivity of the HPLC method (APPENDIX P) that was employed. Ultraviolet detection (254 nm) was used to

visualise and quantify SAH and SAM. However, the levels of these two metabolites in whole embryo tissues were below the detection limit and could therefore not be quantified. Chromatograms of hepatic tissue extracts, obtained from the mothers, displayed severe interference from unknown metabolite peaks. Although the peaks for SAM and SAH were visible in these extracts, the mentioned interference made it impossible to quantify these two metabolites. A more sensitive method is needed to quantify SAM and SAH in whole embryos and hepatic tissues obtained from the mothers.

Homocystine levels in urine samples from control and HNV treated experimental mice were also below the detection limit of the analytical method (APPENDIX Q) employed. Even by using a relatively high homocystine isotope concentration as carrier, the sensitivity of the method remained problematic. A more sensitive method is essential to quantify the total homocysteine concentrations in 10-day-old mouse embryos, rather than quantify the urinary homocystine levels of the mothers as an indication of altered homocysteine levels.

4.4.4.1 The effect of HNV on DNA methylation in pregnant mice and their fetuses

The methylation status of DNA was assessed in the livers of pregnant females and in their unborn offspring, as described in APPENDIX D. The control group consisted of 6 mothers and the experimental group of 9 mothers. The experimental group was treated with 450 mg/kg HNV on days 7, 8 and 9, while the controls received saline.

4.4.4.1.1 DNA methylation status in the livers of pregnant female mice

DNA methylation in the livers of pregnant female mice appeared to be normally distributed ($p = 0.671$; Shapiro-Wilk W-test). Although a tendency in the inhibitory action of HNV on the DNA methylation status of the mothers was observed, no statistically significant effect could be demonstrated ($p = 0.45$; Student T-test). The mean DNA methylation in control mice was 2.73 ± 0.44 % and that of the HNV-

treated females was 2.49 ± 0.63 %, representing an 8.6 % decrease in the methylation of DNA.

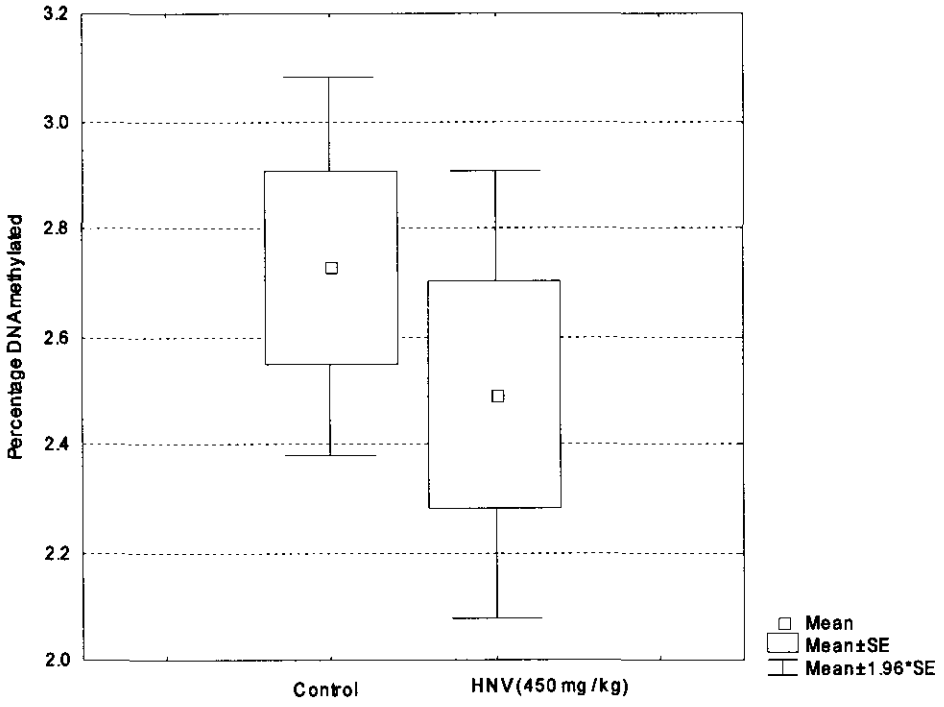

Figure 4.14. Box and Whisker plot of the percentage methylated DNA in control and HNV treated mice (450 mg/kg).

The DNA methylation status of the HNV treated mothers did not appear to differ significantly from the controls ($p = 0.45$). Experimental mice were, however, only treated for 3 days with HNV before they were sacrificed. The methylation status of the DNA in the mothers can apparently not be expected to change significantly in short term studies, such as the one reported here, since it is dependent on the intracellular concentration of S-adenosylmethionine (SAM). If the concentration of SAM decreases, it would probably take some time before the DNA methylation status of the animals would be affected. Chronic exposure to the toxin (HNV), may affect a more pronounced decrease in DNA methylation status.

4.4.4.1.2 The effect of HNV on the DNA methylation status of developing embryos

DNA methylation in the 10-day-old mouse embryos appeared to be normally

distributed (p = 0.137; Shapiro-Wilk W-test). β-Hydroxynorvaline had a statistically significant effect on the DNA methylation status of the mouse embryos (p = 0.01; Student T-test). The mean percentage of methylated cytosine residues was reduced from 3.38 ± 0.32 % in the controls to 2.92 ± 0.36 % in the HNV treated embryos. This represented a reduction of 13.7 % in the methylated cytosine residues.

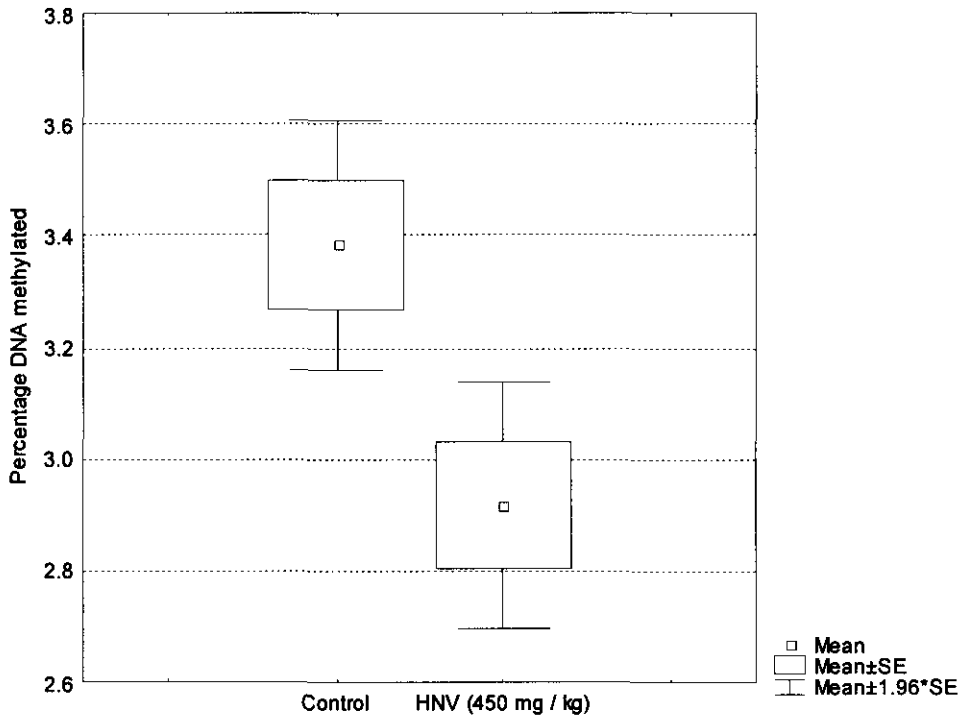

Figure 4.15. Box and Whisker plot of the percentage methylated DNA in control and HNV treated embryos (450 mg/kg).

A negative effect on DNA methylation in developing embryos may cause NTD. Studies by other researchers indicated that disruption of DNA methylation by a null mutation of the DNA methyltransferase gene resulted in a distorted neural tube at 9.5 days *p.c.* in the *in vitro* mouse embryo model (Lei, 1996). The DNA of these embryos was highly demethylated compared to normal embryos.

In the present study, β-hydroxynorvaline exhibited a statistically significant effect on the methylation status of developing embryos *in utero*. The developing embryos were exposed to HNV *via* oral administration of the amino acid to the pregnant mothers on days 7, 8 and 9 of gestation. On day 10 *p.c.*, the experimental

embryos displayed a lower content of methylated cytosine (2.92 ± 0.36 %), compared to that of the control group (3.38 ± 0.32 %). This effect proved to be statistically significant (Student's T-test: $p = 0.01$). On the other hand, mothers treated with HNV did not exhibit a lower methylation status compared to untreated mothers ($p = 0.45$). This observation may indicate that the methylation status of the mothers appears to remain unchanged in the short term, while DNA methylation in the rapidly developing embryos was compromised.

Tissue-specific methylation patterns are established during embryonic development and involve *de novo* methylation and demethylation. During the preimplantation stage of mouse embryonic development, genome wide demethylation occurs, resulting in hypomethylation of the genome at the blastula stage. Following implantation, methylation of cytosine residues is initiated, resulting in a rapid increase in the methylation status of genomic DNA (Monk, 1987; Kafri, 1992).

Due to the rapidly net increase in the DNA methylation status of the developing embryo, the demand for *de novo* methylation is very high. Inhibition in the flow of one-carbon units through the folic acid cycle and/or the methylation cycle may result in decreased SAM levels. A shortage in the supply of SAM, necessary of the timely methylation of DNA, may result in the hypomethylation of DNA and NTD formation.

4.4.4.2 The effect of HNV on polyamine biosynthesis

Polyamine levels were measured in pregnant female Hanover-NMRI mice and their unborn fetuses. The control group consisted of 8 females and the experimental group of 10 animals. Controls were treated orally with saline on days 7, 8 and 9 of *p.c.*, while experimental animals received 450 mg/kg β-hydroxynorvaline. Animals were sacrificed on day 10 *p.c.*, the embryos removed and prepared as described (Section 4.3.1).

4.4.4.2.1 Polyamine levels in the livers of pregnant female mice

(a) The levels of free polyamines

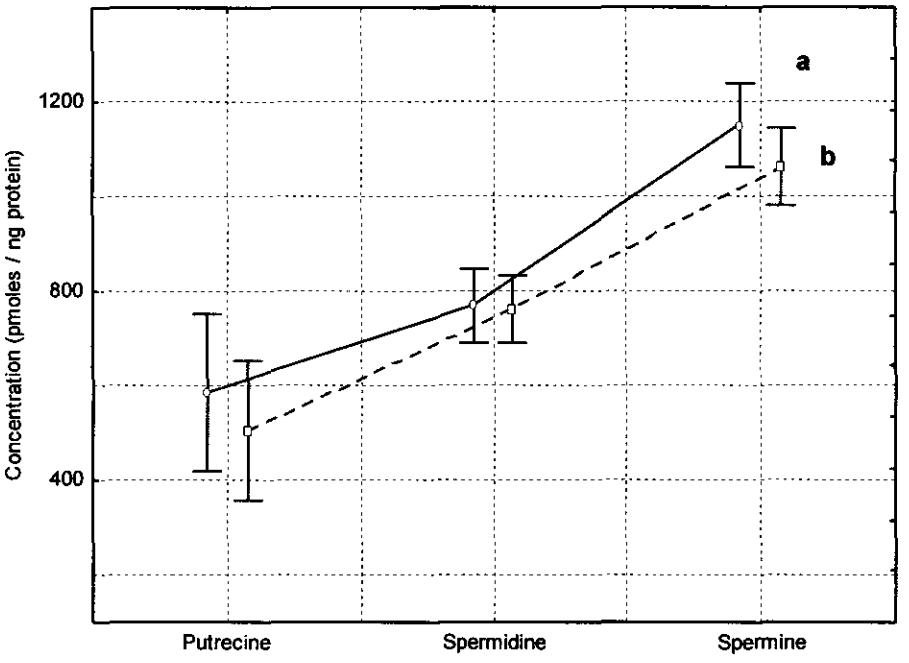

Figure 4.16. Polyamine concentrations in the livers of pregnant female mice. (a) Control group; (b) experimental group.

Table 5.4. The Levene Test of homogeneity of variances on hepatic polyamine levels in control and experimental mice.

	Levene's Test for Homogeneity of Variances Effect: none Degrees of freedom for all F's: 1, 16			
	MS Effect	MS Error	F	p
Putrescine	669.956	24357.08	0.027506	0.870354
Spermidine	6429.369	3128.79	2.054905	0.170969
Spermine	6190.890	4302.36	1.438951	0.247772

Variances in the control and experimental groups are not the same ($p > 0.05$; Levene Test for homogeneity of variance). Therefore a non-parametric method (Mann-Whitney U test) was used to test for significant differences between the control and experimental groups.

Table 5.5. The Mann-Whitney U Test on median hepatic polyamine levels in control and experimental mice.

variable	Mann-Whitney U Test By variable Dosis Marked tests are significant at p <.05000 Rank Sum Group 1	Rank Sum Group 2	U	Z	p-level	Z adjusted	p-level	Valid N Group 1	Valid N Group 2	2*1sided exact p
Putrescine	91.00000	80.00000	25.00000	1.332785	0.182603	1.332785	0.182603	8	10	0.203071
Spermidine	72.00000	99.00000	36.00000	-0.355409	0.722283	-0.355409	0.722283	8	10	0.761826
Spermine	90.00000	81.00000	26.00000	1.243933	0.213525	1.243933	0.213525	8	10	0.236985

HNV does not appear to display a statistically significant effect on polyamine levels in the liver of pregnant female mice ($p > 0.05$).

(b) Effect of HNV on the putrescine/spermine ratio

Putrescine is metabolised to spermidine and ultimately to spermine, using 2 molecules of S-adenosylmethionine (Section 4.2.4.2). Reduced SAM levels may inhibit polyamine synthesis, which in turn may lead to an increase in putrescine levels and decreased spermine concentrations. The putrescine/spermine ratio in the experimental animals may, therefore, prove to be higher and may serve as a more sensitive indicator of the effect of HNV on polyamine levels.

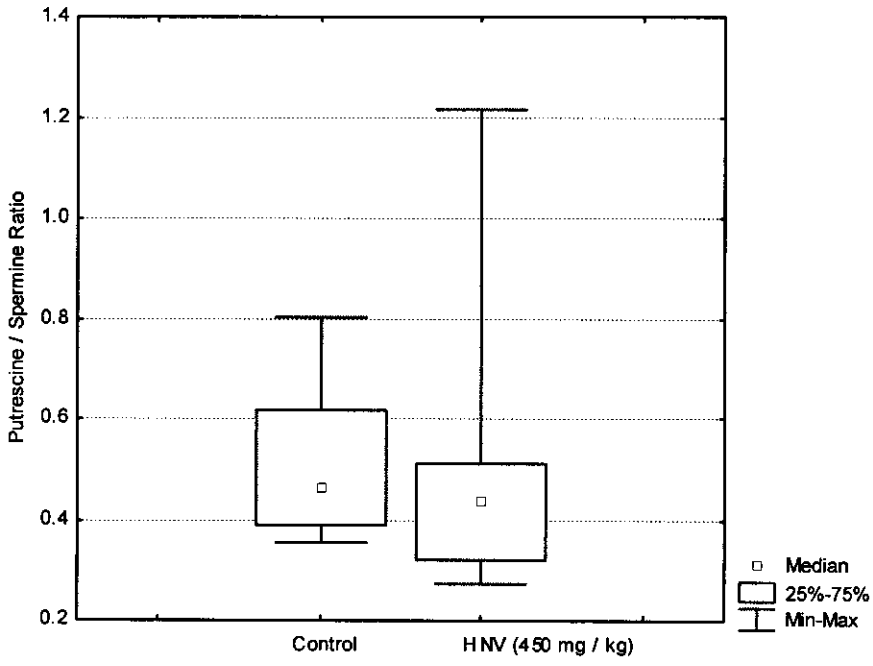

Figure 4.17. Box and Whisker plot of the putrescine/spermine ratio in the liver of the mothers.

The putrescine/spermine data were normally distributed ($p < 0.001$; Shapiro-Wilk W test). HNV did not appear to have a significant effect on the putrescine/spermine ratio in pregnant female mice ($p = 0.534$; Mann-Whitney U test). The mean ratio of the control mice was 0.51 ± 0.17 and that of the HNV-treated mice 0.49 ± 0.27.

4.4.4.2.2 The effect of HNV on polyamine levels in 10-day-old embryos

Polyamine levels were measured in 10-day old mouse embryos. Embryos from a single mother were pooled and polyamine levels measured in the 600 x *g* supernatant (Section 4.3.1, p 77).

(a) The concentrations of free polyamines

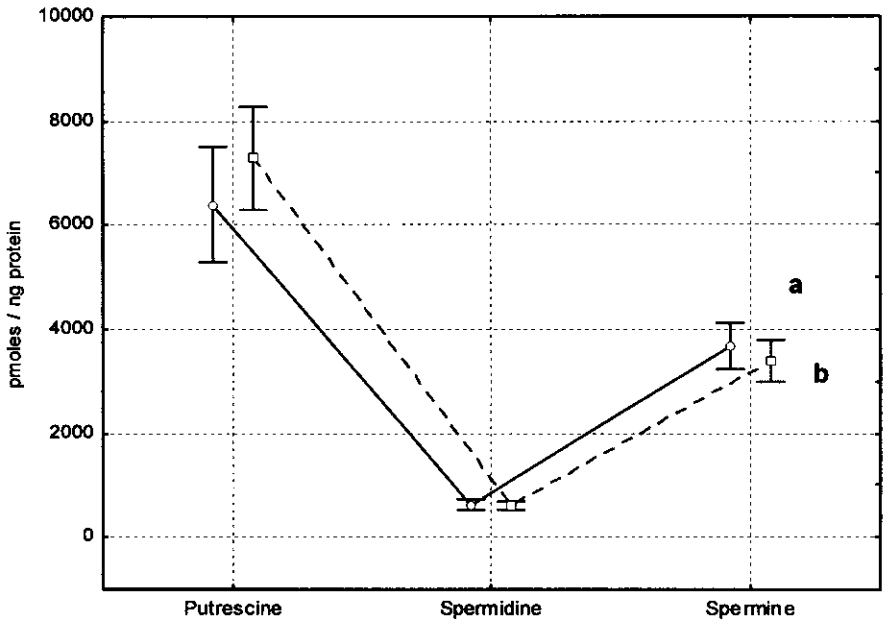

Figure 4.18. Polyamine concentrations in 10-day-old embryos. (a) Control group; (b) experimental group.

Variances in the different groups were not similar ($p > 0.05$; Levene Test for homogeneity of variance). A non-parametric method (the Mann-Whitney U test)

was therefore applied to test the results for significant differences between the control and experimental groups.

Table 5.7. The Levene Test for homogeneity of variances on embryonic polyamine levels (control vs experimental embryos).

	Levene's Test for Homogeneity of Variances Effect: none Degrees of freedom for all F's: 1, 16			
	MS Effect	MS Error	F	p
Putrecine	822639.3	852671.7	0.964779	0.340606
Spermidine	7518.2	7679.7	0.978970	0.337181
Spermine	77942.1	67911.5	1.147701	0.299925

Table 5.8. The Mann-Whitney U Test on differences in median polyamine values in control and HNV-treated (450 mg/kg) embryos.

	Mann-Whitney U Test By variable Dosis Marked tests are significant at p <.05000									
variable	Rank Sum Group 1	Rank Sum Group 2	U	Z	p-level	Z adjusted	p-level	Valid N Group 1	Valid N Group 2	2*1sided exact p
Putrecine	61.00000	110.0000	25.00000	-1.33278	0.182603	-1.33278	0.182603	8	10	0.203071
Spermidine	80.00000	91.0000	36.00000	0.35541	0.722283	0.35541	0.722283	8	10	0.761826
Spermine	86.00000	85.0000	30.00000	0.88852	0.374260	0.88852	0.374260	8	10	0.408245

HNV did not appear to have exerted a statistically significant effect on the polyamine levels of 10-day-old mouse embryos ($p > 0.05$).

(b) The putrescine/spermine ratio in the fetus as an indicator of altered polyamine synthesis

The putrescine/spermine data did not appear to be normally distributed ($p = 0.034$; Shapiro Wilk W-test). HNV displayed no apparent statistically significant effect on this ratio in developing mouse embryos ($p = 0.13$; Mann-Whitney U test). The mean ratio of the control embryos was 1.75 ± 0.30 and that of the HNV-treated embryos 2.20 ± 0.65, representing a 25.6 % increase.

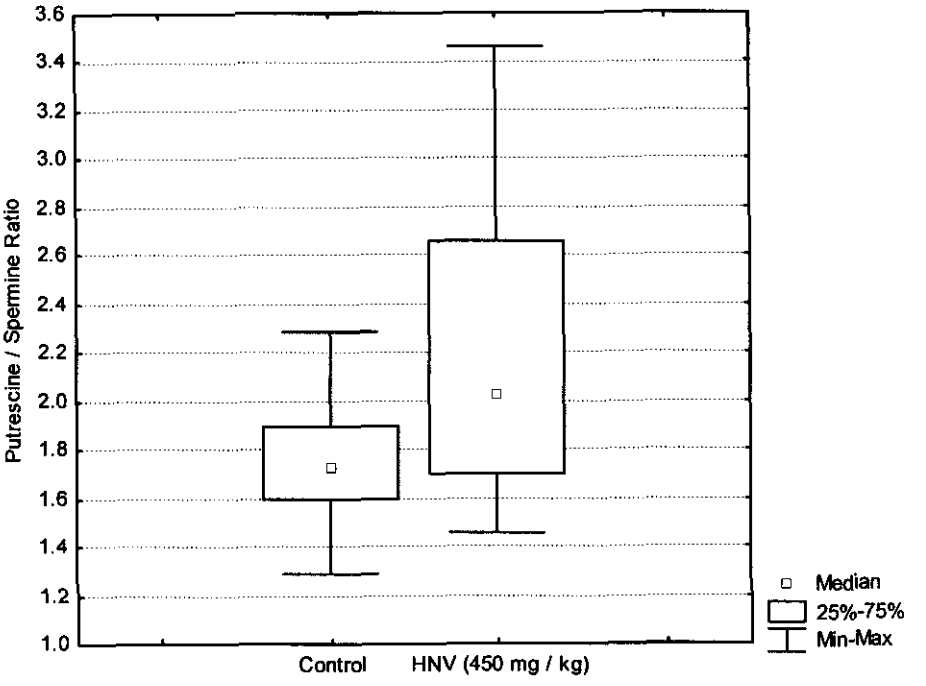

Figure 4.19. Box and Whisker plot of the putrescine/spermine ratio in 10-day-old mouse embryos.

(c) Altered ornithine concentrations as an indicator of reduced polyamine synthesis

Ornithine levels were determined in the 10-day-old embryos. Since the data were apparently normally distributed ($p = 0.602$; Shapiro-Wilk W test), a students T-test was used to test for statistical significances between control and HNV treated embryos.

The mean ornithine concentration increased from 4.4 µmol/g protein to 5.3 µmol/g protein (Figure 4.20). This represented a 19.5 % increase and appeared to be statistically significant ($p = 0.003$; Student T-test). Increased ornithine concentrations may be an indication of reduced polyamine synthesis, since it is a precursor of polyamine biosynthesis.

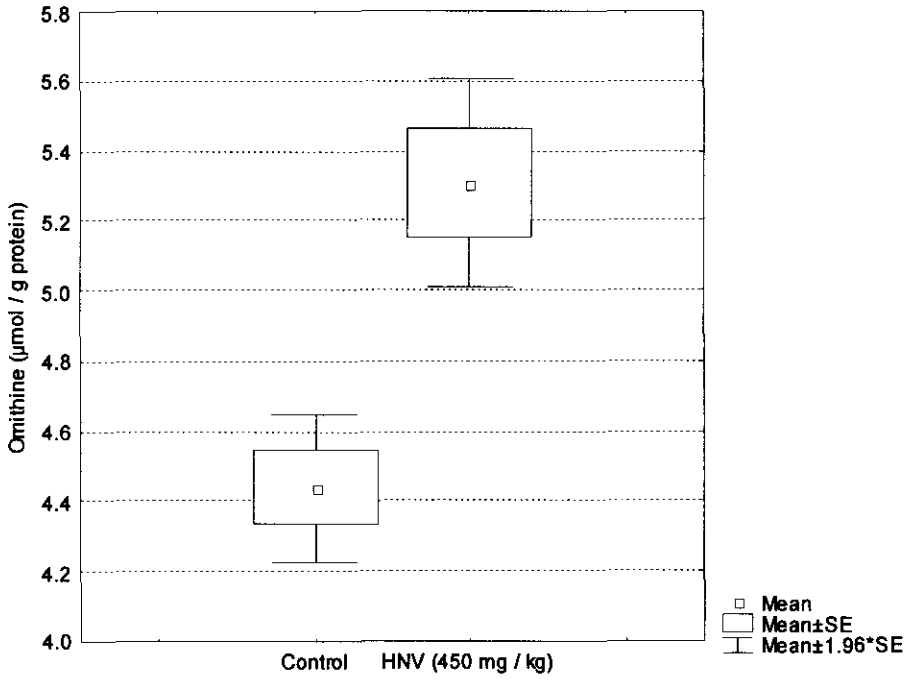

Figure 4.20. Ornithine concentrations in 10-day-old mouse embryos.

(d) The effect of HNV on polyamine levels in individual animals.

The average putrescine/spermine ratio of the control group was 1.75 ± 0.30, while that of the experimental group was 2.20 ± 0.65. However, not all the embryos were affected to the same extend by exposure to HNV. Some of the embryos in the experimental group were affected more than others, with their Put/Spm ratios as high as 3.46 (1.98 times that of the control mean). Most of the embryo samples displayed a Put/Spm ratio within the normal range (compared to the control group). In a number of embryos elevated Put/Spm ratios was observed, possibly due to different responses of the mothers to HNV.

4.4.4.3 Effect of HNV on carnitine biosynthesis

As mentioned before (4.2.4.3) , carnitine (L-3-hydroxy-4-*N,N,N*-trimethyl-aminobutyrate) is an important biomolecule, involved in a number of important metabolic processes (i.e. transport of long chain fatty acids and peroxisomal β-oxidation products into the mitochondrial matrix, modulation of the intramitochondrial acyl-CoA/CoA ratio, storage of energy in the form of

acetylcarnitine, detoxification of poorly metabolised acyl derivatives, etc.). L-carnitine is synthesised from trimethyl-L-lysine (TML), derived from post-translationally *N*-methylated proteins (i.e. myosin, actin, cytochrome *c*, calmodulin, histones, etc.). *N*-methylation of protein bound L-lysine residues is catalysed by specific methyltransferases, with SAM as methyl donor and the subsequent lysosomal hydrolysis of these proteins generates TML which is then used in the synthesis of L-carnitine.

Some of the metabolic effects caused by HNV on the metabolism of HNV-treated experimental animals could be ascribed to altered SAM levels. Decreased SAM levels will influence carnitine biosynthesis and may lead to a carnitine shortage. In a number of metabolic disorders, carnitine assumes the role of a detoxification agent, facilitating the removal of excess acyl moieties (Fontaine, 1996). Decreased carnitine synthesis and depleted free intracellular L-carnitine levels, may then exert a dramatic effect on the metabolism of pregnant female mice and their fetuses.

4.4.4.3.1 HNV and carnitine biosynthesis in pregnant female mice

Total carnitines (free- and acyl-carnitines) were determined in the urine samples of control and HNV-treated, pregnant female mice and the tissues of their unborn offspring. The Shapiro-Wilk W test was used to determine the normality of the distribution of urine data. Data obtained on urine analyses appeared to be non-normally distributed ($p = 0.025$) while data obtained on the embryos complied with the criteria for normal distributions. A Mann-Whitney U test was subsequently employed to test for the statistical significance of the data obtained for the mothers (urine samples), while the Student's T-test was applied on data obtained from embryos.

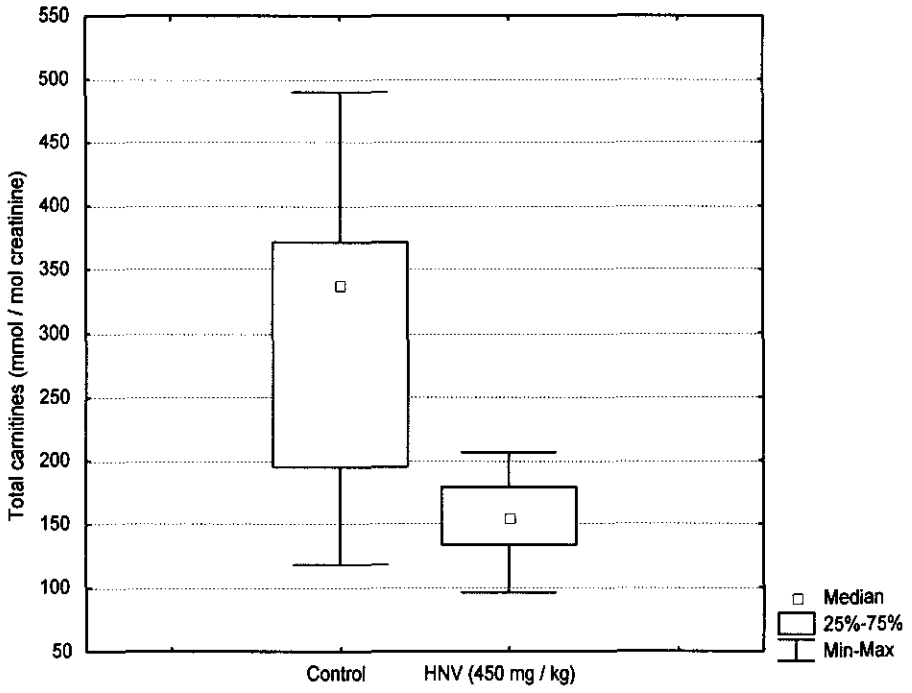

Figure 4.21. Total urinary carnitines in control and HNV-treated pregnant female mice.

HNV appeared to exhibit a statistically significant effect ($p = 0.017$; Mann-Whitney U test) on the total carnitine concentration in the urine samples, collected from pregnant mothers. The mean total carnitine concentration in control animals was 302.8 ± 113.5 mmol/mol creatinine. An apparent decrease (48.4 %) was observed in HNV-treated animals (mean total carnitine concentration = 156.3 ± 33.5 mmol/mol creatinine).

The concentration of trimethyllysine was quantified in urine of pregnant female mice and the data did not appear to be normally distributed ($p = 0.002$; Shapiro-Wilk).

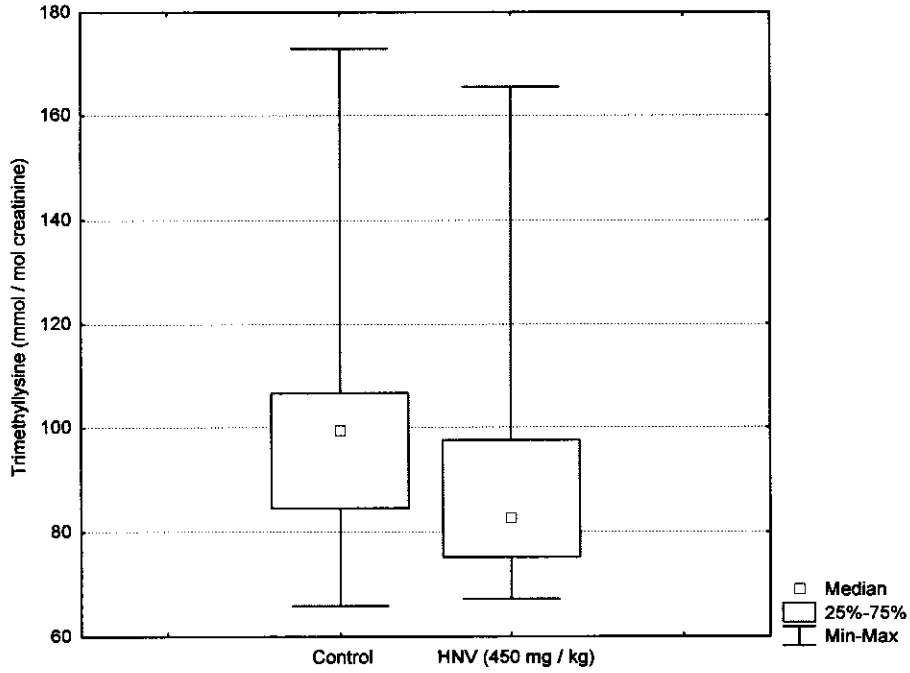

Figure 4.22. Urinary trimethyllysine concentrations of pregnant female mice.

Although the mean trimethyllysine concentration of the HNV treated experimental mice was 12.8 % lower than the control group (90.7 ± 28.8 vs. 104.0 ± 29.9 mmol/mol creatinine), HNV did not appear to significantly influence trimethyllysine levels ($p = 0.131$; Mann-Whitney U test). Decreased carnitine synthesis, due to possible depleted stocks of SAM may have led to lower trimethyllysine concentrations and ultimately to lower total carnitine levels.

Since the availability of trimethyllysine is the rate-limiting factor for carnitine synthesis (Davies, 1986), lowered trimethyllysine concentrations may lead to decreased carnitine biosynthesis. *In vitro* experiments with rat embryos in methionine-deficient media resulted in NTD and lowered trimethyllysine concentrations (Coelho, 1990). Although the actual cause of NTD in this experiment was never determined, altered trimethyllysine (and most probably lowered carnitine synthesis) could have been involved in the resultant NTD. Since carnitine is essential for detoxification and the transport of fatty acids in the mitochondria, one can expect that lowered carnitine levels in pregnant female mice, treated with HNV, most probably affected the detoxification of HNV and may also influence fatty acid metabolism and hence energy generation.

4.4.4.3.2 Embryonic carnitine levels and HNV

Embryonic total carnitine levels were normally distributed (p = 0.344; Shapiro-Wilk) and HNV appeared to exert a statistically significant effect on this parameter (p = 0.050; Student's T-test). The mean total carnitines concentration, observed in control embryos was 36.6 ± 4.9 µmol/g protein, compared to the levels measured in HNV treated experimental embryos (mean total carnitines = 44.4 ± 5.7 µmol/g protein) (Figure 4.23), a 21.2 % increase.

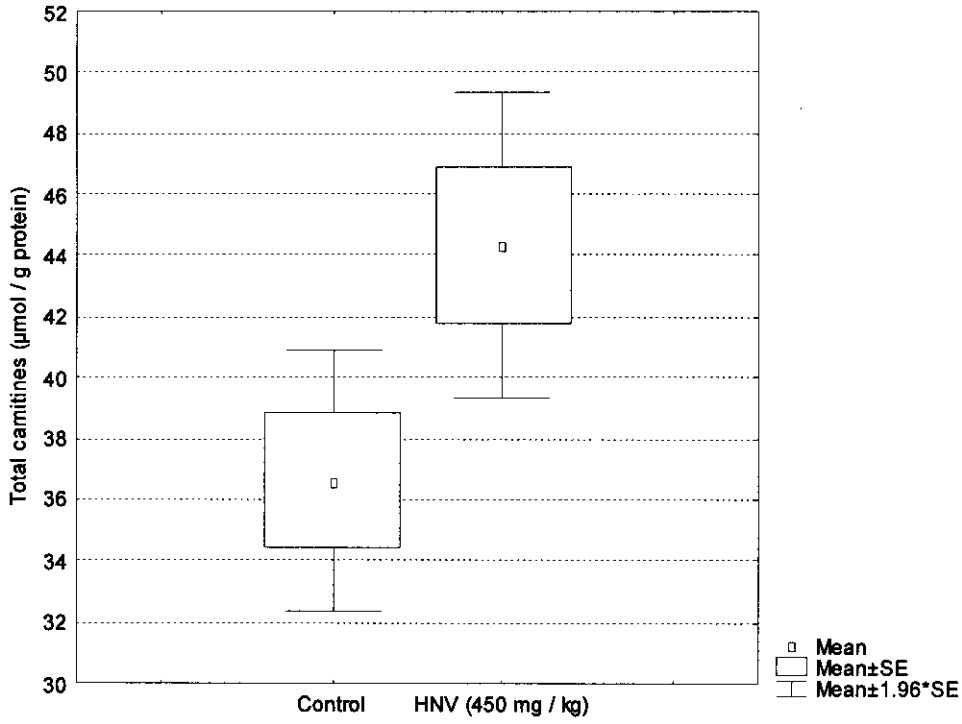

Figure 4.23. Total carnitines in 10-day-old mouse embryos.

The increase in total carnitines seen in the 10-day-old mouse embryos is not consistent with the expected results. However, in the mothers, a decrease in total carnitines was observed, as anticipated. This is probably due to lower SAM levels inhibiting normal carnitine biosynthesis. The paradoxical increase in total carnites in the embryos can however, not be explained at this moment in time.

4.4.4.4 Effect of HNV on specific enzymes involved in the flow of one-carbon units through the folate and remethylation cycles

Several studies suggested that serine and glycine occupy a unique metabolic position in the fetus. The fetus relies on the endogenous synthesis of serine and glycine, and changes in the regulation of fetal serine and glycine biosynthesis and utilisation appear to be the only mechanisms available for the fetus to regulate the supply of these two amino acids. Serine and glycine interconversion is catalysed by the cytosolic and mitochondrial isoforms of serine hydroxymethyltransferase, cSHMT and mSHMT, respectively, as well as the glycine cleavage system (GCS). This interconversion is especially important when there is a need for one-carbon cofactors (Xue, 1999).

Enzyme levels were measured in pregnant female Hanover-NMRI mice and their unborn fetuses. The control group consisted of 8 females and the experimental group of 10 animals. Controls were treated orally with saline on days 7, 8 and 9 of *p.c.*, while experimental animals received 450 mg/kg β-hydroxynorvaline. Animals were sacrificed on day 10 *p.c.*, the embryos removed and prepared as described (Section 4.3.1).

4.4.4.4.1 The effect of HNV on the enzyme activity in the livers of pregnant female mice:

(a) Effect of HNV on the catalytic activity of cytosolic serine hydroxymethyltransferase (cSHMT)

Data on the catalytic activity of cSHMT appeared to be normally distributed ($p = 0.430$; Shapiro-Wilk). Although the results in adult mice indicated a tendency of HNV to lower catalytic activity of the hepatic cSHMT, the effect did not appear to be statistically significant ($p = 0.562$; Student's T-test). The mean cSHMT activity in control mice was 1.93 ± 0.34 $\mu mol.min^{-1}.mg\ protein^{-1}$, while the mean hepatic cSHMT activity levels in HNV treated experimental mice was 1.81 ± 0.39 $\mu mol.min^{-1}.mg\ protein^{-1}$, a decrease of approximately 6.1 %.

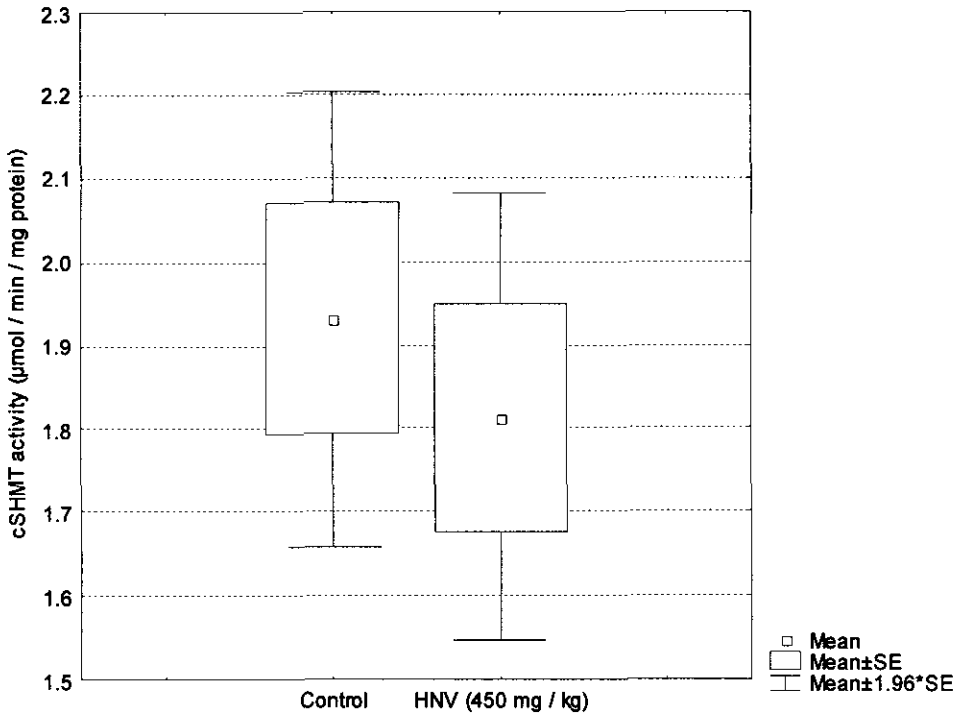

Figure 4.24. Cytosolic serine hydroxymethyltransferase (cSHMT) activity in livers of pregnant female mice.

(b) Effect of HNV on the catalytic activity of mitochondrial serine hydroxymethyltransferase (mSHMT)

The data for the catalytic activity of hepatic mSHMT appeared to be normally distributed ($p = 0.361$; Shapiro-Wilk). Although the mean catalytic activity of hepatic mSHMT in HNV-treated adult female mice (mean = 14.51 ± 5.01 µmol. min^{-1}.Unit CS^{-1}) was 20.2% higher than that observed in the controls (12.08 ± 1.85 µmol.min^{-1}.Unit CS^{-1}) the effect did not appear to be statistically significant ($p = 0.285$; Student's T-test).

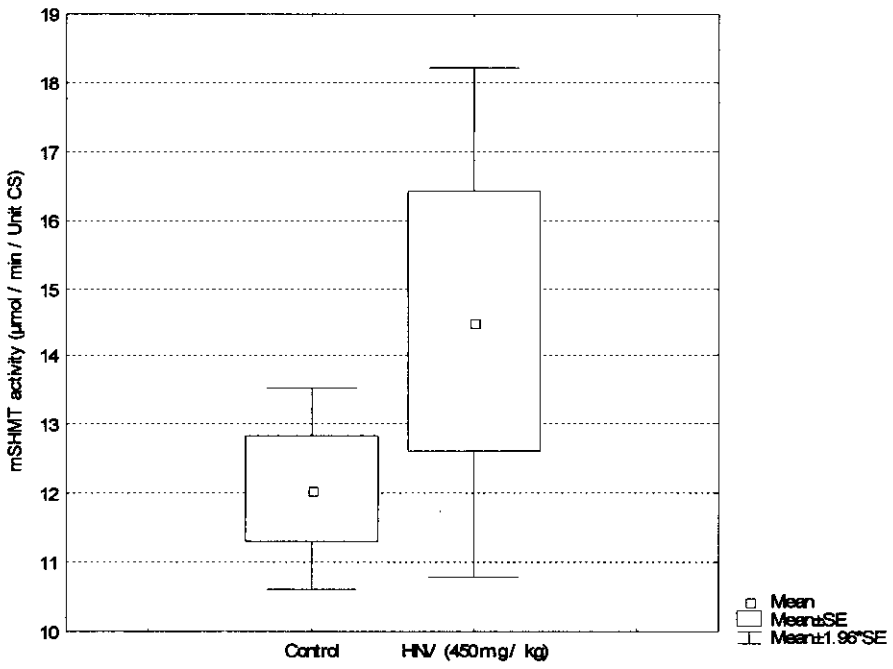

Figure 4.25. Mitochondrial serine hydroxymethyltransferase (mSHMT) activity in livers of pregnant female mice.

(c) Effect of HNV on the catalytic activity of mitochondrial glycine cleavage system (GCS) activity in pregnant female mice

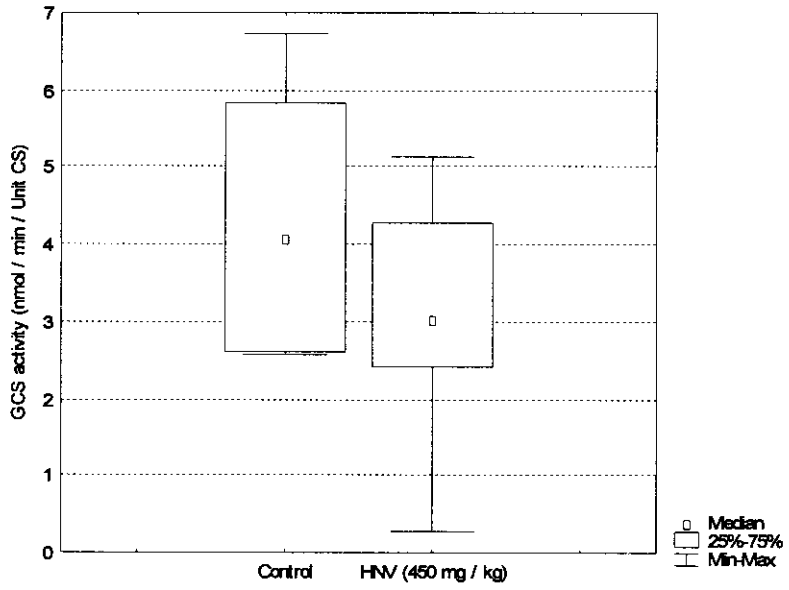

Figure 4.26. Glycine cleavage system activity in liver of pregnant female mice.

The Shapiro-Wilk W test indicated that the data on the catalytic activity of the GCS was normally distributed ($p = 0.863$) and the Student's T-test was employed to test

for statistical significance between the two groups. The mean GCS activity of HNV-treated mice (3.11 ± 1.54 nmol.min^{-1}.U CS^{-1}) apparently did not differ significantly (0.192; Student's T-test) from that of the controls (4.32 ± 1.72 nmol.min^{-1}.U CS^{-1}), although a tendency of HNV treatment to lower the catalytic activity of the mitochondrial GCS (28.01%) could be clearly observed.

4.4.4.4.2 Effect of HNV on enzyme activity in 10-day-old mouse embryos

(a) Effect of HNV on cytosolic serine hydroxymethyltransferase (cSHMT)

Data for the catalytic activity of embryonic cSHMT appeared to be normally distributed (p = 0.889; Shapiro-Wilk). HNV apparently displayed no statistically significant effect on the catalytic activity of cSHMT in adult female mice (p = 0.165; Student's T-test). However, a strong tendency towards an inhibition (32.1%) of embryonic cSHMT activity by HNV was observed in HNV treated experimental embryos (mean catalytic cSHMT activity = 0.19 ± 0.06 µmol.min^{-1}.mg protein^{-1}), compared to the activity of the cSHMT in control embryos (mean catalytic cSHMT activity = 0.28 ± 0.10 µmol.min^{-1}.mg protein^{-1}).

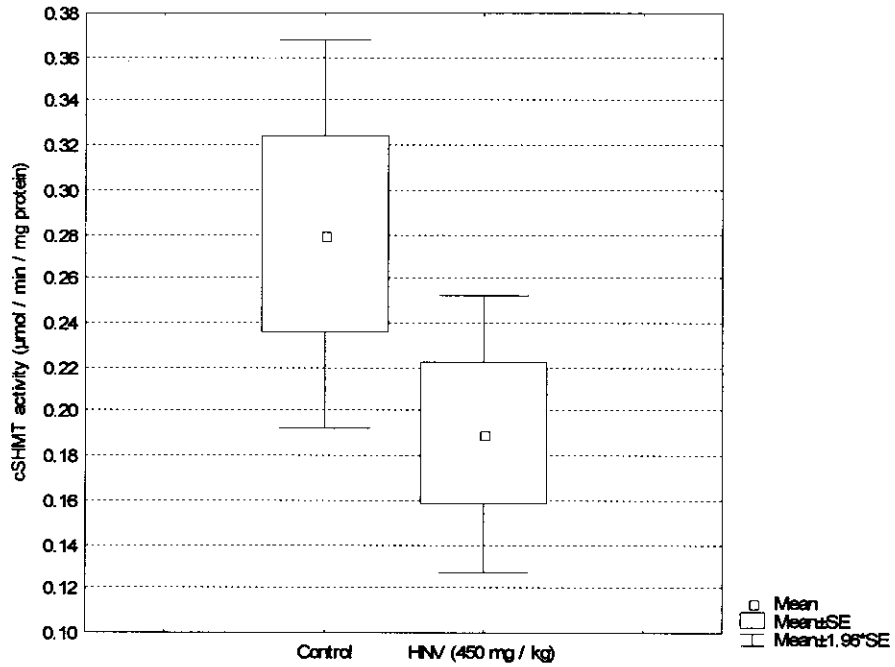

Figure 4.27. Cytosolic serine hydroxymethyltransferase (cSHMT) activity in 10-day-old mouse embryos.

(b) Effect of HNV on mitochondrial serine hydroxymethyltransferase (mSHMT)

The data obtained on the catalytic activity of embryonic mSHMT appeared to be normally distributed (p = 0.260; Shapiro-Wilk). Although no statistically significant effect on the catalytic activity of embryonic mSHMT-levels could be demonstrated (p = 0.378; Student's T-test), the mean embryonic cSHMT activity of the HNV treated embryos (25.48 ± 7.69 µmol.min^{-1}.Unit CS^{-1}.Unit CS^{-1}) was 24.6% lower than that of the control embryos (33.77 ± 22.02 µmol.min^{-1}).

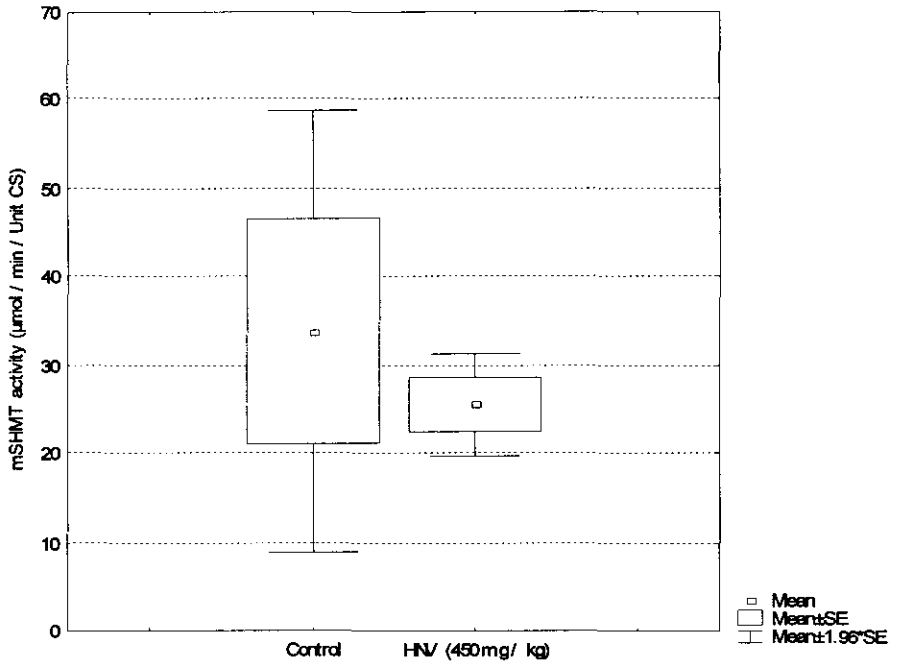

Figure 4.28. Mitochondrial serine hydroxymethyltransferase (mSHMT) activity in 10-day-old mouse embryos.

(c) Effect of HNV on the catalytic activity of the glycine cleavage system (GCS) in 10-day-old mouse embryos

Data on the catalytic activity of the embryonic GCS appeared to be normally distributed (Shapiro-Wilk W test; p = 0.127). The Student's T-test was therefore used to test for statistical significance between groups. The mean GCS activity of the HNV-treated embryos (3.66 ± 1.47 nmol.min^{-1}.U CS^{-1}) was approximately 19.38% lower than in control embryos (4.54 ± 1.99 nmol.min^{-1}.U CS^{-1}). However,

no statistical significance could be illustrated for this observation ($p = 0.418$; Student's T-test).

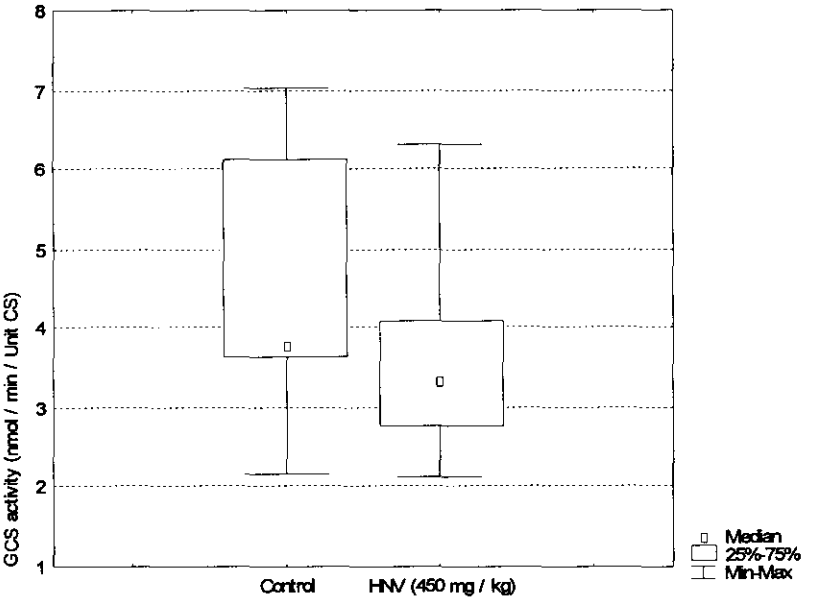

Figure 4.29. Glycine cleavage system activity in 10-day-old mouse embryos.

HNV did not significantly influence the activity of cSHMT, mSHMT of the GCS in pregnant females and their fetuses, although clear tendencies were observed:

cSHMT activity was reduced in both HNV exposed mothers and embryos, compared to controls. This enzyme is responsible for the supply of one carbon units for the synthesis of purines, thymidine and methionine from homocysteine (Girgis, 1997; Gregory, 2000; Herbig, 2002). Since the activity of cSHMT was reduced in HNV exposed animals, compared to controls, one can conclude that this inhibition may be partly responsible for the reduced flow of one carbon units in the mice ([^{3}H]-thymidine incorporation test; Section 4.4.1). Such an inhibition will not only cause a reduced one carbon flow, but may also be responsible for the inhibition of DNA synthesis and methylation, polyamine synthesis and carnitine biosynthesis.

In the case of mSHMT, the pregnant mothers and the embryos responded differently towards an HNV challenge. Relative to the controls, hepatic mSHMT

activity in HNV treated mothers was increased. However, in whole embryos, the opposite effect was observed. This difference in response of the mothers and their embryos was not anticipated. A probable explanation for this phenomenon may be that upregulation of hepatic mSHMT expression occurred in the mothers, but not in whole embryos. The inhibition of carnitine biosynthesis (Section 4.4.4.3) probably contributed to a greater demand for glycine, essential for detoxification of toxic HNV derived metabolites. Since mSHMT is purportedly responsible for the predominant proportion of glycine synthesis (Narkewicz, 1996a), an upregulation of the mSHMT gene seems to be a logical explanation for the apparent paradoxical increase of hepatic mSHMT activity in the mothers.

Both mothers and embryos treated with HNV exhibited lower GCS activity, compared to controls. Although this inhibition was not statistically significant, the tendency was clear, especially in the embryos. Lowered GCS activity is normally associated with higher glycine levels, since this enzyme complex is the major biochemical pathway for the catabolism of glycine (Yoshida, 1972). Inhibition of the GCS by HNV and/or its metabolites therefore could lead to elevated glycine levels, essential for detoxification. However, according to Hamosh (1995), the GCS activity in 2-day old rat neonates was only a third of the levels normally expressed in the adult rat. This might indicate that, by implication, the serine/glycine interconvertion in this study was most probably more influenced by SHMT than the GCS.

4.4.4.4.3 The effect of HNV on the transsulfuration route

β-Hydroxynorvaline inhibits cystathionine-β-synthase (CBS) *in vitro* (Section 4.4.3). Because of its structural resemblance to L-serine, HNV is probably a competitive inhibitor for CBS, compromising the activity of this important enzyme. Condensation of HNV with homocysteine may result in the formation of 3-ethylcystathionine and the resultant intracellular accumulation of homocysteine. The formed 3-ethylcystathionine will probably quickly be catabolised by CGL to produce 3-ethylcysteine and 2-ketobutyric acid (Figure 4.30). This potential effect of HNV may influence the normal activity of the enzyme since CBS will most

probably display different affinities for its natural substrate, serine and the potential competitive inhibitor, HNV. CBS activity measurements in the mouse embryonic tissues proved to be problematic, because of the relative insensitivity of the CBS assay employed (APPENDIX O).

Inhibition of CBS and the resultant flux of metabolites through the transsulfuration route may be followed by investigating the organic acid profile in the urine of HNV treated animals. The presence of urinary 3-ethylcysteine will be an indication that HNV may have condensed with homocysteine to produce 3-ethylcystathionine, altering the normal course of transsulfuration. 3-Ethylcysteine was synthesised enzymatically using the method of Kraus (1987). The method is described in detail in APPENDIX O.

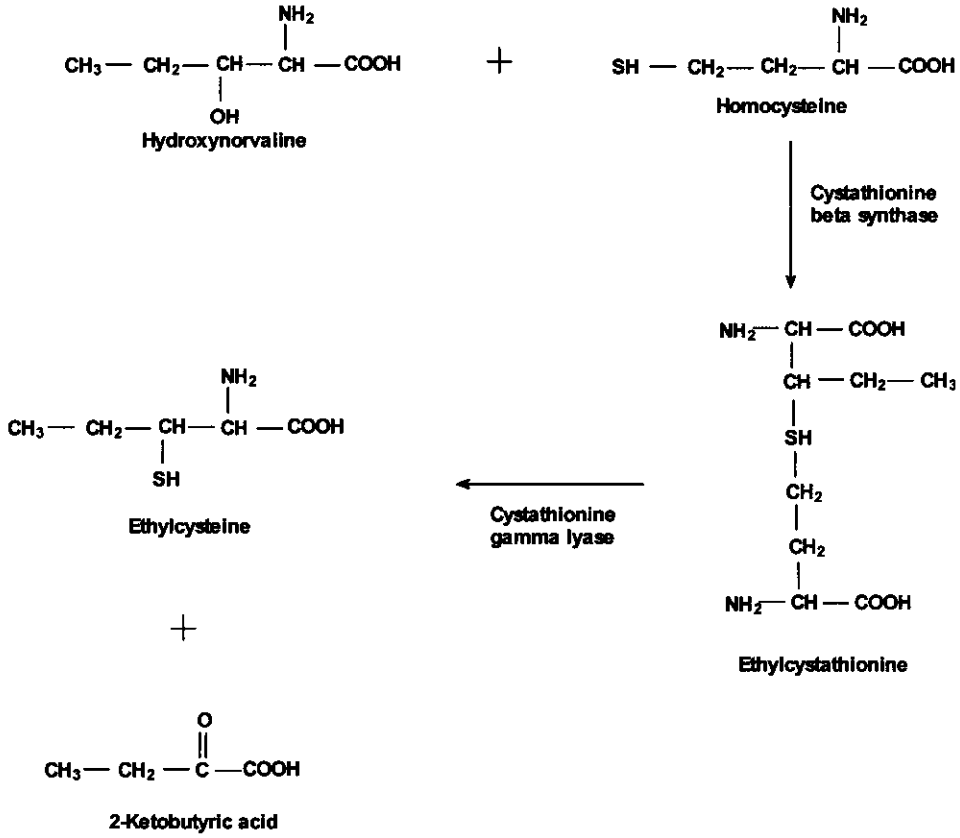

Figure 4.30. Proposed synthesis of ethylcysteine from β-hydroxynorvaline in the mouse.

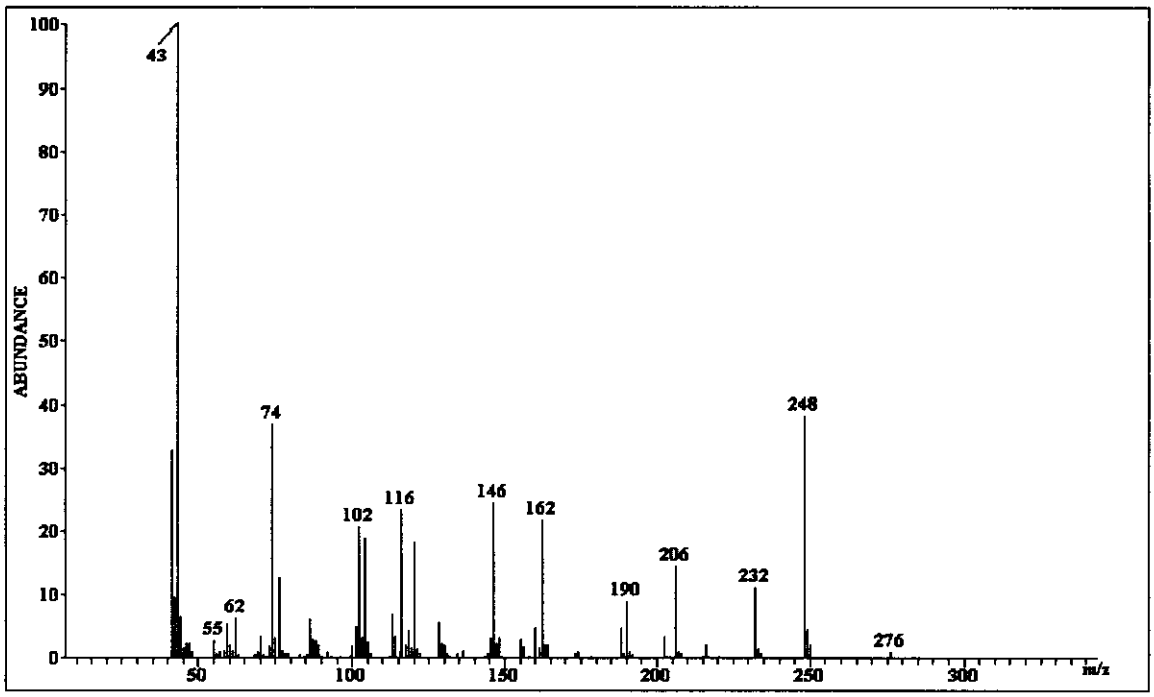

Figure 4.31. Electron ionisation spectrum of the derivatised cysteine standard

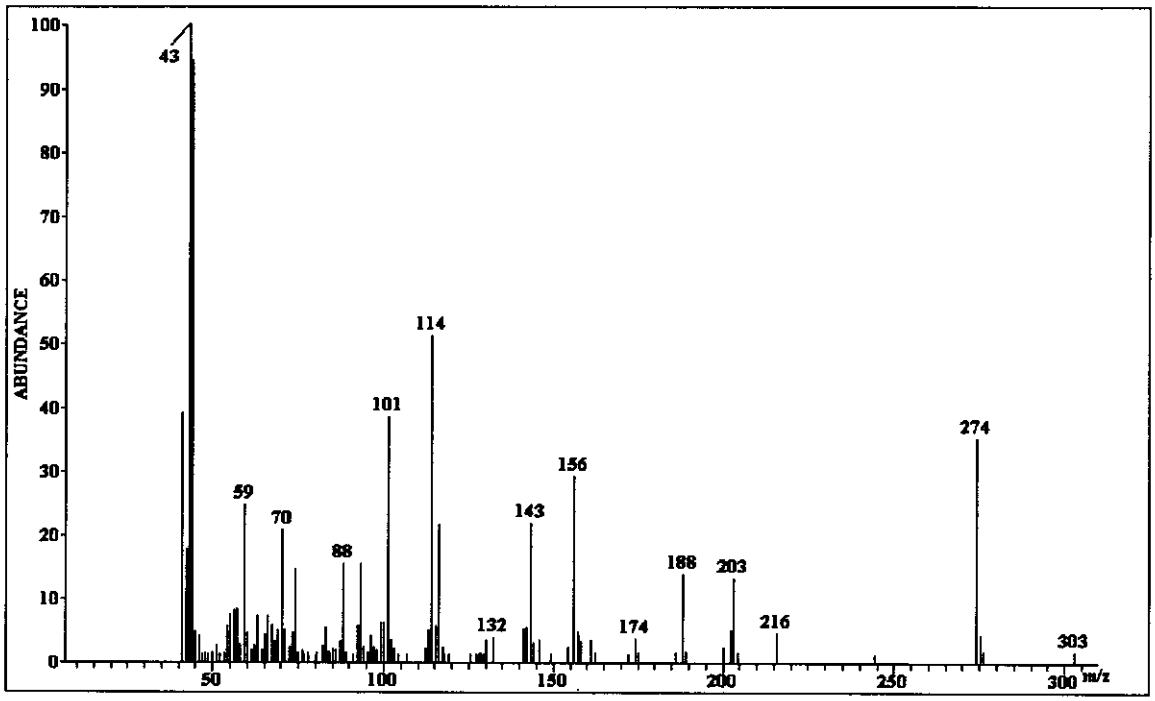

Figure 4.32. Electron ionisation spectrum of enzymatically synthesised, derivatised 3-ethylcysteine

Sufficient amounts of enzymatically synthesised 3-ethylcysteine could not be isolated and purified to confirm the structure of this novel metabolite by nuclear magnetic resonance (NMR) or infrared (IR) spectroscopy. However, the GC retention time of the synthesised 3-ethylcysteine (6.8 ± 0.2 min) proved to be very close to that of standard cysteine (7.6 ± 0.1 min). An electron ionisation spectrum of the synthesised 3-ethylcysteine was compared to an ionisation spectrum of standard cysteine and proved to be very similar. The latter result confirmed the structure of the enzymatically produced 3-ethylcysteine.

The spectra of both standard cysteine and enzymatically synthesised 3-ethylcysteine exhibited characteristic low atomic mass ionisation fragments (i.e. mz $[43]^+$, $[59]^+$, $[74]^+$ and $[88]^+$ respectively). However, spectra of the enzymatically synthesised 3-ethylcysteine displayed ionisation fragments 28 atomic mass units heavier than that observed for standard cysteine. Some of the ionisation fragments were, however, only 27 atomic mass units heavier, due to the loss of a H-atom.

Typical ionisation fragments observed for cysteine were m/z $[104]^+$, $[116]^+$, $[128]^+$, $[146]^+$, $[188]^+$, $[248]^+$ and $[276]^+$. Spectra of ethylcysteine exhibited molecular fragments at m/z $[132]^+$, $[143]^+$, $[156]^+$, $[174]^+$, $[216]^+$, $[276]^+$, and $[303]^+$. These fragments corresponded to that of cysteine, but were all 27 or 28 atomic mass units heavier than the corresponding fragment for cysteine. The fragments observed in the 3-ethylcysteine ionization spectra were similar to the anticipated ionisation fragmentation pattern for 3-ethylcysteine. The additional ethyl-group (-CH_2CH_3) on carbon 3 of the 3-ethylcysteine molecule was apparently responsible for the increase in the m/z of 28 atomic mass units of the ionisation fragments, produced from standard cysteine. Although the mass of the ethyl-group is 29 atom mass units, the molecule loses one H-atom for the addition of the ethyl-group, resulting in a 28 atom mass unit increase in mass, compared to cysteine.

Chemical synthesis of 3-ethylcysteine will obviously be necessary for the absolute confirmation of the structure of this novel metabolite. To accomplish this, a better approach may be to employ purified CBS in the synthesis of 3-ethylcystathionine. It may be possible that sufficient amounts of this intermediary compound could be isolated and its structure confirmed by NMR and IR spectroscopy. For the present

study, however, the formation of 3-ethylcysteine could only be provisionally ratified from EI ionisation spectra, following GC fractionation. Results obtained during the *in vitro* inhibition studies executed on CBS may corroborate the present inference that the 3-ethylcysteine, observed in metabolic profiles of urines collected from animals treated with HNV, was produced from HNV by CBS, following initial transsulfuration of the HNV to 3-ethylcystathionine and subsequent cleavage of the intermediate product by CGL.

3-Ethylcysteine was identified in urine samples from pregnant females treated with β-hydroxynorvaline. This result may be taken to confirm that the catalytic activity of cystathionine-β-synthase (CBS) was affected by HNV, because it had most probably acted as a competitive inhibitor (substrate analogue) of CBS. Inhibition of CBS may therefore effectively increase the levels of homocysteine. This result may in turn be responsible for an inhibition in the rate of one-carbon flux through the remethylation cycle and in so doing, may actively contribute to the induction of the observed NTD in mouse embryos, since increased homocysteine levels is considered a risk factor for NTD (Steegers-Theunissen, 1994; Mills, 1995).

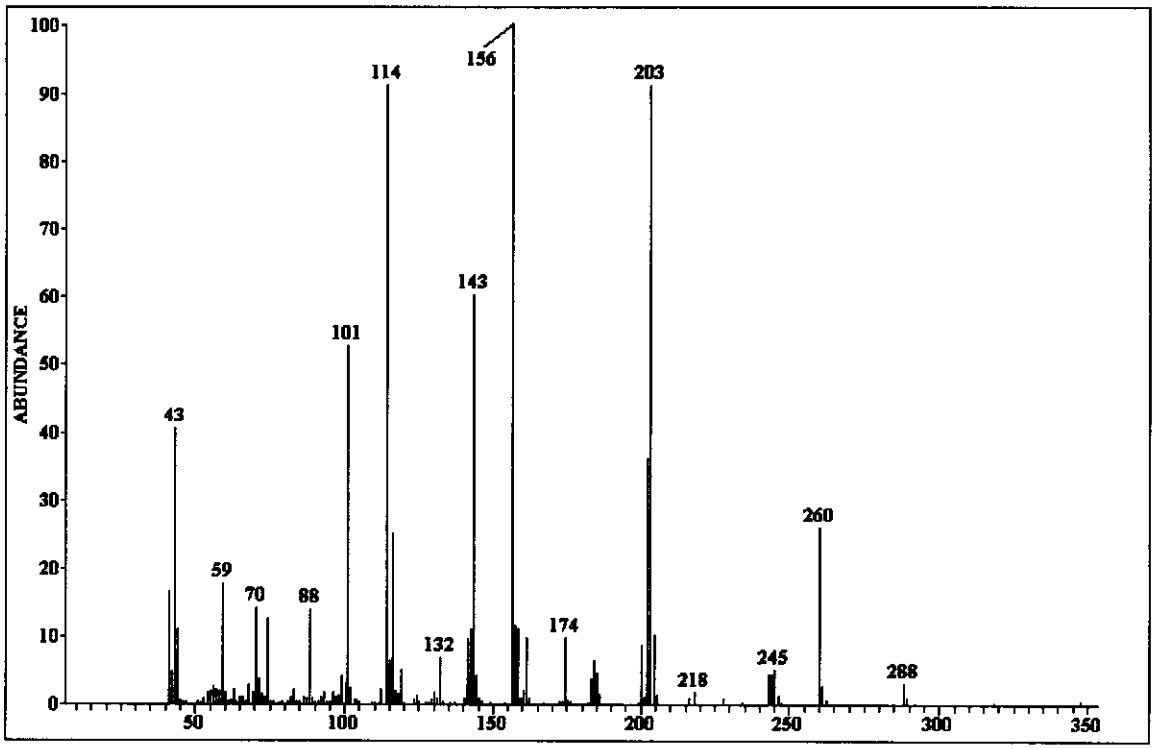

Figure 4.33. Electron ionisation spectrum of derivatised urinary 3-ethylcysteine. (Mouse treated orally with 450 mg/kg HNV).

4.5 DISCUSSION

HNV clearly influences the flow of one-carbon units. Incorporation of [^{3}H]-thymidine in developing mouse embryos was greatly affected by the presence of HNV (Fig. 4.8). Although the increased incorporation of the radio-active nucleotide could also be due to an increased rate of DNA synthesis, *in vitro* studies indicated that this was not the case. HNV inhibited DNA synthesis in chicken embryo fibroblasts indicating that the increased [^{3}H]-thymidine incorporation in mouse embryos can most probably be ascribed to a reduced flow of one-carbon units, rather than an increased rate of DNA synthesis.

DNA methylation was significantly decreased in the developing embryos harvested from pregnant mothers, treated with HNV, as compared to controls. *In vitro* studies with mouse embryos indicated that DNA methylation is essential for normal embryonic development. Loss of the ability to methylate DNA, due to a mutation in the DNA MTase gene, resulted in a distorted neural tube at 9.5 days p.c. and at the same time drastically reduced methylation levels (Lei, 1996). The reduced DNA methylation in experimental HNV treated animals may be a probable cause of the NTD observed in embryos exposed to NTD.

Polyamine biosynthesis appeared to have been affected by HNV. Although this inhibition was not statistically significant (95 % confidence level), the tendency was very clear. Polyamines play a critical role in cell proliferation and differentiation, especially during embryonic development (Goyns, 1982; Haukanes, 1990; Pillai, 1997; Khuhawar, 2001). One can therefore anticipate that disturbances in the biosynthesis of these important biomolecules may detrimentally affect the normal development of the embryo. In this study, HNV did not exhibit a large effect on polyamine biosynthesis (Figure 4.16 and Figure 4.18). One can therefore argue that the observed NTD was most probably not due to inhibition of polyamine biosynthesis. However, due to the critical role of polyamines in embryonic development, even small changes in polyamine concentrations may influence normal embryonic development. The results of this study can therefore not exclude the inhibition of polyamine synthesis as a cause of NTD.

Carnitine biosynthesis was negatively affected by HNV. Pregnant females treated with HNV exhibited dramatically reduced total urinary carnitine levels, in comparison with control animals. Trimethyllysine levels were also reduced in the HNV treated animals, although not statically significant on the 95 % confidence level ($p = 0.131$). This result supports the observed inhibition of carnitine biosynthesis. Due to the essential role of carnitine in detoxification and fatty acid transport, the effect of reduced total carnitine levels may have severe implications for the developing mouse embryos.

Since HNV is a well known toxin, detoxification is essential for normal embryonic development. Low carnitine levels will probably affect the transport of fatty acids into mitochondria, inhibiting β-oxidation and hence energy production. Alternatively, an increased demand for glycine biosynthesis may occur due to an increased need to detoxify HNV metabolites. Glycine conjugation is a known mechanism of detoxification and following depletion of carnitine, the embryos will probably be more dependent on glycine as a conjugating agent for detoxification. The ultimate effect may be an inhibition of the normal flow of one-carbon units since glycine levels are affected by cSHMT, mSHMT and the GCS.

S-Adenosylmethionine, S-adenosylhomocysteine and homocysteine levels could not be quantatively measured in developing embryos due to analytical limitations. Therefore one can only speculate about the direct effect of HNV on the concentrations of these metabolites. However, the indirect effect of HNV on one carbon metabolism (decreased DNA methylation, polyamine synthesis and carnitine biosynthesis) indicates that the concentration of one and/or more of these three metabolites (SAM, SAH and homocysteine) was affected by HNV.

The actual cause of the reduced flow of one carbon units can probably be ascribed to a reduced catalytic activity of cSHMT and/or CBS. Pregnant females and their embryos exposed to HNV exhibited lower cSHMT catalytic activity than that observed in controls. The observed inhibition was not statistically significant (95 % confidence level), but the tendency was very clear. *In vitro* studies confirmed that HNV is a mild competitive inhibitor of the catalytic activity of SHMT. The demand for one carbon units is especially high during embryonic development and lower

cSHMT activity will result in a reduced flow of one carbon units. cSHMT is essential for the supply of one-carbon units to sustain processes like DNA synthesis and methylation (Herbig, 2002).

The catalytic activity of CBS is also inhibited *in vitro* by HNV. This inhibition is most probably competitive and reversible in nature. In pregnant female mice treated with HNV, 3-ethylcysteine was identified in urine samples. This product could only have been formed if HNV acted as a substrate for CBS. This purported "inhibition" of CBS (probably due to a lower affinity for HNV compared to the natural substrate, L-serine), may be the cause of the reduced flow of one carbon units observed in this study.

CHAPTER 5

THE EFFECT OF β-HYDROXYNORVALINE ON THE METABOLISM OF PREGNANT FEMALE MICE

5.1 INTRODUCTION

β-Hydroxynorvaline (HNV) is a well known toxic, non-protein amino acid and had been investigated by a number of researchers over the past two decades (Section 2.5). HNV appeared to be responsible for toxic effects such as:

- the miscleavage of rat preprolactin to prolactin in rat pituitaries (Hortin, 1981);
- the inhibition of asparagine-linked glycosylation (Polonoff, 1982);
- the inhibition of O-glycosylation (Blough, 1986);
- the inhibition of the herpes virus thymidine kinase and DNA polymerase (Massare, 1987);
- increased intracellular degradation of collagen in human fetal lung fibroblasts (Barile, 1989);
- the inhibition of steroidogenesis in rat adrenal cortex cells (Green, 1991);
- the inhibition of the assembly and secretion of procollagen in chicken embryo fibroblasts (Christner, 1975).

Most, if not all, of these toxic effects relate to the fact that HNV is structurally related to L-threonine. An important prerequisite for the precipitation of all of these observed toxic effects, appears to be the prior incorporation of HNV into the structure of the protein or peptide. Due to the fact that at least one of the four stereoisomers of HNV is a near perfect structural analogue of L-threonine, it can slip through the relatively strict editing procedures controlling protein synthesis, to replace L-threonine in the primary structure of a target protein or peptide. This proved to be possible, since HNV could apparently be activated by the same

aminoacyl-tRNA-synthase involved in the activation of L-threonine, prior to incorporation into peptides/proteins (Christner, 1975).

None of the published papers, referring to the toxic properties of HNV contained any proof that HNV or HNV metabolites could effectively compromise the catalytic activity of any particular enzyme as either a reversible competitive, non-competitive or irreversible inhibitor. Never before has HNV been associated with teratogenic events, however, once HNV was visualised as a potential L-serine analogue, numerous other probable scenarios could be considered to be important in explaining the toxic capabilities of HNV.

Serine is generally regarded as the most important donor of one-carbon units (Herbig, 2002). As a potential serine analogue and inhibitor of SHMT, we postulated that apart from numerous other probable options, HNV could disrupt, or adversely affect the flux of one-carbon units in intermediary metabolism. In the process, HNV could potentially emulate a folate deficiency, effecting subnormal methylation of homocysteine, diminished SAM production, defective biomethylation, lower levels of DNA synthesis and eventually compromise embryonic development.

Experimental investigations (Chapter 3) subsequently proved that HNV can induce NTD in developing chicken and mouse embryos, when the embryos were exposed to the toxic amino acid during the developmental window, associated with closure of the neural tube. HNV also appeared to inhibit the synthesis of thymidine and DNA itself (Section 4.4.1). Other results proved that HNV detrimentally affected DNA methylation (Section 4.4.4.1), polyamine synthesis (Section 4.4.4.2) and carnitine biosynthesis (Section 4.4.4.3).

HNV, like the protein amino acids threonine and isoleucine, contains two chiral carbon atoms (α- and β-carbon atoms). Commercially available HNV and HNV synthesised according to the method of Sunko *et al.* (1955) are mixtures of four stereoisomers i.e. L,L-, L,D-, D,L- and D,D-HNV. According to the Cahn-Ingold-Prelog rule of the nomenclature of asymmetric compounds, the HNV stereoisomers can also be denoted as R,R-, S,S-, R,S- or S,R-HNV (Figure 5.1).

The stereoisomeric mixture of HNV actually consists of two pairs of enantiomers that can usually not be properly resolved by classical chromatographic techniques or by mass spectroscopy.

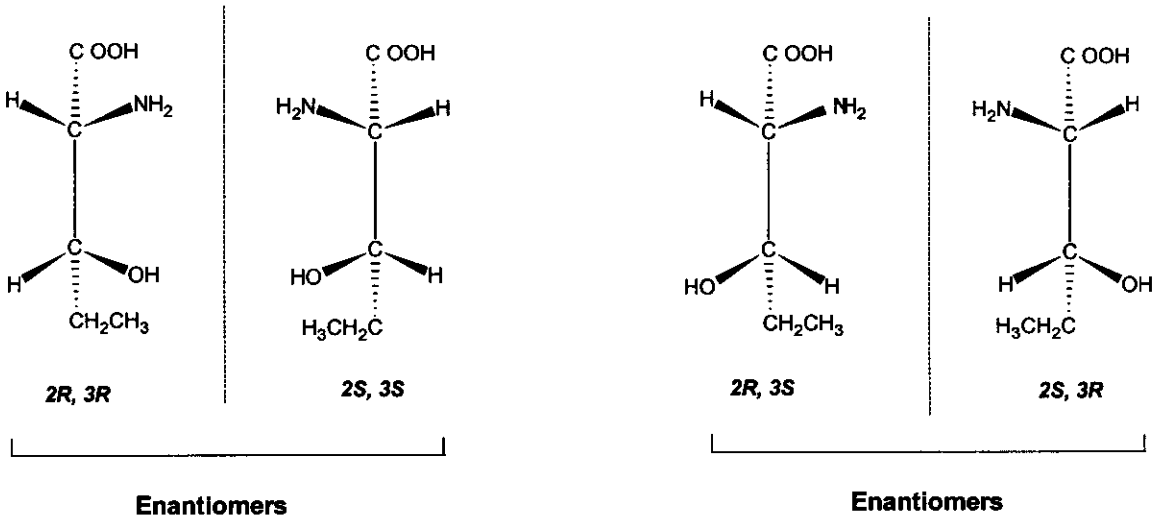

Figure 5.1. The four stereoisomers of β-hydroxynorvaline (2-amino-3-hydroxypentanoic acid).

Since amino acids with the L-or S-configuration of the α-carbon atom are the only stereoisomers incorporated into proteins and because these stereoisomers are more readily metabolised than the D- or R-form (relative to the α-carbon atom), selected stereoisomers of HNV may be metabolised in the mice. The relative molar ratios of the four HNV stereoisomers in the urine samples appear to be a useful tool which may be used to determine if any selective catabolic breakdown of the HNV stereoisomers does indeed occur in the mouse.

Toxins, including HNV seldom exhibit highly selective and specific activities; one should expect that HNV's toxic effects would hardly be limited to one-carbon metabolism and the immediate ramifications of that scenario, discussed above. Catabolic breakdown of β-hydroxynorvaline could also potentially lead to the production of a number of metabolites that could in themselves cause a ripple effect throughout intermediary metabolism as a whole. The catabolic fate of HNV was subsequently investigated.

5.2 β-HYDROXYNORVALINE AND INTERMEDIARY METABOLISM: HYPOTHESES AND APPROACH

A pre-emptive analytical biochemical approach was followed to identify probable unknown metabolites, resulting from the catabolic breakdown of HNV. This approach was previously employed in the Biochemistry Department of the PU for CHE with great success (Mienie, 1994). In principle, the approach will be based on the prior prediction of probable metabolites that may result from the catabolic breakdown of HNV dosed to experimental animals. Commercially or synthesised standards will then be used to obtain electron ionisation mass spectra of the proposed metabolites. The spectra will then be employed for the positive identification of the proposed metabolites in the urine of HNV treated experimental pregnant female mice.

5.2.1 Postulated catabolic fate of HNV in the mouse model

The anticipated catabolic breakdown of HNV is formulated in Figure 5.2. The first reaction in the catabolism of an amino acid usually entails removal of the α-amino group with the express purpose of excreting excess nitrogen and to degrade the remaining carbon skeleton to reusable metabolic intermediates. During the transamination reaction, the amino acid is usually converted to a keto acid, while α-ketoglutarate is converted to glutamate. The catabolic breakdown of HNV may therefore commence with transamination to yield 2-keto-3-hydroxypentanoic acid. Reduction of the latter intermediate may lead to the formation of 2,3-dihydroxypentanoic acid, or 2,3,-dihydroxyvaleric acid (DHPA). DHPA is an organic acid and may potentially be catabolised *via* β-oxidation of fatty acids. Decarboxylation of 2-keto-3-hydroxypentanoic acid may render 2-hydroxybutyryl-CoA and hydrolysis of the latter compound may lead to the formation of 2-hydroxybutyric acid, a probable branch point in the catabolic breakdown of HNV.

Theoretically 2-hydroxybutyric acid may either be carboxylated to form 3-methyloxaloacetate, or oxidised to render 2-ketobutyric acid. If the reaction would proceed in the direction of methyloxaloacetate, the latter may be condensed

with acetyl-CoA to form 4-methylcitrate in the first reaction of the tricarboxylic acid cycle (TCA cycle) and the resultant 4-methylcitrate converted to 4-methylisocitrate by the action of aconitase. The subsequent conversion of 4-methylisocitrate, to 4-methyl-2-ketoisocitrate would not be possible since the methyl-group in the C4-position of the 4-methylisocitrate would hinder the catalytic action of isocitrate dehydrogenase. Blocking the action of isocitrate dehydrogenase will probably seriously compromise the flux of intermediates through the TCA cycle, leading to systemic accumulation of TCA intermediates. Elevated concentrations of TCA-intermediates may then be excreted in the urine of HNV-treated mice.

Oxidation of 2-hydroxybutyric acid will render 2-ketobutyric acid and the latter compound may be metabolised to propionyl-CoA, with the subsequent formation of methylmalonyl-CoA and ultimately succinyl-CoA, a TCA cycle intermediate.

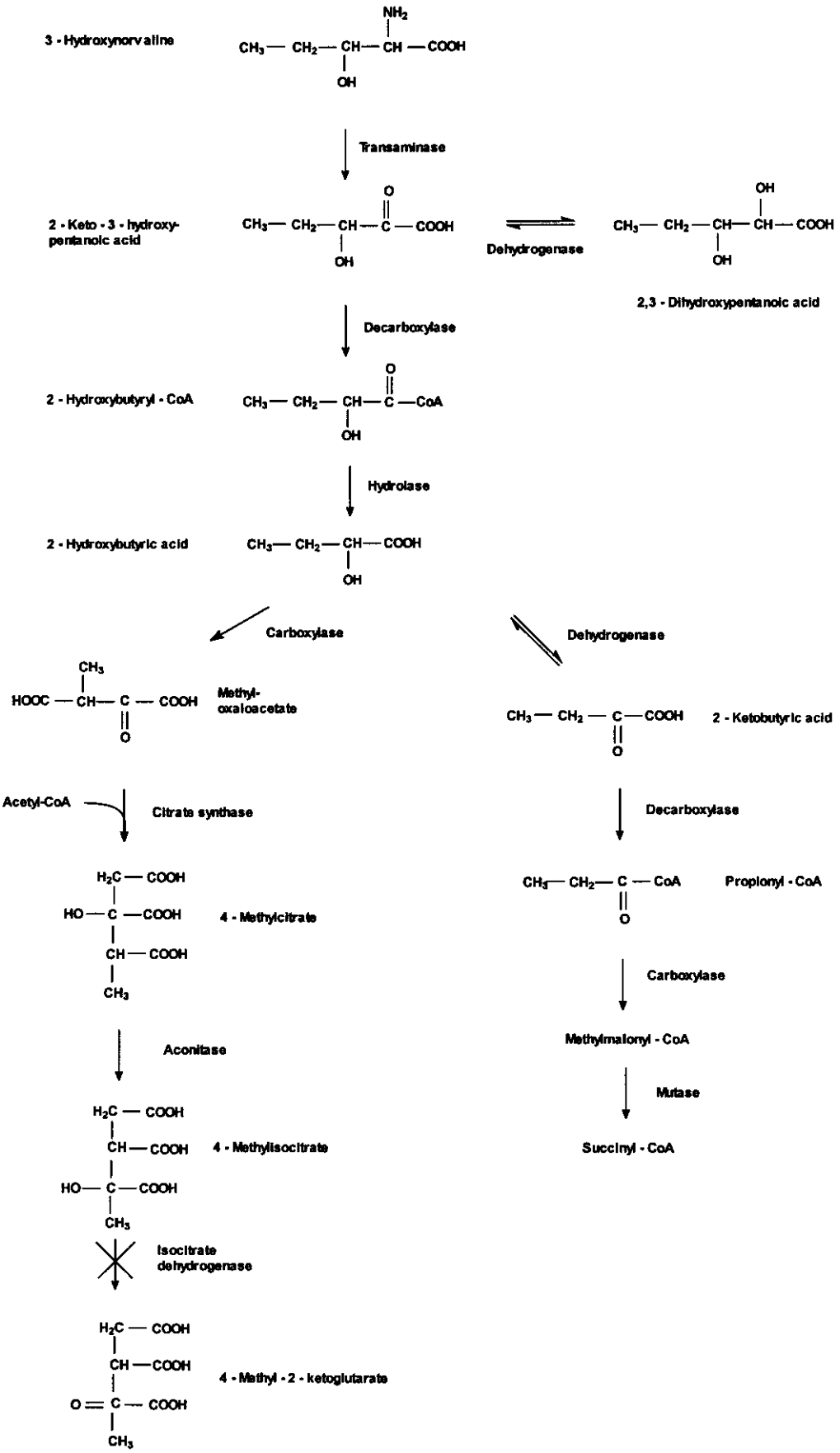

Figure 5.2. Proposed metabolic fate of β-hydroxynorvaline.

5.2.2 Postulated effects of HNV metabolites on the β-oxidation of fatty acids

As described above (Section 5.2.1), the catabolic breakdown of HNV may lead to the biosynthesis of DHPA, which in turn may be converted to 2,3-dihydroxyvaleryl-CoA. Acyl-CoA metabolites are catabolised by β-oxidation to acetyl-CoA and an acyl-CoA derivative that is two carbon units shorter than the original acyl-CoA (Figure 5.3). 2,3-Dihydroxyvaleryl-CoA cannot be catabolised by α-oxidation since it is a short-chain fatty acid. β-Oxidation of 2,3-dihydroxyvaleryl-CoA may, however, be problematic due to the hydroxy-group in the 2-position. By mere inspection, it can be inferred that this hydroxyl-group may negatively affect the activity of one or more of the enzymes involved in β-oxidation of fatty acids. Such an inhibition may, however, also affect the catabolism of other β-oxidisable acyl-CoA derivatives, leading to the excretion of elevated levels of acyl-CoA derivatives in the urine of HNV treated animals. These acyl-CoA derivatives may also conjugate with glycine and eventually be excreted in the mouse urine as acylglycines.

To investigate the proposed catabolic breakdown of HNV, the occurrence of organic acids in urine samples from control and HNV-treated pregnant female mice were investigated by GC-MS, employing a standardised method. Excretion of elevated free fatty acids or acylglycines may indicate that β-oxidation is influenced by certain HNV-metabolites.

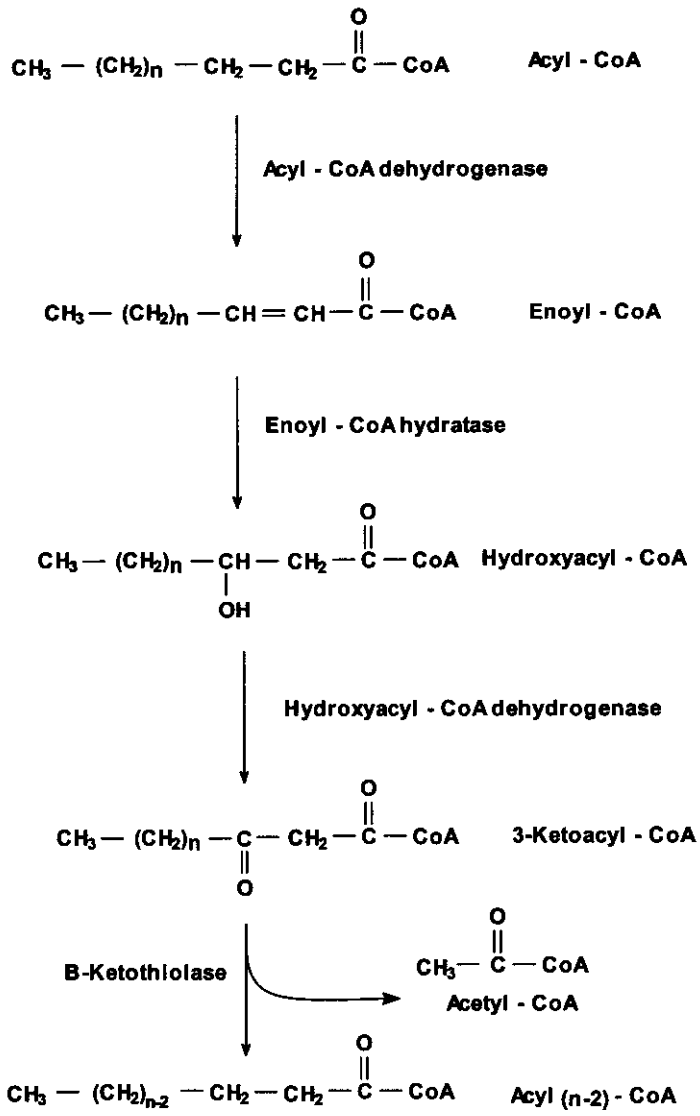

Figure 5.3. β-Oxidation of fatty acids.

5.2.3 A brief summary of hypotheses to be investigated

(i) β-Hydroxynorvaline stereoisomers will be catabolised in the pregnant female mice.

(ii) 2,3-Dihydroxypentanoic acid (DHPA) may form from HNV catabolism.

(iii) Formed DHPA may influence β-oxidation of other fatty acids.

5.3 MATERIALS AND METHODS

5.3.1 Experimental animals

Hanover-NMRI mice were used to study the catabolism of β-hydroxynorvaline and the effect of its metabolites on selected metabolic processes. The same urine samples, employed in the investigation of the effect of HNV on one-carbon metabolism (Chapter 4) were used for this investigation. In the experiment referred to, the urine samples were collected from 8 saline treated, pregnant females (controls) and 10 pregnant females, treated with HNV (450 mg/kg body mass) on days 7, 8 and 9 of gestation. Urine samples were collected over a 24-hour period (day 9 to 10), while the females were kept in metabolic cages and then used for all the relevant analyses. Thymol was added to the urine collecting vessel to prevent any microbial growth in the urine during the 24-hour collection period.

5.3.2 Analytical methods used

In order to determine the metabolic fate and relative molar ratios of the four HNV stereoisomers in the mouse model, a small sample of the HNV standard, as well as a urine sample from a mouse treated with 450 mg/kg HNV were first isolated by cation exchange chromatography and then derivatized with (-)-2-butanolic HCl and acetic anhydride (APPENDIX J). The derivatised samples were analysed by GC-MS. The mixture of four stereoisomers can usually not be completely fractionated by GC alone. During the derivatisation process, the enantiomeric pairs are converted to diastereoisomers differing in physical properties (melting point, boiling point, solubility, etc.) and which are separable and can be speciated by means of standard chromatographic methodologies, including GC-MS.

Organic acids were extracted from urine samples by means of liquid-liquid extraction. TMS-derivatives of the isolated organic acids were prepared following reaction with BSTFA and TMCS, prior to analysis by GC-MS. Phenylbutyric acid was used as an internal standard to assist in the quantification of the urinary organic acids (APPENDIX I).

Amino acids and carnitines (free carnitine and acylcarnitines) were determined with electrospray ionisation tandem mass spectrometry (ESI-MS-MS). The method was briefly discussed in Chapter 4 and is discussed in detail in APPENDIX K.

2,3-Dihydroxypentanoic acid was chemically synthesised. *Trans*-2-pentenoic acid was hydroxylated with hydrogen peroxide to form 2,3-dihydroxypentanoic acid (APPENDIX N). The latter was isolated, derivatised and analysed with the method described for organic acids (APPENDIX I).

5.3.3 Statistical methods

Results were expressed as the mean ± standard error of the mean (SEM). The Shapiro-Wilk W-test was used to determine if the data were normally distributed. The Student's T-test was used to determine the statistical significance of normally distributed data sets and the Kruskal-Wallis non-parametric test was employed if the data appeared to be non-normally distributed or skewed ($p < 0.05$; 95% confidence interval).

5.4 RESULTS

5.4.1 Catabolic fate of β-hydroxynorvaline in the mouse model

The first objective was to determine whether the mice exhibited a metabolic preference for any of the four HNV stereoisomers present in the stereoisomeric mixture, employed in the toxicity experiments.

A partial chromatogram, obtained for the fractionation of the derivatised stereoisomers in a sample of synthesised, standard HNV appear in Figure 5.4 below. Although it was not immediately possible to identify the individual stereoisomers in the chromatogram, it is clear that the original enantiomeric pairs (peaks 1 & 2 and 3 & 4) were well resolved. The concurrent EI mass spectra, however, confirmed the identity of the HNV (Figure 5.5). The relative molar ratios of the stereoisomers were calculated as 1:1:0.25:0.25 (areas of peaks 1:2:3:4).

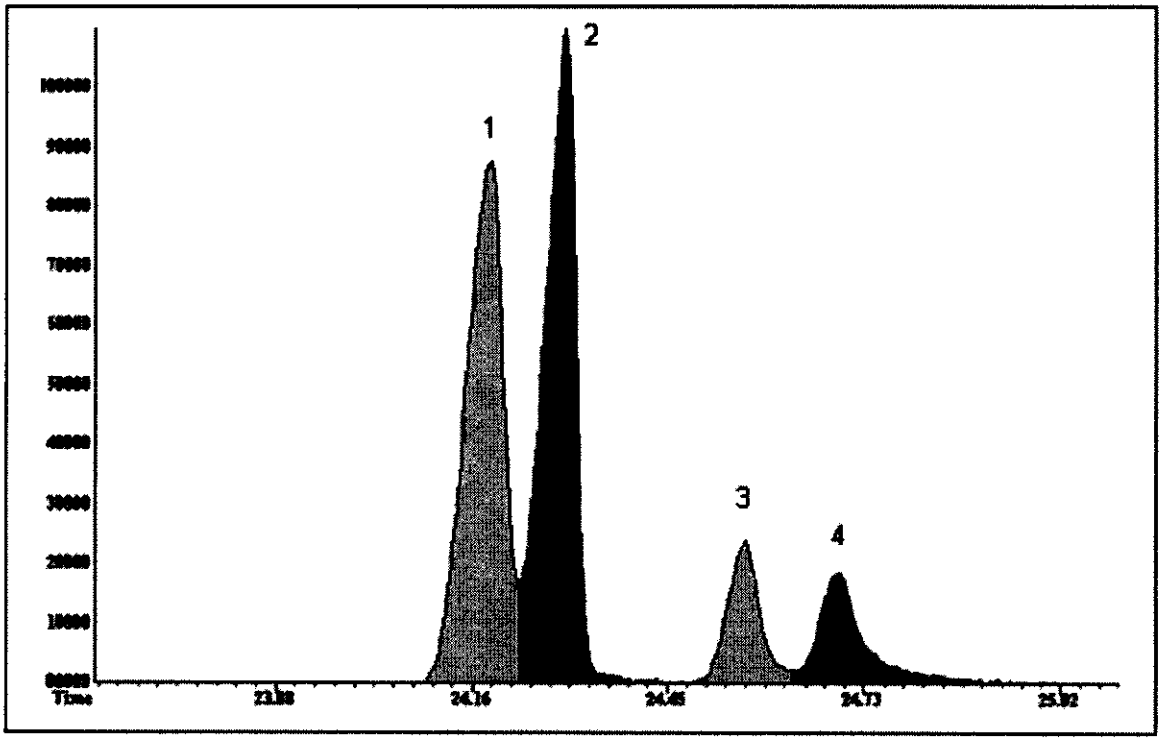

Figure 5.4. Part of the total ion chromatogram for the four isomers of commercially available β-hydroxynorvaline.

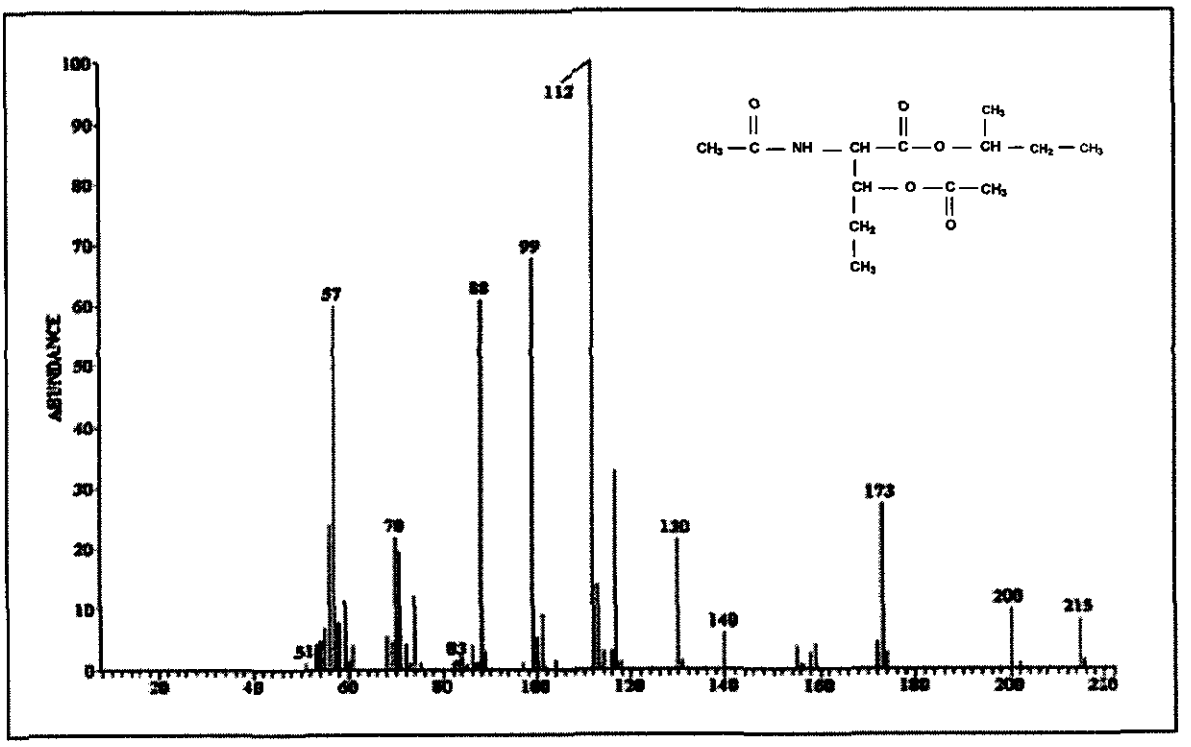

Figure 5.5. Electron ionisation spectrum of N,O-acetyl-(-)-2-butyl ester of commercially available β-hydroxynorvaline.

GC fractionation of the urine sample, collected from the mouse treated with HNV (450 mg /kg body mass), revealed that only two of the stereoisomers (Peaks 1 & 3) were preferably catabolised (Figure 5.6). Based on the knowledge that mostly amino acids with a L- or S-configuration of the α-carbon atom can be metabolised in mammalian systems, it can be inferred that the stereoisomers associated with these two peaks (Peaks 1 and 3) may exhibit the L- or S-configuration around the α-carbon atom of the molecules. The relative molar ratios of the stereoisomers were 0.05:1:0.01:0.25 (Peaks 1:2:3:4) in the mouse urine sample. The identity of the relevant peaks was again confirmed with the EI mass spectra (Figure 5.7), obtained during GC-MS analysis.

The relative molar ratios of the metabolised isomers in the urine sample were altered significantly in comparison to those in the standard synthesised HNV, confirming that metabolic preference occurred.

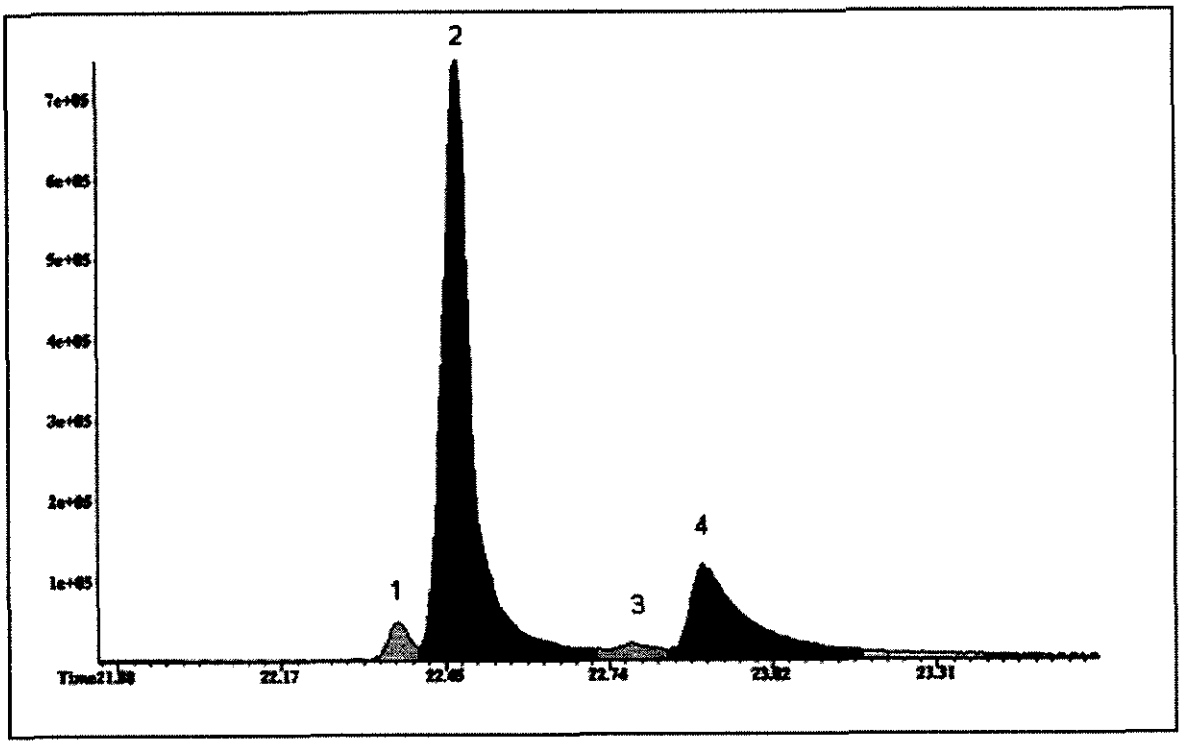

Figure 5.6. **Part of the total ion chromatogram for the separation of the four isomers of β-hydroxynorvaline from a urine sample of an HNV-treated mouse.**

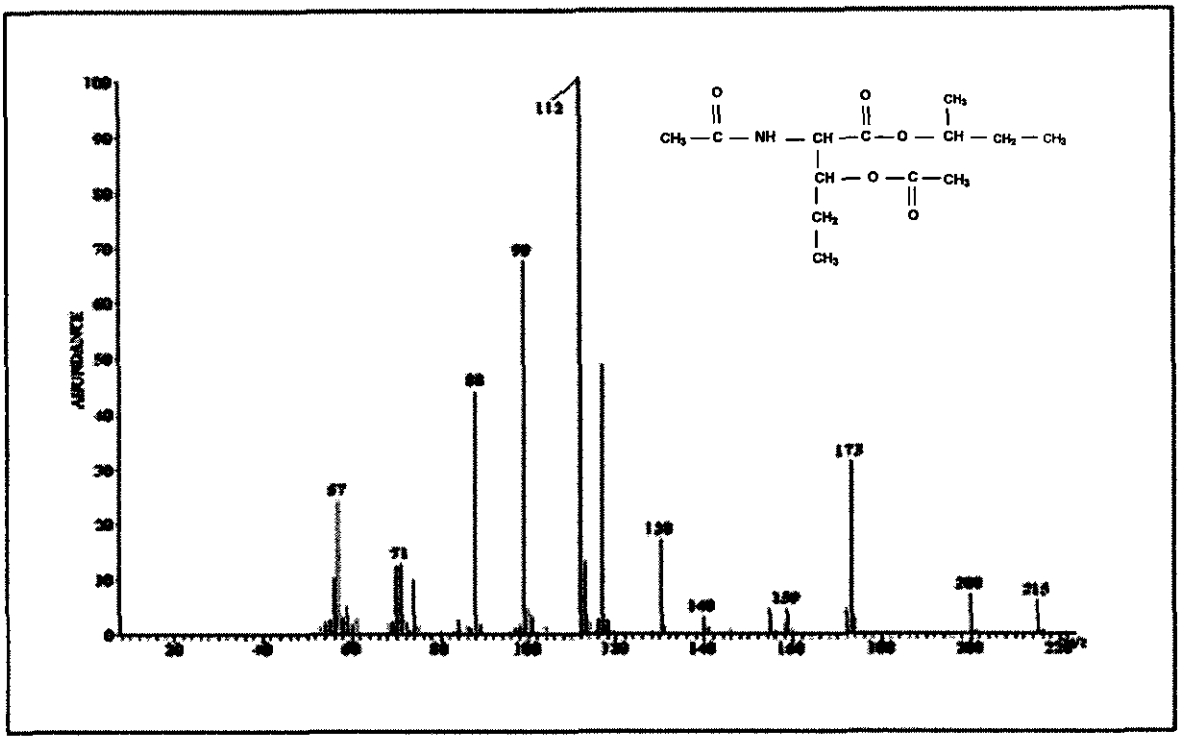

Figure 5.7. **Electron ionisation spectrum of N,O-acetyl-(-)-2-butyl ester of β-hydroxynorvaline detected in the urine of an HNV-treated mouse.**

5.4.2 2,3-Dihydroxypentanoic acid (DHPA) appears to be the main metabolite of HNV-catabolism

In order to determine if the metabolic deamination of β-hydroxynorvaline actually occurred in the mouse as previously postulated, either 2-keto-3-hydroxypentanoic acid and/or 2,3-dihydroxypentanoic acid (DHPA) had to be synthesised. The synthetic product(s) could then be used to obtain EI mass spectra in order to confirm the molecular identity of the DHPA observed in the urine of HNV treated mice.

The chemical synthesis of 2-keto-3-hydroxypentanoic acid (KHPA) was considered to be potentially problematic because of the instability of the keto-group. Most of the synthesised KHPA standard would eventually also be converted to the DHPA derivative during the derivitisation reaction, and this probable outcome could render positive identification of DHPA in the chromatograms of HNV mouse urines uncertain. The synthesis of DHPA therefore appeared to be a more attractive approach. 2,3-Dihydroxypentanoic acid was chemically synthesised from trans-2-pentenoic acid following hydroxylation with hydrogen peroxide (APPENDIX N). A small sample of the synthesised DHPA was isolated with standard liquid-extraction procedure (APPENDIX I) and derivatised with BSTFA and TMCS, prior to analysis by GC-MS.

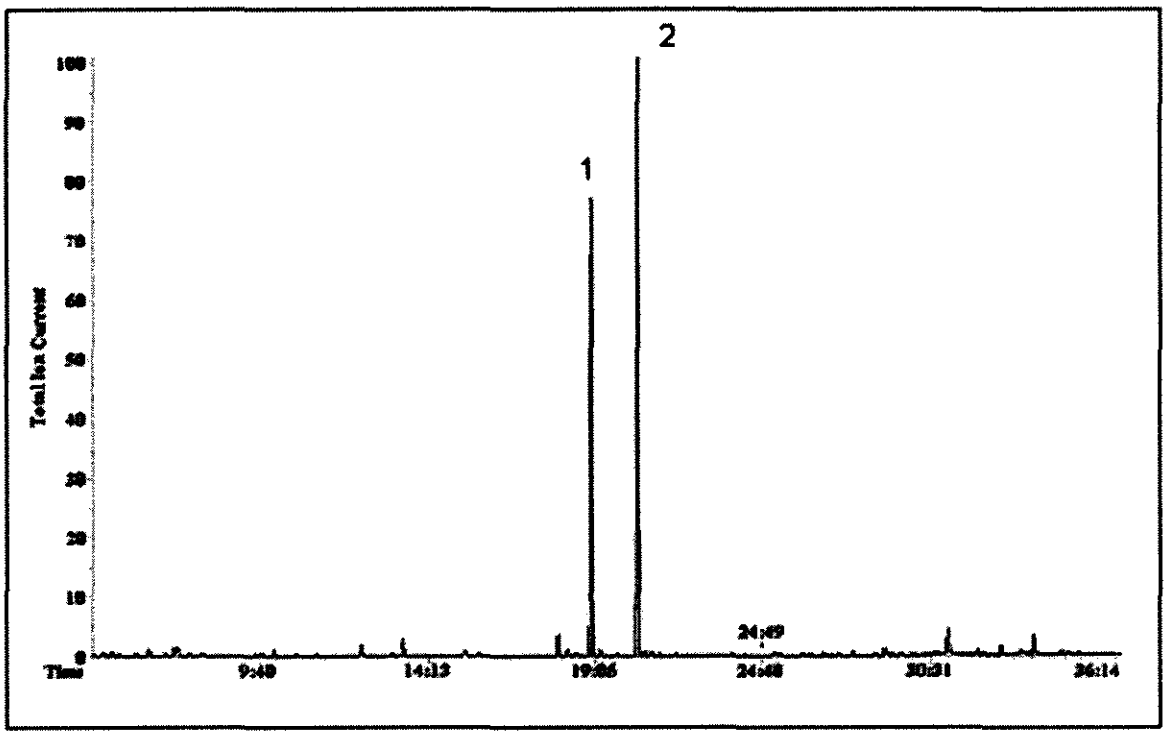

Figure 5.8. **Total ion chromatogram of the TMS-derivative of chemically synthesised 2,3-dihydroxypentanoic acid.** (1) 2,3-dihydroxypentanoic acid; (2) Phenyl butyric acid (Internal standard).

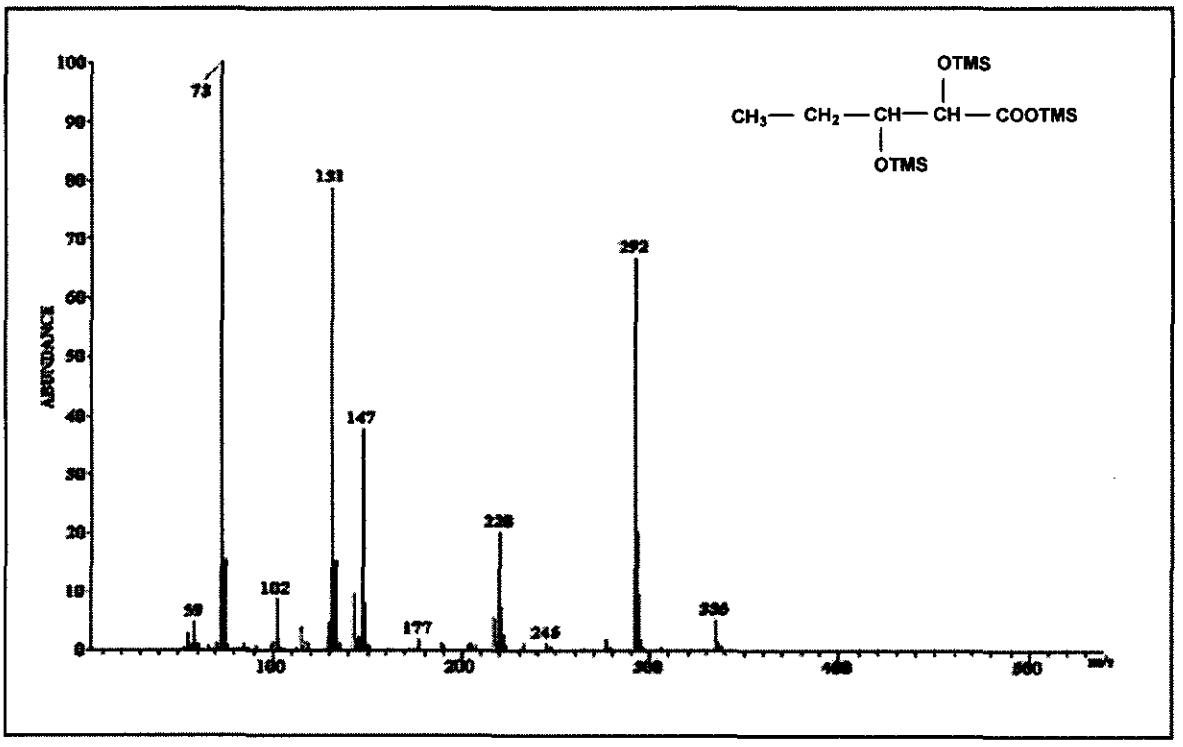

Figure 5.9. **Electron ionisation spectrum of the TMS-derivative of chemically synthesised 2,3-dihydroxypentanoic acid.**

Inspection of the collected GC-MS data and concurrent EI spectra of significant metabolic intermediates, appearing in the GC chromatogram (Figure 5.11) of derivatised urinary metabolites from a HNV treated females, confirmed the presence of the proposed metabolite, DHPA. DHPA actually proved to be the main urinary HNV-metabolite present in the urine of HNV-treated mice. Two well resolved peaks, corresponding to two stereoisomers of DHPA were detected in the chromatograms. No attempt was made to isolate and identify the individual stereoisomers. Concurrent EI mass spectra of the two peaks observed in the HNV treated mouse urine samples (Figure 5.12) were compared to EI mass spectra obtained for the synthesised DHPA (Figure 5.9) and confirmed the molecular identity of the urinary DHPA.

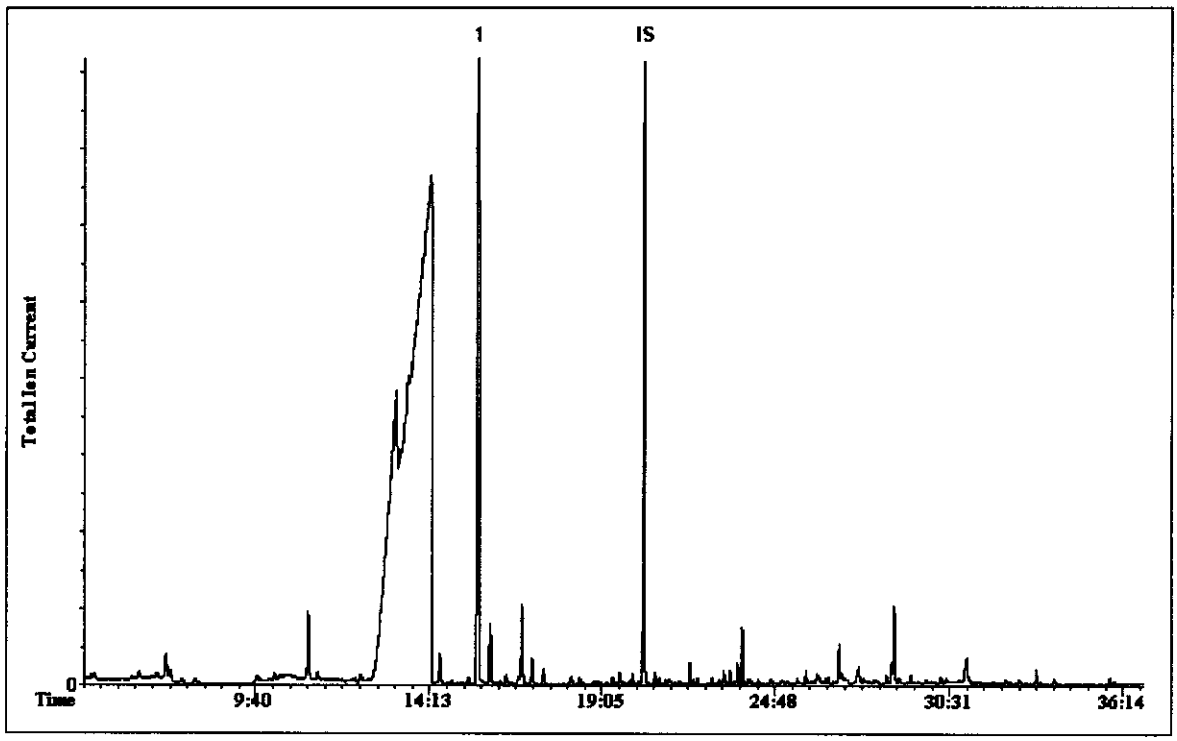

Figure 5.10. Urinary organic acid profile of a control mouse. (1) Thymol; (IS) 3-phenylbutyric acid (internal standard).

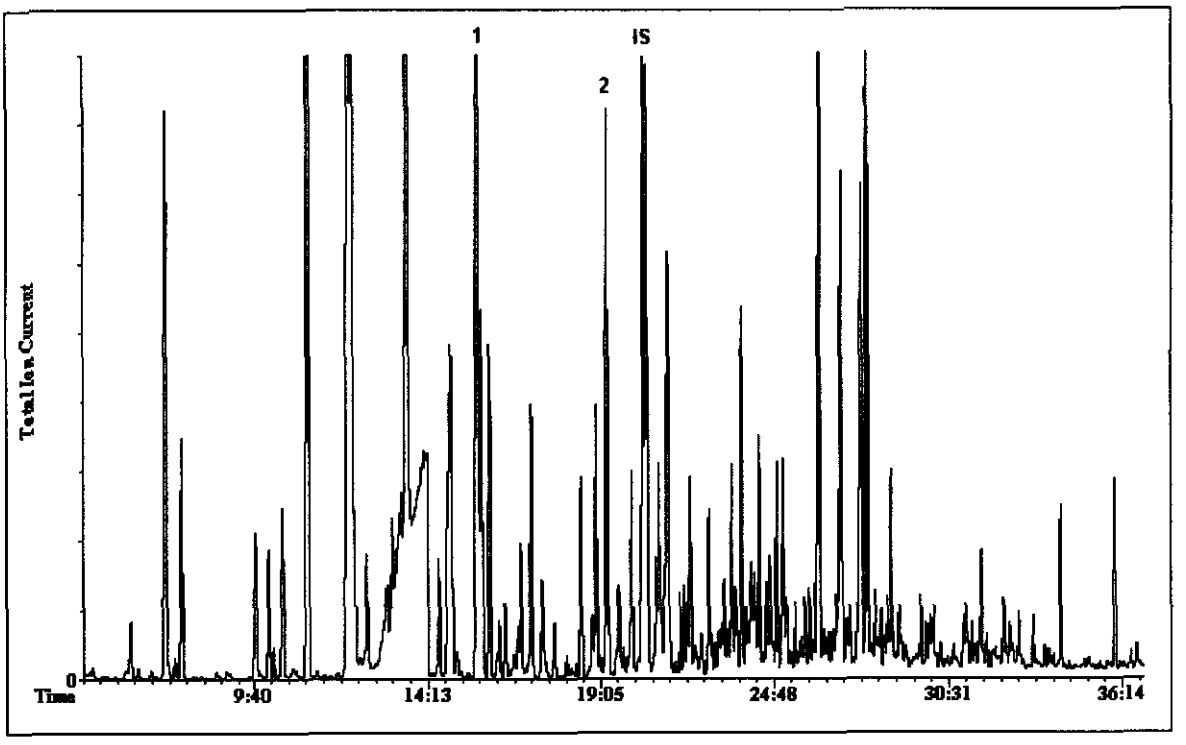

Figure 5.11. Urinary organic acid profile of a pregnant female mouse treated with 450 mg/kg HNV. (1) Thymol; (2) 2,3-dihydroxypentanoic acid; (IS) 3-phenylbutyric acid (internal standard).

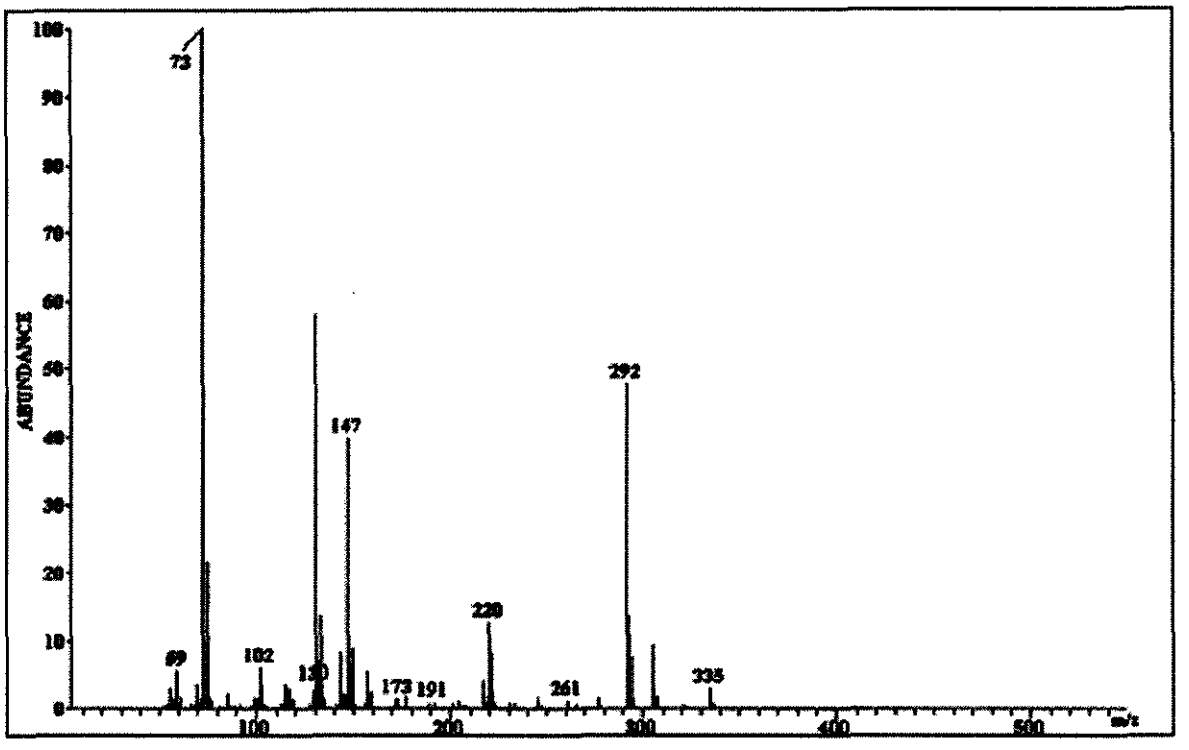

Figure 5.12. Electron ionisation spectrum of the TMS-derivative of urinary 2,3-dihydroxypentanoic acid. (Mouse treated orally with 450 mg/kg HNV).

Our results clearly indicated that specific stereoisomers of HNV were metabolised by the mouse in the same way that amino acids are normally metabolised in mammalian systems (Section 5.4.1, Figure 5.2 and Figure 5.13). Transamination of HNV most probably gave rise to 2-keto-3-hydroxypentanoic acid, which was then subsequently converted to 2,3-dihydroxypentanoic acid by a dehydrogenase enzyme.

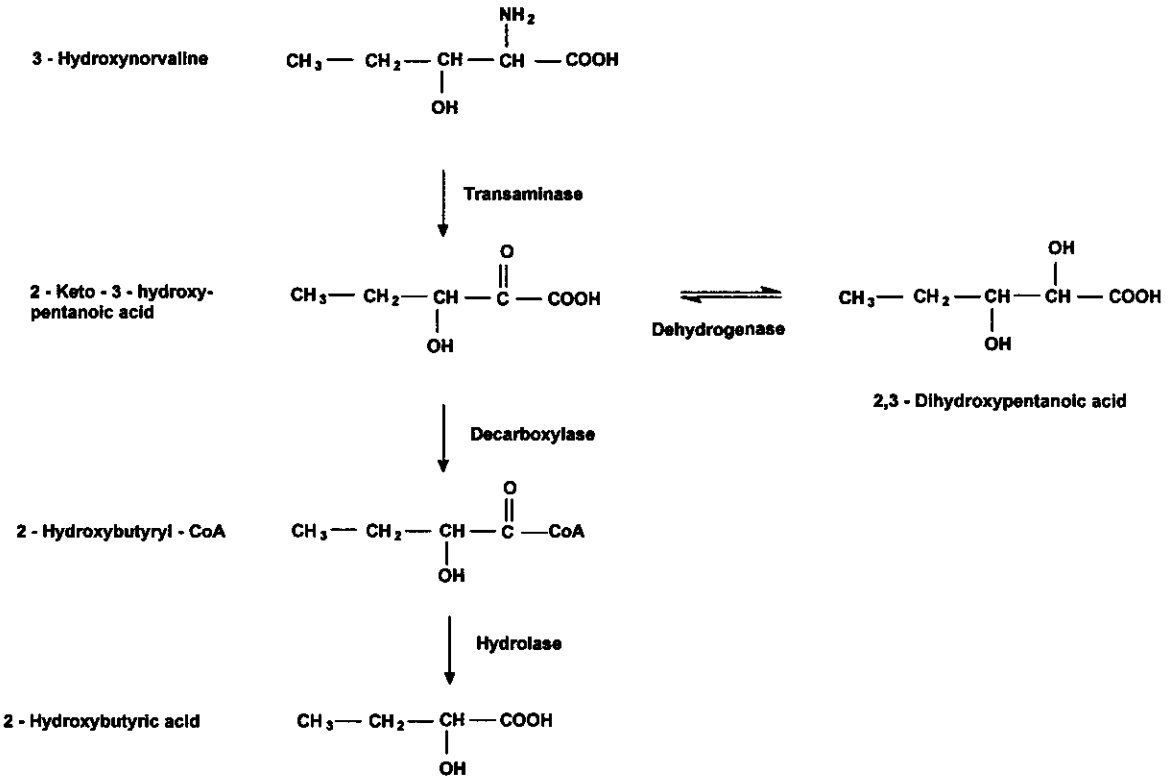

Figure 5.13. Proposed synthesis of 2,3-dihydroxypentanoic acid from β-hydroxynorvaline in the mouse.

5.4.3 Probable effects of HNV metabolites on β-oxidation

β-Oxidation of fatty acids occurs in the mitochondria. Fatty acids are activated by the long chain acyl-CoA synthetase enzyme to form acyl-CoA derivatives. A carnitine shuttle system is needed to transport long chain fatty acids across the inner mitochondrial membrane, into the mitochondrial matrix. Once inside the mitochondrial matrix, the fatty acid is released by transacylation in the acyl-CoA form. The latter compound can then be catabolised *via* β-oxidation, through a

series of reactions ultimately producing acetyl-CoA and an acyl-CoA derivative, two carbon units shorter than the original acyl-CoA (Figure 5.3).

The biochemical manifestations of fatty acid oxidation disorders include deficient production of energy-yielding metabolites (acetyl-CoA and ketone bodies) and the accumulation of free fatty acids and toxic acyl-CoA derivatives upstream of the enzymatic/metabolic block. This will lead to the formation of dicarboxylic acids and hydroxy-dicarboxylic acids from fatty acids via ω- and ω-1-oxidation. Acyl-CoA esters can be converted to their corresponding acylglycines (mediated through the action of glycine-N-acyltransferase) and acylcarnitines. The metabolic purposes of the production of the acylglycines and acylcarnitines are detoxification and the ultimate replenishment of the free CoA stores. A secondary detrimental effect may be a depletion of free L-carnitine due to the formation of excessive levels of acylcarnitines (Sim, 2002) from an induced accumulation of excessive levels of metabolic intermediates. This phenomenon may eventually affect the flow of fatty acids into the mitochondria and the ultimate production of energy (ATP) by the mitochondria.

2,3-Dihydroxyvaleryl-CoA, a β-hydroxynorvaline metabolite, can potentially influence β-oxidation of fatty acids. If the 2,3-dihydoxyvaleryl-CoA is transported to the mitochondria, it can potentially be catabolised by β-oxidation. Due to the hydroxy-group on the C2-atom of the HNV molecule, the activity of one or more of the enzymes involved in β-oxidation of fatty acids may be compromised. If an intermediate is formed that cannot be completely broken down *via* β-oxidation, this metabolite may accumulate and subsequently inhibit the catabolism of other fatty acids. Glycine conjugates (acylglycines) and acylcarnitines may also be excreted in large quantities *via* the urine, a clear indication that β-oxidation is affected by HNV metabolites. To investigate this probable outcome, organic acids occurring in the urine samples from control and HNV-treated, pregnant female mice were analysed by GC-MS employing the standardised method.

Table 5.1. Urinary organic acid concentrations of control and HNV-treated pregnant female mice.

Metabolite	Control (mean)	HNV-treated (mean)
Acyl-CoA metabolites		
Butyryl-glycine	0	148.8
Isobutyryl-glycine	0	161.6
Valeryl-glycine	0	20.4
Isovaleryl-glycine	0.4	153.9
Crotonyl-glycine	0	110.0
3-Methyl-crotonyl-glycine	0	6.6
Hexanoyl-glycine	1.6	45.9
Hydroxyacyl-CoA metabolites		
3-Hydroxy-caproic acid	11.9	113.7
Ketoacyl-CoA metabolites		
3-Ketocaproic acid	3.1	17.6
3-Ketovaleric acid	0	10.3

Concentrations in mmol/mol creatinine

Quantitative data derived from organic acid profiles is summarised in Table 5.1 in a highly abbreviated form, unequivocally demonstrated that HNV affected β-oxidation through an inhibition of the β-ketothiolase step of β-oxidation. Mice treated with HNV excreted relatively large quantities of glycine conjugates (acylglycines), as compared to control mice. Glycine conjugates are normally not detected in mammalian urine in large quantities. Elevated levels may therefore be regarded as an indication of the accumulation of fatty acid intermediates (acyl-CoA), due to a metabolic block in β-oxidation of fatty acids (Sim, 2002).

Hydroxyacyl-CoA and ketoacyl-CoA derivatives are also increased in HNV treated experimental mice, although low concentrations of these metabolites were also detected in controls. The ketoacyl-CoA derivatives can normally be cleaved by β-ketothiolase to produce acetyl-CoA and an acyl-CoA derivative, two carbon units

shorter than the original acyl-CoA. Inhibition of this enzyme will cause an accumulation of all the preceding intermediates, prior to the metabolic block with the subsequent excretion of the accumulating metabolic intermediates into the urine.

The attempted β-oxidation of 2,3-dihydroxyvaleryl-CoA to hydroxyacetyl-CoA may encounter several problems, since the hydroxy-group in the 2-position (Figure 5.14) may effect steric hindrance and render the reaction non-feasible. Since the metabolic profile exhibited a block at the β-thiolase enzyme step, it can be inferred that the intermediate produced from 2,3-dihydroxyvaleryl-CoA could not be metabolised by β-ketothiolase. Increased levels of metabolites were observed for intermediates up to the formation of the ketoacyl-CoA. It would therefore appear that 2,3-dihydroxyvaleryl-CoA could only be metabolised up to this point in the β-oxidation route. 2-Hydroxy-3-keto-butyryl-CoA could therefore not be cleaved by β-ketothiolase to produce acetyl-CoA and hydroxyacetyl-CoA. The inability of the enzyme to metabolise the intermediate will inhibit the thiolytic cleavage of other 3-ketoacyl-CoA derivatives, causing a metabolic block in the catabolism of fatty acids in general.

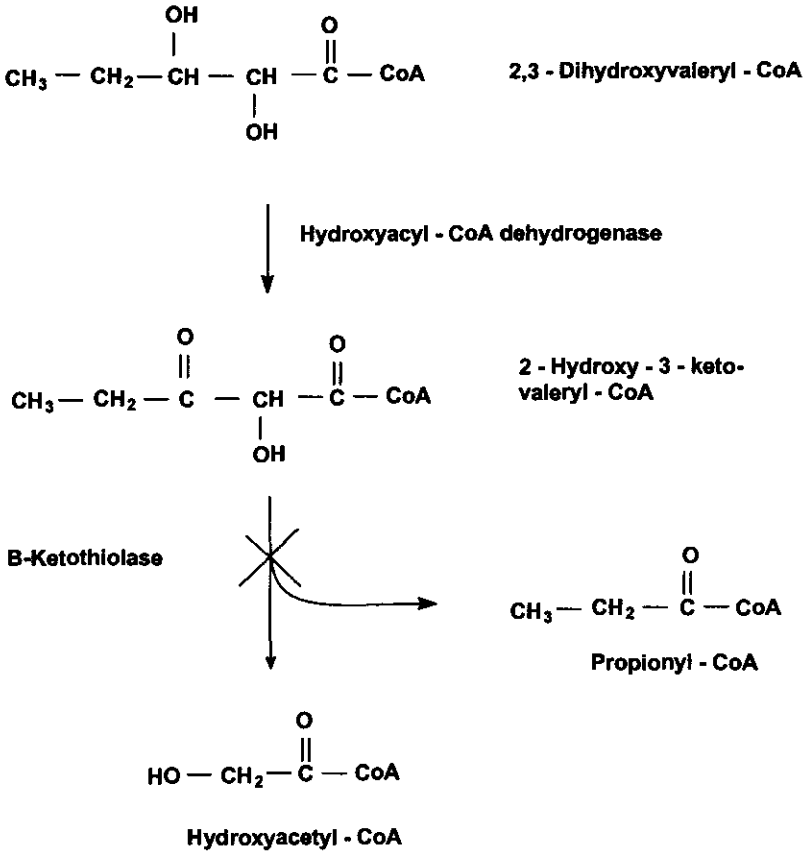

Figure 5.14. Schematic diagram of the proposed catabolism of 2,3-dihydroxyvaleryl-CoA by β-oxidation.

5.4.4 Isoleucine catabolism and HNV-metabolites

At least four different thiolases occur in mammalian tissue. All of them are capable of acting on acetoacetyl-CoA, but only two can utilise 2-methylacetoacetyl-CoA as a substrate (Middleton, 1973; Middleton, 1983). A cytosolic acetoacetyl-CoA thiolase, specific for acetoacetyl-CoA, can be activated by K^+, or inhibited by CoA but not by other substrates and functions in ketone body synthesis and utilisation. A peroxisomal 3-oxoacyl-CoA thiolase with a broad chain-length specificity functions in the peroxisomal β-oxidation of fatty acids (Miyazawa, 1980; Miyazawa, 1981). A similar 3-oxoacyl-CoA thiolase functions in the β-oxidation of fatty acids in the mitochondria. This enzyme also displays broad chain-length specificity, is not stimulated by K^+ and is not inhibited by CoA or high concentrations of the other substrates (Sweetman, 1995). The mitochondrial acetoacetyl-CoA thiolase is specific for both 2-methylacetoacetyl-CoA and acetoacetyl-CoA. This enzyme is

stimulated about fourfold by K^+ and is inhibited by high substrate concentrations, but not by coenzyme A. Its function in most tissues is the catabolism of isoleucine. In the liver it also functions in β-oxidation of fatty acids and in ketogenesis through the synthesis of acetyl-CoA and acetoacetyl-CoA for 3-hydroxy-3-methylglutaryl-CoA (HMGCoA) synthesis.

In the mouse model, β-hydroxynorvaline metabolites appear to inhibit β-ketothiolase (3-oxoacyl-CoA thiolase and/or mitochondrial acetoacetyl-CoA thiolase) in the β-oxidation route. 3-Oxoacyl-CoA thiolase is involved in the cleavage of medium- and long-chain ketoacyl-CoA derivatives and mitochondrial acetoacetyl-CoA thiolase assists with the cleavage of short-chain ketoacyl CoA derivatives. Mitochondrial acetoacetyl-CoA is also involved in the catabolism of L-isoleucine. The thiolase enzyme involved in the catabolism of leucine is often referred to a 2-methylacetoacetate thiolase, although it is the same enzyme as the one involved in β-oxidation of fatty acids. Since metabolic profiles of HNV-treated female mice suggested that β-ketothiolase may be inhibited, it could be inferred that isoleucine catabolism may also be affected by HNV-metabolites.

L-Isoleucine is catabolised exclusively in muscle cells, since these cells contain branched-chain amino acid aminotransferases, essential for the catabolism of branched-chain amino acids. The catabolic breakdown of isoleucine starts with a transamination reaction to form 2-keto-3-methylvalerate. The latter is transported to the mitochondria where progressive catabolic breakdown ultimately leads to the formation of 2-methylacetoacetyl-CoA (Figure 5.15). This metabolite is then cleaved by 2-methylacetoacetate thiolase to produce acetyl-CoA and propionyl-CoA. Accumulation of intermediate metabolites from the isoleucine catabolic route should be quite prominent in the urinary metabolic profiles if HNV metabolites inhibited the 2-methylacetoacetate thiolase. To investigate this, the presence and quantities of the relevant intermediate metabolites were determined in control and HNV treated experimental mice urine samples employing the same standard method for organic acid analysis previously described.

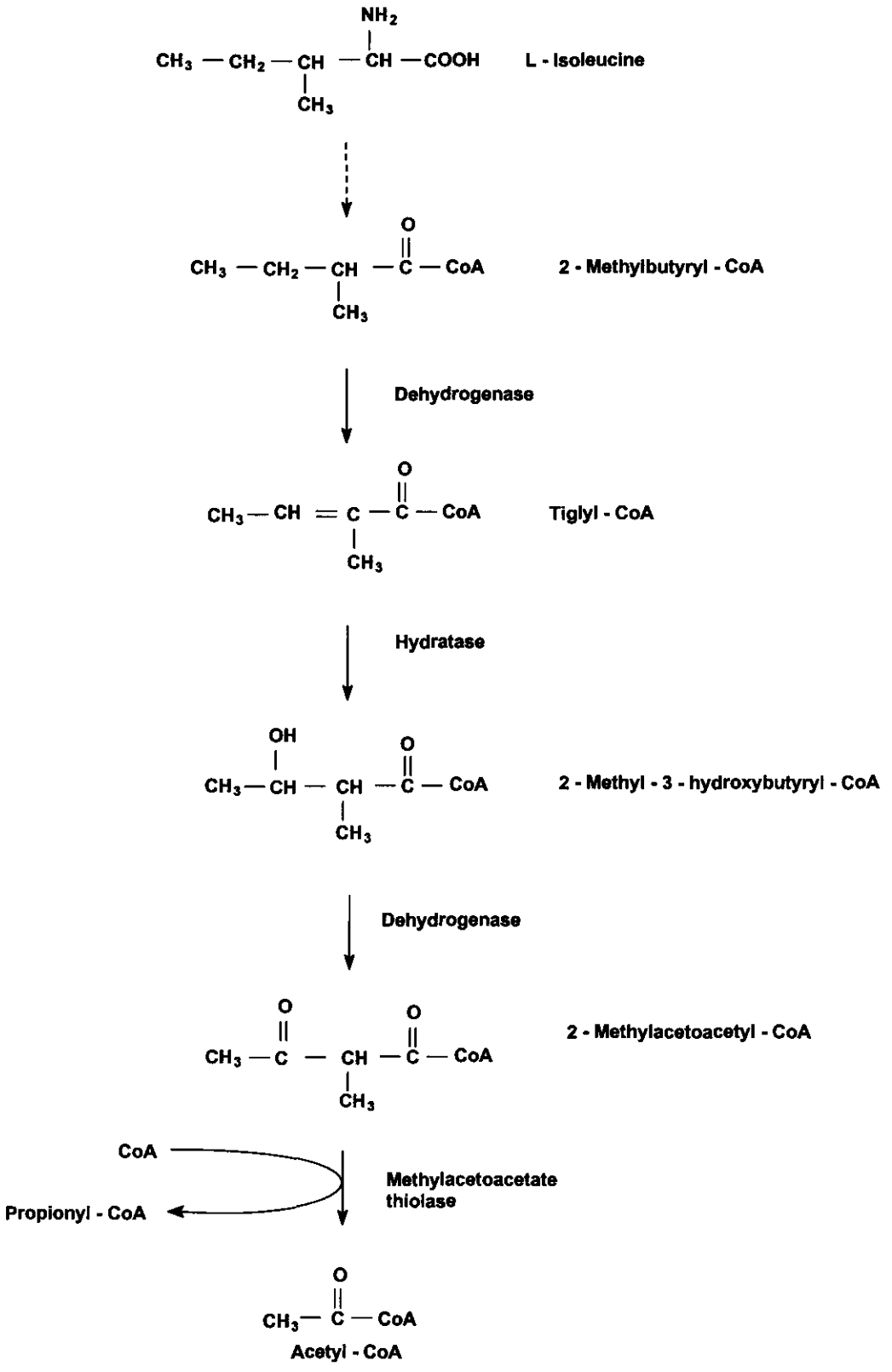

Figure 5.15. Schematic diagram of isoleucine catabolism.

Table 5.2. Urinary organic acid concentrations of control and HNV-treated pregnant female mice.

Metabolite	Control (mean)	HNV-treated (mean)
Tiglylglycine	0	27.6
2-Methyl-3-hydroxybutyric acid	0	22.7
2-Methylacetoacetate	0	13.5
Isoleucine/leucine	1119.9	799.8

Concentrations in mmol/mol creatinine. Although the mean isoleucine/leucine concentration decreased in the experimental animals, it was not statistically significant.

The resultant profiles indicated that relatively high levels of intermediate catabolic metabolites, derived from isoleucine, were indeed excreted in the urine of HNV treated mice. Control mice, on the other hand, excreted no detectable levels of either tiglylglycine or 2-methyl-3-ketobutyric acid (2-methylacetoacetic acid). These two intermediates were, however, excreted in HNV treated mice and seemed to point to a possible metabolic block in isoleucine catabolism. The mean isoleucine/leucine concentration in the HNV treated mice was lower than the control mice, although the difference was not statistically significant.

2,3-Dihydroxyvaleryl-CoA (2,3-dihydroxypentanoyl-CoA), a major HNV-metabolite, was most probably the most important metabolite involved in the inhibition of isoleucine catabolism. Two possible explanations exist for the inhibition of isoleucine catabolism by HNV-metabolites. The isoleucine catabolic route can potentially catabolise 2,3-dihydroxyvaleryl-CoA, since it closely resembles the structure of 2-methyl-3-hydroxybutyryl-CoA, an intermediate in isoleucine catabolism. Catabolic conversion of 2,3-dihydroxyvaleryl-CoA will lead to the formation of 2-hydroxy-3-ketovaleryl-CoA (Figure 5.16). The latter metabolite may perhaps not be effectively utilised by methylacetoacetate thiolase as a substrate in the production of propionyl-CoA and hydroxyacetyl-CoA.

The inability of methylacetoacetate thiolase to cleave 2-hydroxy-3-ketovaleryl-CoA may lead to an accumulation of the latter compound, amplifying the inhibitory effect of HNV metabolites on methylacetoacetate thiolase. The inhibition of the

latter enzyme may ultimately adversely affect the catabolic breakdown of L-leucine. This may in turn lead to an accumulation of relatively high levels of leucine related intermediates in the tissues and blood of HNV treated animals, followed by excretion of these metabolites in the urine of such animals. Secondly, the inhibition of methylacetoacetyl-CoA thiolase may be directly caused by 2,3-dihydroxyvaleryl-CoA itself, if the latter HNV derived metabolite can not be converted to 2-hydroxy-3-keto-valeryl-CoA by the dehydrogenase enzyme. If this was the case, accumulating levels of 2,3-dihydroxyvaleryl-CoA may be responsible for a direct inhibition of methylacetoacetyl-CoA thiolase.

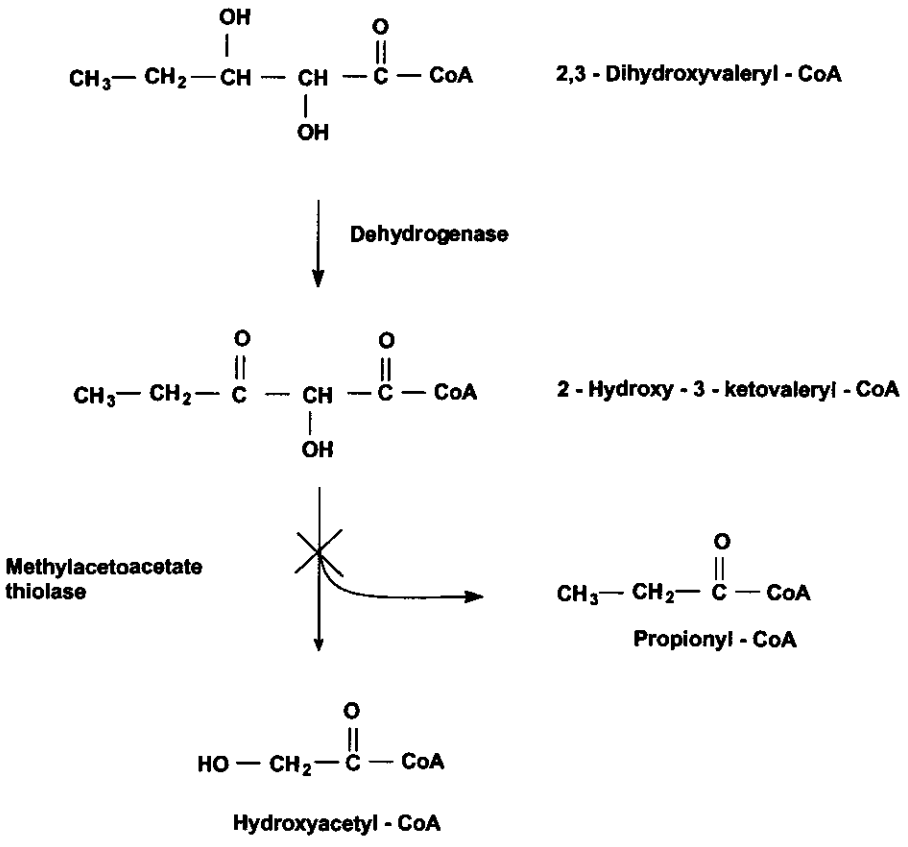

Figure 5.16. Schematic diagram of the proposed effect of 2,3-dihydroxy-valeryl-CoA on isoleucine catabolism.

β-Ketothiolase (3-oxothiolase) is a generic name for a group of enzymes. Originally, a defect in any one of these enzymes was referred to as a "β-ketothiolase defect". However, patients with defects in various subtypes of thiolases are known to display a variety of clinical and biochemical abnormalities.

Due to this problem, it became preferable to use a more specific nomenclature to describe a specific defect.

2-Methylacetoacetyl-CoA thiolase deficiency was first described in 1971. Daum *et al.* (1971) studied a 6-year-old boy with metabolic acidosis and identified 2-methylacetoacetic and 2-methyl-3-hydroxybutyric acids in his urine. A more thorough metabolic study was conducted more recently on twin brothers with 2-methylacetoacetyl-CoA thiolase deficiency (Fontaine, 1996). The main clinical features included important staturo-ponderal delay, frequent infectious rhinopharyngitis episodes and acute metabolic acidosis. Biochemical analysis revealed excessive excretion of tiglylglycine, 2-methyl-3-hydroxybutyrate, 3-hydroxyisovalerate, 2-methylglutaconate, adipate and 2-methylacetoacetate. Blood carnitine levels were altered with increased total and esterified carnitines and an increase in the acylcarnitine:free carnitine ratio.

Experimental mice treated with HNV excreted abnormally high levels of tiglylglycine, 2-methyl-3-hydroxybutyrate, 2-methylacetoacetate, adipate, 3-hydroxyisovalerate and 2-methylglutaconate. Some of these metabolites appear to be characteristic of a 2-methylacetoacetyl-CoA thiolase (mitochondrial acetoacetyl-CoA thiolase) deficiency. The most characteristic elevated urinary metabolite of a deficiency of 2-methylacetoacetyl-CoA thiolase is 2-methyl-3-hydroxybutyrate. This is often accompanied by elevated 2-methylacetoacetate concentrations. Most 2-methylacetoacetyl-CoA thiolase deficient patients also excrete tiglylglycine, however, some do not (Sweetman, 1995). The excreted 2-methylglutaconate is derived from the decarboxylation of tiglyl-CoA. One may therefore conclude that β-hydroxynorvaline metabolites induce a 2-methyl-acetoacetyl-CoA thiolase deficiency in pregnant female mice.

In mitochondrial disorders, L-carnitine not only stimulates acyl-CoA oxidation pathways whose capacities are reduced, but also acts as a detoxification agent that facilitates the removal of these acyl moieties. In the twins affected by a 2-methyacetoacetyl-CoA thiolase deficiency, blood carnitine levels were altered. Total and esterified carnitines were increased as well as the acylcarnitine:free carnitine ratio (Fontaine, 1996).

Table 5.3 Urinary carnitine concentrations of control and HNV-treated pregnant female mice.

Metabolite	Control (mean)	HNV-treated (mean)
Free carnitine	280.4	132.9
Acetylcarnitine	22.0	22.9
Isovalerylcarnitine	0.35	0.38
Octanoylcarnitine	0.07	0.17

Concentrations in mmol/mol creatinine. Due to analytical limitations, only these carnitines were quantified. See APPENDIX K for a more detailed discussion.

Free carnitine stores were dramatically depleted in HNV-treated experimental animals, compared to that observed in the controls (Table 5.3). This decrease was statistically significant ($p = 0.023$; Mann-Whitney U test). The mean free carnitine in control mice urine was 280.4 ± 119.9 mmol/mol creatinine and that in the HNV treated experimental mice was only 132.9 ± 30.0 mmol/mol creatinine, a 53 % decrease.

β-Hydroxynorvaline also exhibited a statistically significant effect ($p = 0.023$; Mann-Whitney U test) on the mean acylcarnitine:free carnitine ratio of these pregnant female mice (Figure 5.17). The mean acylcarnitine:free carnitine ratio in control mice urine was 0.10 ± 0.06 and that in the HNV treated experimental mice was 0.18 ± 0.07, an 80 % increase. This increase was consistent with an induced mitochondrial disorder and a 2-methyacetoacetyl-CoA thiolase deficiency (Fontaine, 1996).

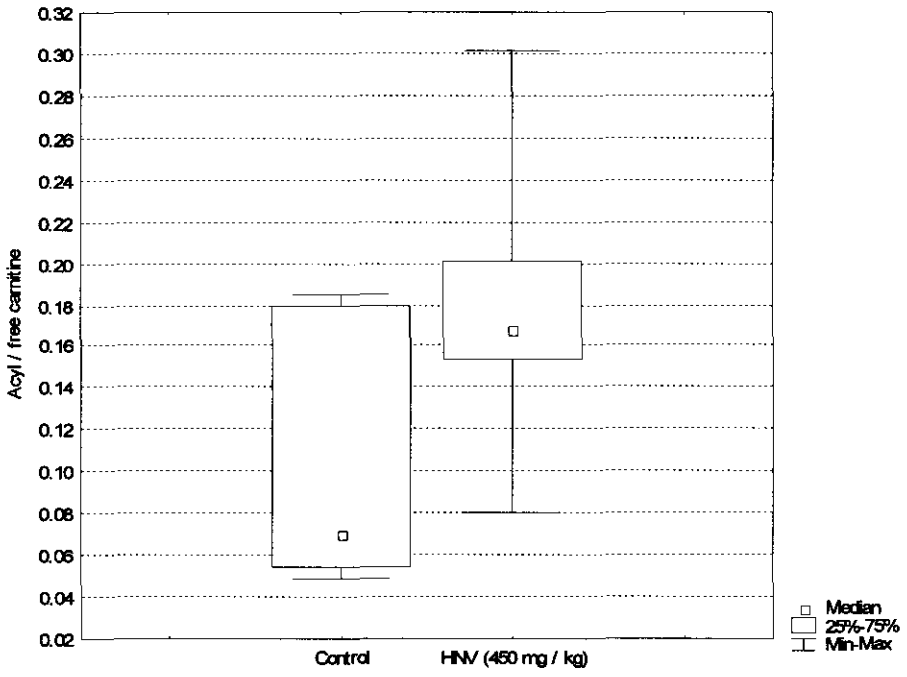

Figure 5.17. Acylcarnitine:free carnitine ratio in urine of pregnant female mice.

5.4.5 Inhibition of ketone body metabolism by 2,3-dihydroxypentanoic acid

Ketone body metabolism also involves a thiolase enzyme, cytosolic acetoacetate thiolase. Ketone bodies (acetone, acetoacetate and D-3-hydroxybutyrate) are formed during ketogenesis form fatty acids, derived from triacylglycerol. Certain amino acids are also ketogenic (leucine, isoleucine, lysine, phenylalanine, tyrosine and tryptophan).

During starvation, ketone bodies are used as respiratory "fuel". D-3-hydroxy-butyrate is converted to acetoacetate before it is activated by succinyl-CoA to form acetoacetyl-CoA (Figure 5.18). Acetoacetate thiolase is responsible for the cleavage of acetoacetyl-CoA to produce two molecules acetyl-CoA. The acetyl-CoA can then be catabolised *via* the citric acid cycle to produce ATP and NADH. More ATP is eventually produced from the NADH by the process of oxidative phosphorylation.

Since β-hydroxynorvaline metabolites appeared to be able to inhibit mitochondrial acetoacetyl-CoA thiolase, it is probable that it may also affect the activity of

cytosolic acetoacetyl-CoA thiolase. Inhibition of cytosolic acetoacetyl-CoA thiolase will lead to elevated 3-hydroxybutyric acid and acetoacetate (3-ketobutyric acid) levels in the urine of mice treated with HNV. This notion was subsequently investigated in urine samples from control- and HNV-exposed mice.

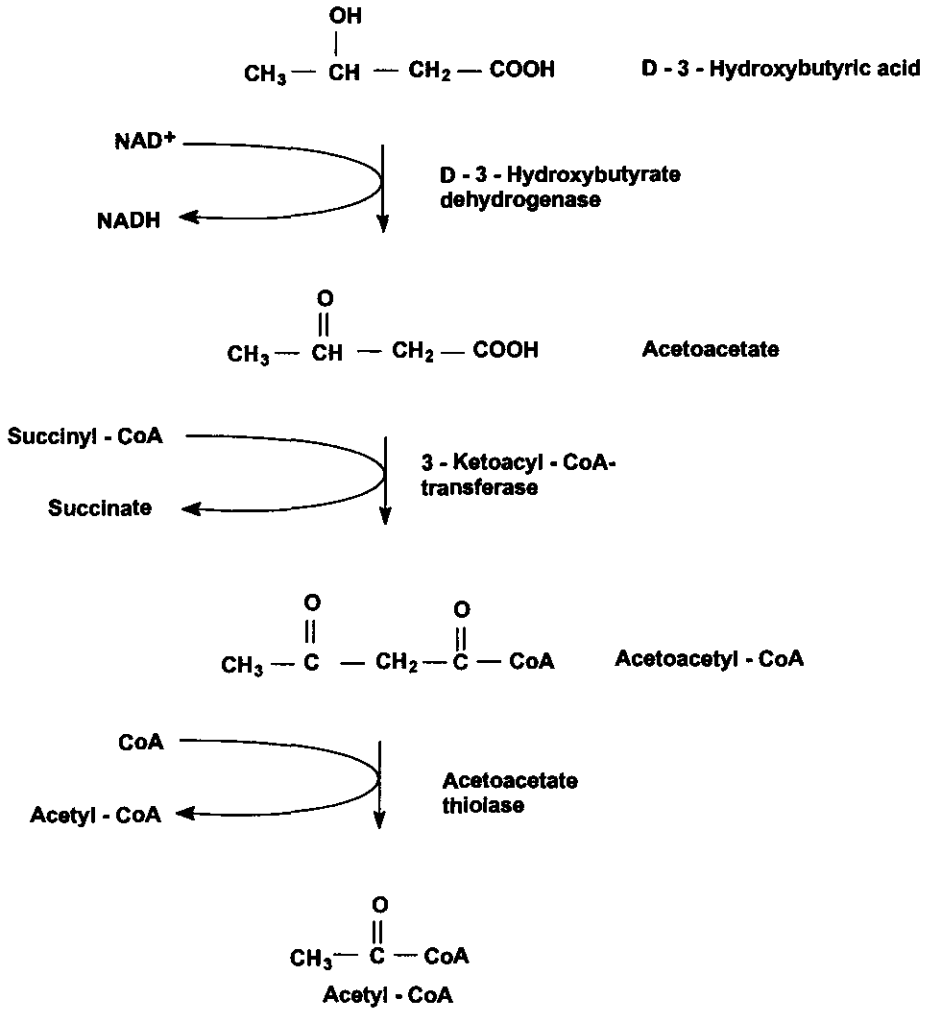

Figure 5.18. Schematic diagram of ketone body utilisation.

Table 5.4. Urinary organic acid concentrations of control and HNV-treated pregnant female mice.

Metabolite	Control (mean)	HNV-treated (mean)
3-Hydroxybutyric acid	20.2	474.8
3-Ketobutyric acid	0.9	655.3

Concentrations in mmol/mol creatinine.

Ketone body utilisation was greatly affected by β-hydroxynorvaline. HNV-treated experimental mice excreted relatively large quantities 3-hydroxybutyric acid and 3-ketobutyric acid, compared to the controls. The excretion of 3-hydroxybutyric acid in the experimental mice was approximately 25 fold higher than that of the control animals. The controls excreted virtually no 3-ketobutyric acid, but the HNV treated mice excreted on average 655 mmol 3-ketobutyric acid per mol creatinine (approximately a 1000-fold increase).

The inhibition of cytosolic acetoacetyl-CoA thiolase was most likely due to the catabolism of 2,3-dihydroxypentanoic acid (Figure 5.19). This metabolite is structurally related to the structure of 3-hydroxybutyric acid, the primary substrate for ketone body utilisation. DHPA was probably converted to 2-hydroxy-3-ketopentanoic acid through the action of hydroxybutyrate dehydrogenase. The resultant keto acid, 2-hydroxy-3-ketopentanoic acid, was probably transformed to 2-hydroxy-3-ketovaleryl-CoA and the latter compound then cleaved by acetoacetate thiolase to form propionyl CoA and hydroxyacetyl-CoA. The organic acid profiles, however, suggested that the acetoacetate thiolase may have been unable to perform this step. As a result, 2-hydroxy-3-ketovaleryl-CoA accumulated and may have contributed to the inhibition of acetoacetate thiolase and eventual under utilisation of ketone bodies as an energy source.

Cytoplasmic acetoacetyl-CoA thiolase deficiency was first reported by De Groot *et al.* (1977). A 4-month old first born child from unrelated parents presented with delayed motor development, ataxic and choreoathetoid movements, involuntary eye movements and hypertonia. Blood lactate and pyruvate levels were constantly above normal with high blood 3-hydroxybutyrate and acetoacetate concentrations. Another case was reported with cytosolic acetoacetyl-CoA thiolase deficiency, associated with mental retardation (Bennett, 1984). The boy also excreted elevated 3-hydroxybutyrate and acetoacetate. Enzyme analysis on cultured fibroblasts revealed a probable defect in cytosolic acetoacetyl-CoA thiolase, displaying about 50% of the activity of control fibroblasts. Mitochondrial acetoacetate thiolase activity was apparently normal.

The metabolic profiles presented in mice treated with HNV appear to be consistent with a β-ketothiolase defect. The inhibitory effect of the HNV-metabolites did not appear to be limited to a single thiolase enzyme but to the activity of all the cellular thiolases. As a result, the metabolic profiles of HNV-treated animals were typical that of a mitochondrial acetoacetyl-CoA thiolase defect combined with a cytosolic acetoacetyl-CoA Thiolase defect. Energy generation in the HNV-treated animals was therefore not only limited through an inhibition of β-oxidation, but also *via* an inhibition of ketone body utilisation, an effect clearly confirmed by altered [3-hydroxybutyrate]/[acetoacetate] ratios in the HNV treated experimental animals. These actions of HNV obviously pose severe consequences for the pregnant mice and their developing embryos.

According to reported data, the [3-hydroxybutyrate]/[acetoacetate] ratio is directly proportional to the [NADH]/[NAD^+] ratio in the mitochondria (Williamson, 1967) due to the action of 3-hydroxybutyrate dehydrogenase (Equation 5.1). This enzyme is very active in the liver and can therefore be assumed that it catalyses a reaction that operates close to equilibrium (Williamson, 1967). Therefore the [NADH]/[NAD^+] ratio can be calculated by employing Equation 5.1 (Modified from Williamson, 1967):.

$$\frac{[3\text{-}hydroxybutyrate]}{[acetoacetate]} = \frac{[NADH]}{[NAD^+]} \times \frac{1}{K_{HBD}} \qquad \textbf{(5.1)}$$

Where:

[3-hydroxybutyrate] = the concentration of 3-hydroxybutyrate

[acetoacetate] = the concentration of acetoacetate

[NADH] = the concentration of NADH

[NAD^+] = the concentration of DNA^+

K_{HBD} = the apparent equilibrium constant for the 3-hydroxybutyrate dehydrogenase reaction.

The [3-hydroxybutyrate]/[acetoacetate] ratio is approximately 20:1 in the control mice but changed to 0.7:1 in the experimental mice, therefore indicating a severe limitation in the production of NADH. The [NADH]/[NAD^+] ratio plays an important role in the regulation of the intracellular redox state and is often considered a valuable measure of the metabolic state of an organism. Many metabolic enzymes

appear to be regulated by the [NADH]/[NAD$^+$] ratio, including the glycolytic enzyme glyceraldehyde 3-phosphate dehydrogenase and the pyruvate dehydrogenase complex, which converts pyruvate to acetyl-CoA, a substrate for the citric acid cycle.

A number of human diseases have been associated with changes in the [NADH]/[NAD$^+$] ratio (Lin, 2003). Most importantly, an altered [NADH]/[NAD$^+$] ratio have been positively linked to cellular apoptosis (Luo, 2001; Vaziri, 2001). In the case of HNV treated pregnant mice, changes in the [NADH]/[NAD$^+$] ratio may have affected the stability and transcriptional level of p53, a proapoptotic protein factor in cells, causing an abnormal increase in the rate of cellular apoptosis in developing mouse embryos.

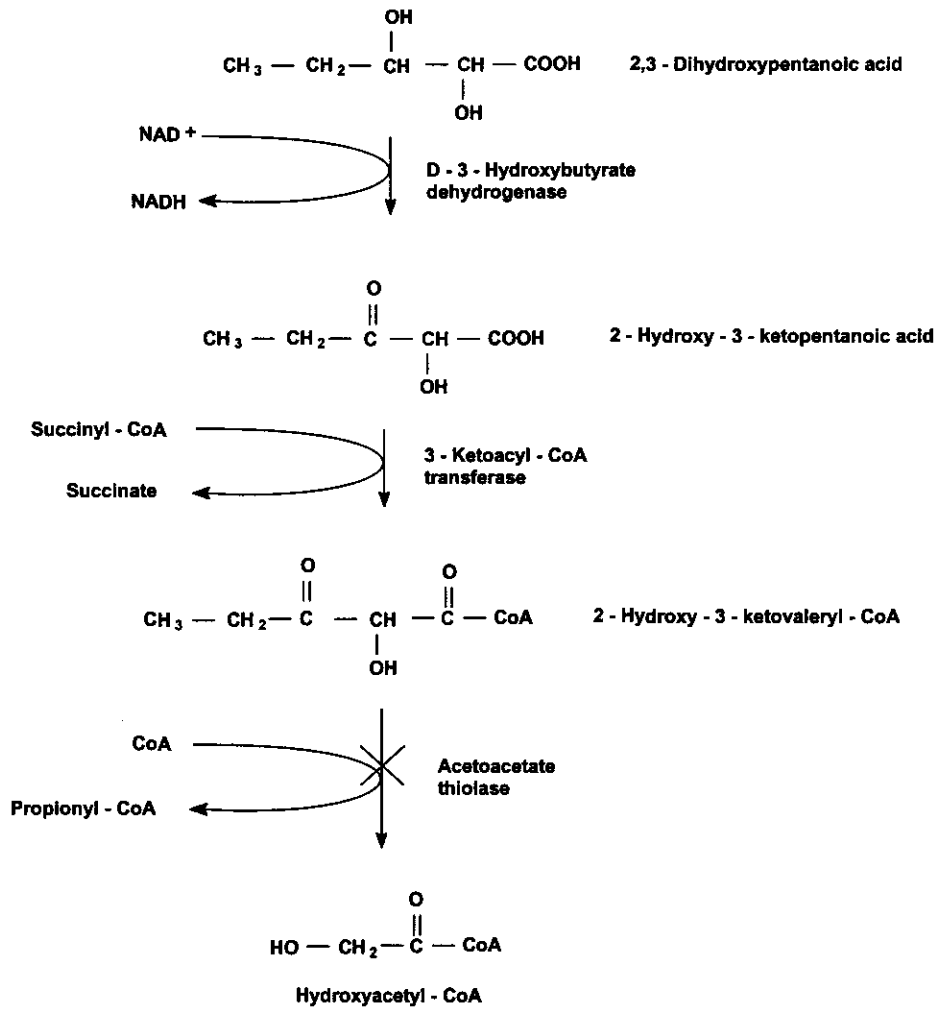

Figure 5.19. Schematic diagram of the proposed effect of 2,3-dihydroxypentanoic acid on ketone body utilisation.

5.5 DISCUSSION

Our results clearly indicate that selective catabolic breakdown of two of the four β-hydroxynorvaline stereoisomers, most probably the two L-isomers, occurred in HNV treated female mice (Figure 5.6).

Metabolic profiles obtained from HNV treated females (non-pregnant and pregnant) were employed in piecing together the events involved in the catabolic breakdown of HNV. The main HNV-metabolite in the urine samples of HNV treated mice was 2,3-dihydroxypentanoic acid (DHPA; Figure 5.11). This metabolite was most probably the result of an initial transamination of HNV to form 2-keto-3-hydroxypentanoic acid, the immediate precursor of DHPA.

Based on analyses of the urinary metabolic profiles of HNV treated mice (Figure 5.11), 2,3-dihydroxyvaleryl-CoA appeared to have inhibited β-oxidation (Figure 5.14). Systemic accumulation of β-oxidation intermediates led to their subsequent urinary excretion in elevated concentrations. A relatively large fraction of the acyl-CoA derivatives may have been conjugated with glycine in mice treated with HNV and the resultant acylglycines subsequently excreted in their urine.

Isoleucine catabolism was also apparently detrimentally affected by the metabolic havoc, created by the catabolic products, derived from β-hydroxynorvaline. The metabolic intermediates that were excreted pointed towards a HNV-induced mitochondrial acetoacetyl-CoA thiolase defect. Information, inferred from the metabolic profiles obtained for HNV treated experimental mice, was consistent with the inhibition of the mitochondrial acetoacetyl-CoA thiolase enzyme.

However, the data also supported the conclusion that cytoplasmic acetoacetyl-CoA thiolase was affected in a similar fashion. As a result, drastically decreased [3-hydroxybutyrate]/[acetoacetate] ratios could be calculated from organic acid profiles of HNV treated females, in comparison to the ratios observed in the profiles of control females. The [3-hydroxybutyrate]/[acetoacetate] ratio was previously reported to be directly proportional to the [NADH]/[NAD^+] ratio (Williamson, 1967), and it could be inferred that the concentration of NADH had

decreased and/or that the concentration of NAD^+ had increased. It can therefore be inferred that a serious metabolic energy shortage may have caused gross problems for the developing embryos in pregnant females treated with the toxic amino acid.

CHAPTER 6

DISCUSSION AND CONCLUSIONS

6.1 INTRODUCTION

Neural tube defects are a constellation of folate-responsive congenital defects that frequently occur in humans. This condition displays a multi-factorial aetiology and may be caused by genetic and environmental factors. The British Medical Council, the Budapest trials and numerous other studies proved beyond doubt that a woman's risk for a NTD-affected pregnancy is substantially reduced by periconceptional folate supplementation (Medical Research Council [MRC] Vitamin Study Group, 1991; Czeizel, 1992).

The most important objective of this study was to ascertain whether HNV exhibited teratogenicity in selected animal models. Equally important was the more specific objective to elucidate some of the mechanisms involved in the teratogenic action of HNV. The teratogenicity of HNV has not yet been described before. Almost all the known toxic attributes of HNV were ascribed to effects observed, following the substitution of L-threonine by HNV in proteins. No report has yet appeared which refers to the metabolic fate of HNV in animal systems or to any competitive, non-competitive or irreversible inhibitory action of this toxin on the catalytic activity of any known enzyme.

In this chapter, the major aspects of this study are summarised to emphasise the contribution made to unravel the catabolic fate of HNV, its effect on intermediary metabolism and its teratogenic action in selected animal models.

6.2 THE INDUCTION OF NEURAL TUBE DEFETCS IN ANIMAL MODELS WITH β-HYDROXYNORVALINE

The chicken and mouse embryo models have been used extensively for experimental investigations into the aetiology of and mechanisms associated with neural tube defects. These two models also proved to be the best representative animal models for these studies because of similarities in neurulation, observed in human embryos and these animal models (George, 1995; George, 2003).

(a) HNV-induced NTD in 10-day-old chicken embryos.

Embryos exposed to HNV exhibited various congenital abnormalities (Table 3.1). These defects included encephalocele, anencephaly, spina bifida, incomplete closure of skull roofs and abnormal tail buds. Numerous non-specific defects were also observed (26%). In the HNV treated group, 8.4 % of the embryos displayed neural tube defects, while no NTD occurred in control embryos ($p = 0.01$).

In a separate dose-response study, HNV teratogenicity in chicken embryos proved to be concentration dependent ($p = 0.076$; Fisher's exact probability test) (Figure 3.1). No abnormalities were observed in the control group, which had received saline alone. In this experiment, up to 18.5 % NTD were induced at the highest dosed concentration level of HNV (300 μM). Results, obtained in separate experiments varied considerably. In the dose-response experiment the incidence of NTD was much higher (18.5 %) than in the first investigation (8.4 %). This apparent discrepancy may be ascribed to the use of relatively small experimental subgroups ($n_i < 30$) in the investigation.

Growth inhibitory effects on body mass, body length, toe length and beak length of developing chicken embryos, based on developmental criteria (Hamburger and Hamilton, 1951), were also HNV concentration dependent (Figures 3.2, 3.4, 3.6 and 3.8). HNV exerted a statistically significant inhibitory effect on growth and development of chicken embryos in most cases.

(b) HNV induced NTD in 18-day-old mouse embryos.

Up to 17.1 % NTD were induced in mouse embryos of pregnant mothers by HNV (Figure 3.10). As in the chicken embryo model, the effect of HNV on the mouse embryos was also concentration dependent ($p < 0.001$). HNV did not only cause NTD in embryos, but also exhibited general embryotoxic effects, i.e. growth inhibitory effects ($p < 0.001$) and high embryo mortality, i.e. 33.9 % in the embryos of mothers that were dosed with 600 mg/kg of HNV ($p < 0.001$).

6.3 THE EFFECT OF HNV ON ONE-CARBON METABOLISM

Neural tube defects have been positively linked to folic acid metabolism (Medical Research Council [MRC] Vitamin Study Group, 1991; Czeizel, 1992). Numerous studies focussed on different aspects of one-carbon metabolism (i.e. folate cycle, remethylation cycle, transsulfuration, etc.) in an attempt to unravel the cause(s) of NTD.

As stated before, folate metabolism plays a very important role in a large number of essential biochemical processes in animal cells. These include purine, thymidine and methionine biosynthesis, serine/glycine interconversion and the metabolism of histidine and formate. Folate is also indirectly involved in the formation of S-adenosylmethionine (SAM), an important biomethylating agent responsible for more than a hundred known biomethylation reactions (Heby, 1981; Selhub, 1992; Bailey, 1999; Herbig, 2002). *Via* SAM, folic acid is indirectly linked to the biosyntesis of carnitine, polyamines, cysteine and glutathione as well as to DNA methylation and gene regulation and numerous other methylation reactions (Heby, 1981; Selhub, 1992).

(a) HNV inhibits the flow of one-carbon units

[^{3}H]-Thymidine incorporation was employed to determine the effect of HNV on the flow of one-carbon units and thymidine biosynthesis, *via* the folate cycle

(CH_2-THF). HNV exhibited a statistically significant effect ($p < 0.001$) on the incorporation of [^{3}H]-thymidine into the DNA of developing mouse embryos *in utero* (Figure 4.8). The mean [^{3}H]-thymidine incorporation into control embryos was 1.11 ± 0.23 dpm/mg DNA, while that in HNV-treated embryos amounted to 1.51 ± 0.38 dpm/mg DNA (36 % increase).

Chicken embryo fibroblast (CEF) cultures were subsequently used to determine the concentration dependent effect HNV on the rate of DNA synthesis (Figure 4.10). At relatively low HNV concentrations, the cell viability still appeared to be high (> 97 %), on par with controls (100%). However, DNA synthesis was dramatically decreased (45 %) in comparison to controls. These results indicate that HNV effectively inhibits DNA synthesis.

No data of the effect of HNV on one-carbon metabolism in mammalian systems has ever been published. However, Massare *et al.* (1987) proved that HNV inhibits the synthesis of DNA in the herpes virus, by altering the catalytic activity of viral thymidine kinase (TK) and DNA polymerase (DNApol). These researchers concluded that the inhibitory action of HNV observed on the viral TK and DNApol may have been the result of (a) incorporation of HNV into the primary structures of TK and DNApol, resulting in the formation of mutant enzymes with compromised catalytic activities; (b) HNV inhibited the formation of regulatory viral polypeptides and compromised their cellular functions; (c) HNV caused the formation of altered viral polypeptides that were more labile towards *in situ* proteolytic degeneration.

We have no proof that the inhibitory effects of HNV on DNA synthesis observed in the present study can not be ascribed to the substitution of L-Thr by HNV in proteins. However, this investigation specifically focused on the probability that HNV may also act as an analogue of L-Ser, compromising the catalytic activities of enzymes using L-Ser as a substrate. Christner *et al.* (1975) managed to illustrate that HNV can be activated by the aminoacyl-tRNA-synthase, specific for L-Thr in fibroblasts. It is more probable that both L-Thr substitution and L-Ser anti-metabolic effects may play a role in all of the toxic effects of HNV, exhibited in the chicken and mouse embryo model systems, employed in this investigation.

(b) The effect of HNV on the in vitro catalytic activity of selected enzymes

The *in vitro* catalytic activities of both SHMT and CBS appeared to have been compromised by HNV, suggesting that this toxic amino acid can also act as a L-serine analogue (Figures 4.11 and 4.13). The observed inhibitory effects of HNV on these both enzymes appeared to be competitive in nature. Since both of these enzymes are involved in one-carbon metabolism, it was assumed that their catalytic activity may have been compromised by HNV in the developing embryos. The latter effect may have caused a concomitantly reduced flux of one-carbon units through the folate and remethylation cycles, which may have obvious implications for a number of important metabolic processes, dependent on one-carbon unit flux.

The [^{3}H]-thymidine incorporation study seemed to indicate that a reduced flow of one-carbon units in developing embryos may indeed have been caused by HNV (Figure 4.8). It was therefore assumed that the concentrations of SAM, SAH and/or homocysteine may also have been altered. However, the levels of SAM, SAH and homocysteine could not be properly quantified in developing embryos, due to limitations in the sensitivity of the analytical methods that were employed. It is therefore only possible to speculate about the direct effect of HNV on the concentrations of these metabolites. In vascular endothelial cells (VEC), the addition of homocysteine inhibited DNA synthesis ([^{3}H]-thymidine incorporation test) and increased the concentration of SAH, with the resultant lowering of SAM (Lee, 1999). Therefore, it may be possible that the elevated [^{3}H]-thymidine incorporation displayed in the mouse embryos is related to lowered SAM levels.

(c) Inhibition of DNA methylation

There was an indication that DNA methyation in HNV treated pregnant female mice was reduced (8.6 %), although a statistically significant inhibitory tendency ($p = 0.45$) was not observed (Figure 4.14). However, DNA methylation in the embryos was significantly reduced ($p = 0.01$). The mean percentage methylated cytosine residues was reduced from 3.38 ± 0.32 % in the controls to 2.92 ± 0.36 %

in the embryos exposed to HNV, representing a 13.7 % reduction (Figure 4.15). DNA methylation is critical for regulation of gene expression. Reduced DNA methylation may lead to altered gene expression with catastrophic consequences for the developing embryo. Lei *et al.* (1996) illustrated that mice homozygous for a mutation in the DNA methyltransferase gene displayed highly demethylated DNA and a distorted neural tube at 9.5 days *p.c.*

(d) Inhibition of polyamine synthesis by HNV

The concentrations of the polyamines (Put, Spd, Spm) were altered by HNV in both pregnant female and their embryos (Figures 4.16 and 4.18), although the observed effects were not statistically significant (95 % confidence level). The ratios of putrescine/spermine (Put/Spm) in both the mothers and embryos proved to be a better indicator of the effect of HNV on polyamine biosynthesis (Figures 4.17 and 4.19). However, these effects were also not statistically significant (mothers: $p = 0.53$; embryos: $p = 0.13$). The mean Put/Spm ratio of the HNV-treated embryos was 2.20 ± 0.65, compared to a value of 1.75 ± 0.30 in the controls (25.6 % increase).

Ornithine is the direct metabolic precursor of polyamines. Total ornithine concentrations in the embryos exposed to HNV, were significantly increased (Figure 4.20) from 4.4 µmol/g protein (controls) to 5.3 µmol/g protein (HNV exposed). This represented a 19.5 % increase, which proved to be statistically significant ($p = 0.003$). Although polyamine levels were not dramatically altered by HNV, the increased ornithine levels corroborated the inference that polyamine biosynthesis may have been compromised by HNV.

The catalytic activity of the enzymes involved in polyamine synthesis was, however, not determined in pregnant females or their fetuses. Therefore one can not exclude the direct inhibition of any of the enzymes by HNV and/or any of its metabolites. However, this possibility appears to be remote since HNV does not display a close structural resemblance to any of the metabolites involved in polyamine biosynthesis. Therefore it may be inferred that the inhibited polyamine

synthesis, as indicated by the altered putrescine/spermine ratios and increased ornithine levels, were most probably caused by reduced SAM levels in the developing embryos.

(e) The effect of carnitine biosynthesis

Total urinary carnitines in pregnant females was significantly reduced in HNV exposed pregnant females, compared to controls ($p = 0.017$), although the effect was not statistically significant on the 95 % confidence interval (Figure 4.21). The mean total carnitine concentration in control pregnant females was 302.8 ± 113.5 mmol/mol creatinine and 156.3 ± 33.5 mmol/mol creatinine in HNV treated pregnant females. An apparent decrease (48.4 %) was therefore observed in the HNV-treated animals.

The carnitine precursor, trimethyllysine, was also quantified in the urine of pregnant females. The mean level of this metabolite in HNV-treated pregnant female urine samples was 90.7 ± 28.8 mmol/mol creatinine and that of the controls 104.0 ± 29.9 mmol/mol creatinine. This decrease (12.8 %) did not prove to be statistically significant on the 95 % confidence level ($p = 0.131$).

SAM is used for the methylation of L-lysine residues in some of the newly synthesised proteins to produce protein bound trimethyllysine. Hydrolysis of these proteins will release trimethyllysine, essential for carnitine synthesis. Therefore, if SAM levels were limited by HNV, methylation of proteins would be limited, resulting in lowered trimethyllysine and carnitine levels.

Inspection of the organic acid profiles indicates the presence of highly elevated levels of metabolites and metabolite conjugates in the urines of HNV treated pregnant females, compared to control pregnant females (Figures 5.10 and 5.11). Carnitine, glycine and glutathione conjugation are known mechanisms employed in the restoration of homeostatic levels of these metabolites. Ultimately, intracellular levels of free carnitine, glycine and even glutathione may be depleted. The observed lowering of carnitine levels in the HNV-treated pregnant females

may therefore be attributed to either one or both of the following events: (a) the inhibition of carnitine biosynthesis (b) a depletion of free carnitine stores.

Decreased production of cellular energy may result because the transport of long-chain fatty acids into the mitochondria to be oxidised *via* β-oxidation can not reach optimal levels. Ultimately, the resultant energy shortage that will follow may pose dire consequences for the developing embryos.

(f) The effect of HNV on the catalytic activity of selected enzymes

The catalytic activity of selected enzymes involved in the flow of one-carbon units was measured in control and HNV treated animals. SHMT uses L-serine as a natural substrate and is a key enzyme in the supply of one-carbon units derived from L-Ser. L-Ser is also a natural substrate for CBS. CBS is important in the removal of excess levels of homocysteine *via* transsulfuration. GCS on the other hand plays an important role in the glycine/serine flux although L-Ser is not its natural substrate. Metabolic antagonism, caused by HNV, of any of these enzymes may ultimately affect the flow of one-carbon units and may impair the glycine/serine flux.

Although not statistically significant, the catalytic activity of cSHMT was reduced in both HNV exposed mothers (6.1 %; $p = 0.56$) and embryos (32.1 %; $p = 0.17$), compared to controls (Figure 4.24 and 4.27). The effect of HNV on the embryos was clearly more prominent than in the mothers. It is possible that this result may support earlier observations that HNV reduced thymidine biosynthesis and probably also DNA synthesis in developing mouse embryos and CEF. This could be the result of an HNV-induced decrease in cSHMT activity, because this enzyme is responsible for the main supply (>80 %) of one carbon units for the synthesis of purines, thymidine and methionine (Girgis, 1997; Gregory, 2000; Herbig, 2002). Ultimately, the reduced cSHMT activity may have been responsible for the altered flow of one-carbon units. Inhibition of cSHMT activity therefore appears to be one of the most likely causes of the inhibition of

polyamine and carnitine biosynthesis, with the resultant reduction in DNA methylation observed in pregnant female mice and embryos exposed to HNV.

In the case of mSHMT, the pregnant mothers and the embryos responded differently towards an HNV challenge (Figures 4.25 and 4.28). Relative to the controls, hepatic mSHMT activity in HNV treated mothers was increased by 20.2 % ($p = 0.29$). However, in whole embryos, the opposite effect was observed (24.6 % decrease; $p = 0.38$). A probable explanation for this phenomenon may be that upregulation of hepatic mSHMT expression occurred in the mothers, but not in whole embryos.

Reduced free carnitine levels probably contributed to a greater demand for glycine, essential for the detoxification of the elevated levels of metabolites, induced by HNV. Since mSHMT is purportedly the most important metabolic entity, involved in the control of glycine synthesis (Narkewicz, 1996a), an upregulation of the mSHMT gene seems to be a logical explanation for the apparent paradoxical increase of hepatic mSHMT activity in the mothers (Figure 4.25).

Both mothers and embryos treated with HNV exhibited lower GCS activity, compared to controls (not statistically significant; Figures 4.26 and 4.29). GCS enzyme complex is the major biochemical entity responsible for the catabolic breakdown of glycine and reduced GCS activity is therefore normally associated with increased glycine levels (Yoshida, 1972). An HNV-induced inhibition of the GCS may theoretically result in an increase in glycine levels, essential for the detoxification of excess levels of potentially toxic metabolites, present in the cells. However, according to Hamosh (1995), GCS activity in 2-day old rat neonates represented only a third of the levels normally expressed in the adult rat. Therefore, by extrapolation, we postulate that the altered one-carbon flux observed in this study was more likely caused by the inhibition of SHMT, rather than the inhibition of GCS.

3-Ethylcysteine (EC) was observed in the urines of HNV-treated pregnant females (Figure 4.33). The presence of this metabolite is an indication that HNV acted as a

substrate for CBS and was subsequently condensed with homocysteine. The resulting enzymatic product, 3-ethylcystathionine, could have been rapidly catabolised to 3-ethylcysteine and 2-ketobutyric acid by a highly reactive cystathionine-γ-lyase (CGL). *In vitro* studies indicated that the catalytic activity of CBS was inhibited by HNV (Figure 4.13). The nature of this inhibition could not be determined, due to problems experienced with the CBS assay employed in this study (APPENDIX O).

The presence of 3-ethylcysteine was never before reported in a biological system. However, 3-methylcysteine was recently synthesised by Jhee *et al.* (2002.), using yeast cystathionine β-synthase. L-Allothreonine and L-homocysteine were used as substrates in this reaction.

By means of extrapolation from the *in vitro* phenomenon to what may have occurred *in vivo* in the HNV exposed embryo, it may be speculated that the simultaneous inhibitory action of HNV on SHMT, CBS and the GCS caused a disruption in the generation and flux of one-carbon units, with subsequent detrimental effects on embryonic development.

6.4 THE EFFECT OF β-HYDROXYNORVALINE ON THE METABOLISM OF PREGNANT FEMALE MICE

(a) The catabolism of HNV

Our results clearly indicate that HNV is catabolised in the mouse. Selective catabolic breakdown of two of the four β-hydroxynorvaline stereoisomers, most probably the two L-isomers, occurred in HNV treated female mice (Figure 5.6). The relative molar ratios of the stereoisomers in commercially available HNV were calculated as 1:1:0.25:0.25 (Figure 5.4). However, the relative molar ratios of the stereoisomers in a mouse urine sample were 0.05:1:0.01:0.25 (Figure 5.6). This change in the relative molar ratios of the stereoisomers confirmed that selected HNV stereoisomers were catabolised in the mouse.

(b) DHPA as the main HNV metabolite

The catabolic breakdown of HNV in the mouse has never been reported before. The obvious next step was to identify HNV metabolites that may have been produced and their influence on the intermediary metabolism of the HNV treated pregnant females and their embryos. 2,3-Dihydroxypentanoic acid (DHPA; Figure 5.11) proved to be the main urinary HNV metabolite. This metabolite was most probably the result of an initial transamination of HNV to form 2-keto-3-hydroxy-pentanoic acid, the immediate precursor of DHPA. Two well resolved peaks, corresponding to two stereoisomers of DHPA were detected.

(c) The effect of HNV on β-oxidation in the pregnant female mouse

Inferences drawn from the urinary organic acid profiles (Figure 5.11) of HNV-treated pregnant females indicate that β-oxidation of fatty acids may have been dramatically affected in these animals (Table 5.1). Numerous urinary acylglycines were detected in highly elevated levels in females exposed to HNV compared to the negligible levels observed in control females. The metabolic profiles clearly revealed an inhibition of the β-ketothiolase step of β-oxidation, resulting in an accumulation of the preceding intermediates prior to the metabolic block, with the subsequent excretion of the accumulating metabolic intermediates into the urine.

The urinary organic acid profiles also indicated that HNV exerted a negative effect on the catabolic breakdown of isoleucine. Elevated levels of tiglylglycine, 2-methyl-3-hydroxybutyric acid and 2-methylacetoacetate were observed in HNV treated pregnant females, although none of these metabolites were detectable in the urines of pregnant female controls (Table 5.2). These results support the inference that β-ketothiolase was severely inhibited.

Based on data extracted from organic acid profiles, ketone body utilisation was severely affected by β-hydroxynorvaline. HNV-treated pregnant female mice excreted large quantities of 3-hydroxybutyric acid and 3-ketobutyric acid in their urine compared to the controls (Table 5.4). Urinary 3-hydroxybutyric acid excretion

was approximately 25-fold higher in HNV-treated pregnant females than in control animals. Control females excreted virtually no 3-ketobutyric acid, but the HNV treated mice excreted on average 655 mmol 3-ketobutyric acid per mol creatinine (approximately a 1000-fold increase). The altered ketone body levels suggested that cytosolic acetoacetyl-CoA thiolase may have been strongly inhibited by HNV and/or HNV metabolites.

HNV-treated pregnant female mice displayed urinary organic acid profiles frequently observed in humans with a ketothiolase defect. The pregnant females excreted abnormally high levels of tiglylglycine, 2-methyl-3-hydroxybutyrate, 2-methylacetoacetate, adipate, 3-hydroxyisovalerate and 2-methylglutaconate (Table 5.2). Biochemical analysis of twins with a 2-methylacetoacetyl-CoA thiolase defect revealed that excessive amounts of tiglylglycine, 2-methyl-3-hydroxy-butyrate, 3-hydroxyisovalerate, 2-methylglutaconate, adipate and 2-methyl-acetoacetate were excreted in their urine (Fontaine, 1996). The most characteristic elevated urinary metabolite of a typical 2-methylacetoacetyl-CoA thiolase defect is 2-methyl-3-hydroxybutyrate. Excessive levels of this metabolite is often accompanied by elevated 2-methylacetoacetate concentrations. Most patients with a 2-methylacetoacetyl-CoA thiolase defect also excrete tiglylglycine, however, there are some that do not (Sweetman, 1995).

In mitochondrial disorders, L-carnitine not only stimulates acyl-CoA oxidation pathways of which the metabolic capacities have been reduced, but also acts as a detoxification agent facilitating the removal of excessive levels of acyl compounds (Fontaine, 1996). Blood carnitine levels were altered in the twins with the 2-methyacetoacetyl-CoA thiolase deficiency. Their total and esterified urinary carnitines were also increased, as well as the acylcarnitine:free carnitine ratio. This ratio was also altered in HNV-treated pregnant female mice, compared to that observed in saline treated pregnant controls (Figure 5.17).

Free carnitine stores in HNV treated pregnant females were drastically depleted, compared to that observed in saline treated pregnant controls (Table 5.3). The mean free urinary carnitine concentration of the control urine was 280.4 ± 119.9 mmol/mol creatinine compared to a mean of only 132.9 ± 30.0 mmol/mol

creatinine obsereved in HNV treated pregnant mice, a 53 % decrease. This decease proved to be statistically significant ($p = 0.023$). The mean urinary acylcarnitine:free carnitine ratio of HNV treated pregnant mice (0.18 ± 0.07) was also significantly increased (80 % increase; $p = 0.023$) compared to the ratio observed in control animals (0.10 ± 0.06) (Figure 5.17). This increase was consistent with an induced mitochondrial disorder and a 2-methyacetoacetyl-CoA thiolase deficiency (Fontaine, 1996).

Cytoplasmic acetoacetyl-CoA thiolase deficiency was first reported by De Groot *et al.* (1977). A four-month old first born child from unrelated parents presented with delayed motor development, ataxic and choreoathetoid movements, involuntary eye movements and hypertonia. Blood lactate and pyruvate levels were constantly above normal with high blood concentrations of 3-hydroxybutyrate and acetoacetate. Another case was reported with cytosolic acetoacetyl-CoA thiolase deficiency, associated with mental retardation in a male child (Bennett, 1984). This boy also excreted elevated 3-hydroxybutyrate and acetoacetate. Enzyme analyses on cultured fibroblasts from the affected boy revealed a probable defect in cytosolic acetoacetyl-CoA thiolase. The enzyme displayed only about 50% of the catalytic activity, measured in fibroblasts obtained from healthy, control subjects. Mitochondrial acetoacetate thiolase activity in this case was apparently normal.

As explained before, the metabolic profiles observed in pregnant female mice treated with HNV are consistent with a β-ketothiolase defect. The inhibitory effect of the HNV-metabolites, however, does not appear to target a single thiolase enzyme but seems to affect the activity of a variety of cellular thiolases. As a result, HNV-treated animals exhibited a mitochondrial acetoacetyl-CoA thiolase defect combined with a cytosolic acetoacetyl-CoA thiolase defect. Energy generation in the HNV treated animals may have been diminished because certain steps in the β-oxidation of acyl compounds have been detrimentally affected. However, energy depletion could also result, following an inhibition of the utilisation of ketone bodies. These effects have been clearly confirmed by the manifestation of altered [3-hydroxybutyrate]/[acetoacetate] ratios in the HNV treated experimental animals (Table 5.4). These actions of HNV obviously pose severe consequences for the pregnant mice and their developing embryos.

6.5 FINAL CONCLUSIONS

1. β-Hydroxynorvaline (HNV) is a teratogen, causing neural tube defects in the chicken and mouse embryo models. HNV is also capable of inducing a variety of other congenital defects (i.e. omphalocele) and embryotoxic effects (growth, lethality) in these models.

2. HNV inhibits the flow of one-carbon units through the folate and remethylation cycles, resulting in:
   (i) decreased DNA synthesis
   (ii) decreased DNA methylation
   (iii) inhibition of polyamine biosynthesis
   (iv) lowered total carnitine levels, probably due to:
      - depletion of free carnitine stores because of the detoxification of vast amounts of accumulatiing metabolites that are generated as a result of HNV toxicosis
      - reduced biosynthesis of carnitine
   (v) altered serine/glycine interconversion mainly due to the inhibition of cSHMT and to a lesser degree the inhibition of the GCS

3. HNV affects transulffuration by acting as a substrate for CBS, culminating in the biosynthesis of 3-ethylcysteine.

4. Selected HNV stereoisomers are catabolised in pregnant female mice, with the production of 2,3-dihydroxypentanoic acid (DHPA) as the main urinary metabolite.

5. HNV induces a β-ketothiolase defect in the pregnant females by inhibiting the following metabolic processes:
   (i) β-oxidation of fatty acids
   (ii) isoleucine catabolism
   (iii) ketone body utilization

6.6 SHORTCOMINGS OF AND PROBLEMS ENCOUNTERED IN THIS INVESTIGATION

(i) The chicken embryo model

Several characteristics of the *in ovo* chicken embryo model may complicate any investigation into the effect of teratogenic substances (i.e. β-hydroxynorvaline) on embryonic development in man. The *in ovo* chicken embryo model does not really portray the exact situation of the human embryo *in utero* and numerous uncertainties concerning the exact nature and concentration(s) of the toxic species, responsible for the induction of congenital defects in the embryos may contribute to inaccuracies and lack of relevancy of inferences drawn from experimental results. The chicken embryo can therefore not be regarded as a suitable, representative model for teratogenic studies, relevant to man.

One of the greatest disadvantages of the *in ovo* chicken embryo model experienced in the present study was the large variations observed in the outcomes (i.e. incidence of NTD) of consecutive experiments. This phenomenon may be explained by the fact that not all of the embryos within subgroups were exposed to exactly the same dose of HNV inside the eggs. This problem may be ascribed to either one or both of the following factors:
(a) the position of the toxin containing droplet on the bottom of the air sac membrane, relative to the embryo, attached to it.
(b) the large variation in the sizes and therefore the volumes of individual eggs, used in the investigation (intra- and interbatch).

During dosage of the eggs, a 50 µl aliquot of the HNV solution (initial concentrations: 75, 150 and 300 mM HNV) was injected into the air sack and the resultant droplet of saline solution, containing the toxin, was then located on the inner membrane at the bottom of the air sac. The position of the embryo on this membrane, relative to the position of the toxin containing droplet may have varied considerably from egg to egg. To expose the embryo to HNV, the toxin must diffuse through the air sac membrane into the contents of the egg (i.e. egg yolk, etc.) to come into contact with and to be absorbed by the developing embryo. Due

to the different positions of individual embryos on the membrane, the embryos were probably not all exposed to the same *in ovo* concentrations of HNV. The volumes of individual eggs varied considerably, which would have affected the dilution and final concentration of the dosed HNV and as a result, the final exposure levels of the individual embryos to HNV.

By exposing individual embryos to different concentrations (doses) of HNV during embryonic development, the quantity and quality of the effects observed in the embryos displayed high variability. Various indicators of growth inhibition were measured (i.e. body mass, body length, beak length and toe length). The apparent differential effects of the toxin on the selected growth and developmental indicators for individual embryos within subgroups differed considerably, most probably due to the fact that the embryos were exposed to different HNV concentrations (doses) *in ovo*. These problems and the fact that the non-invasive assessment of a variety of biochemical and/or metabolic biomarkers was not possible (i.e. no urine or blood samples can be collected), limited the use of the chicken embryo model. A decision was made to switch to the mouse model.

(ii) Pooling of mouse embryos from one mother to form a single sample

In order to assess all the biochemical and/or metabolic biomarkers targeted in this study, relatively large amounts of urine and tissues (i.e. liver, whole embryo) were needed. For the enzyme assays on whole embryos, at least 300 mg of tissue were required to execute a single batch of analyses (mSHMT, GCS and CS). Isolated mitochondria were required for the analysis of mSHMT, GCS and CS in liver and whole embryo tissues. The quantitative yield of mitochondria from liver tissue and whole embryos varied considerably within batches and between different experiments and this problem inflated the amount of tissue required to complete an experiment. A single 10-day old mouse embryo weighs approximately 50 mg each. It was therefore a necessity to pool embryos from single mothers and for this purpose, all the embryos from a single mother (6 – 13 embryos/litter) had to be pooled to generate one sample. By pooling the embryos of each mother, enough tissue was obtained to perform all the necessary analyses. However, the number

of samples per experiment decreased, affecting the statistical power of experiments and consequently the statistical significance of the data.

It is also possible that another concomitant problem may have affected the statistical significance of the data. Although the NMRI mice used in this study are highly inbred and therefore great individual genomic differences are not expected, some of the embryos showed NTD (responders) while the rest of the embryos were unaffected by the toxin (non-responders). It is therefore expected that some metabolic difference might exist between the responders and non-responders that could be measured. By combining the responders and non-responders in a single sample, the non-responders largely neutralised the effect that would have been clear in the responders. If a small difference existed between the control and experimental groups, this difference might have been masked/neutralised by the non-responders. This is probably the cause of numerous tendencies seen in this study while the results were not statistically significant on the 95 % confidence level. If these analyses could be performed on individual embryos, the results most probably would have been statistically significant.

(iii) The half-life of polyamines

The half-life of polyamines is relatively long. The apparent half-life of spermidine may vary between 7 and 42 days and that of spermine between 11 and 42 days (Heby, 1981). Therefore, a rapid reduction in the concentration of individual polyamines, due to inhibition of its biosynthesis, would most probably not occur. Because polyamines play a critical role in cell proliferation and differentiation, especially during embryonic development, minor changes in polyamine concentrations might influence the normal development of the embryo. In this study, β-hydroxynorvaline did not have a statistically significant effect on polyamine synthesis (95 % confidence interval). This is most probably due to the long half-life of polyamines and/or the pooling of embryos. Therefore one cannot conclude that polyamines are not involved in the aetiology of neural tube defects. On the contrary, due to its essential role in embryonic development, polyamines remain an attractive point of investigation into the aetiology of neural tube defects.

6.7 FUTURE PERSPECTIVES

(i) Serine hydroxymethyltransferase

Inhibition of SHMT with a more specific inhibitor might shed more light on the role of this important enzyme during embryonic development. Another alternative is the development of a knockout mouse model. Due to the importance of this critical enzyme for normal cellular function, a knockout mouse (homozygous defect) will probably not be viable. A knockdown model (heterozygous defect), on the other hand, may be more helpful to elucidate the role of SHMT during embryonic development.

(ii) Carnitine biosynthesis

Some authors suggested that SHMT may also be involved in carnitine biosynthesis (Henderson, 1982; Vas, 2002). Carnitines play a critical role in the transport of fatty acids and the detoxification of excess levels of potentially toxic metabolites. Inhibition of carnitine synthesis will influence the β-oxidation of fatty acids, and hence energy production as well as detoxification. Specific inhibitors of carnitine biosynthesis may be useful to study the role of impaired carnitine synthesis in the aetiology of NTD.

(iii) Polyamines

The role of polyamines may prove to play a more prominent role in the development of NTD than was previously believed. Inhibition of polyamine synthesis with a specific inhibitor may result in the induction of NTD. Due to the relatively long half-life of polyamines ($t_{½}$ = 7 – 42 days), it may be necessary to increase the duration of exposure of experimental animals to the toxin in order to deplete polyamine levels.

(iv) Detoxification

Coakley *et al.* (1986) reported that numerous short chain carboxylic acids (i.e. valproate, methoxyacetate, butarate, etc.) may be teratogenic. Glycine conjugation is mainly responsible for the detoxification of short chain carboxylic acids during organic acidurias. Since the detoxification process utilise glycine, the glycine/serine interconversion will be affected in the developing embryo. The embryo rely on endogenous synthesis of serine and glycine, and changes in the regulation of fetal serine and glycine biosynthesis and utilisation appear to be the only mechanisms available for the fetus to affect the supply of these two amino acids. Serine and glycine are interconnected through the actions of cSHMT, mSHMT and the GCS. All of these enzymes also utilise tetrahydrofolate (THF) as a co-substrate. Therefore, detoxification (glycine conjugation) of organic acids may indirectly affect the normal flow of one-carbon units and may induce NTD.

(v) Sphingolipid biosynthesis

L-Serine is involved in sphingolipid biosynthesis. Palmitoyl-CoA and L-serine are converted to 3-ketosphinganine by serine palmitoyltransferase in the first reaction of sphingolipid synthesis. β-Hydroxynorvaline can potentially influence sphingolipid synthesis by inhibiting serine palmitoyltransferase, or an intermediate metabolite may be formed that could not be cleaved by one of the next enzymes involved in sphingolipid synthesis (similar to the observed effect of HNV-metabolites on ketone body utilisation). Since sphingolipids are essential membrane components that play a vital role in cellular differentiation, proliferation and apoptosis (Perry, 1998), the potential inhibition of sphingolipid biosynthesis by HNV may be another aspect of HNV teratogenicity that should be investigated.

APPENDIX A

Assessing the level of [^{3}H]-thymidine incorporation in developing mouse embryos

The effect of 3-hydroxynorvaline (HNV) on DNA synthesis was investigated by measuring the quantitative incorporation of ^{3}[H]-thymidine into the genomic DNA of developing mouse embryos. The method used was essentially that of Botero-Ruiz *et al.* (1997).

1. Reagents, materials, buffers and solutions

(i) Reagents and materials

[^{3}H]-Labelled thymidine ([methyl-^{3}H]-thymidine: specific activity: 5.0 Ci/mmol) was purchased form Amersham, U.K. Tris-HCl, SDS, NaCl, EDTA, DNase-free RNase were purchased from Sigma Chemical Company. Hydroxyquinoline was obtained from BDH and phenol was purchased from Merck Chemicals. Chloroform and isoamyl alcohol was purchased from Sigma Chemical Company. Unless otherwise stated all chemical reagents were of the highest purity (~99%). Eppendorf tubes were purchased from Merck.

(ii) Buffers and solutions

- **Digestion Buffer:**
  - 100 mM NaCl
  - 10 mM Tris-HCl, pH 8
  - 25 mM EDTA, pH 8
  - 0.5 % sodium dodecyl sulfate
  - 1 mg/ml DNase-free RNase
- **Buffered phenol:**
  - 0.5 g hydroxyquinoline (BDH)
  - 500 ml liquefied phenol (Merck), buffered with 50 mM Tris, pH 8
- **Phenol / chloroform / isoamyl alcohol extraction buffer:**
  - 25 ml buffered phenol
  - 24 ml chloroform
  - 1 ml isoamyl alcohol
- **Ammonium acetate:**
  - 7.5 M solution prepared in water

2. Methods

(i) Administration of [^{3}H]-thymidine to pregnant female mice

Each mouse received 10 µCi [^{3}H]-thymidine on day 9 of gestation (0.1 ml of a 100 µCi/ml solution prepared in saline). [^{3}H]-Thymidine was administered with a 23-guage needle through the *vena caudalis* in the tail of the mouse.

(ii) Isolation of DNA

High molecular weight DNA was isolated by employing the classic phenol extraction method (Strauss, 1987). Frozen tissue samples (preparation described in APPENDIX C) were used for the isolation of DNA. The 600 x *g* pellet was suspended in 500 µl H_2O and homogenised on ice with a tight fit Potter Elvejham homogeniser (Glas-Col).

An aliquot (200 µl) of the pellet suspension was used for the isolation of DNA. The 600 x *g* suspension was mixed with 800 µl digestion buffer in a polypropylene reaction vial (Eppendorf®). The samples were incubated at 50 °C for 12 hours in a temperature-controlled horizontal platform shaker.

After 18 hours of DNase-free RNase digestion, the samples were thoroughly extracted with an equal volume of phenol/chloroform/isoamyl alcohol. Samples were centrifuged for 10 minutes at 1700 x *g* to separate the organic and aqueous phases. The aqueous phase was transferred to a clean tube and ½ a volume of ammonium acetate added. Two volumes of ice cold 100 % ethanol were subsequently added to precipitate the DNA. The precipitated DNA was recovered by centrifugation at 1700 x *g* for 2 minutes. The DNA containing pellet was rinsed with 70 % ethanol, the ethanol decanted and the remaining pellet air-dried. The dried DNA residue was redissolved in 300 µl H_2O.

(iii) Quantification of extracted DNA

The concentration of DNA in the extracted samples was quantified spectrophotometrically (Beckman DU® 7500 double beam spectrophotometer). The absorbance of individual samples was measured

at 260 nm and 320 nm, respectively (pure, double stranded DNA absorbs UV light at 260 nm; a 50 µg/µl DNA solution ideally displays an absorbance reading of 1 absorbance unit). Background absorption was measured at 320 nm. The concentration of the extracted DNA was calculated *(Equation A1)*:

$$\text{dsDNA} = \frac{(A_{260} - A_{320})}{50\ \text{ng.}\mu\text{l}^{-1} \times DF} \qquad \textit{(A1)}$$

Where: [dsDNA] = the concentration of the double stranded DNA ($ng.\mu l^{-1}$)
A_{260} = absorbance of the samples at 260 nm
A_{320} = the absorbance of the samples at 320 nm
DF = the dilution factor

(iv) Quantification of the amount of [^{3}H]-thymidine incorporated into DNA

A MINAXI Tri-carb® 4000 liquid scintillation counter was used to quantify radioactive DNA content of the isolated DNA. Aliquots (300 µl) of the isolated DNA were thoroughly mixed with 3 ml Ultima Gold™ XR liquid scintillation counter cocktail (Packard) and then monitored for radioactivity. An external standard was used for calculating quenching (standard curve). The DNA concentration was used to calculate the [^{3}H]-thymidine content of DNA (Equation A2):

$$[^3\text{H}]\text{-Thymidine content of DNA} = \frac{(A_s - A_b)}{\text{DNA}_{vol} \times [DNA]} \qquad \textit{(A2)}$$

Where: A_s = disintegrations per minute measure in sample
A_b = disintegrations per minute measure in blank
DNA_{vol} = Sample volume (µl)
[DNA] = concentration of DNA in sample ($\mu g.\mu l^{-1}$)

APPENDIX B

Quantification of the inhibition of DNA synthesis in chicken embryo fibroblast cultures

The extent to which DNA synthesis was affected by β-hydroxynorvaline (HNV) was also measured in chicken embryo fibroblasts by means of a slightly modified fluorescence method of Bester *et al* (1994).

1. Reagents, materials, buffers and solutions

(i) Reagents and materials

Hoechst 33258 or bisbenzamide: 2-[4-hydroxyphenyl)-5-[4-methyl-1-piperazinyl]-2,5–bis-1*H*-benzimidazole] was purchased from Sigma Chemical Company. This reagent does not possess inherent fluorescence, but forms fluorescent complexes with the adenine-thymidine base pairs of DNA, occurring in both single and double stranded DNA.

Penicillin/Streptomycin, fetal bovine serum and DMEM were obtained from Gibco. Proteinase-K, sodium cholate, SDS and MTT were all purchased from Sigma Chemical Company. The 24-well Nunc cell culture plates were bought from AEC-Amersham. Phosphate buffered saline was bought from Bio-Whittaker.

(ii) Buffers and solutions

SDS solution

10 mM Tris-HCl, pH 7
2 % sodium dodecyl sulfate

Proteinase K solution

10 mM Tris-HCl, pH 7
2 mg/ml proteinase K

NaCl solution 1

10 mM Tris-HCl, pH 7
4 M NaCl

NaCl solution 2

10 mM Tris-HCl, pH 7
0.5 M NaCl

Cholate solution

10 mM Tris-HCl, pH 7
3.11 mM Cholate
0.5 M NaCl

Hoechst solution 1

10 mM Tris-HCl, pH 7
0.5 M NaCl
2.34 µM Hoechst

2. Methods

(i) Preparation of chicken embryo fibroblasts (CEF)

CEF were prepared from 10-day-old chicken embryos. Chicken embryos were harvested under sterile conditions. Skin was surgically removed and cut up into small tissue blocks of approximately 1 mm^3. The pieces of skin were placed in a 25 cm^2 tissue culture flask without any media/fluids. The flask was set in the upright position of 15 minutes for the tissue to adhere to the bottom of the flask. After the flask was carefully returned to the original position, 1.5 ml complete media was added and the biopsy incubated at 37 °C for 2 weeks.

CEF were cultured in DMEM containing 10 % fetal bovine serum (v/v) and 1 % Pen/Strep (v/v). CEF were seeded into a 24 well plates (100 000 cells per well). The cultures were subsequently incubated for 24 hours (37 °C, 5 % CO_2) to allow the cells to adhere to the bottoms of the individual wells. After 24 hours, the medium was removed from the wells and 500 µl fresh medium added.

(ii) Exposure of CEF to β-hydroxynorvaline

The CEF were subsequently exposed to HNV, following the addition of D,L-HNV to the wells (final HNV concentration range: 0 - 315 µM, respectively). The CEF were incubated for 24 hours at 37 °C before total DNA content and cell viability were measured.

(iii) Quantification of DNA in CEF

DNA was quantified according to the method of Bester *et al.* (1994). CEF monolayers were washed twice with 10 mM Tris-HCl, pH 7. SDS solution was added (200 µl) and the plate gently tilted until the monolayer formed a viscous mixture. NaCl solution 1 was added (200 µl), as well as proteinase K solution (50 µl) and the reaction mixture then incubated at 65 °C for 1 hour. While still warm, cholate solution (200 µl) was added and shaken well. NaCl solution 2 was added (350 µl) and the mixture sonified on a low energy setting.

Following the addition of Hoechst 33258 to the lysed cells, the fluorescence in the individual wells was measured in a Biotek FL600 microtitre plate reader (Bio-Tek instrument Inc.; excitation wavelength = 350 nm; emission wavelength = 460 nm). The correlation coefficient of the fluorescence-concentration relationship was determined to monitor the linearity of the calibration standards.

(iii) Cell viability of CEF in cultures

Cell viability was measured with the MTT assay. Colourless tetrazolium salts can be converted by metabolically active mitochondrial succinate dehydrogenase to form deep purple coloured formazan salts. The concentration of the formazan product can be colourimetrically quantified following dissolution of the crystals. A colourless solution is normally obtained with metabolically inactive mitochondria, occurring in non-viable cells. MTT (4,5-dimethylthiazol-2-yl]-5-diphenyltetrazolium bromide) was employed to determine the viability of the CEF.

CEF were cultured in 24-well plates and exposed to HNV as described in Section 2 (ii). The cells were washed twice with PBS to remove serum and media. 20 µl MTT-solution (5 mg/ml in PBS) was added to each well and the plates incubated at 37°C to allow the formazan crystals to form. After 5 hours, 200 µl dimethyl sulfoxide (DMSO) was added to dissolve the crystalline product. Optical density was subsequently measured in a Biotek FL600 microtitre plate reader (Bio-Tek instrument Inc.), at a wavelength of 560 nm. Background absorption was measured at 630 nm and subtracted automatically by the plate reader. A graph was constructed from the data (mean value of the optical densities versus the concentration of HNV).

APPENDIX C

Isolation of mitochondria from hepatic tissue and whole embryos

Mitochondria were isolated to determine the effect of HNV on mitochondrial enzymes (mSHMT, GCS, CS) in the livers of pregnant female mice and whole embryos. The method of Kalbag and Palekar (1990) was used for the isolation.

1. Reagents, materials, buffers and solutions

(i) Reagents and materials

Sucrose, Hepes, mannitol and ethylene glycol-bis (2-aminoethyleter)-N,N,N',N'-tetra acetic acid were all of the highest purity and purchased from the Sigma Chemical Company.

(ii) Buffers and solutions

- **Homogenisation buffer:**
    - 70 mM sucrose,
    - 5 mM Hepes
    - 220 mM mannitol
    - 0.2 mM ethylene glycol-bis (2-aminoethyleter)-N,N,N',N'-tetra acetic acid

2. Methods

Tissue samples were homogenised on ice in 8 volumes of the homogenisation buffer, using a tight-fit Potter Elvejham homogeniser (Glas-Col). Samples were centrifuged in polypropylene Eppendorf® reaction vials for 10 minutes at 600 x *g* (4°C) to remove nuclei and membranes.

The 600 x *g* supernatant was transferred to a clean Eppendorf® reaction vial and recentrifuged for 25 minutes at 9500 x *g* (4°C). The resulting supernatant was removed and the 9 500 x *g* pellet resuspended in 7 ml homogenisation buffer. Suspended mitochondrial samples were recentrifuged for an additional 25 minutes at 9 500 x *g* (4°C).

Following removal of the supernatant, the washed 9 500 x *g* pellet was resuspended in homogenisation buffer (600 µl for the liver preparations and 400 µl for the whole embryo samples), prior to use in enzyme assays. Protein content was determined with the bicinchoninic acid (BCA) method (Smith, 1985).

APPENDIX D

Quantification of the inhibition of DNA methylation in maternal and embryonic tissues by 3-hydroxynorvaline

The extent to which DNA methylation was affected by 3-hydroxynorvaline (HNV) was measured in liver samples form pregnant mice and whole embryos by means of tandem mass spectrometry. A slightly modified method of Friso *et al.* (2002) was employed.

1. Reagents, materials, buffers and solutions

(i) Reagents and materials

Isotopically labelled cytosine (Cytosine-2-^{13}C-1, 3 -$^{15}N_2$) was purchased form Cambridge Isotope Laboratories, Inc. Tris-HCl, SDS; NaCl, EDTA, DNase-free RNase were purchased from Sigma Chemical Company. Hydroxyquinoline, was obtained from BDH and phenol was purchased from Merck Chemicals. Chloroform and isoamyl alcohol were purchased from the Sigma Chemical Company. Unless otherwise stated all chemical reagents were of the highest purity (~99%). Eppendorf tubes were purchased from Merck.

(ii) Buffers and solutions

- **Digestion Buffer:**
  - 100 mM NaCl
  - 10 mM Tris-HCl, pH 8
  - 25 mM EDTA, pH 8
  - 0.5 % sodium dodecyl sulfate
  - 1 mg/ml DNase-free RNase
- **Buffered phenol:**
  - 0.5 g hydroxyquinoline (BDH)
  - 500 ml liquefied phenol (Merck), buffered with 50 mM Tris, pH 8
- **Phenol / chloroform / isoamyl alcohol extraction buffer:**
  - 25 ml buffered phenol
  - 24 ml chloroform
  - 1 ml isoamyl alcohol

2. Methods

(i) Isolation of DNA from livers and whole embryos

Frozen tissue samples (preparation described in APPENDIX C) were used for the isolation of DNA. The 600 x *g* pellet was suspended in 500 µl H_2O and homogenised on ice, using a tight fitting Potter-Elvejham homogeniser (Glas-Col). High molecular weight DNA was isolated by the classic phenol extraction method as described in Section 2(ii) of APPENDIX A. DNA was quantified spectrophotometrically as described in Section 2(iii) of APPENDIX A.

(ii) Hydrolysis of DNA isolated from tissues

High molecular weight DNA was hydrolysed to the corresponding free bases with formic acid. Isolated high molecular weight DNA (10 µg) was added to a small glass insert used for the LC-MS. Isotopically labelled cytosine (Cytosine-2-^{13}C-1,3-$^{15}N_2$) was used as an internal standard. One nmole of internal standard was added (20 µl of a 50µM stock solution) and the sample dried under vacuum.

Following the addition of formic acid (20 µl; 98 %) the insert was sealed within a GC-MS vial and the DNA sample hydrolysed (150 °C, 45 minutes). After the samples were cooled down, the vials were opened, the small glass inserts removed and the contents dried under vacuum. The resultant dried residues were redissolved in 100 µl 40 % CH_3CN, 60 % H_2O (containing 1 % HCOOH) and analysed immediately.

(iii) Electrospray ionisation tandem mass spectrometric (ESI-MS-MS) analyses of 5-methylcytosine in DNA samples

ESI-MS-MS analyses were executed on a VG Quattro II triple quadrupole instrument (Micromass, UK). For the identification and quantification of the DNA bases, the first MS was set to scan for the positive ion mass/charge ratio (*m/z*) of the individual bases (Pseudo molecular ions or parent ions). Collision induced dissociation (CID) with argon gas was employed in the

fragmentation of these molecules. The second MS was set to scan for the mass/charge ratio of the daughter ions of the bases. The detection of a specific daughter ion in the second MS, corresponding to the correct parent ion in the first MS was the main objective for the quantification of the specific DNA bases.

Conditions of the ESI-MS-MS analysis

	Source (ES^+)
Capillary	3.50 kVolts
HV Lens	0.50 kVolts
Cone	35 Volts
Skimmer Offset	5 Volts
Skimmer	1.5 Volts
RF Lens	0.2 Volts
Source Temperature	90 °C

		MS1		MS2
Ion Energy		1.0 Volts		1.0 Volts
Ion Energy Ramp		0.0 Volts		0.0 Volts
LM Resolution		12.0		13.0
HM Resolution		12.0		13.0
Lenses	(# 5)	100 Volts	(# 7)	250 Volts
	(# 6)	5 Volts	(# 8)	40 Volts
			(# 9)	5 Volts
Multiplier		750 Volts		

Nitrogen was used as drying and nebulizing gas. Flow rates for drying and nebulising were set at 350 and 20 $L.h^{-1}$, respectively.

The mobile phase consisted of 40 % CH_3CN and 60 % H_2O (1 % HCOOH). A constant volumetric flow rate of 250 µl/min was maintained. The injection volume was 25 µl. No chromatographic separation was used and samples were directly injected into the MS.

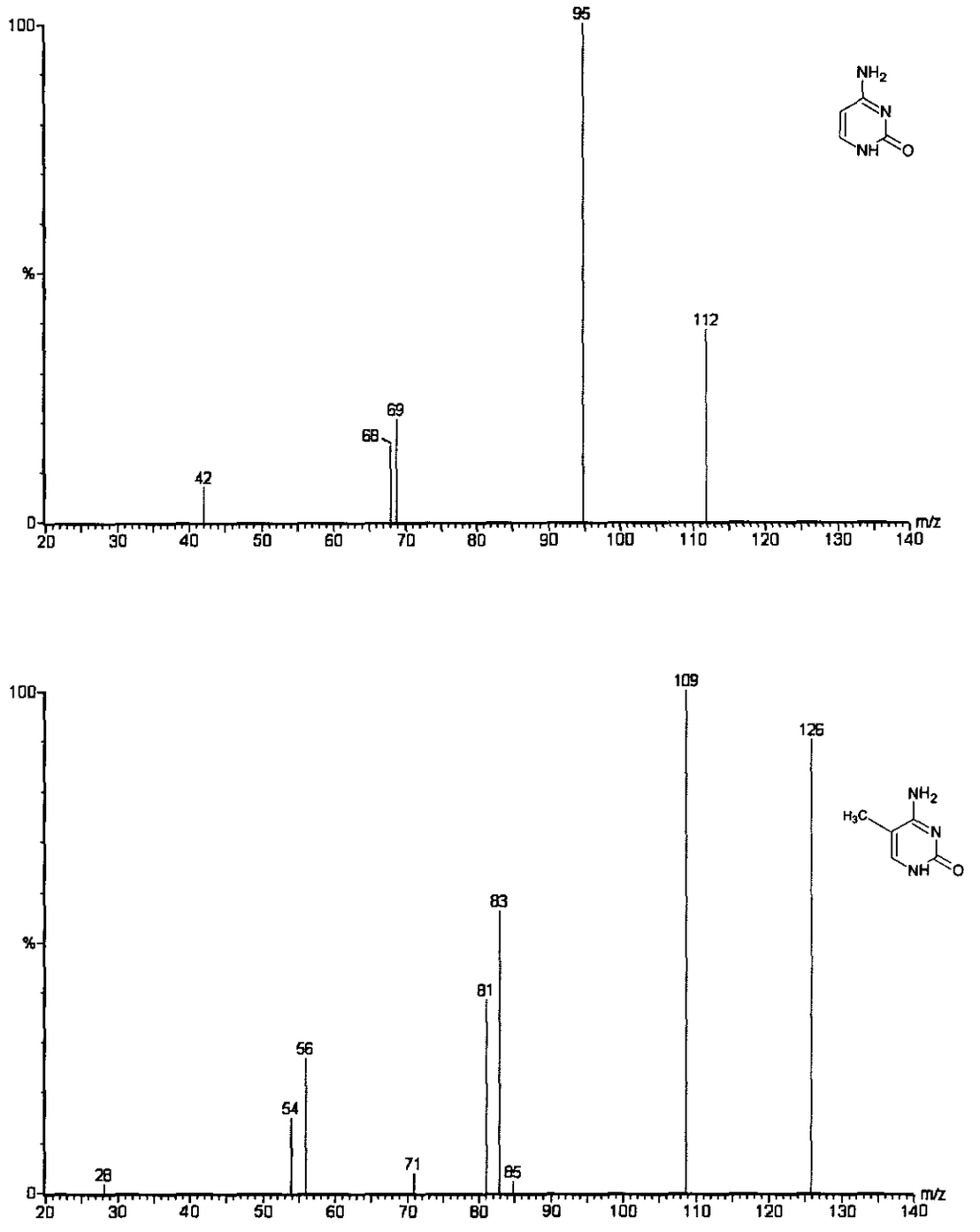

Figure D1. Daughter ion spectrums on the LC-MS. (a) Spectrum of cytosine; (b) spectrum of 5-methylcytosine.

Unique *m/z* ratios were selected form the daughter ion spectra of the compounds for the detection of the various molecular species. The first MS was set to scan for a mass/charge ratio (*m/z*) of 112, 115 and 128. The second MS scanned for the daughter ions (*m/z* = 95, 97 and 109).

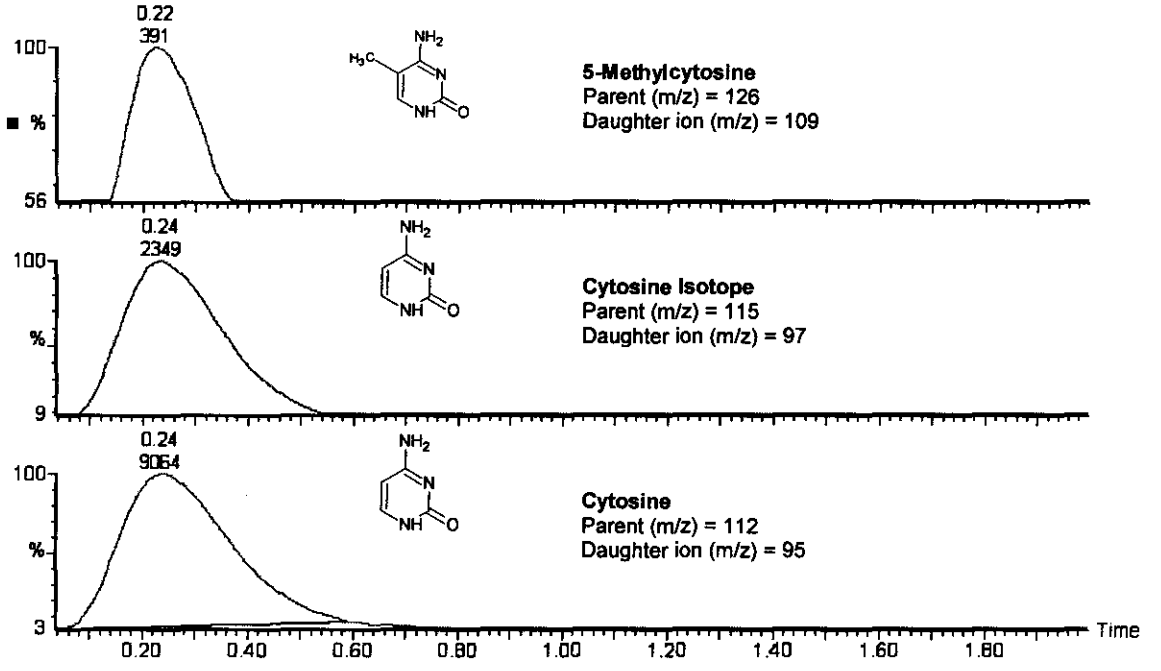

Figure D2. Multiple Reaction Monitoring chromatograms of 5-methylcytosine, cytosine and the cytosine isotope. (Cytosine-2-^{13}C-1, 3 -$^{15}N_2$).

(iv) Validation of the method

Calibration curves were constructed following the analysis of 12 standards. These standards contained increasing concentrations of cytosine and 5-methylcytosine, while the concentration of the internal isotope was constant in all the samples. This was essential to be sure that the quantification would be in the linear range of the tandem MS and therefore would be accurate and reproducible. The standards were analysed with the method described.

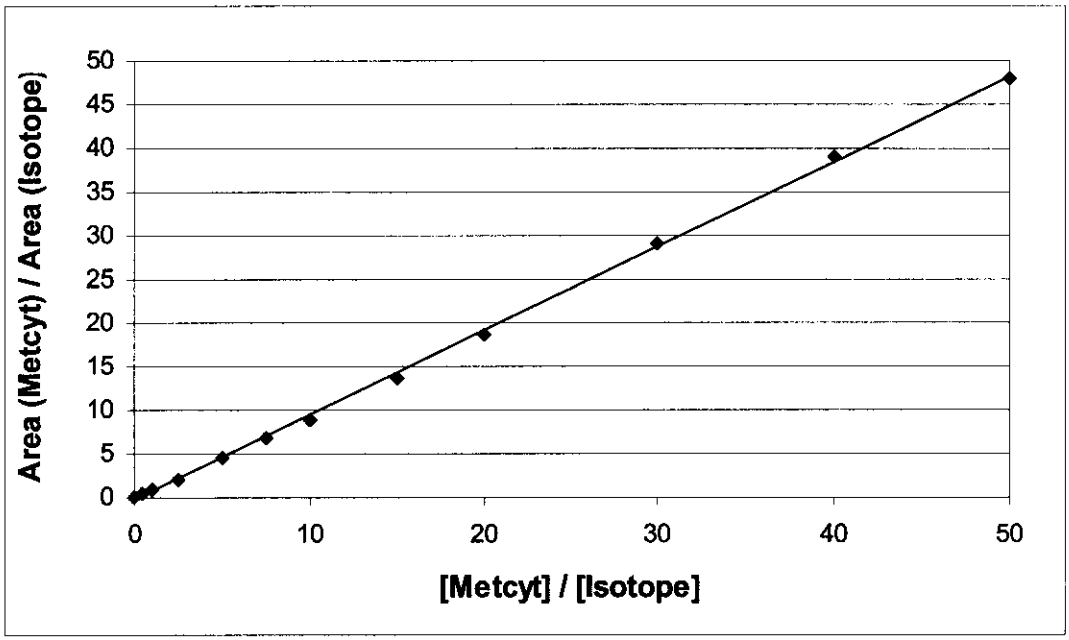

Figure D3. Calibration curve of 5-methylcytosine (Metcyt) compared to the internal standard. (R^2 = 0.9995; response factor = 1.08).

The response factor was calculated (Equation D1) and employed in the quantification of 5-methylcytosine.

(v) Calculation of the response factor for the quantification of 5-methylcytosine levels in DNA hydrolysates

$$\text{Response factor} = \frac{\text{Response IS} \times [\text{analyte}]}{\text{Response (analyte)} \times [\text{IS}]} \qquad \textit{(D1)}$$

Where: Response IS = the response of the internal standard (isotope)
[analyte] = the concentration of the analyte
Response (analyte) = the response of the analyte
[IS] = the concentration of the internal standard (isotope).

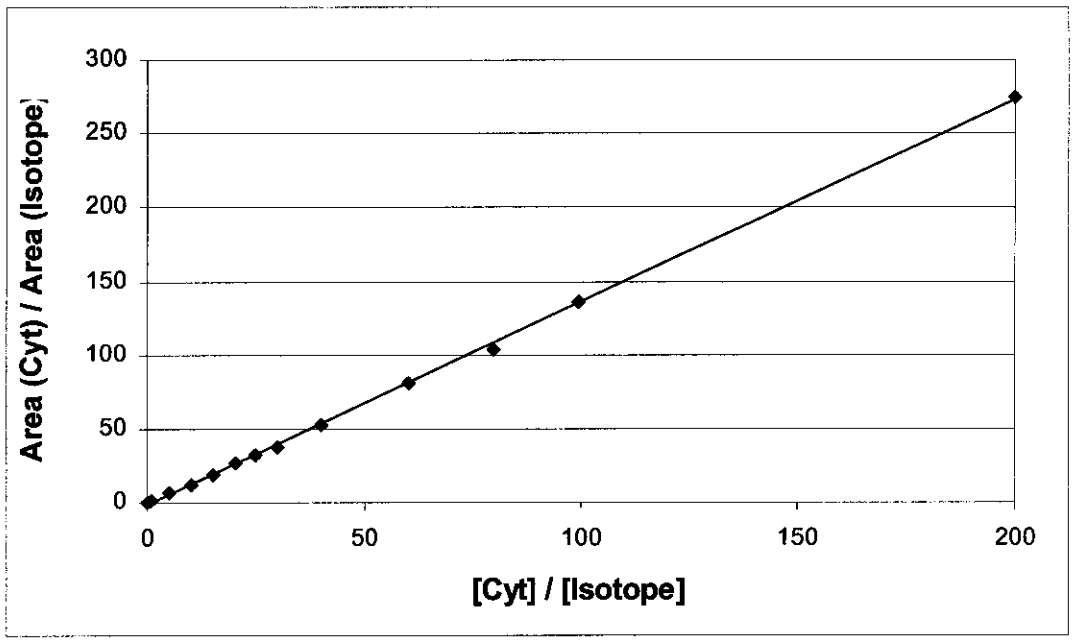

Figure D4. Calibration curve for cytosine compared to the internal standard. (R^2 = 0.9995; response factor = 0.83).

Excellent linearity was obtained for both cytosine and 5-methylcytosine (R^2 = 0.9995) within the relevant concentration range.

(vi) Precision of the 5-methylcytosine analysis

To determine the precision of the analysis, five identical standards were analysed. The standards contained 5 nmoles of each analyte (cytosine, 5-methylcytosine and internal standard). The samples were analysed with the described method and the precision calculated (Table D1):

Table D1. Precision for the quantification of cytosine and 5-methylcytosine.

Assay No.	Cytosine (pmole)	Methylcytosine (pmole)
1	4876	4961
2	4782	4901
3	5425	5382
4	4794	5176
5	5254	4558
Mean	**5026**	**4996**
SD	**294.5**	**309.6**
RSD	**5.86**	**6.20**

(SD = standard deviation; RSD is the relative standard deviation, calculated as SD/Mean x 100)

Although slightly high, the analytical variation of 6.20 %, obtained for the quantification of 5-methylcytosine in isolated DNA samples, by means of the described method was regarded to be acceptable for the assessment of DNA methylation status. Quantification of 5-methylcytosine and isotopically labelled cytosine (Cytosine-2-^{13}C-1,3-$^{15}N_2$) was based on the integration of the area under the analyte peaks in the chromatograms generated by the LC-MS-MS. Since no chromatographic separation of the various molecular species was undertaken, the peaks observed in the chromatograms appeared to be skewed and did not represent an ideal Gaussian distribution of analyte concentration as a function of time. This phenomenon may therefore be responsible for inaccuracies in peak integration and the relatively high RSD of >5 % obtained. Chromatographic separation, prior to tandem MS, will probably eliminate this problem.

(vii) Apparent validity of the method employed for the quantification of 5-methylcytosine levels in DNA hydrolysates

Calf thymus DNA was analysed to determine if results obtained with this method were comparable to published data. Purified calf thymus DNA was hydrolysed and analysed according to the described methods. The methylation status of DNA (% methylated) was calculated (Equation D2):

$$\%\ Methylated\ DNA = \frac{[Metcyt]}{[Metcyt]+[Cyt]} \times 100 \qquad \textbf{(D2)}$$

Where: [Metcyt] = concentration of 5-Methylcytosine
[Cyt] = concentration of cytosine.

Duplicate samples of calf thymus DNA were analysed. The results indicated that 5.95 ± 0.28 % of the genomic DNA was methylated. The reported normal range of calf thymus DNA methylation is 5.7 – 6.8 %, with a mean of 6.5 % (Hall, 1971). Levels of DNA methylation obtained with the ESI-MS-MS method employed in this study proved to be linear, reproducible and relatively accurate compared to published data.

APPENDIX E

Quantification of the effect of β-hydroxynorvaline on polyamine synthesis in maternal and embryonic tissues

High performance liquid chromatography (HPLC) was employed for the quantification of polyamines in the livers of pregnant mice and their unborn offspring. A modified method of Marcé *et al.* (1995) was used.

1. Reagents, materials, buffers and solutions

(i) Reagents and materials

Dansyl chloride (5-Dimethylaminonaphthalene-1-sulfonyl chloride) was purchased form Fluka Biochemika. All other reagents were of the highest purity and were obtained from Sigma Chemical Company.

(ii) Buffers and solutions

- Perchloric acid solution: 0.4 mol/l $HClO_4$
- Sodium bicarbonate solution: 2.5 M, preheated at 37 °C
- Dansyl chloride solution: 5 mg/ml in acetone, freshly prepared
- Proline solution: 100 mg/ml in water, freshly prepared
- Diaminohexane stock solution A (internal standard A): 250 µM prepared in 0.4 M $HClO_4$
- Diaminohexane stock solution B (internal standard B): 10 µM prepared in 0.4 M $HClO_4$

(iii) HPLC specifications

The chromatographic system consisted of a HPLC pump (Dionex model P580A HPG) with an ASI-100 automated sample injector. An online Dionex degasser (Model DG-2410) was used. Fluorescence detection was achieved with a Dionex RF 2000 fluorescence detector (excitation at 340 nm, emission at 540 nm). A Cosmosil 4.6 X 250 mm, 5C18-MSII column was used (Waters, code 38020-41) and protected by a guard column (4 mm X 2 mm I.D.) containing a silica-based C18 sorbent packing.

2. Methods

(i) Sample preparation

Tissue samples were prepared as described (APPENDIX C). Fresh mouse liver tissue was used for the standardisation and validation of the analytical methods. Samples of liver tissue (50 mg) were homogenised on ice in four volumes 0.4 M $HClO_4$ in a Potter-Elvejham homogeniser (Glas-Col). After centrifugation for 10 minutes at 16 000 x *g* (4 °C), the supernatants were removed and frozen at –70 °C until they were used. Quantification of polyamines in experimental animals were performed on the 9 500 x *g* supernatant, obtained during the isolation of mitochondria from the livers of pregnant female mice and their unborn fetuses (APPENDIX C). These samples were stored at –70 °C until analysed.

Frozen tissue sample supernatants were thawed on ice. For the optimisation and validation reactions, 200 µl of the samples were taken for derivatisation. Due to the small available volumes of the experimental samples, only 50 µl aliquots were used for derivatisation. Diaminohexane, the internal standard, was added (100 µl) from a stock solution prepared in 0.4 M $HClO_4$ (stock solution A for the spermine/spermidine analysis and stock solution B for the putrescine analysis). Saturated Na_2CO_3 was added (200 µl of a 2.5 M solution), as well as 400 µl dansyl chloride (100 mg/ml prepared in acetone). After the mixture was vigorously mixed for 10 seconds (Vortex), it was incubated overnight at room temperature (25 °C).

A proline stock solution (100 µl of a 100 mg/ml solution) was added and incubated for 30 minutes in the dark at room temperature to react with the excess dansyl chloride. The dansylated polyamines were extracted twice in 500 µl toluene. Extracts were pooled and dried under vacuum for 15 minutes. Dried samples were dissolved in 100 % acetonitrile (1000 µl and 500 µl for spermine/spermidine and putrescine determinations, respectively), prior to analysis.

(ii) Quantification of spermine and spermidine

Marcé *et al.* (1995) used a single HPLC analysis to quantify spermine, spermidine and putrescine. The concentrations of spermine and spermidine are considerably higher in the eukaryotic cell than that of putrescine (Marcé, 1995). In order to ensure precision and accuracy in the analysis of all three the target polyamines, two different variations of the method, published by Marcé *et al.* (1995) were developed for the quantification of spermine and spermidine (Method 1) and putrescine (Method 2).

(iii) HPLC procedure for the separation of spermine and spermidine (Method 1)

HPLC conditions and instrument settings

- Gradient protocol:
  - Initial conditions: Acetonitrile:H_2O (70:30)
  - Ramp: 70:30 to 100:0 within 4 minutes; maintain at 100:0 for 6 minutes and return to initial conditions within 30 seconds
  - Equilibrate at initial conditions for 10 minutes, prior to next run
- Column: Cosmosil 5C18-MSII column (150 mm x 4.6 mm)
- Volumetric flow rate 1.0 ml/min
- Auto sampler temperature: 25 °C
- Column oven temperature: 25 °C
- Upper pressure limit: 200 bar
- **Fluorescence detector settings**
  - Excitation wavelength: 340 nm
  - Emmision wavelength: 540 nm
  - Emmision gain: 4.0
  - Emmision response: 0.5
  - Emmision sensitivity: Low
  - Emmision step: Auto
  - Emmision average: On

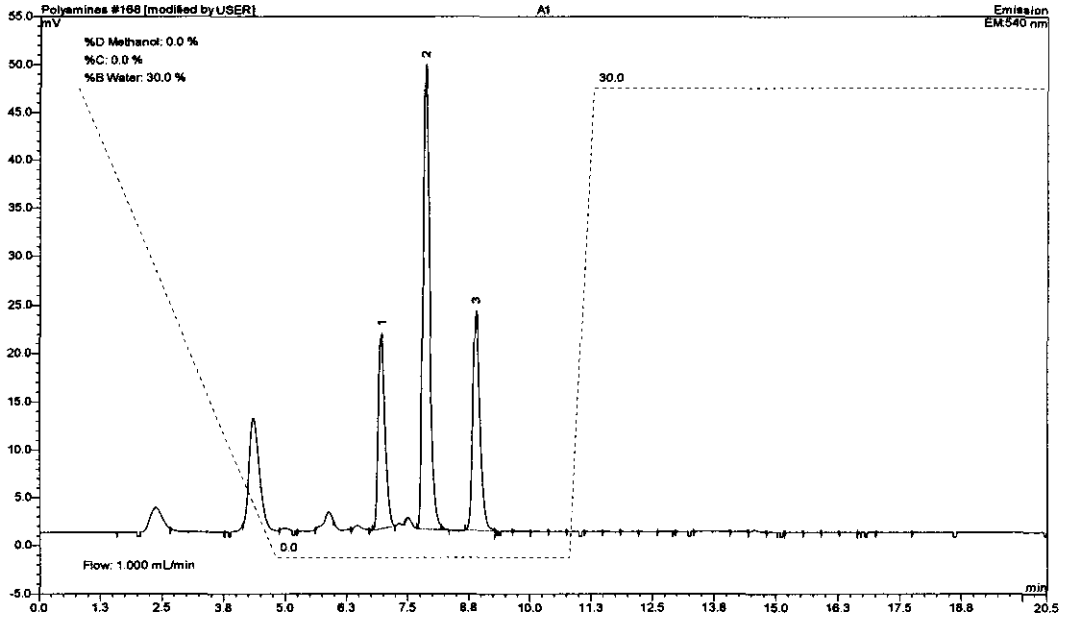

Figure E1. Separation of dansylated standard polyamines. (1) Internal standard, Diaminohexane;(2) Spermidine; (3) Spermine.

(iv) Validation of the spermine/spermidine assay

Calibration curves were obtained by analysing 7 standards, each in duplicate. All the samples were analysed with the method described in Section E2 (iii).

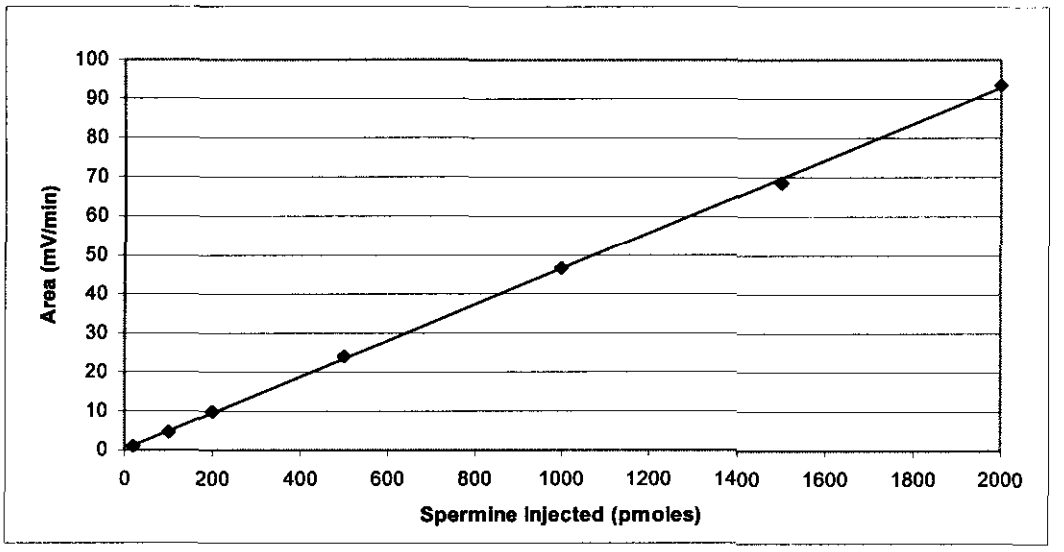

Figure E2. Calibration curve of spermine compared to the internal standard. (R^2 = 0.9997, the response factor = 1.83).

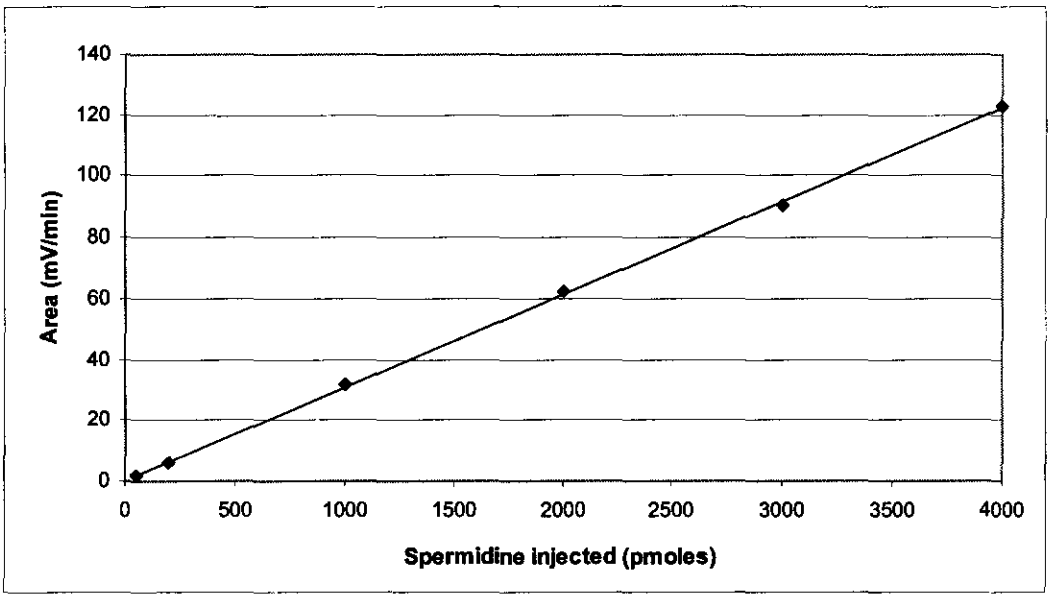

Figure E3. Calibration curve of spermidine compared to the internal standard. (R^2 = 0.9995, the response factor = 1.20).

Excellent linearity was obtained for both spermine and spermidine (R^2 > 0.9995) over the relevant concentration ranges.

(v) Precision of the spermine/spermidine assay

Five identical standards were prepared and analysed as described in Section E2 (iii). The relative standard deviation was calculated from this data.

Table E1. Precision of spermine and spermidine assays.

Assay No.	Spermine (nmole/g)	Spermidine (nmole/g)
1	350.05	1034.99
2	326.08	992.94
3	346.54	1025.35
4	327.06	1014.94
5	350.65	949.86
Mean	**340.08**	**1003.62**
SD	**12.434**	**33.870**
RSD	**3.66**	**3.37**

SD = standard deviation; RSD is the relative standard deviation (calculated as SD/Mean x 100)

The RSD for both the spermine and spermidine analysis was below 4 %, which is acceptable for an analytical technique.

(vi) Quantification of putrescine (Method 2)

The initial column conditions were similar to those used for the separation and quantification of spermine and spermidine (Method 1; acetonitrile:water, 70:30; Section (iii). Ramp changes differed from the previous method: the initial 70:30 ratio of acetonitrile:water was increased to 100:0 within 60 seconds. The latter phase was maintained for 8 minutes, before the gradient was returned to the initial conditions (acetonitrile:water, 70:30) within 60 seconds. The column was also equilibrated for at least 10 minutes prior to injection of the next sample.

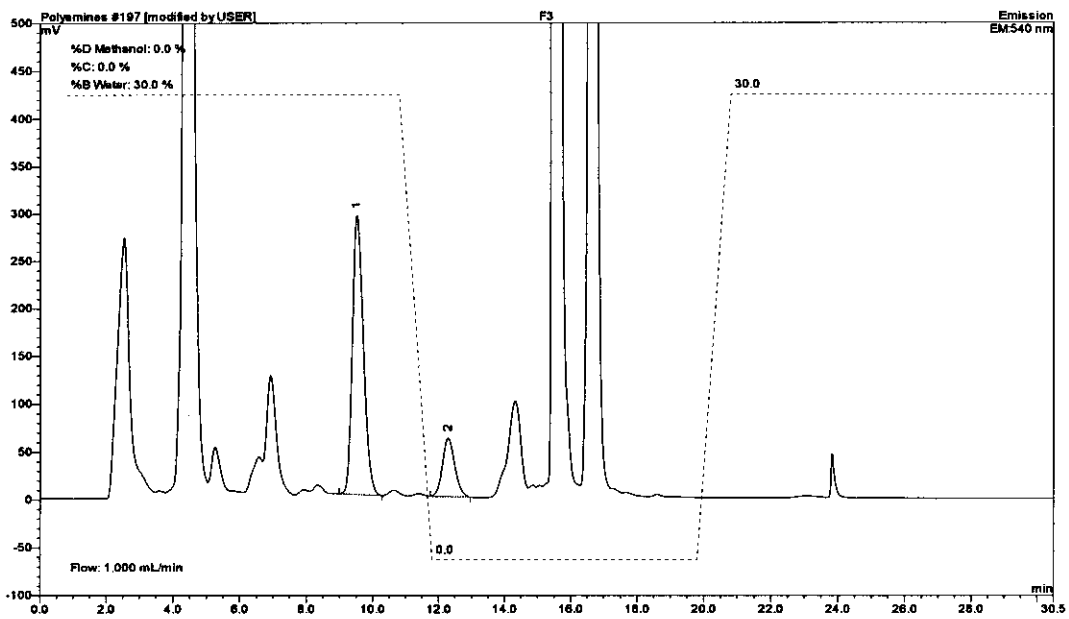

Figure E4. Chromatogram of dansylated standard polyamines. (1) Putrescine; (2) Diaminohexane (IS).

(vii) Validation of the putrescine assay

A calibration curve was obtained by analysing 5 standards in duplicates. All the samples were analysed with the described method (Section E2 (vi)).

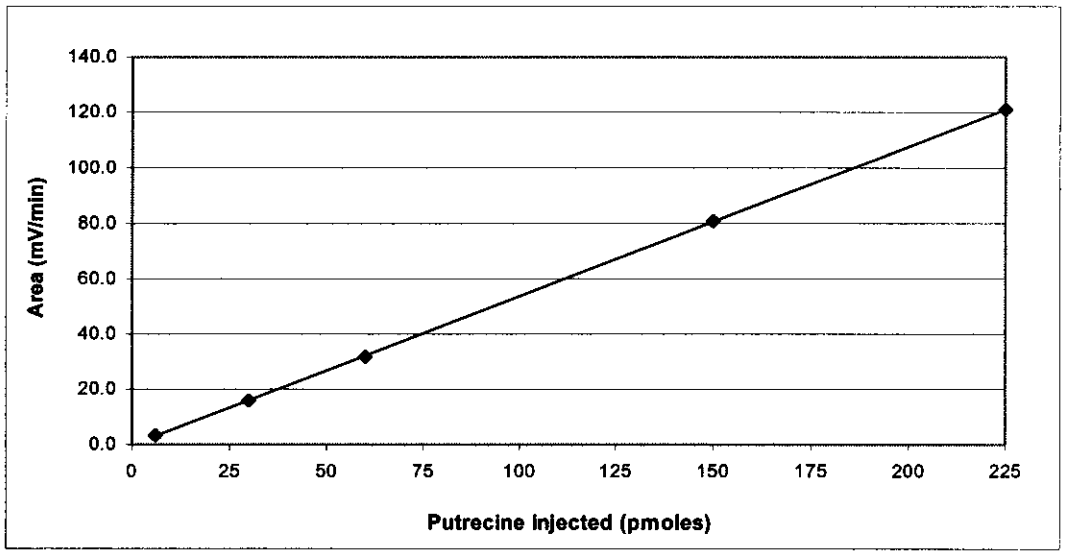

Figure E5. Calibration curve for putrescine compared to the internal standard. (R^2 = 1.0000, the response factor = 0.75).

Excellent linearity was obtained (R^2 > 0.9999) for putrescine calibration over the relevant concentration range. The method therefore proved to be highly sensitive throughout this concentration range. It was regarded to be acceptable for analysing the relatively low levels of putrescine in experimental females and their embryos.

(viii) Precision of the putrescine assay

To determine the precision of the analytical method, 5 identical standards were derivatised and analysed with the described method (Section E2 (vi)). The relative standard deviation was calculated to demonstrate the precision of the putrescine analysis:

Table E2. Precision of the putrescine assay.

Assay No.	Putrescine (nmole/g)
1	15.03
2	14.42
3	14.61
4	14.40
5	14.51
Mean	**14.59**
SD	**0.258**
RSD	**1.76**

SD = standard deviation; RSD is the relative standard deviation (calculated as SD/Mean x 100)

The RSD of 1.76 % was deemed to be acceptable for the analysis of putrescine.

(ix) Calculation of the response factors for polyamine quantification (Equation E1)

$$RF = \frac{\text{Response IS} \times [\text{analyte}]}{\text{Response (analyte)} \times [\text{IS}]} \qquad \textit{(E1)}$$

Where: RF = response factor

Response IS = the response of the internal standard (Diaminohexane)

[analyte] = the concentration of the analyte

Response [analyte] = the response of the analyte

[IS] = the concentration of the internal standard (Diaminohexane).

(x) Apparent validity of the method employed in the analysis of spermine, spermidine and putrescine

Polyamine levels were measured in liver homogenates from pregnant Hanover-NMRI females. Freshly prepared sample supernatants were derivatised as described in Section E2 (i) and analysed (in triplicate) with the described methods.

TABLE E3. Quantification of polyamines in liver homogenate.

Polyamine species	Mean value (nmole/g)	Standard deviation	RSD
Putrescine	14.59	0.29	1.76
Spermidine	1003.62	33.87	3.37
Spermine	340.08	12.43	3.66

Mean of 3 replicates; RSD is the relative standard deviation (calculated as SD/Mean x 100)

Results on polyamine levels in the livers of Hooded-Lister rats, published by Marcé *et al*, (1995) revealed the following: Observed mean levels were 57 ± 16 nmoles/g for putrescine, 2055 ± 195 nmoles/g for spermidine and 1210 ± 165 nmoles/g of fresh liver tissue for spermine. The polyamine levels found in our study (Hanover-NMRI mouse, table 5.3) differ to some extent from the concentrations of the same compounds measured in the Hooded-Lister rat by Marcé *et al.* (1995). These 2 data sets appear not to be exactly comparable and they most probably reflect species differences in the levels of the polyamines.

APPENDIX F

Optimisation and standardisation of the serine hydroxymethyltransferase (SHMT) assay

A modified method of Geller *et al.* (1989) was employed in the analysis of the effect of β-hydroxynorvaline (HNV) on the catalytic activity of serine hydroxymethyltransferase (SHMT; EC 2.1.2.1) in pregnant female mice and their embryos. SHMT is a key enzyme in the folate cycle and plays a major role in one-carbon metabolism with important consequences for the remethylation of homocysteine and biomethylation.

1. Reagents, materials, buffers and solutions

(i) Reagents and materials

Radioactively labelled serine (L-[3-^{3}H]-serine: specific activity 33.0 Ci/mmol) was purchased form Amersham, U.K. All other reagents were of the highest purity and purchased from Sigma Chemical Company, unless otherwise stated.

(ii) Buffers and solutions

- Reaction buffer: Tris-HCl: 500 mM, pH 8
- Phosphate buffer: 500 mM, pH 8
- EDTA (ethylenediaminetetraacetic acid) solution: 50 mM
- DTT (dithiotreitol) solution: 60 mM
- PLP (pyridoxal 5'-phosphate) solution: 50 mM
- L-Serine solution: 10 mM L-serine containing [^{3}H]-serine (2 mCi/mmol)
- THF (tetrahydrofolate) solution: 32 mM prepared in 50 mM Tris-HCl, pH 8

2. Methods

(i) Basic principle of the Geller et al. (1989) assay

SHMT activity is best measured by means of a radiometric assay. The enzyme acts on a pool of L-serine, spiked with 3-[^{14}C]-L-serine. During the enzyme reaction, the methylene group, originating from the hydroxymethyl group (i.e. the 3-^{14}C carbon) of 3-[^{14}C]-L-serine is transferred to the co-substrate, tetrahydrofolate (THF), by SHMT. Unlabelled glycine (Gly) and radiolabelled N^5,N^{10}-[^{14}C]-methylene tetrahydrofolate ($^{14}CH_2$-THF) are produced from the 3-[^{14}C]-L-serine during the reaction. The labelled THF-derivative is then extracted from the reaction mixture onto a DEAE-cellulose anion-exchange solid phase (filter paper). Unreacted, 3-[^{14}C]-L-serine and other reaction products are removed by filtration and subsequent washing of the solid phase, prior to assessing the quantity of $^{14}CH_2$-THF remaining on the paper.

(ii) Modifications of the Geller et al (1989) method

Due to the low specific activity of the ^{14}C-derivatives, the quantity of dpm measured for assays was relatively low, creating problems for the sensitivity of the enzyme assay. The SHMT assay was subsequently modified to obtain higher levels of sensitivity and standardised for this investigation. The [^{14}C]-serine used by Geller *et al.* (1989) as substrate for the SHMT was replaced with [^{3}H]-serine. The specific activity of the tritiated substrate was nearly 10^3 times higher than its [^{14}C]-equivalent and this step alone increased the sensitivity of the SHMT assay significantly.

(iii) Separation of N^5,N^{10}-[^{3}H]methylene tetrahydrofolate ([^{3}H]-CH_2-THF) and unreacted [^{3}H]-serine

The effectivity of the solid phase separation of unreacted [^{3}H]-serine and the SHMT produced [^{3}H]-N^5,N^{10}-methylene tetrahydrofolate ([^{3}H]-CH_2-THF) was investigated. An aliquot of the enzyme reaction mixture was adsorbed onto a Whatman® DEAE cellulose paper circle (2.3 cm, Whatman International Ltd, England), secured in a sealed vacuum manifold. The unreacted [^{3}H]-serine was displaced from the cellulose paper with five

portions of water of 5 ml each. Optimal removal of almost all of the unreacted [^{3}H]-serine could be achieved in this step. The optimal volume of the reaction mixture which could be adsorbed onto the cellulose paper, without exceeding the binding capacity of the anion exchange paper for the [^{3}H]-CH_2-THF, was 50 µl.

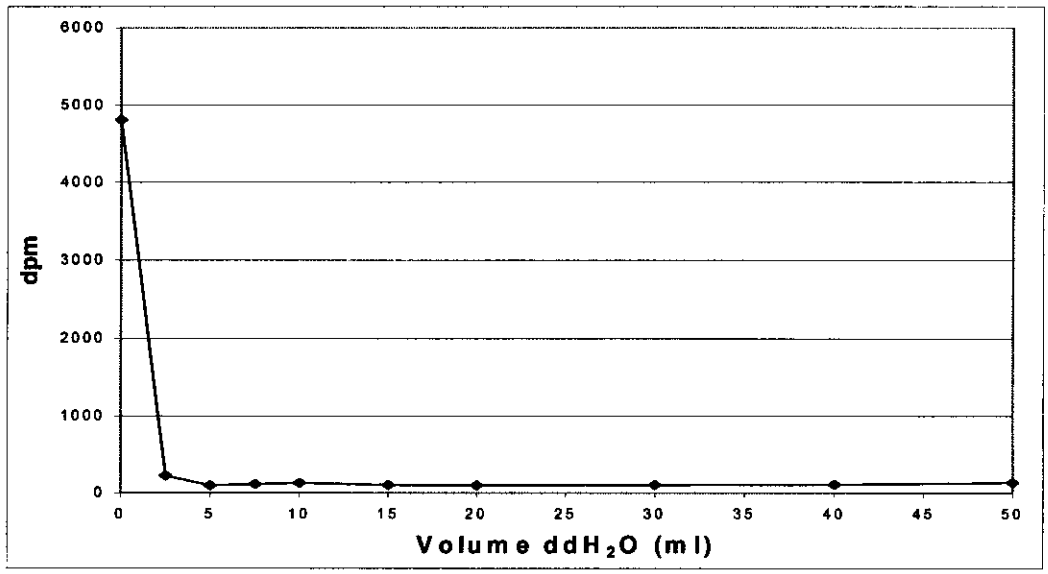

Figure F1. Determination of the optical volume water to remove the unreacted [^{3}H]-serine from the solid state anion extraction phase.

(iv) The effect of different buffers on the rate of the catalytic activity of SHMT

The effect of the type of buffer on the SHMT enzyme reaction was investigated. Apart from the prescribed Tris-HCl buffer (500 mM, pH 8), a phosphate buffer with similar concentration and pH was employed in the assay. A significant inhibition of the rate of SHMT activity by the phosphate buffer (56.7%), as compared to the Tris-HCl buffer, was evident from the results (Figure F2). A similar inhibitory effect of the phosphate buffer was previously reported by Geller *et al.* (1989).

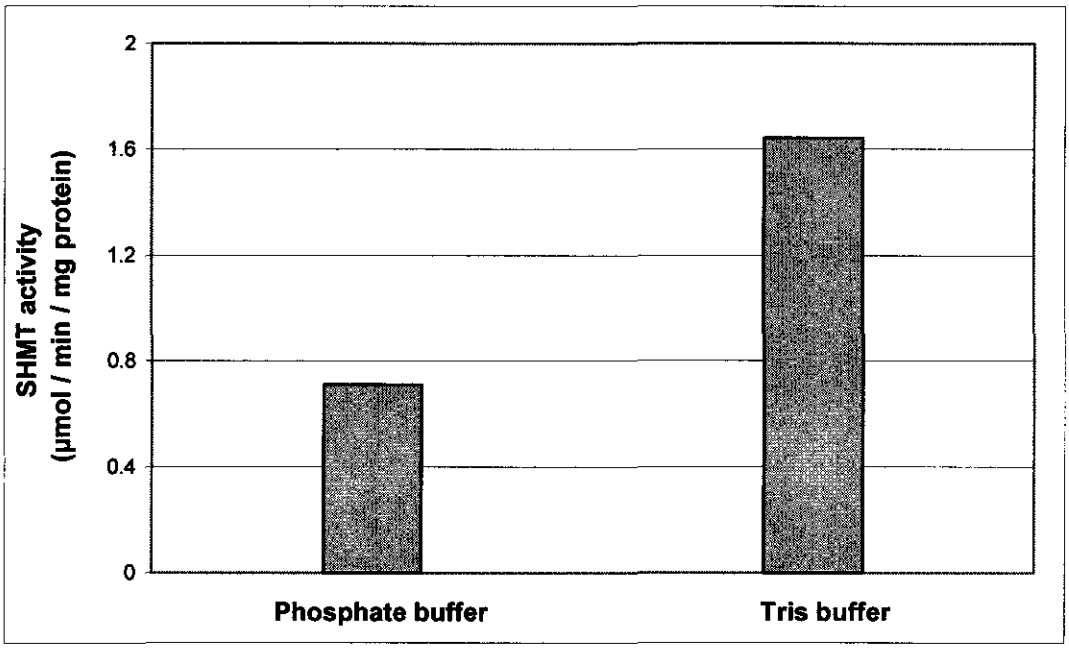

Figure F2. The effect of different buffers on the activity of SHMT.

(v) The effect of increasing PLP-concentrations on the SHMT assay

The reaction mixture employed by Geller *et al.* (1989) for the assay of SHMT activity in rat liver and lens tissue contained 0.25 mM pyridoxal 5'-phosphate (PLP). Since PLP may form a Schiff base with [^{3}H]-serine, the resulting radiolabelled serine-PLP complex may also bind to the DEAE cellulose disk and cause a high background radioactivity. The PLP concentration must therefore be kept as low as possible in order to avoid a high background, which may render the SHMT assay insensitive. However, PLP is an essential coenzyme of SHMT and a too low concentration of PLP in the reaction mixture may result in low enzyme activity.

The effect of increasing PLP concentrations (0 - 1.0 mM) on the SHMT assay was therefore investigated. Addition of increasing concentrations of PLP to the reaction mixture had no apparent effect on SHMT activity. The enzyme activity appeared to remain relatively constant over this concentration range (Figure F3) and it was subsequently inferred that mouse liver SHMT is naturally saturated with PLP.

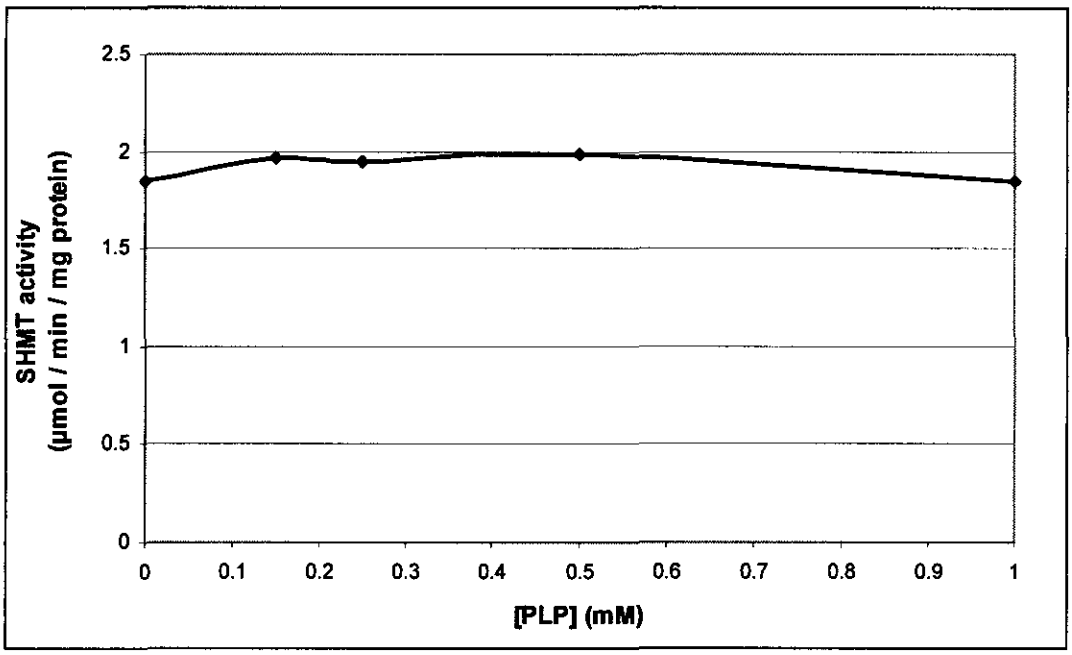

Figure F3. The effect of increasing PLP concentrations on the activity of SHMT.

According to Schirch (1982), purified SHMT contains one tightly bound PLP molecule per subunit, which can only be removed enzymatically. Since addition of supplemental PLP to the enzyme reaction mixture had no effect on SHMT activity (Fig. F3), and due to the fact that added PLP may result in a high background, all SHMT assays were subsequently performed without supplemental PLP.

(vi) The effect of serine and THF concentrations on SHMT activity

SHMT activity was measured at various concentrations of the substrate, serine (0 - 10 mM) in an effort to increase the sensitivity of the SHMT assay (Figure F4) and to determine an optimum substrate level for inhibition studies. A concentration of 2 mM serine was selected. At this concentration, serine did not appear to be rate limiting and no substrate inhibition was observed (Palmer, 1995).

A similar approach was used to determine the optimum THF concentration. SHMT activity was measured at 2 mM serine and varying concentrations of THF (0 - 12 mM). No substrate inhibition was observed up to 12 mM THF (Figure F5). THF is highly sensitive to oxidation, and its concentration in the

reaction mixture was therefore kept high (12 mM) in order to prevent it from becoming rate limiting.

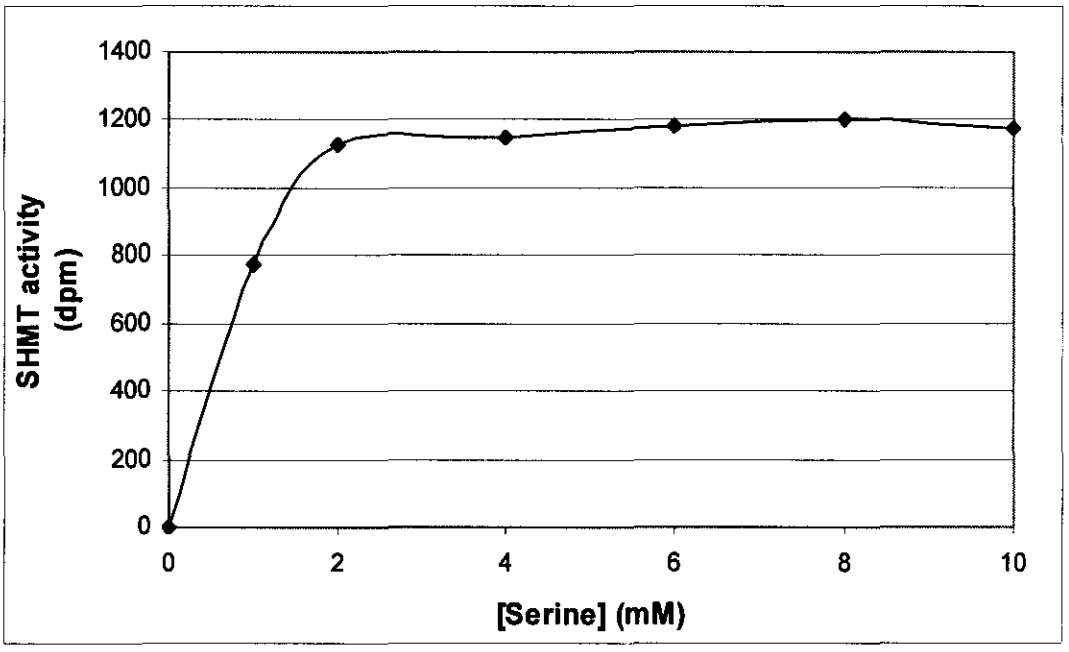

Figure F4. The effect of increasing serine concentration on the activity of SHMT.

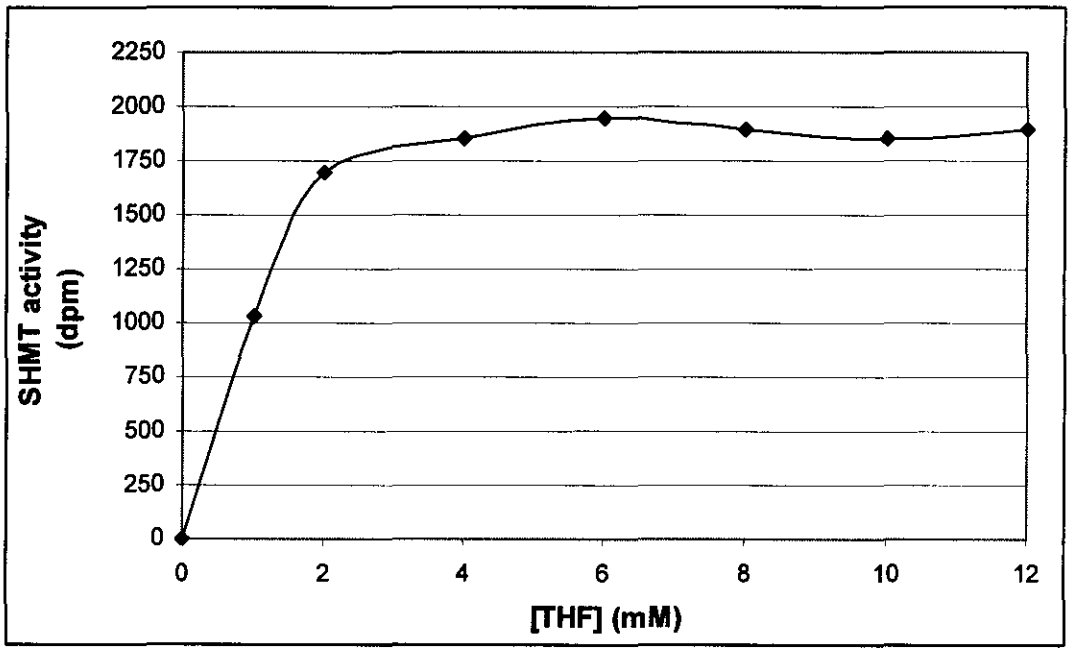

Figure F5. The effect of increasing THF concentration on the activity of SHMT.

(vii) Quantitative extraction of [^{3}H]-CH_2-THF from the DEAE solid phase

In the method employed by Geller *et al.* (1989), [^{3}H]-CH_2-THF is quantified by assessing the radioactivity adsorbed onto the DEAE cellulose solid phase filter paper with a liquid scintillation counter. The DEAE cellulose filter papers, containing the adsorbed [^{3}H]-CH_2-THF, were initially suspended in scintillation cocktail within the counting vials and then counted. The problem with this approach was that the DEAE cellulose paper appeared to cause a considerable amount of quenching of the energy of emitted β-particles, within the sample, resulting in relatively low and inconsistent results (dpm values).

When samples were left suspended in the scintillation cocktail for approximately two days, the quantity of radioactivity (dpm values) increased up to 300%, compared to that in recently counted samples. This phenomenon was ascribed to the gradual dissolution of the DEAE cellulose bound [^{3}H]-CH_2-THF into the scintillation liquid.

To overcome the problem of quenching, the DEAE cellulose bound [^{3}H]-CH_2-THF was decomposed into free, unlabelled THF and [^{3}H]-formaldehyde, following the addition of hydrochloric acid (final concentration: 0.1M) to the sample (Figure F6). DEAE cellulose fibres in the suspension were subsequently pelleted by centrifugation (16 000 x *g* x 3 min), the clear supernatant containing the released [^{3}H]-formaldehyde solution transferred to a scintillation vial, scintillation cocktail added and the quantity of [^{3}H]-formaldehyde in the sample assessed with a liquid scintillation counter.

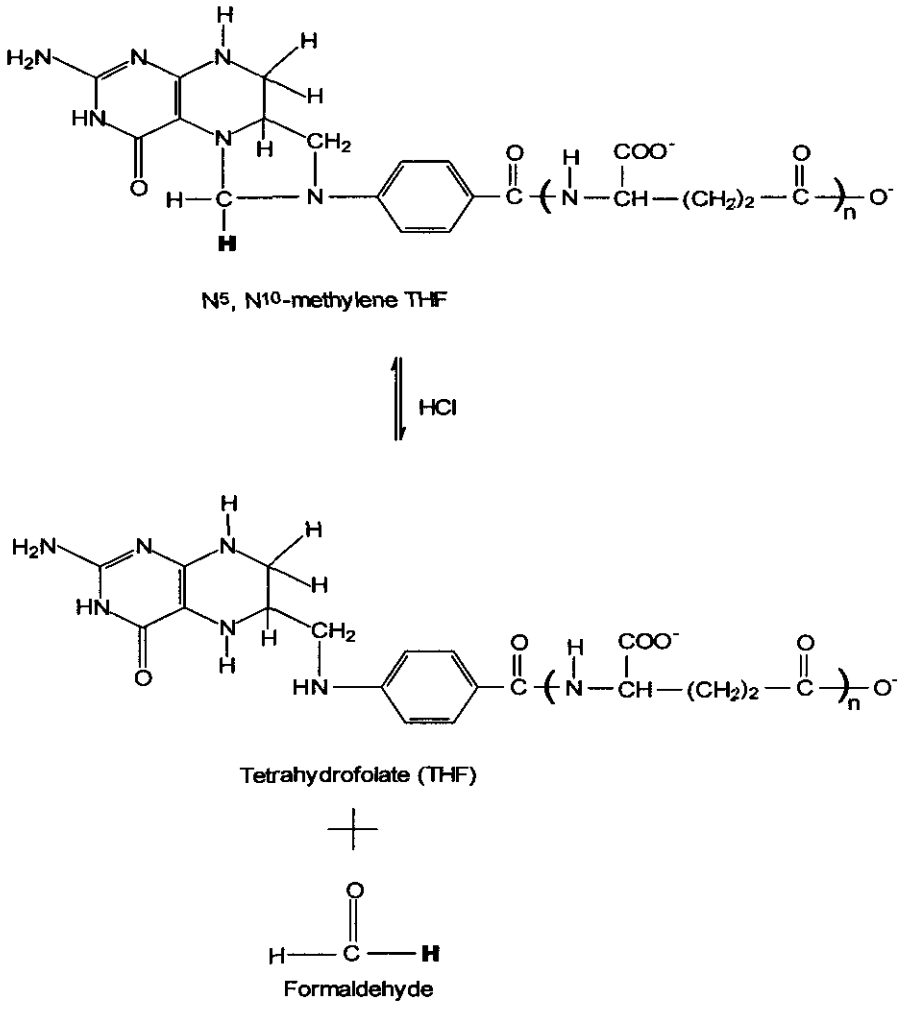

Figure F1. Conversion of [^{3}H]-CH2-THF to [^{3}H]-formaldehyde and unlabelled THF by HCl.

Since formaldehyde is relatively volatile, attempts were made to "trap" the radioactive [^{3}H]-formaldehyde product in a "non-volatile" form. Derivitisation of the [^{3}H]-formaldehyde with 2,4-dinitrophenylhydrazine to form [^{3}H]-formaldehyde-2,4-dinitrophenyl-hydrazine did not to have any beneficial effect on the recovery of radioactivity. Enzyme assays were therefore executed without "trapping" the acid-released [^{3}H]-formaldehyde.

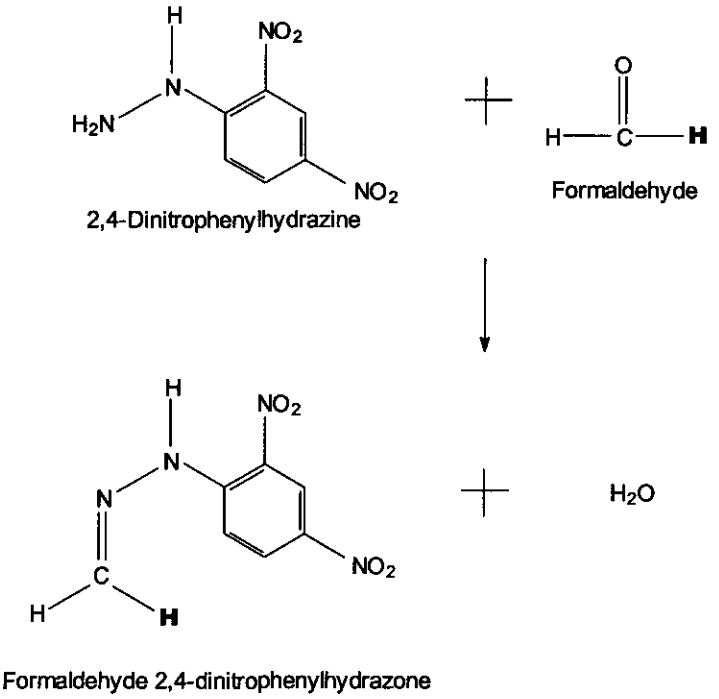

Figure F2. Proposed reaction of [^{3}H]-formaldehyde with 2,4-dinitrophenyl-hydrazine to form [^{3}H]-formaldehyde-2,4-dinitrophenylhydrazine and water.

(viii) The validated SHMT assay

A complete assay reaction mixture in a final volume of 200 µl contains 50 mM Tris-HCl buffer (pH 8.0), 2.5 mM ethylenediaminetetraacetic acid (EDTA), 3 mM dithiotreitol, 12 mM tetrahydrofolate (THF), 2 mM serine containing [^{3}H]-serine (2 mCi/mmol), and 200 µg protein (liver homogenate or isolated mitochondria). Enzyme reactions were initiated with the addition of [^{3}H]-serine solution (40 µl) and the reaction mixtures incubated for 15 minutes at 37°C. The reactions were terminated by adsorbing aliquots (50 µl) of the reaction mixtures onto Whatman® DEAE cellulose filter paper circles secured in a vacuum manifold. Assays were executed in triplicate to minimize variations in results. The cellulose papers were thoroughly washed with distilled water (5 x 5 ml portions) at a flow rate of 5 ml/minute.

The DEAE cellulose filter papers were removed, individually placed in a 1.5 ml plastic Eppendorf® reaction vials and 1 ml 0.1 N HCl added. The vials were tightly sealed and vigorously shaken to disintegrate the filter papers and to form a fibre suspension. Samples containing the acidified DEAE cellulose fibre suspension were incubated for 30 minutes at room temperature, regularly shaken every 10 minutes, and then centrifuged (16 000 x *g* for 3 minutes at 4°C). An aliquot (750 µl) of each sample supernatant was transferred to a scintillation vial and dissolved in Ultima Gold™ XR liquid scintillation cocktail (3 ml). Proper dissolution was ensured by vortexing each sample. The [^{3}H]-formaldehyde content of individual samples was quantified with a MINAXI Tri-carb® 4000 liquid scintillation counter. An external quench standard series (standard curve) was employed to correct for quenching. Enzyme activity was subsequently calculated using Equation F1:

$$SHMT\ activity = \frac{(Sample\ dpm - Blank\ dpm)}{SA \times TP} \times CF \qquad \textbf{(F1)}$$

Where: SHMT activity is expressed as µmol.min^{-1}.mg protein^{-1}

Sample dpm = disintegrations per minute observed in samples

Blank dpm = disintegrations per minute observed in blanks (background dpm)

SA = the specific activity of the [^{3}H]-serine substrate, expressed as dpm/nmole

TP = the total protein (mg) in the reaction mixture

CF = correction factor

(ix) Linearity of the SHMT assay with regard to protein content

In order to express the activity of an enzyme in absolute terms (specific activity), it is necessary to ensure that the assay procedure measures the maximum reaction velocity proportional to enzyme activity. Under these conditions, the ratio of velocity/enzyme concentration should be constant and can be used to express the activity of the enzyme quantitatively (Tipton, 1992). A graph of reaction velocity against enzyme concentration should theoretically be a straight line passing through the origin (zero activity at zero enzyme concentration). Enzyme activity under these conditions should only be influenced by the concentration of the enzyme and its catalytic

activity and is independent of the concentration of the substrates (non rate-limiting). Since the SHMT assay is an end point analysis, it was essential to assess the linearity of the assay. The upper and lower limits of protein concentration where the reaction velocity of the enzyme was still linear were determined.

The linearity of the cytosolic (cSHMT) and mitochonrial SHMT (mSHMT) assays, developed to measure enzyme activity in liver tissue of pregnant female mice and their 10-day-old unborn fetuses, was investigated. After homogenates were prepared from the livers of the mothers and whole embryos, mitochondria were isolated as described in APPENDIX C. The 9 000 x *g* supernatant was used for the cSHMT assay and the isolated mitochondria (9 000 x *g* pellet) for the mSHMT assay.

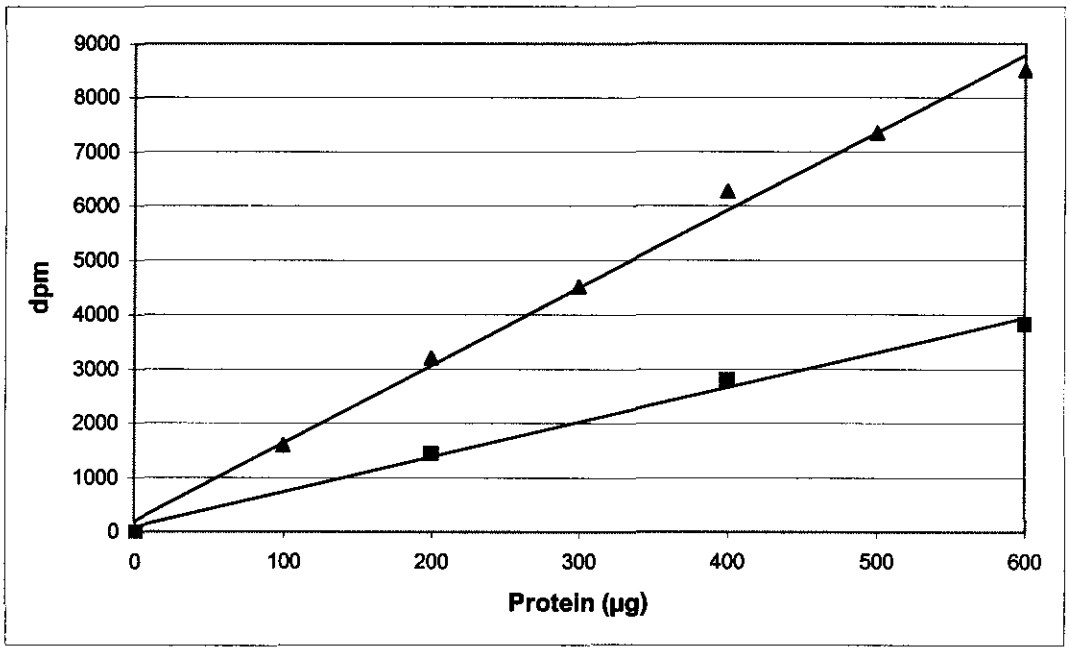

Figure F3. Linearity of the hepatic cSHMT and mSHMT assays. (pregnant female mice. (▲) cSHMT (R^2 = 0.9954); (▪) mSHMT (R^2 = 0.9945).

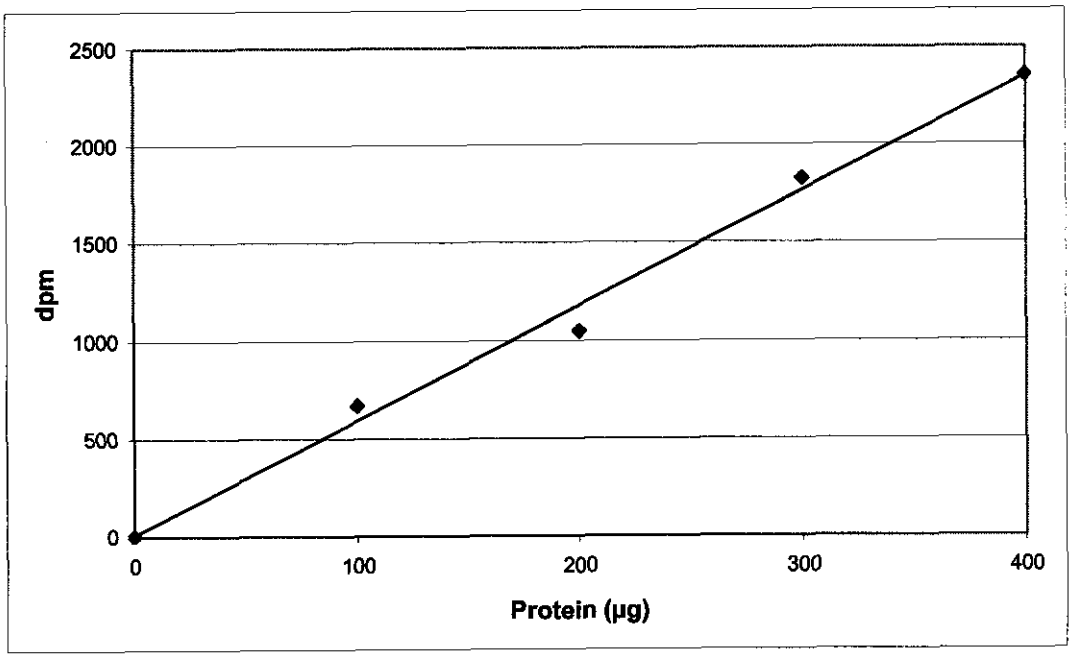

Figure F4. Linearity of the cSHMT assay in mouse embryos. ($R^2 = 0.9925$).

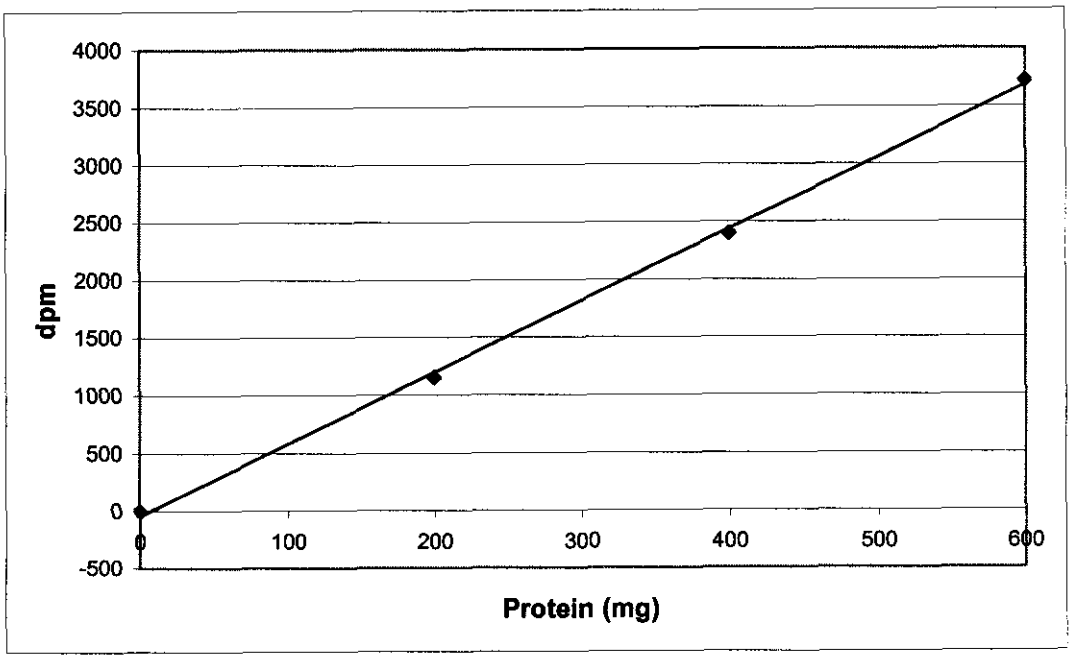

Figure F5. Linearity of the mSHMT assay in mouse embryos. ($R^2 = 0.9992$).

(x) Precision of the SHMT assay

Precision of measurements is defined as the level of agreement between replicate measurements (Bergmeyer, 1983) and is also termed the intra batch variation of the analytical method. To determine the precision of the SHMT assay, a liver homogenate was used. Nine identical samples were taken from a single liver homogenate and analysed according to the described method. The standard deviation (SD) and relative standard deviation (RSD) was calculated to demonstrate the variation in the results generated with the standardised analytical method. These measures of variation correspond to the conventional expressions variance and analytical variability (Bergmeyer, 1983).

Table F1. Precision of the SHMT assay.

	SHMT activity ($\mu mol.min^{-1}.mg\ protein^{-1}$)
1	1.90
2	1.81
3	1.54
4	1.56
5	1.67
6	1.78
7	1.89
8	1.69
9	1.50
Mean	**1.70**
SD	**0.14**
RSD	**8.31%**

SD = standard deviation; RSD is the relative standard deviation (calculated as SD / Mean x 100)

The relative standard deviation of an enzyme analysis should be less than 10 % (Cleland, 1967). The RSD of 8.31 % obtained with the standardised method is therefore acceptable for an analytical enzymatic method.

APPENDIX G

Optimising the glycine cleavage system assay

The method of Kalbag and Palekar (1990), as modified by Brits (2004) was employed in the investigation of the effect of HNV on the catalytic activity of the glycine cleavage system (GCS: EC2.1.2.1) in pregnant female mice and their embryos. The GCC complex is an integral part of the inner mitochondrial membrane and consists of three units, each catalysing a specific step in the catalytic reaction, where the substrate glycine is converted to ammonia and carbon dioxide. This enzyme complex also plays an important role in the flux of one-carbon units between the cytosol and the mitochondria.

1. Reagents, materials, buffers and solutions

(i) Reagents and materials

Radioactively labelled glycine ([1-^{14}C]-glycine) with a specific activity of 56.0 mCi/mmol was purchased form Amersham, U.K. All other reagents were of the highest purity and purchased from Sigma Chemical Company, unless stated otherwise.

(ii) Buffers and solutions

- Reaction buffer: 400mM Tris-HCl, pH 8
- NAD^+ (β-nicotinamide adenine dinucleotide) solution: 10 mM
- Mercaptoethanol solution: 50 mM
- PLP (pyridoxal 5'-phosphate) solution: 2.5 mM prepared in 40 mM Tris-HCl, pH 8
- THF (tetrahydrofolate) solution: 32 mM prepared in 40 mM Tris-HCl, pH 8
- Glycine solution: 100 mM glycine solution containing [1-^{14}C]-glycine (25.0μCi/mmol)

2. Methods

(i) Basic principle of the Kalbag and Palekar (1990) assay

The assay is based on the oxidative cleavage of glycine, spiked with [1-^{14}C]-glycine with the resultant production of CO_2, ($^{14}CO_2$) and NH_4^+. β-Nicotinamide adenine dinucleotide (NAD^+) is used as a coenzyme in the reaction. In the process, tetrahydrofolic acid (THF) is converted to N^5,N^{10}-

methylene THF and NAD^+ is reduced (NADH + H^+). The CO_2 and $^{14}CO_2$ produced in the reaction, is absorbed by a solution of potassium hydroxide (KOH) in a sealed-off reaction vial and can be quantified with a liquid scintillation counter. Enzyme activity is proportional to the net amount of radio labelled $^{14}CO_2$ released in the course of the reaction.

(ii) The GCS assay

A complete assay reaction mixture (1000 µl) contained Tris-HCl buffer (80 mM, pH 8.0), pyridoxal-5-phosphate (PLP; 0.25 mM), β-nicotinamide adenine dinucleotide (NAD^+; 1.0 mM), mercaptoethanol (5.0 mM), tetrahydrofolate (THF; 0.5 mM), the substrate glycine spiked with [1-^{14}C]-glycine (10 mM) and approximately 1500 µg of protein (isolated mitochondria from liver or whole embryos).

The enzyme reaction was initiated with the addition of substrate and the reaction mixture incubated for 30 minutes at 37°C in a sealed Warburg flask. The flasks were agitated continuously during their incubation to assist with the release of CO_2 and $^{14}CO_2$ produced during the enzyme reaction. The released CO_2 was absorbed in a solution of KOH (2 M; 200 µl), contained in an Eppendorf® tube, inserted into the sealed reaction vessel. After incubation, the reaction was terminated by the addition of 1 ml HCl (5 N) to the reaction mixture. The flask was shaken for an additional 60 minutes to facilitate the release and KOH absorption of CO_2, generated by the enzyme. Aliquots (190 µl) of the CO_2 and $^{14}CO_2$ containing KOH solutions were subsequently transferred from the reaction flasks to scintillation vials, 3 ml Ultima Gold™ XR liquid scintillation counter cocktail (Packard) added to the solutions and the samples vortexed to ensure proper mixing of the contents. [^{14}C]-CO_2 was quantified with a MINAXI Tri-carb® 4000 liquid scintillation counter. An external standard quench series (standard curve) was used to correct for quenching. Enzyme activity was calculated with Equation G2:

$$GCS\ activity = \frac{(Sample\ dpm - Blank\ dpm)}{SA \times TP} \times CF \qquad \textbf{(G2)}$$

Where: GCS activity is expressed as nmol.min^{-1}.mg protein^{-1}

Sample dpm = disintegrations per minute observed in samples

Blank dpm = disintegrations per minute observed for background

SA = specific activity of [1-^{14}C]-glycine,(dpm / nmole)

TP = the total amount of protein (mg) in the reaction mixture

CF = Correction factor

(iii) The GCS activity relative to citrate synthase (CS) activity

Citrate synthase was used as a marker enzyme (See Appendix H). Since protein concentration alone is not very accurate as a means of expressing the specific activity of mitochondrial enzymes, CS was used as an internal standard against which the activity of other enzymes can be normalised, since it is a known marker enzyme for mitochondrial content. The activity of the GCS was subsequently calculated with Equation G.3:

$$GCS\ activity = \frac{GCS\ activity}{Citrate\ synthase\ activity} \qquad \textbf{(G3)}$$

Where: GCS activity is expressed as nmol.min^{-1}.Unit CS^{-1}

GCS activity is expressed as nmol.min^{-1}.mg protein^{1}

One unit of citrate synthase activity = 1 µmol.min^{-1}.mg protein^{1}

(iv) Linearity of the GCS assay

The linearity of the GCS assay, executed on mitochondria isolated from hepatic tissues of pregnant female mice and whole 10-day-old fetuses, was determined.

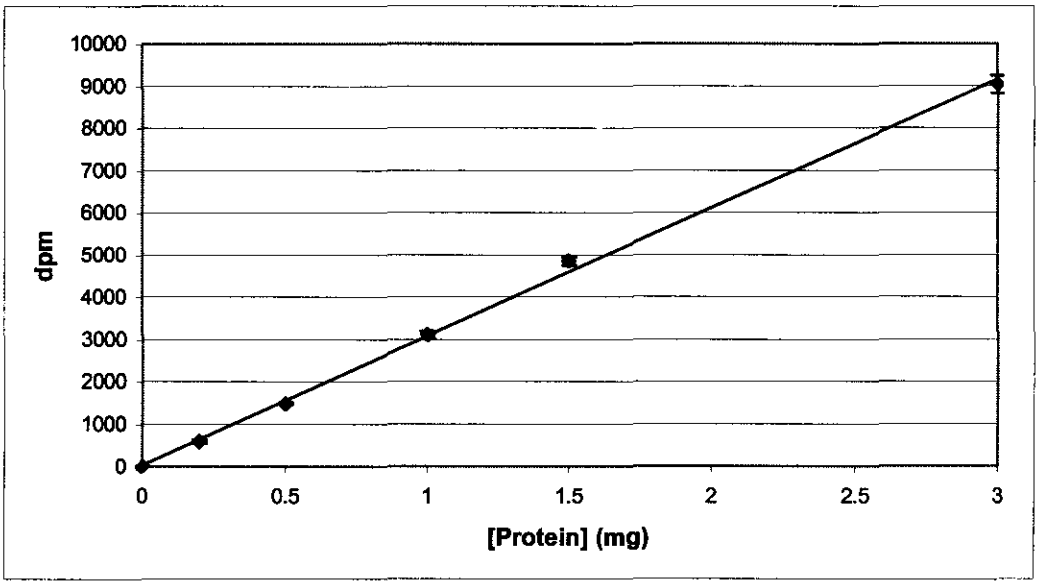

Figure G1. Linearity of the GCS assay in the liver mitochondria of a pregnant female mouse. (R^2 = 0.9984).

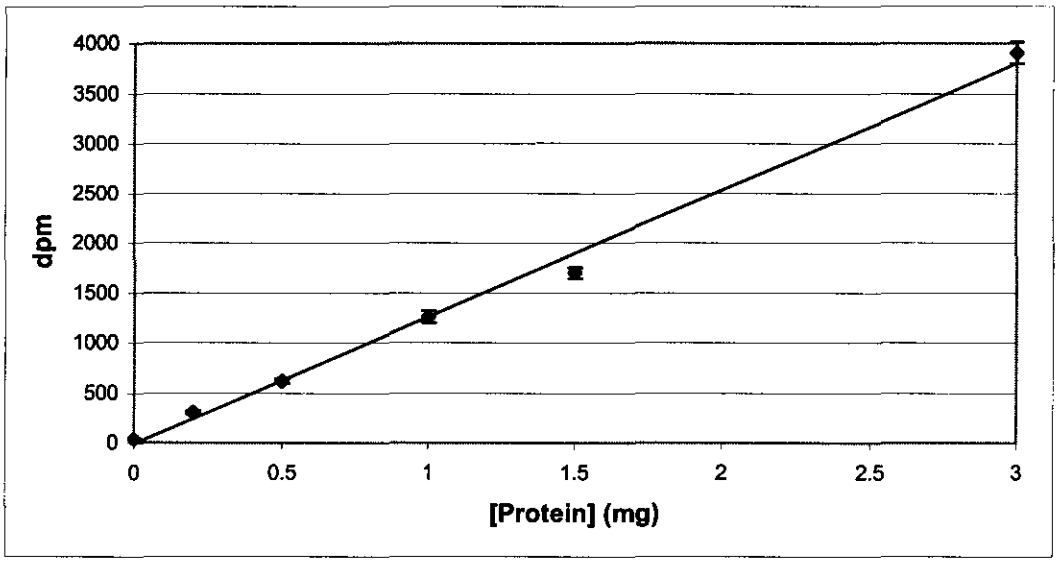

Figure G2. Linearity of the GCS assay in mitochondria isolated from 10-day-old mouse embryos. (R^2 = 0.9944).

(v) Precision of the GCS assay

To determine the precision of the GCS assay, freshly isolated mitochondria from a pregnant female mouse were used. Five identical samples were analysed in duplicate with the described method. The relative standard deviation was calculated to demonstrate the precision of the analytical method.

Table G1. Precision of the GCS assay.

	GCS activity ($nmol.min^{-1}.mg\ protein^{-1}$)
1	1.782
2	1.781
3	1.780
4	1.799
5	1.786
Mean	**1.786**
SD	**0.008**
RSD	**0.438**

SD = standard deviation; RSD is the relative standard deviation (calculated as SD/Mean x 100)

The RSD of 0.44 % was deemed acceptable for an enzymatic analysis.

APPENDIX H

The citrate synthase assay

Citrate synthase (CS) was used as a marker enzyme (internal standard) for the expression of mitochondrial enzyme activity. The method of Robinson *et al.* (1987) was employed.

1. Reagents, materials, buffers and solutions

(i) Reagents and materials

Radioactively labelled glycine ([1-^{14}C]-glycine) with a specific activity of 56.0 mCi/mmol was purchased form Amersham, U.K. DTNB (5,5'dithiobis-[2-nitrobenzoic acid]) was purchased from Boehringer Mannheim. All other reagents were of the highest purity and purchased from Sigma Chemical Company, unless stated otherwise.

(ii) Buffers and solutions

- Reaction buffer: 1 M Tris-HCl, pH 8
- 5,5'dithiobis-[2-nitrobenzoic acid] (DTNB) solution: 0.4 mg/ml in 1M Tris-HCl, pH8 (freshly prepared)
- Oxaloacetate solution: 1.32 mg/ml in water (freshly prepared)
- Acetyl-CoA solution: 6 mM
- Triton X100 solution: 10 % in water (freshly prepared)

2. Methods

(i) The CS assay

Citrate synthase (CS) catalyses the irreversible condensation of oxaloacetate and acetyl-CoA to form citrate and free coenzyme A (CoA) in the first reaction of the Krebs cycle. CS is located inside the mitochondria and is hence used as a marker enzyme to express the activity of other mitochondria-based enzymes. The principle of the CS assay of Robinson *et al.* (1987) is based on the binding of the released CoA to DTNB. This reaction can be measured spectrophotometrically at 412 nm.

A complete assay reaction mixture contained Tris-HCl buffer (100 mM, pH 8.0), 5,5'dithiobis-[2-nitrobenzoic acid] (DTNB, 45 µM), Triton X100 (0.04 %), acetyl-CoA (60 µM) and isolated mitochondria (~ 2 mg protein/ml; 2 µl) in a final volume of 500 µl. The reaction rate was measured spectrophotometrically at 412 nm on a Beckman DU® 7500 spectrophotometer. The initial rate of CS in the absence of substrate was measured as the background activity of the enzyme (A1 = dA_{412}/min). After 2 minutes, 25 µl oxaloacetate solution was added to initiate the reaction. Reaction velocity was measured for 3 minutes at 412 nm (A2 = dA_{412}/min). Citrate synthase activity was calculated (Equation H1). One unit of citrate synthase activity is defined as 1 µmol.min^{-1}.mg protein^{-1}.

$$CS\ activity = \frac{(A2 - A1)}{13.6\ mM^{-1}} \times \frac{0.5}{TP} \qquad \textbf{(H1)}$$

Where: CS activity is expressed as µmol.min^{-1}.mg protein^{-1}

A1 = initial reaction velocity (dA_{412}/min over a 2 minute period)

A2 = the reaction velocity (dA_{412}/min over a 3 minute period)

dA_{412} = change in absorbance at 412 nm

13.6 mM is the molar absorptivity coefficient

Volume correction factor = 0.5

TP = the total amount of protein present in the reaction in mg.

APPENDIX I

Qualitative and quantitative effects of β-hydroxynorvaline on urinary organic acids in HNV treated female mice

The extraction of organic acids with a liquid-liquid extraction procedure is still the most commonly used method although it is less effective than column extraction (Chalmers, 1982). By using more than one solvent, organic acids are more effectively isolated (Erasmus, 1987). In this study, a combination of diethyl ether and ethyl acetate was used for extraction of organic acids. 3-Phenyl butyric acid was employed as an internal standard in the quantification of organic acids.

1. Reagents, materials, buffers and solutions

(i) Reagents and materials

Sodium sulphate was purchased from BDH Laboratory Supplies. All other reagents were of the highest purity and purchased from Sigma Chemical Company.

2. Methods

(i) Organic acid extraction procedure

Creatinine content of urine samples was determined with the picric acid method, originally described by Jaffe (1886) and later modified by Chasson (1961). Internal standard (2.5 µmol/mg creatinine) was added to 0.5 ml urine in a glass Kimax® tube and the pH adjusted to pH = 2 with HCl (5 mol/l). Organic acids were extracted, following the addition of ethyl acetate (6 ml) and diethyl ether (3 ml), respectively to the urine and subsequent shaking for 15 minutes. Phase separation was achieved by centrifugation. The two organic phases were removed, combined and all residual water removed by the addition of a small amount of anhydrous sodium sulphate. The sodium sulphate was removed by centrifugation, the supernatant removed and dried under a N_2 stream at room temperature. This procedure

is referred to as the "standard liquid-extraction procedure" throughout this thesis.

(ii) Derivatisation of organic acids

Organic acids were derivatised with BSTFA (N,O-bis(Trimethylsilyl)-trifluoroacetamide) and TMCS (Trimethylchlorosilane). BSTFA (22.6 µl/µmol creatinine) and TMCS (4.5 µl/µmol creatinine) were added to the dried organic acids and incubated for 30 minutes at 70 °C.

(iii) Gas chromatography mass spectrometry (GC-MS) of TMS-derivatives of organic acids

Gas chromatographic mass spectrometry analyses were performed on a Hewlett Packard 6890 GC, equipped with a split/splitless auto injector (Agilent 7683 series). An SE 30 (25 m x 0.33 mm ID) capillary column was used with helium as a carrier gas at a flow rate of 1 ml/min. Initial oven temperature was 60°C and was maintained for 2 minutes. The temperature was then increased at 4 °C/min up to 120 °C, after which it was increased by 10 °C/min to a final temperature of 280 °C. An inlet temperature of 280 °C was used.

A quadrupole mass spectrometer (HP 5973) was used for GC-MS analyses. In order to obtain an electron ionisation spectrum, the source temperature was kept at 230 °C and the electron energy at 70 eV.

(iv) Quantification of organic acids

Organic acids were quantified, relatively to the internal standard (Equation I1).

$$[Metabolite] = \frac{A_m}{A_{IS}} \times 262.5 \qquad \textit{(I1)}$$

Where: [Metabolite] = the metabolite concentration in mg/mol creatinine

A_m = the peak area obtained from the corresponding signal for the specific metabolite

A_{IS} = the peak area of the internal standard

262.5 = the concentration of the internal standard (µmol/litre).

APPENDIX J

Chiral separation and quantification of the relative molar ratio of β-hydroxynorvaline stereoisomers

Commercially available and synthesised β-hydroxynorvaline (two chiral carbon atoms) consists of 4 stereoisomers: 2R,3R-β-hydroxynorvaline, 2R,3S-β-hydroxynorvaline, 2S,3R-hydroxynorvaline and 2S,3S-β-hydroxynorvaline. Enzymes in mammalian systems are stereo-selective and almost exclusively use the L-form of amino acids in metabolic reactions as substrates. This L-form of amino acids is also denoted as the 2S-form (Cahn-Ingold-Prelog system) and it was therefore assumed that the 2S-isomers of HNV may be more readily metabolised than the 2R-isomers.

In order to investigate the metabolic fate of β-hydroxynorvaline in the mouse model, chiral separation and the relative molar ratios of HNV stereoisomers were deemed essential. The ratio of the various HNV isomers relative to one another could be assessed in commercially available HNV. Following the per os dosage of stereoisomeric HNV to experimental mice, altered relative molar ratios of the stereoisomers in urine samples could be regarded as an indication that some of the isomers were selectively catabolised in the mouse model.

The four HNV stereoisomers consist of two pairs of enantomers and since enantiomers can not be separated from one another by GC alone, chiral derivitisation was deemed necessary to effect complete separation of the four stereoisomers. During the derivatisation process, the enantomers would be converted to diastereoisomers. The latter have different physical properties (melting point, boiling point, solubility, etc.) and can therefore be separated by physical means (Gas chromatography).

1. Reagents, materials, buffers and solutions

(i) Reagents and materials

Dowex® 50, toluene and chloroform were purchased from BDH Laboratory Supplies. All other reagents were of the highest purity and purchased fro the Sigma Chemical Company.

(ii) Buffers and solutions

- R-(-)-2-butanol-(1M)-HCl: Dry HCl gas was passed through an R-(-)-2-butanol solution, until the desired HCl concentration was reached (~1 M)
- Pyridine/acetic acid anhydride solution (1:1; v/v)

2. Methods

(i) Stereo-specific derivatisation of amino acids

Amino acids were isolated from urine with Dowex® 50 and freeze-dried. The isolated amino acids were dissolved in water and transferred to a glass Kimax® tube. The samples were dried under vacuum in the presence of a few drops of toluene. Dried samples were butylated with 100 µl R-(-)-2-butanol-HCl (~1M HCl) at 100 °C for 60 minutes. The samples were again dried under vacuum after a few drops of toluene were added. Acetylation of samples was achieved by the addition of pyridine/acetic acid anhydride solution (100 µl) and incubation at 100 °C for 5 minutes. Samples were again dried under vacuum and dissolved in a small volume of chloroform before it was analysed on the GC-MS.

(ii) Gas chromatography mass spectrometric (GC-MS) separation of HNV-stereoisomers

Gas chromatographic mass spectrometric analyses were performed on a Hewlett Packard 6890 GC, equipped with a split/splitless auto injector (Agilent 7683 series). An SE 30 (25 m x 0.33 mm ID) capillary column was used with helium as a carrier gas at a flow rate of 1 ml/min. Initial oven temperature was 60°C that was maintained for 2 minutes. The temperature was increased at 4 °C/min up to 120 °C, after which it was increased by 10 °C/min to a final temperature of 280 °C. An inlet temperature of 280 °C was used.

A quadrupole mass spectrometer (HP 5973) was used for GC-MS analyses. In order to get an electron ionisation spectrum, the source temperature was kept at 230 °C and the electron energy at 70 eV.

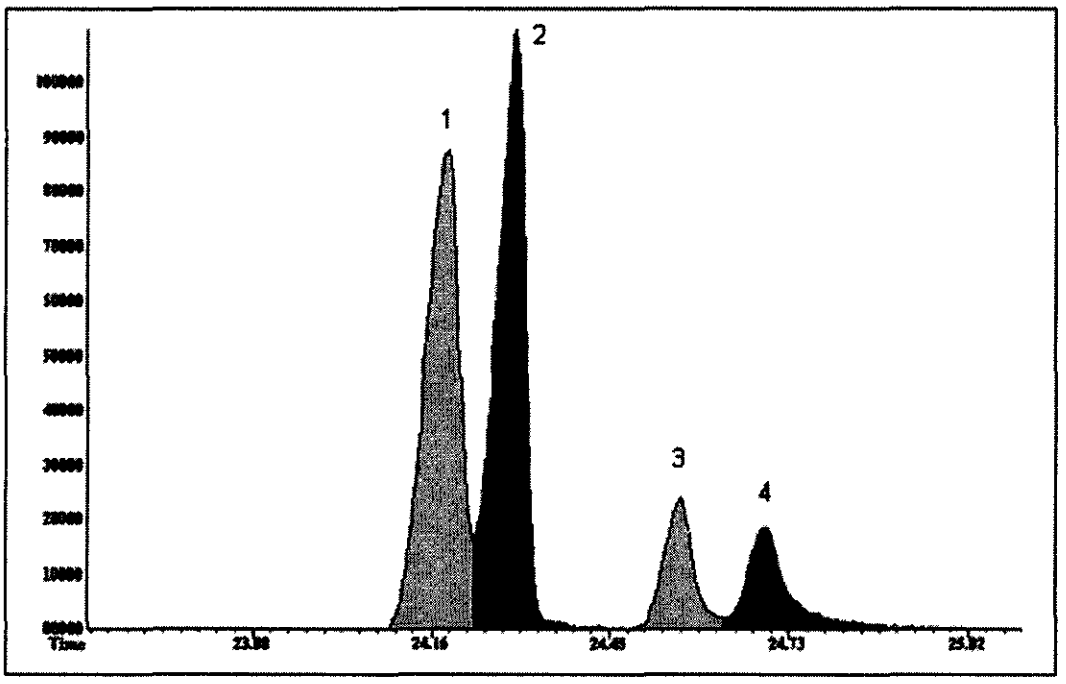

Figure J1. Part of the total ion chromatogram of the four derivatised stereoisomers of commercially available HNV.

APPENDIX K

Quantification of amino acids and acylcarnitines with electrospray ionisation tandem mass spectrometry

Electrospray ionisation tandem mass spectrometry was used for the quantification of amino acids and carnitines since the technology as well as the expertise was available to this study.

1. Reagents, materials, buffers and solutions

(i) Reagents and materials

Amino acids and carnitines were analysed with the isotope dilution method on a tandem mass spectrometer. The amino acid and carnitine isotopes used, as well as their concentrations are given in Table K1. All non-isotopically labelled compounds were purchased from Sigma Chemical Company, unless stated otherwise.

Table K1. Isotopes and their concentration in the isotope mixture used as an internal standard for amino acid and carnitine quantification.

Amino acids	**Concentration**
Glycine- (D2)	16.04 µmol/l
Valine- (D8)	24.05 µmol/l
Isoleucine- (D10)	19.87 µmol/l
Methionine- (methyl-D3)	3.97 µmol/l
Phenylalanine (-ring-D5)	5.77 µmol/l
Lysine- (D4)	10.01 µmol/l
Carnitines	**Concentration**
Carnitine- (methyl-D3)	1.52 µmol/l
Acetyl carnitine- (D3)	0.51 µmol/l
Propionyl carnitine- (D3)	0.13 µmol/l
Isovaleryl carnitine- (D9)	0.11 µmol/l
Octanoyl carnitine- (D3)	0.10 µmol/l
Palmitoyl carnitine- (D3)	0.04 µmol/l

Glycine, valine, methionine and phenylalanine isotopes were purchased from Euriso-top, France; isoleucine, lysine and carnitine isotopes were from Cambridge Isotope Laboratories, Inc; all other isotopically labelled carnitines were synthesised by Dr. Herman J. ten Brink, Academic Hospital, VU, Netherlands.

(ii) Buffers and solutions

- Butanolic-HCl: HCl gas was passed through butanol until the desired concentration was reached (5 mol/l).
- Water/acetonitrile/formic acid solution: (98:1:1; v/v).

2. Methods

(i) Derivatisation and ESI-MS-MS analysis of amino acids and carnitines

Liver homogenates from pregnant female mice and homogenates from their 10-day-old embryos (preparation described in 3.3.2) were diluted 10 times with distilled water. Amino acid isotope mixture (410 µl) was added to each sample (20 µl) in a plastic Eppendorf® reaction vial. Samples were centrifuged for 30 minutes at 16 000 x *g* to remove any particles. The supernatant was again centrifuged at 16 000 x *g* for 20 minutes. The clear supernatant was dried under a nitrogen stream at 55 °C for 40 minutes. Butanolic-HCl was added (200 µl) to the samples and the samples incubated for 15 minutes at 55 °C. Before analysis by electrospray MS/MS, the excess derivatising reagent was removed by evaporation under a constant stream of dry nitrogen gas. The butylated samples were subsequently dissolved in 100 µl $H_2O/CH_3CN/HCOOH$ mixture and analysed. The concentrations of the amino acids and acylcarnites were calculated, employing Equation K2 below:

$$[Metabolite] = \frac{Area\,(metabolite)}{Area\,(isotope)} \times \frac{Isotope\,(pmol)}{Creatinine\,(pmol)} \times CF \qquad \textbf{(K1)}$$

Where:

[Metabolite] = the metabolite concentration in mmol/mol creatinine

Area (metabolite) = the peak area obtained from the corresponding signal for the specific metabolite

Area (isotope) = the peak area of the corresponding isotope

Isotope = the amount of isotope in the sample measured in pmoles

creatinine = the amount of creatinine present in the sample measured in pmoles

CF = concentration correction factor

(ii) ESI-MS-MS analysis of butylated amino acids and acylcarnitines

Butylated amino acids and acylcarnitines display characteristic fragmentation profiles under collision induced decomposition (CID) with

commonly shared ions. These ions could be used for the detection of specific groups of metabolites. Butylated acylcarnitines can be identified by positive precursor ion scan of *m/z* 85. Butylated amino acids display a loss of a butylformate group under CID, always resulting in a loss of a neutral fragment of 102 Da in the case of neutral and acidic amino acids. Basic amino acids always loose an ammonia group as well as the butylformate group, resulting in a neutral loss of 119 Da (Millington, 1990).

Mienie *et al.* (2004) found that direct injection ESI-MS-MS of butylated amino acids and acylcarnitines could lead to false positives. Acetylcarnitine is usually detected by a *m/z* 260 to *m/z* 85 transition. L-Glutamate can, however, also be detected in acylcarnitine profiles, since it also displays a *m/z* 260 to *m/z* 85 transition. This results in the signal obtained from acetylcarnitine being artifactually inflated in the presence of L-glutamate, leading to false positive analyses or overestimation of acetylcarnitine. Due to this reason, all samples were chromatographically fractionated in order to discriminate between individual molecular species.

Analyses were executed on a VG Quattro II triple quadrupole instrument (Micromass, UK), equipped with a Hewlett Packard 1090 HPLC and a Hewlett Packard 1090 auto sampler (Waldbronn, Germany). Samples were separated on a Phenomenex Luna C18 (2) reverse phase column (250 x 2.00 mm, 5 micron), protected by a guard column (4 mm X 2 mm I.D.) that contained a silica-based C_{18} sorbent packing. A mobile phase gradient was used for the chromatographic separation of the amino acids and the carnitines. A flow rate of 0.2 ml/minute was maintained throughout the analysis. Initially the column was eluted with a mobile phase containing 99% water (containing 1% HCOOH) and 1% CH_3CN. The organic component of the mobile phase was gradually increased to 90% CH_3CN:10% H_2O over a 10-minute interval. The mobile phase composition was returned to the initial conditions over 5 minutes, where it was kept constant for 20 minutes for re-equilibration of the C18-column before the next sample was injected. The injection volume was 25 µl.

(iii) Conditions employed in the ESI-MS-MS analysis of amino acids and acylcarnitines

		Source (ES^+)		
Capillary		3.50 kVolts		
HV Lens		0.50 kVolts		
Cone		34 Volts		
Skimmer Offset		5 Volts		
Skimmer		1.5 Volts		
RF Lens		0.2 Volts		
Source Temperature		85 °C		
		MS1	**MS2**	
Ion Energy		1.0 Volts		1.0 Volts
Ion Energy Ramp		0.0 Volts		0.0 Volts
LM Resolution		14.0		13.5
HM Resolution		14.0		13.5
Lenses	(# 5)	100 Volts	(# 7)	250 Volts
	(# 6)	5 Volts	(# 8)	40 Volts
			(# 9)	5 Volts
Multiplier		650 Volts		

Nitrogen was used as drying and nebulizing gas. Flow rates for drying and nebulising were set at 350 and 20 $L.h^{-1}$, respectively.

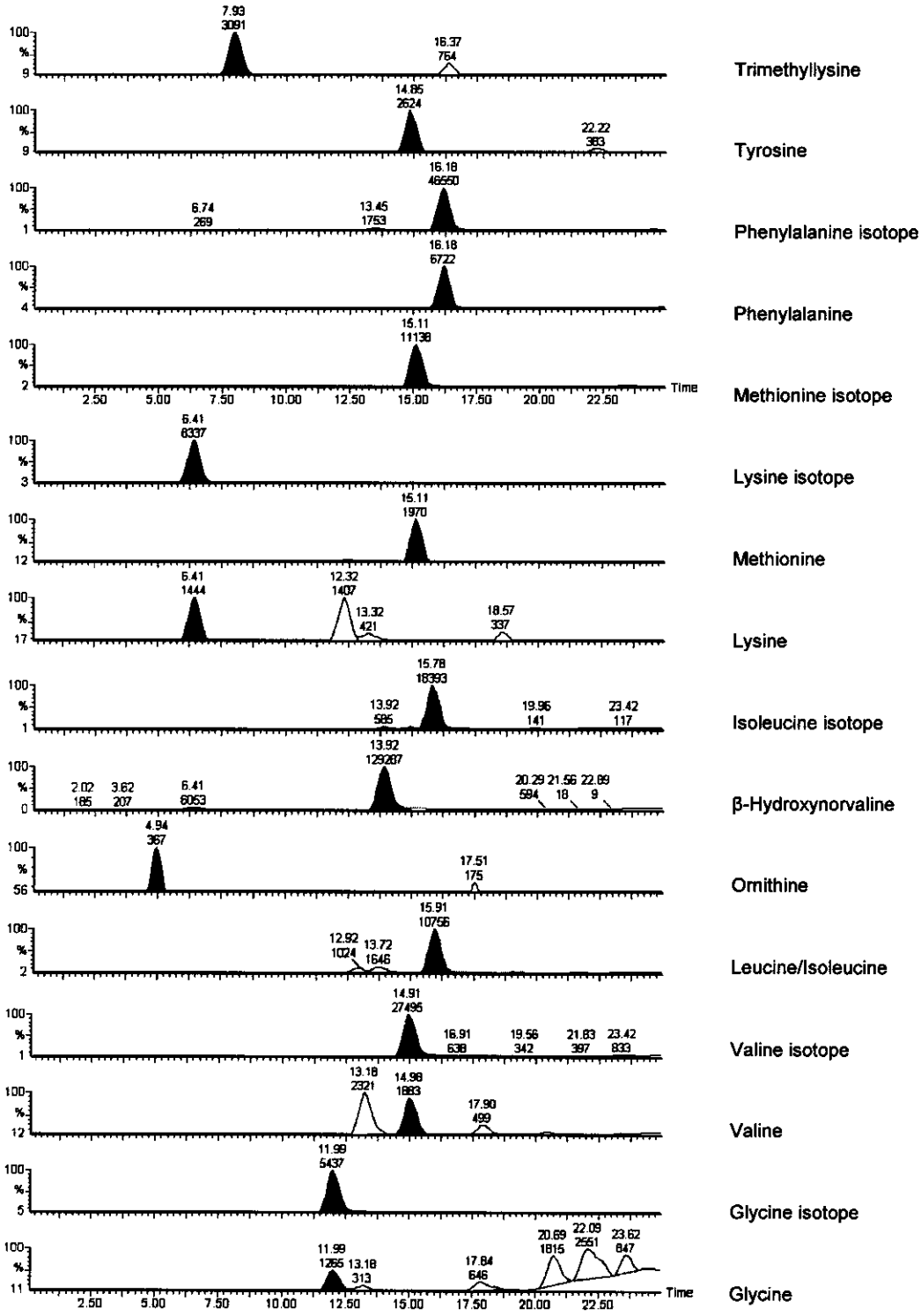

Figure K1. Multiple Reaction Monitoring (MRM) of urinary butylated amino acids. Grey peaks indicate the specific amino acid, corresponding to the correct retention time, while other peaks appear to be non-specific and may generate false positives, as a result of direct injection into the ESI-MS-MS.

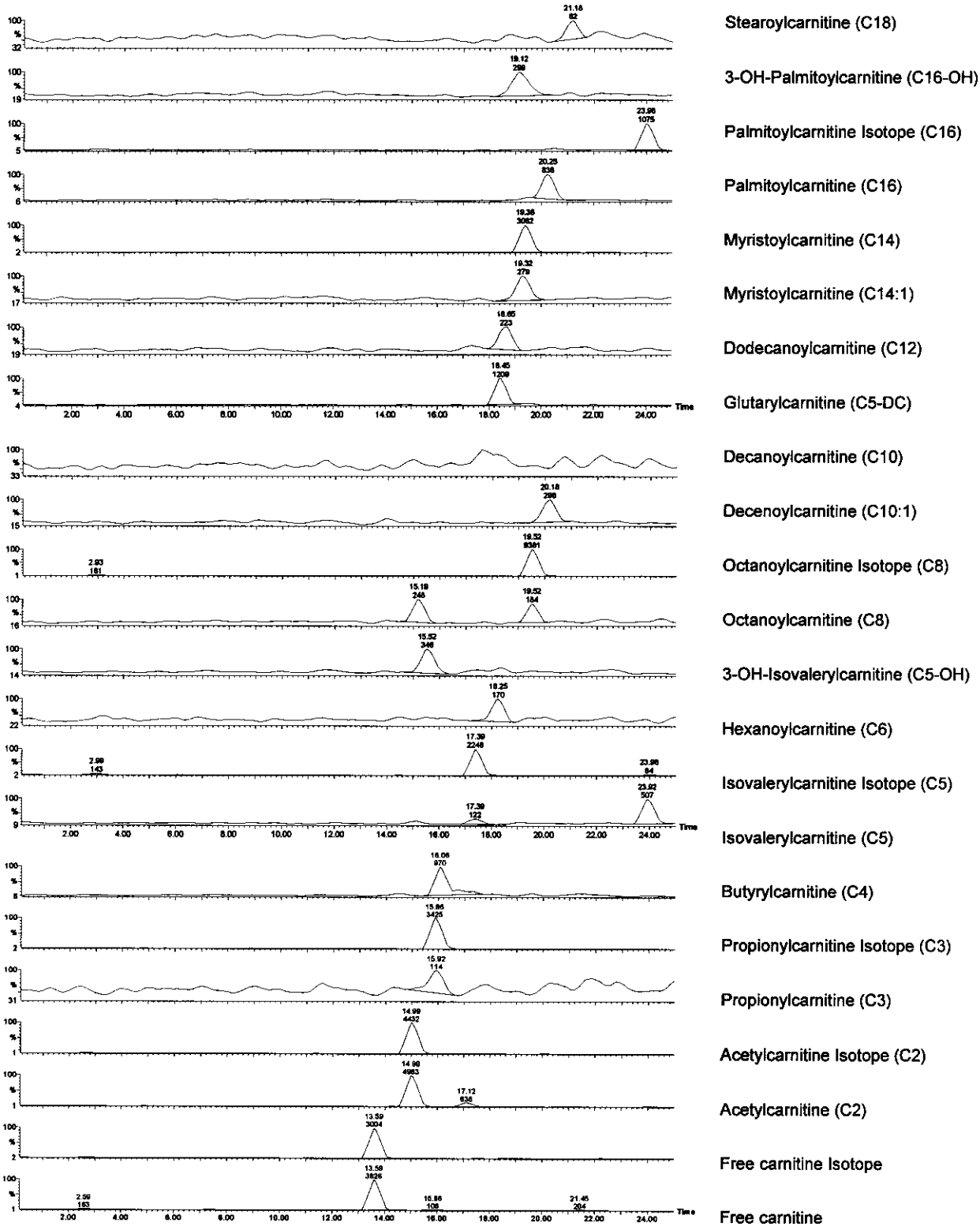

Figure K2. Multiple Reaction Monitoring (MRM) chromatogram of unesterified and esterified carnitines.

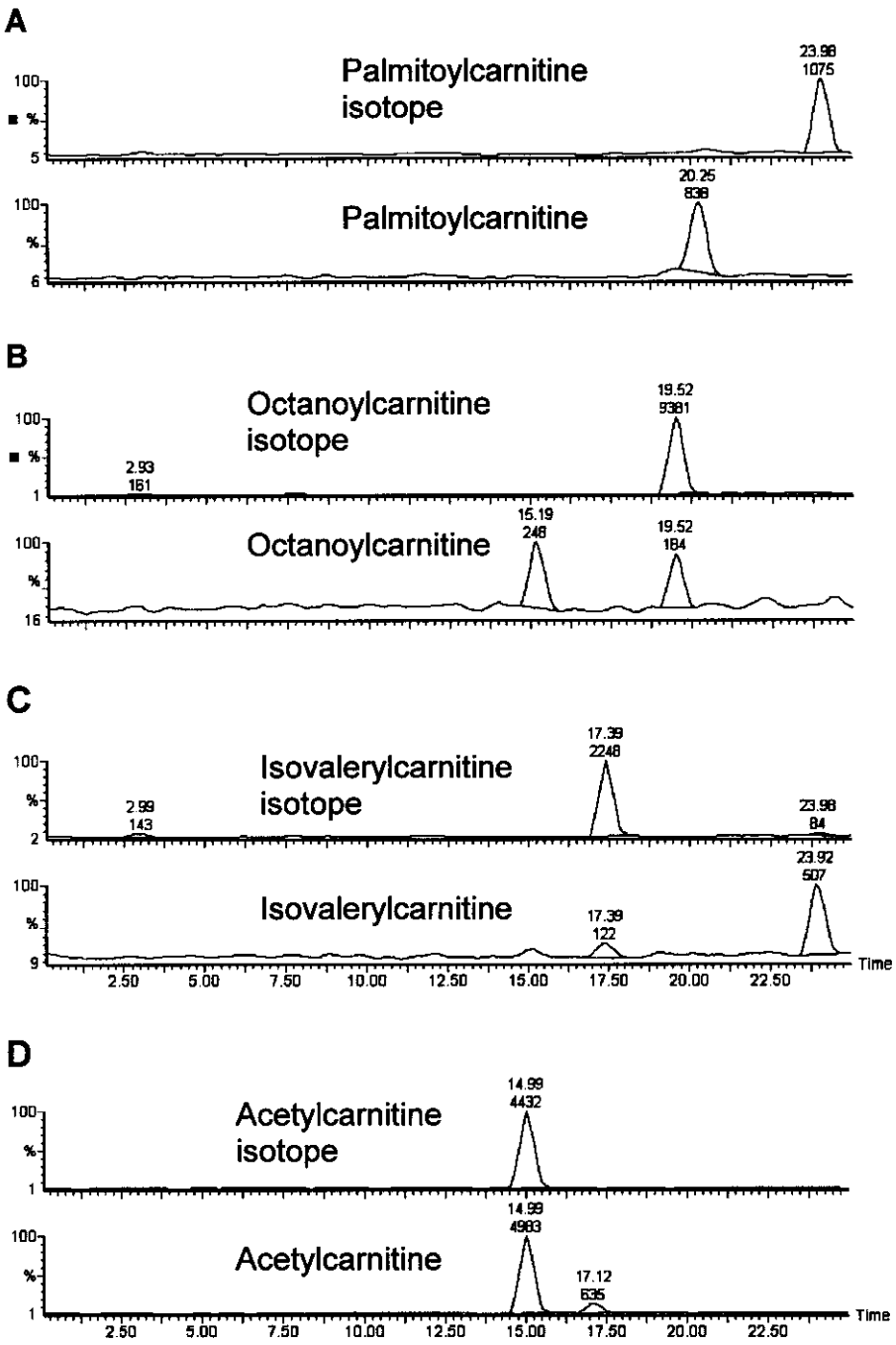

Figure K3. Multiple Reaction Monitoring (MRM) chromatogram of esterified carnitines and their corresponding isotopes. (a) Palmitoylcarnitine isotope (*m/z* 459 to *m/z* 85 transition); palmitoylcarnitine (*m/z* 456 to *m/z* 85 transition); (b) octanoylcarnitine isotope (*m/z* 347 to *m/z* 85 transition); octanoylcarnitine (*m/z* 344 to *m/z* 85 transition); (c) isovalerylcarnitine isotope (*m/z* 311 to *m/z* 85 transition); isovalerylcarnitine (*m/z* 302 to *m/z* 85 transition); (d) acetylcarnitine isotope (*m/z* 263 to *m/z* 85 transition); acetylcarnitine (*m/z* 260 to *m/z* 85 transition).

Better results were obtained, following chromatographic separation of the samples, prior to tandem mass spectrometry, as compared to direct injection. In the initial phase of the analysis, most organic molecules were eluted from the column. The chromatographic separation increased the sensitivity of the assay since fewer molecules were in the ionisation source at a specific point in time, competing for ionisation.

Figure K3 illustrates typical examples of unknown metabolites interfering with the carnitine analysis. Acetylcarnitine (*m/z* 260 to *m/z* 85 transition) is detected at 14.99 minutes, while an unknown metabolite is detected at 17.12 minutes, also showing a *m/z* 260 to *m/z* 85 transition. Quantification of acetylcarnitine by direct injection would normally not discriminate between the acetylcarnitine and the unknown metabolite on the acetylcarnitine chromatogram. This would lead to an erroneous, artifactual 12.7 % increase in the estimation of the concentration of acetylcarnitine, due to the interference with an unknown metabolite.

Quantification of isovaleryl- and octanoyl-carnitine also proved to be problematic due to interference of unknown metabolites. The relative concentration of isovalerylcarnitine would be erroneously increased by 415 % and the concentration of octanoylcarnitine by 135 % if direct injection ESI-MS-MS would be employed. The urine sample analysed in the example chromatogram contained no palmitoylcarnitine (Figure K3. C). However, an unknown compound was detected at 20.25 minutes on the palmitoylcarnitine chromatogram. This compound displayed a *m/z* 456 to *m/z* 85 transition similar to palmitoylcarnitine. Since palmitoylcarnitine would have displayed a retention time of approximately 24 minute (the retention time of it's corresponding stable isotope), this unknown compound was not identical to palmitoylcarnitine. Direct injection ESI-MS-MS would therefore also have erroneously identified and quantified the unknown compound as palmitoylcarnitine. The final concentration of palmitoylcarnitine would have been calculated as 2.55 mmole/mol creatinine (Equation K1), even though the sample actually contained no detectable levels of palmitoylcarnitine.
The interference of unknown compounds in carnitine and amino acid analysis by ESI-MS-MS was encountered regularly. Due to this problem

only acylcarnitines corresponding to their stable isotopes were quantified and used in this study (i.e. free carnitine, acetyl-, isovaleryl-, octanoyl-, and palmitoylcarnitine). Retention times were used for identification of the amino acids, as indicated by their corresponding stable isotopes. Standards were used to determine the retention times of amino acids for which no corresponding stable isotopes were available (i.e. ornithine, tyrosine, trimethyllysine and β-hydroxynorvaline).

APPENDIX L

Analysis of amino acids with the Phenomenex EZ: faast® amino acid analysis kit

Amino acids can be quantified fast and reliably with the PHENOMENEX EZ: faast® AMINO ACID ANALYSIS KIT. The advantage of this method, compared to the electrospray ionisation tandem mass spectrometry for the quantification of amino acids is that this method simultaneously detects almost all the amino acids. It was therefore deemed to be the ideal method to identify the 3-ethylcysteine (Appendix O). The method also provides an electron ionisation spectrum of each individual amino acid, unique to the specific compound and which can be used to positively identify the amino acids.

1. Reagents, materials, buffers and solutions

(i) Reagents and materials

- Phenomenex EZ: faast® amino acid analysis kit (Phenomenex, Inc.).

(ii) Buffers and solutions

- All buffers and reagents were supplied with the Phenomenex EZ: faast® amino acid analysis kit (Phenomenex, Inc.).

2. Methods

(i) Derivatisation of amino acids for GC-MS analysis

Amino acids were extracted onto a solid phase support, desorbed and subsequently derivatised with the Phenomenex EZ: faast® amino acid analysis kit (Phenomenex, Inc.). The method was used as described by the manufacturer.

(ii) Gas chromatography mass spectrometry (GC-MS) of amino acids

Gas chromatographic mass spectrometry analyses were performed on a Hewlett Packard 5890 GC, equipped with a split/splitless auto injector (HP 7673). A ZB-AAA GC column (provided as part of the Phenomenex EZ:

faast® amino acid analysis kit, Phenomenex, Inc.) was used with helium as a carrier gas at a flow rate of 1 ml/min. The initial oven temperature was 120°C and was maintained for 1 minute. The temperature was increased at 15 °C/min up to 200 °C, after which it was increased by 25 °C/min to a final temperature of 310 °C, maintained for 3 minutes.

A quadrupole mass spectrometer (HP 5989A) was used for GC-MS analyses. In order to get an electron ionisation spectrum, the source temperature was kept at 240 °C and the electron energy at 70 eV.

APPENDIX M

Chemical synthesis of β-hydroxynorvaline

Chirally specific β-hydroxynorvaline (HNV) is not commercially available and even the stereoisomeric equivalent, which could be purchased from Sigma Chemical Company was extremely expensive. A decision was made to synthesise HNV for the initial experiments, according to the method of Sunko (1955).

1. Reagents, materials, buffers and solutions

(i) Reagents and materials

All reagents used was of the highest purity and purchased from Sigma Chemical Company

(ii) Buffers and solutions

- Copper (II) sulfate solution: 16 g $CuSO_4.5H_2O$ per 100 ml water (0.64 M)
- Glycine solution: 10 g Glycine per 100 ml water (1.33 M)
- KOH solution: 1 M KOH in water (dissolved O_2 removed by bubbling N_2 gas through the KOH solution for 5 minutes).

2. Methods

(i) Synthesis of copper glycinate

Copper sulfate (50 ml, 32 millimoles) and glycine (50 ml, 66 millimoles) solutions were mixed and stirred for 30 minutes at room temperature. The synthetic reaction mixture was then concentrated on a rotary evaporator (Rotavap). Copper glycinate ($CuGly_2$) crystallized from the concentrated solution, following the addition of methanol. $CuGly_2$ crystals were removed by filtration, washed with methanol and air-dried.

(ii) Synthesis of stereoisomeric HNV

Dry copper glycinate (30 g, 0.12 moles) was dissolved in 300 ml 1 M KOH. Dissolved O_2 was removed by bubbling N_2 gas through the KOH solution for 5 minutes. While the N_2 was bubbled through the alkaline copper sulphate

solution, 90 ml propionaldehyde (1.25 moles) was slowly added. Five minutes after the last propionaldehyde was added, the N_2 gas was turned off and the reaction vial sealed. The reaction mixture was magnetically stirred under a N_2 blanket or 36 hours at 4°C. Propanol was then added to the reaction mixture to facilitate crystallization of the copper hydroxynorvalate ($CuHNV_2$).

The deep blue $CuHNV_2$ crystals were removed by filtration, washed with propanol and air-dried. $CuHNV_2$ (0.1 moles) were dissolved in excess water, thioacetamide (9 grams; 0.1moles) added and the solution stirred for 12 hours. Activated charcoal was added and the suspension stirred for an additional 30 minutes. The fine, black precipitate of copper sulphide and activated charcoal was removed by filtration, the resulting colourless solution concentrated by rotary evaporation and β-hydroxynorvaline crystallized, following the addition of methanol to a final concentration of approximately 80 % methanol. The crystalline HNV was recrystallized from 80% methanol (final yield ~ 60 %).

(ii) Confirmation of the structure of synthesised HNV with GC-MS technology

The structure of the synthesised β-hydroxynorvaline was confirmed with GC-MS, following chiral separation of the four stereoisomers (APPENDIX J).

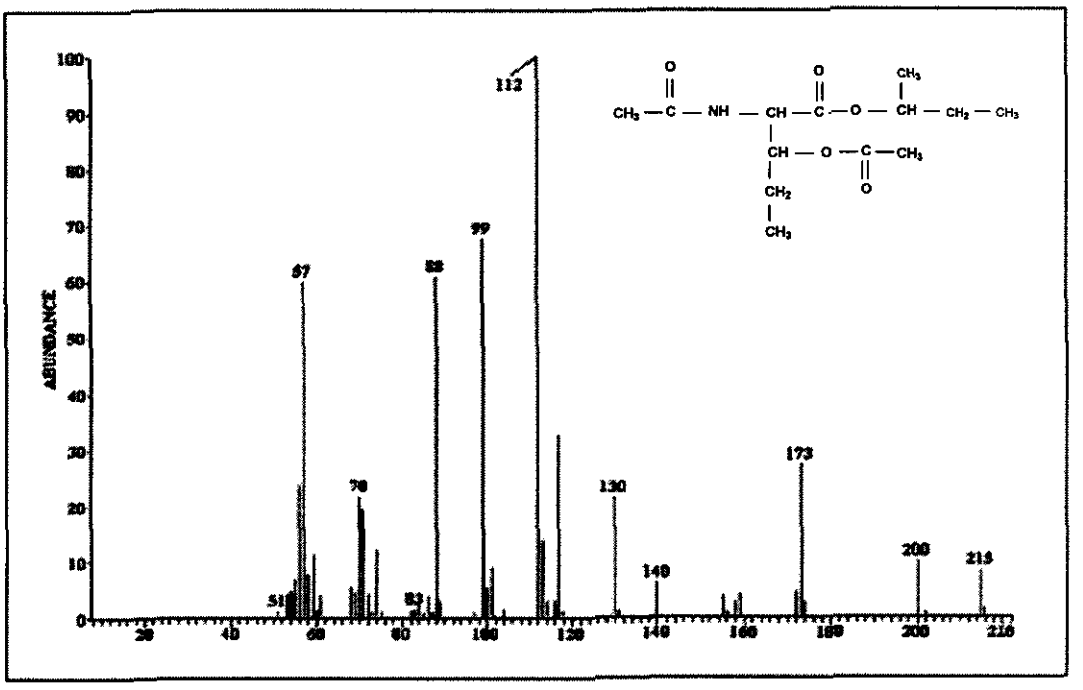

Figure M1. Electron ionisation spectrum of N, O-acetyl- (-)-2-butyl ester of commercially available β-hydroxynorvaline.

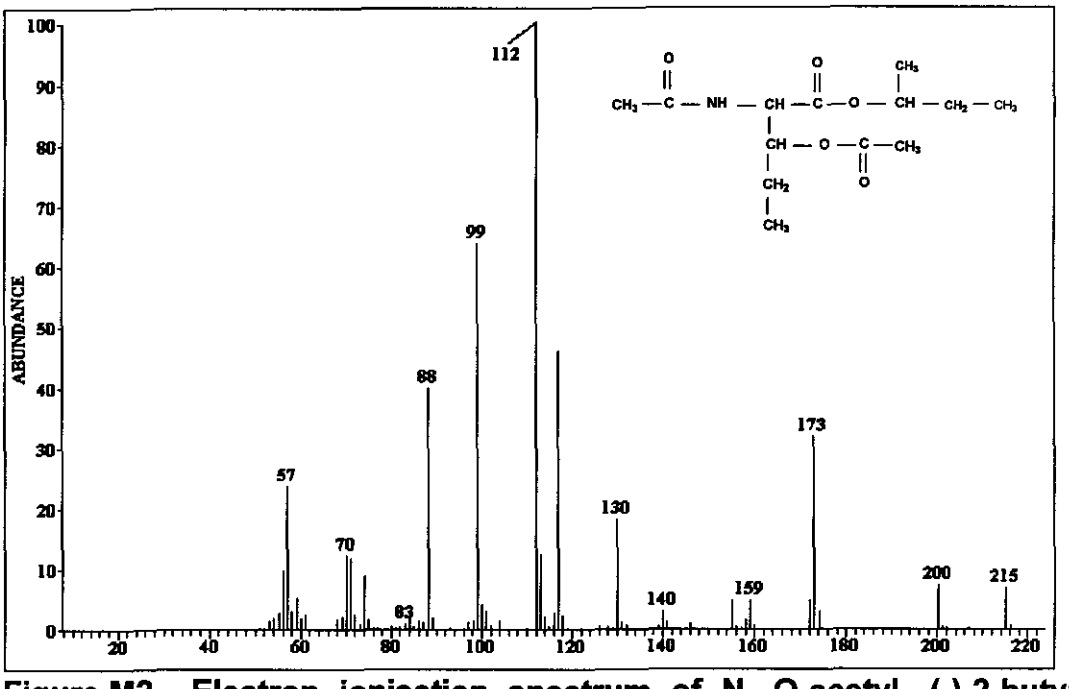

Figure M2. Electron ionisation spectrum of N, O-acetyl- (-)-2-butyl ester of synthesised β-hydroxynorvaline.

The GC retention times and electron ionisation spectra for the standard β-hydroxynorvaline (Sigma Chemical Company) and the synthesised equivalent appeared to be identical and confirmed the identity of the synthesised product.

APPENDIX N

Chemical synthesis of 2,3-dihydroxypentanoic acid

2,3-Dihydroxypentanoic acid (DHPA) is not commercially available. In order to confirm the presence of this compound in biological matrices (i.e. murine urine samples, etc.), generated in the course of this study, it was necessary to execute an in-house synthesis of DHPA. No references to former synthetic efforts to produce this particular compound could be traced. A method aimed at synthesising a compound with a similar functional group was subsequently employed in the synthesis of DHPA (Jordaan, 2000). In the synthesis, executed by Jordaan (2000), *trans*-hydroxylation of an unsaturated organic acid was achieved with hydrogen peroxide and formic acid. Epoxidation, of a double bond, followed by a subsequent S_N2-reaction, was responsible for the formation of the trans-diol product.

1. Reagents, materials, buffers and solutions

(i) Reagents and materials

Trans-2-pentenoic acid was purchased from Fluka. All other reagents were obtained from Sigma Chemical Company and were of the highest purity.

(ii) Buffers and solutions

- H_2O_2 solution: 100 volumes (30 %)

2. Methods

(i) Synthesis of DHPA

Trans-2-pentenoic acid (0.5 ml) was dissolved in 10 ml formic acid (98 %) and stirred at room temperature (RT). Hydrogen peroxide (H_2O_2; 0.4 ml) was added and the reaction mixture refluxed for 30 minutes. Another 0.4 ml aliquot of H_2O_2 was added to the reaction mixture and the mixture then refluxed for an additional 30 minutes. Addition of a final 0.4 ml aliquot of H_2O_2 was followed by refluxing for 120 minutes, after which the reaction

was terminated by adding the reaction mixture in 50 ml H_2O at room temperature (Figure N1).

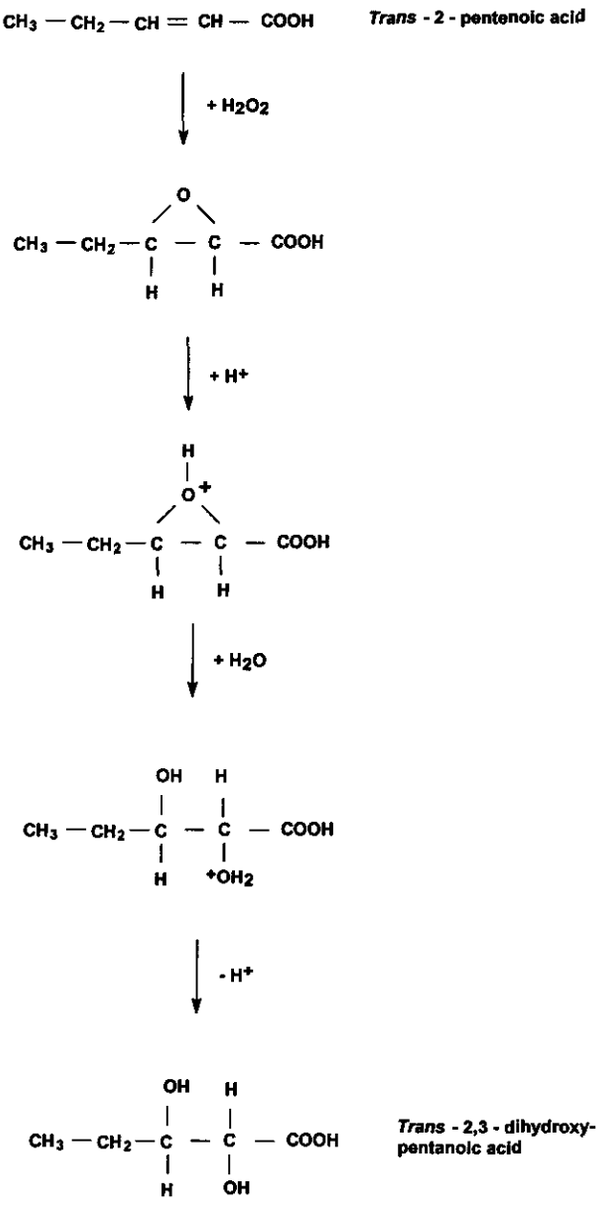

Figure N1. Schematic representation of the chemical synthesis of *Trans*-2,3-dihydroxypentanoic acid from *Trans*-2-pentenoic acid.

(ii) Confirmation of structure of DHPA

The structure of the synthesised DHPA was confirmed by employing GC-MS, as well as IR and NMR spectroscopy. A 300 MHz Varian Gemini 300 MHz Broadband NMR spectrometer and Nicolet Magna-IR 550 Series II

spectrometer with DRIFT and ATR were used for the NMR and IR, respectively.

The GC-MS spectrum of the tri-TMS derivative of DHPA indicate the presence of a molecular ion at m/z 335 (Figure N2) and a number of other fragmentation products, with the m/z 73 species as the most abundant ion. The molecular ion of tri-TMS-DHPA (M^+ = 350 m/z) can not be observed in the mass spectrum, because it is highly unstable and probably lost a methyl group from one of the TMS moieties during EI ionisation to render the m/z 335 species.

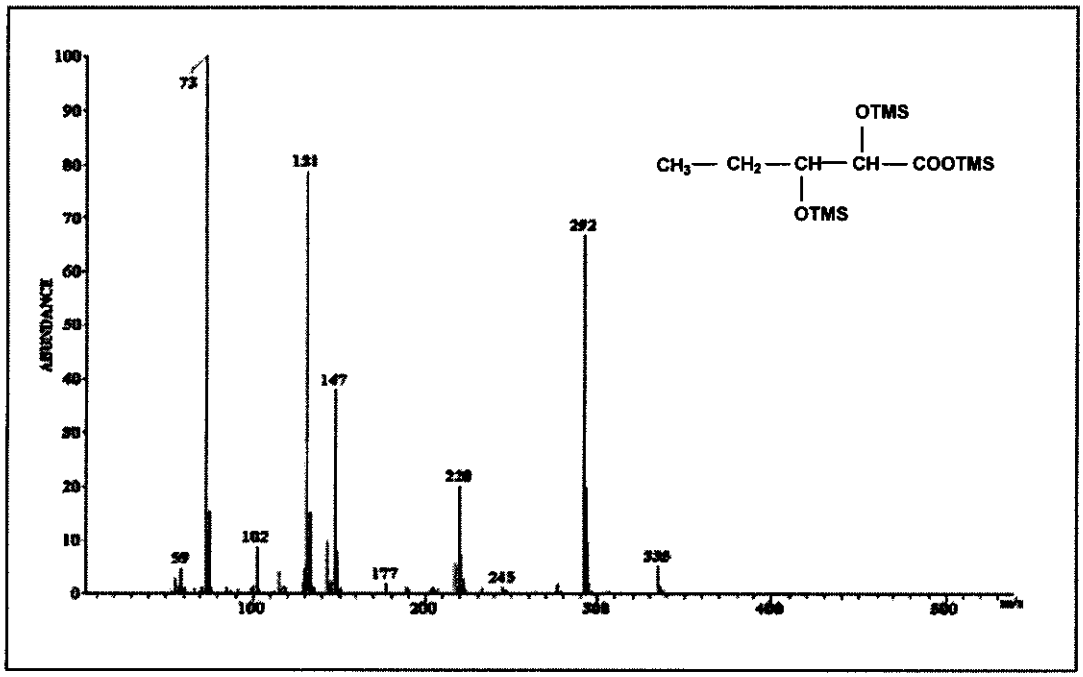

Figure N2. Electron ionisation spectrum of the TMS-derivative of chemically synthesised 2,3-dihydroxypentanoic acid.

The infrared spectrum of DHPA (Figure N3) displayed a strong O–H stretch vibration at 3350 cm^{-1},accompanied by a strong C–H stretch vibration at 1950 cm^{-1}, typical of an aliphatic compound. No signs of aromaticity were indicated. A strong C=O stretch vibration can be observed at 1700 cm^{-1} and a C–O stretch vibration at 1290 cm^{-1}, confirming the presence of a –COOH group. The IR spectrum (Figure N3) corroborates the structural information, derived from the mass spectrum (Figure N2).

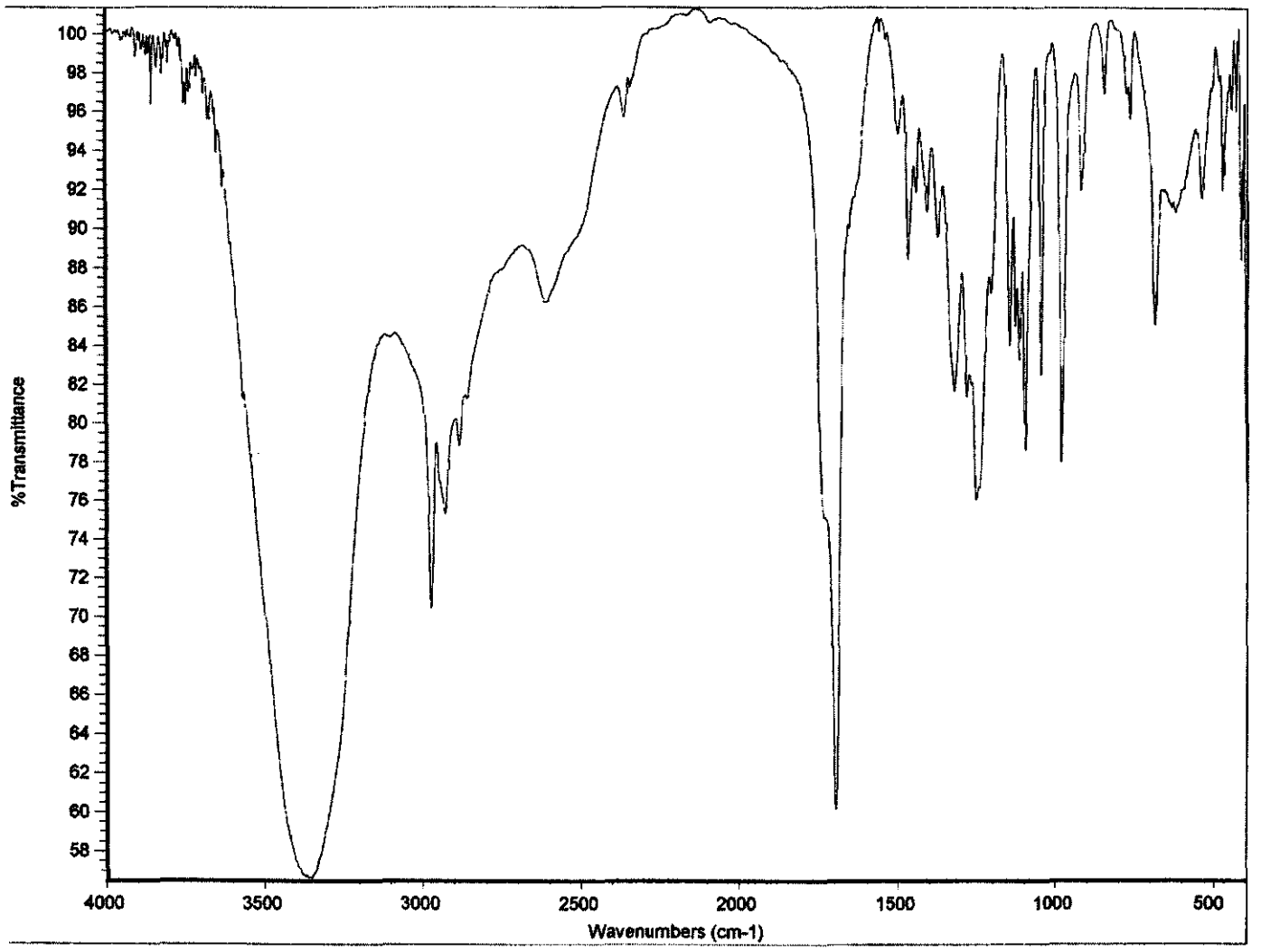

Figure N3. IR spectra of synthesised 2,3-dihydroxypentanoic acid.

The ^{13}C NMR spectrum (Figure N5) of DHPA in DMSO displays signals that can be associated with 5 different carbon atoms in the molecule. DEPT spectra (Figure N7) indicate the presence one CH_3–, one CH_2– and two CH–moieties. An unprotonated C was observed at δ_c 174, corresponding to a –C=O group in the molecule. The ^{13}C NMR spectrum is also supportive of the proposed structure for DHPA.

A signal in the δ_H 5.5 to δ_H 8.9 region which is typical of a –COOH group, is present the ^1H NMR spectrum (Figure N6), of the compound. The signal is not very well defined, due to the rapid exchange of protons. Signals for the ^1H NMR are summarised in Table N1. COSY (Figure N9) and HETCOR (Figure N8) spectra also corroborate the proposed structure of the synthetic product (Fig. N4). A signal corresponding to a –OH group was observed at δ_H 2.5 in the HETCOR spectrum (Figure N8). The other –OH signal may be either masked by the signal at δ_H 2.5, or may be hidden in the δ_H1.4 multiplet.

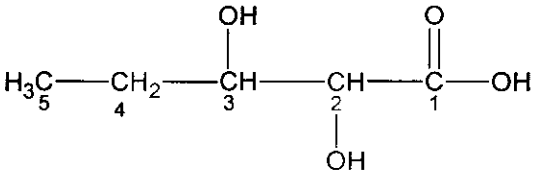

Figure N4. The structure of 2,3-dihydroxypentanoic acid (DHPA).

Table N1. ^1H and ^{13}C NMR data of the synthesised DHPA.

Number	δ_H	δ_C
1		174.311
2	3.8 d	74.263
3	3.45 m	73.419
4	1.4 m	24.985
5	0.85 t	10.102
–OH	2.5 m	
–COOH	5.4 – 8.9 s	

Solvent = DMSO; s = singlet; d = doublet; t = triplet; m = multiplet.

To conclude: all the available spectral data (GC-MS, IR, ^{13}C NMR, ^1H NMR) confirm that the proposed structure of the synthetic product is consistent with that of 2,3-dihydroxypentanoic acid.

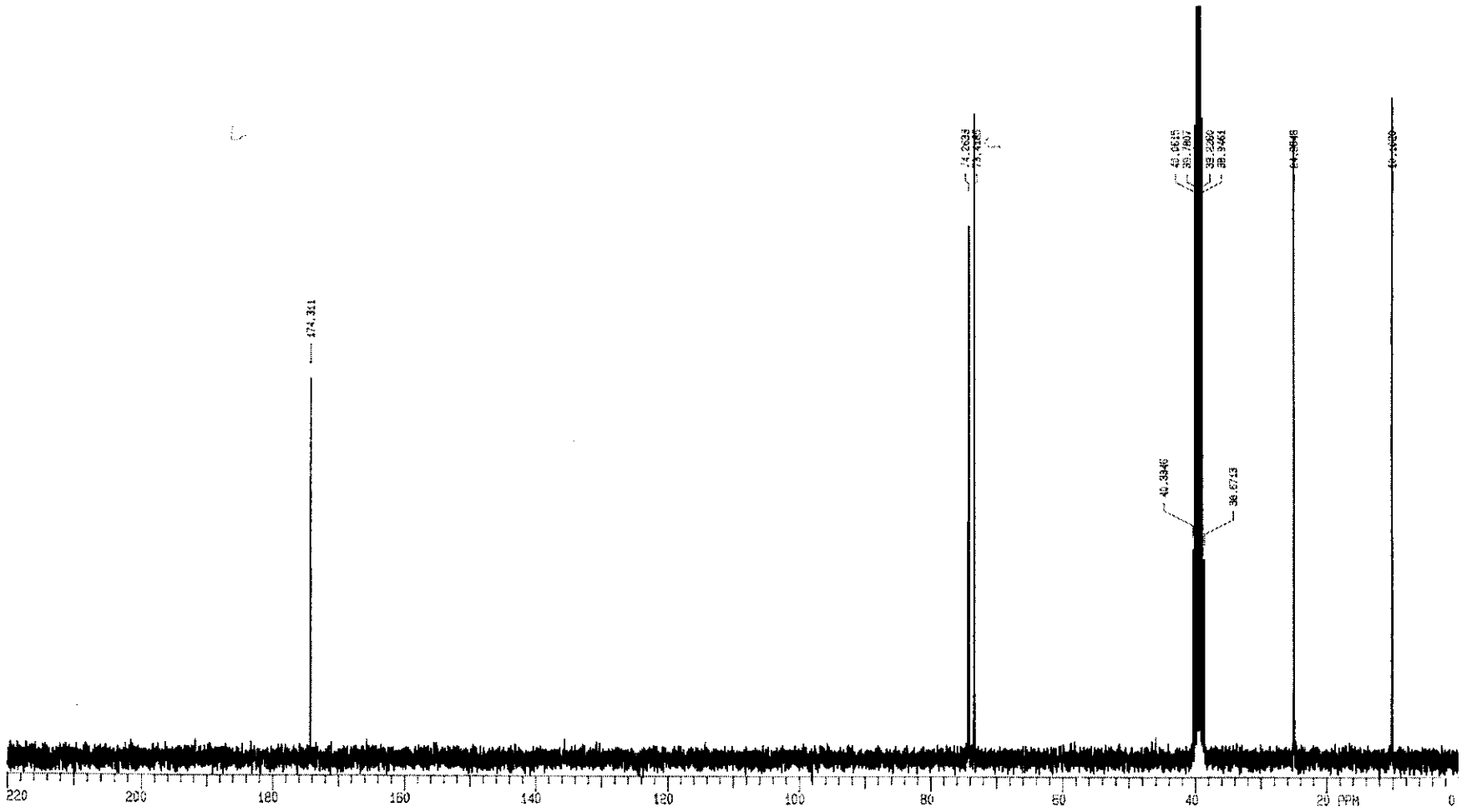

Figure N5. ^{13}C **NMR spectra in DMSO of synthesised 2,3-dihydroxypentanoic acid.**

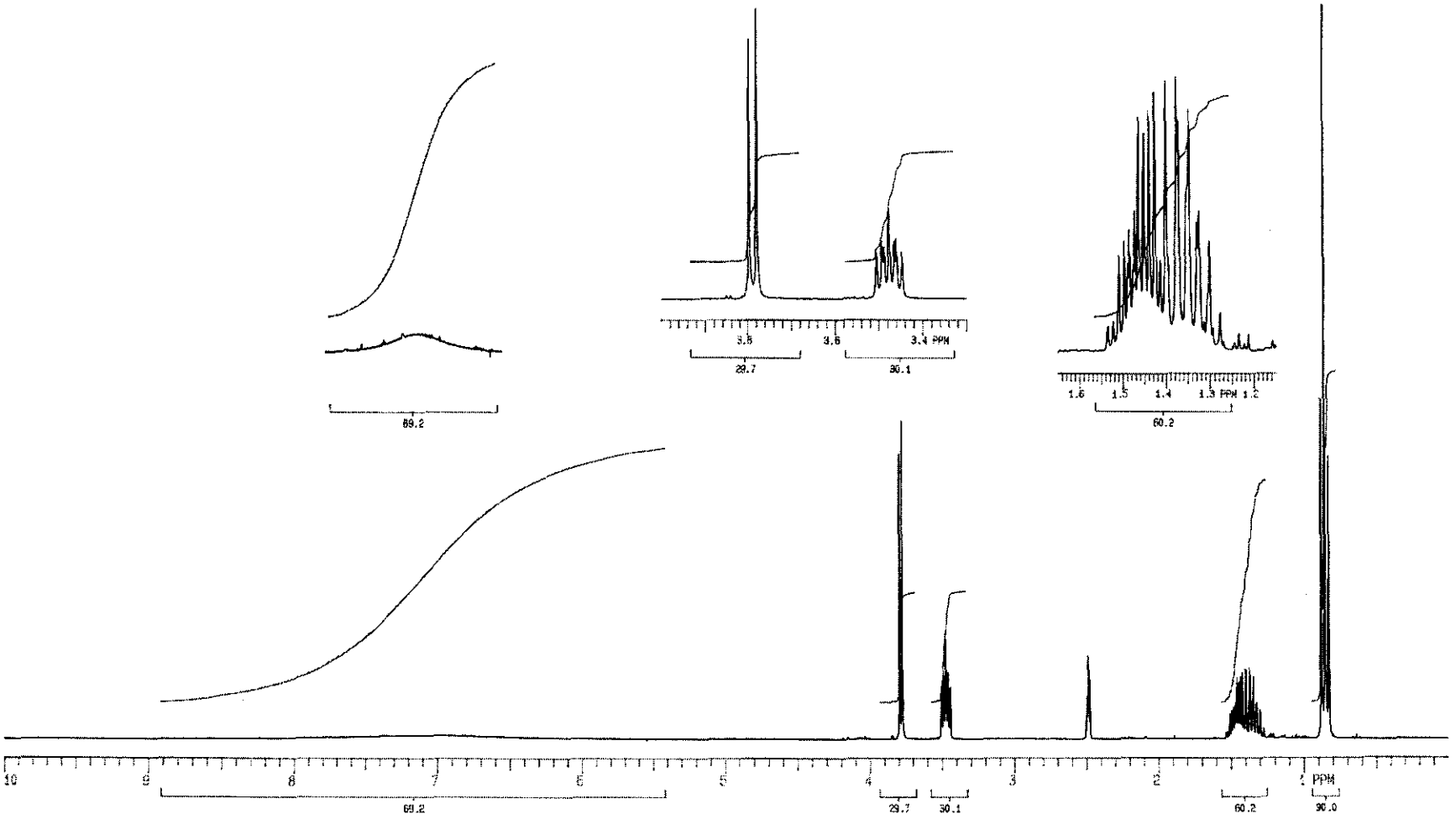

Figure N6. ^{1}H NMR spectra in DMSO of synthesised 2,3-dihydroxypentanoic acid.

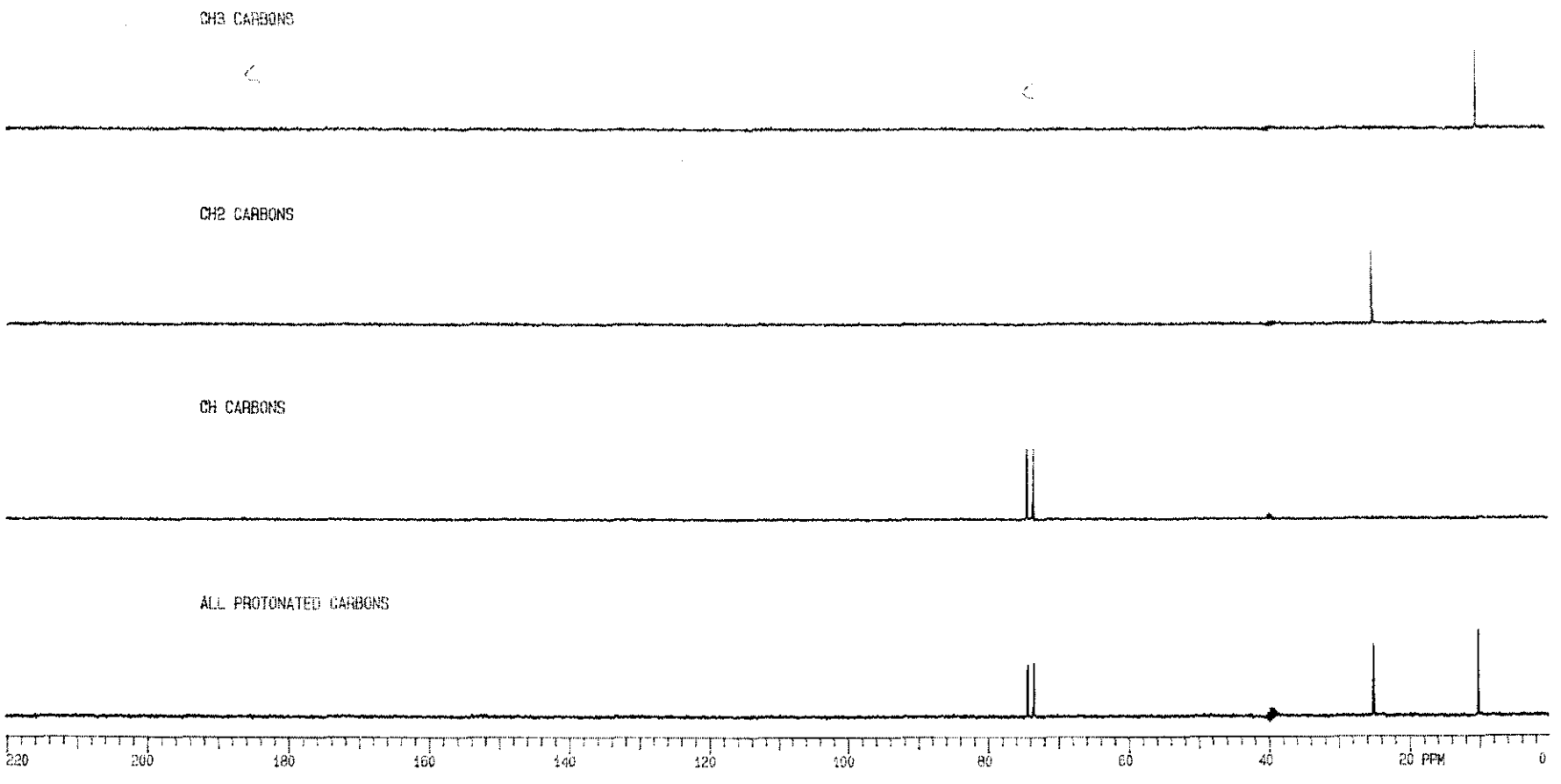

Figure N7. DEPT in DMSO of synthesised 2,3-dihydroxypentanoic acid.

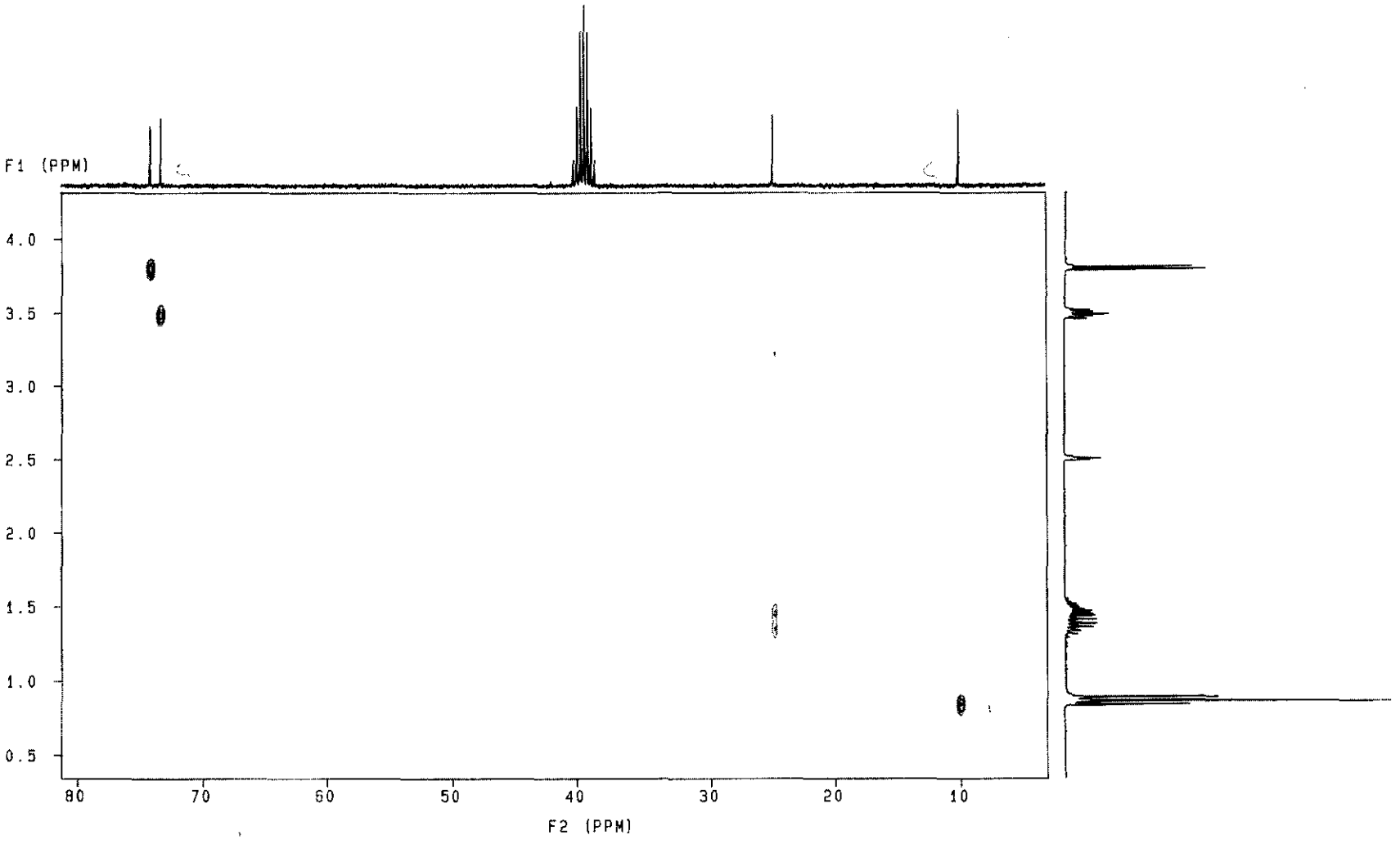

Figure N8. HETCOR in DMSO of synthesised 2,3-dihydroxypentanoic acid.

Figure N9. COSY in DMSO of synthesised 2,3-dihydroxypentanoic acid.

APPENDIX O

Enzymatic synthesis of 3-ethylcysteine

3-Ethylcysteine (EC) is not commercially available. In order to confirm the presence of this compound in biological matrices (i.e. urine, etc.), generated in the course of this investigation, EC was enzymatically synthesised. The synthesis was based on the chemical reaction catalysed by cystathionine β-synthase (CBS) and described by Kraus (1987).

1. Reagents, materials, buffers and solutions

(i) Reagents and materials

All reagents used was of the highest purity and purchased from Sigma Chemical Company

(ii) Buffers and solutions

- Reaction buffer: 500 mM Tris-HCl, pH 8.6
- Dithiothreitol solution: 200mM
- Pyridoxal 5'-phosphate solution: 2 mM
- Bovine serum albumin solution: 10 mg/ml in distilled water
- Perchloric acid solution: 0.4 M
- L-Homocysteine solution: 200 mM

The L-homocysteine solution was prepared by incubating 30.72 mg of L-homocysteine-*S*-thiolactone in 200 µl 5 M NaOH at 37 °C for 5 minutes. The pH was adjusted to 8.6 with ~ 465 µl 2 M HCl and 100 µl 500 mM Tris pH 8.6. Dithiothreitol was added to a final concentration of 20 mM and the volume made up to 1 000 µl with distilled water.

2. Methods

(i) Synthesis of EC

Synthesis of EC was achieved enzymatically by using the *in situ* cystathionine β-synthase (CBS) reaction, naturally operating in mouse liver, under reaction conditions previously described by Kraus (1987). Cystathionine β-synthase normally irreversibly condenses homocysteine and serine to produce cystathionine. The latter is then cleaved

enzymatically by *in situ* cystathionine gamma-lyase (CGL) to produce cysteine and 2-ketobutyric acid.

According to the planned strategy, β-hydroxynorvaline, a potential structural analogue of L-serine would be presented to CBS in a mouse liver homogenate to synthesize the condensation product, 3-ethylcystathionine. Assumptions were made that 3-ethylcystathionine will be produced as an intermediary product. Rapid cleavage of the appropriate carbon-sulphur bond would produce 2-ketobutyric acid and 3-ethylcysteine as the desired transsulfuration product.

The complete reaction mixture contained, Tris-HCl buffer (250 mM, pH 8.6), pyridoxal-5-phosphate (PLP; 0.25 μM), bovine serum albumin (BSA; 0.5 μg), β-hydroxynorvaline (HNV; 5.0 mM), and freshly prepared mouse liver homogenate (50 μl) in a final volume of 400 μl. After a 5-minute pre-incubation at 37 °C, the reaction was initiated with the addition of 50 μl of L-homocysteine (freshly prepared). The reaction mixture was incubated for 3 hours at 37 °C and then terminated with the addition of perchloric acid (0.4 M, 20 μl).

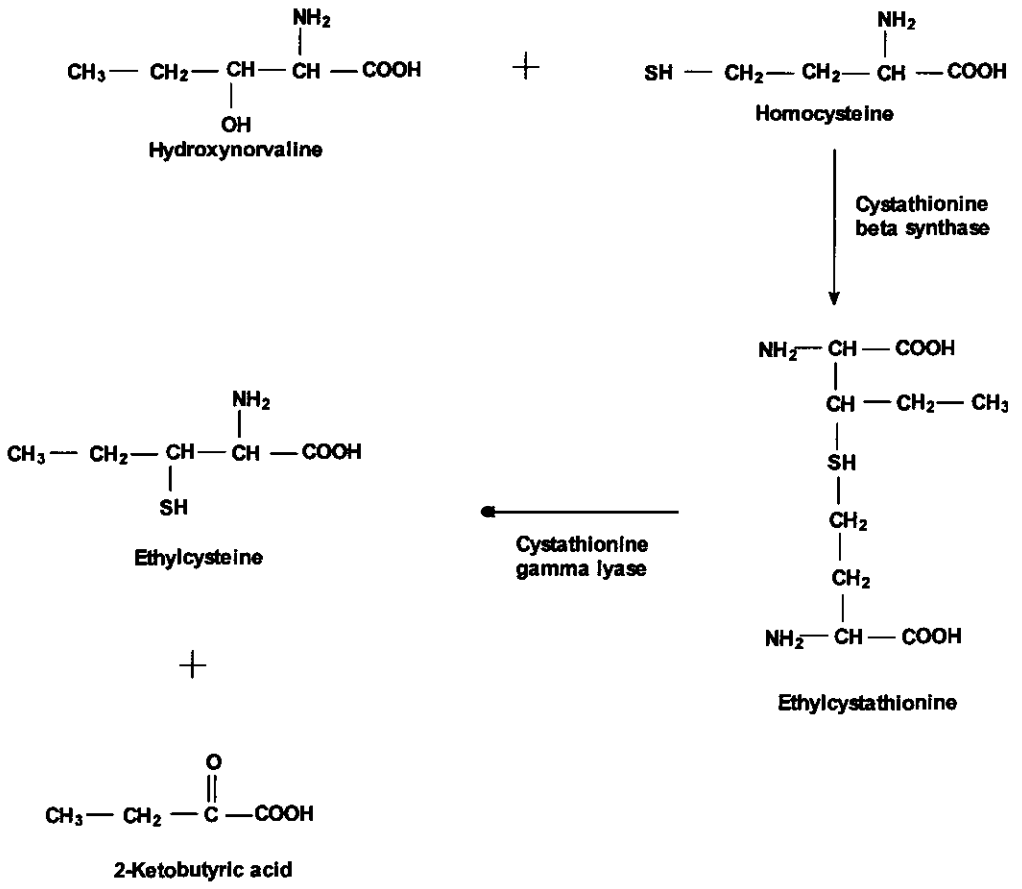

Figure O1. Proposed synthesis of 3-ethylcysteine from β-hydroxy-norvaline in the mouse.

(ii) Confirmation of the structure of the synthesised EC by means of GC-MS

A small aliquot of the synthetic reaction mixture was derivatised with the EZ: faast® amino acid analysis kit and analysed by GC-MS (Appendix L).

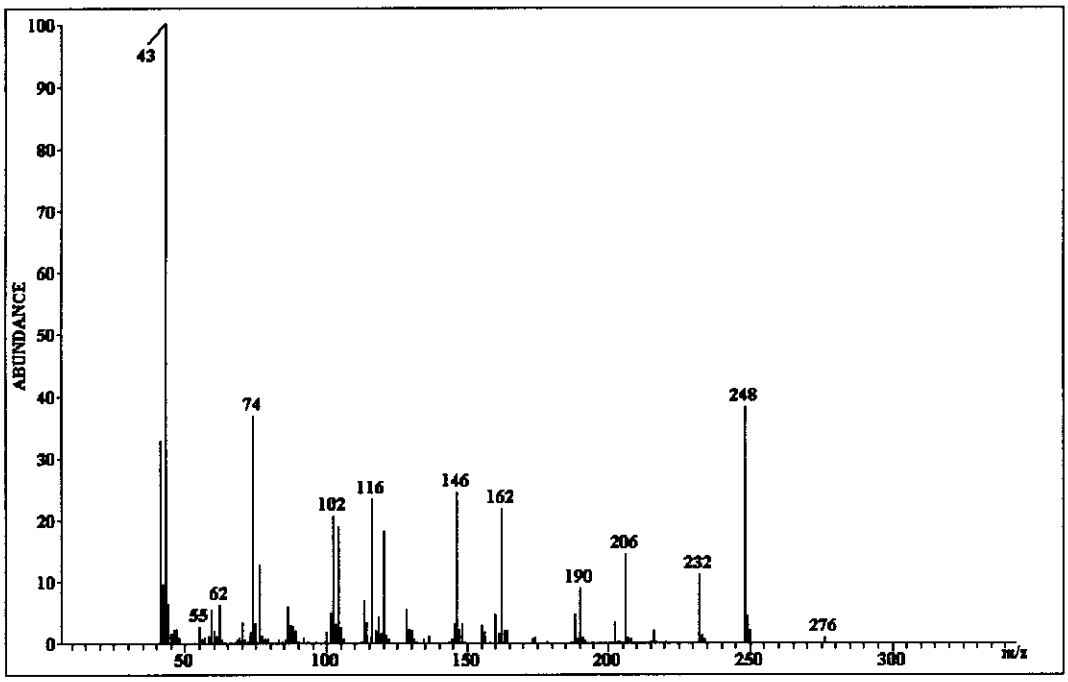

Figure O2. Electron ionisation spectrum of derivatised cysteine standard.

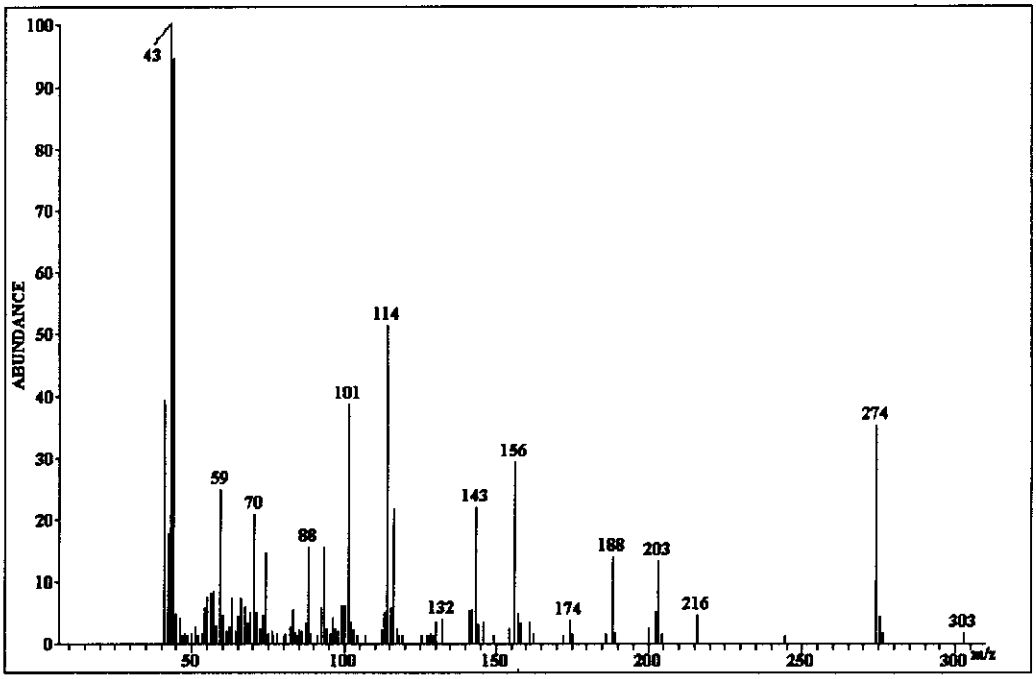

Figure O3. Electron ionisation spectrum of derivatised 3-ethylcysteine. (Enzymatically synthesised).

The enzymatically synthesised 3-ethylcysteine was not isolated for nuclear magnetic resonance (NMR) or infrared (IR) spectrometric confirmation of the structure. The GC-MS data was considered irrefutable proof that the desired synthetic product was, indeed obtained. The GC retention time of

the synthesised 3-ethylcysteine appeared to be very close to that of L-cysteine. The ionisation spectrum contributed final proof that the synthesised product was indeed 3-ethylcysteine.

The L-cysteine derivative exhibited characteristic m/z $[104]^+$, $[116]^+$, $[128]^+$, $[146]^+$, $[188]^+$, $[248]^+$ and $[276]^+$ fragments, while the 3-ethylcysteine derivative rendered fragments at m/z $[132]^+$, $143]^+$, $[156]^+$, $[174]^+$, $[216]^+$, $[276]^+$, and $[303]^+$. These fragments corresponded to that of cysteine and are all 28 or 27 atom mass units heavier than the corresponding fragment for cysteine. This is in line with what could be anticipated from the EI fragmentation pattern of the 3-ethylcysteine derivative. The additional ethyl-group ($-CH^2CH^3$) on 3-ethylcysteine is responsible for the additional 28 atom mass unit increase in molecular mass, relative to the ionisation fragments of the L-cysteine derivative. Although the mass of the ethyl-group is 29 atom mass units, the molecule loses one H-atom for the addition of the ethyl-group, resulting in a net 28 atom mass unit increase in mass, compared to the L-cysteine derivative.

Chemical synthesis of sufficient quantities of 3-ethylcysteine on a preparative scale will be necessary for absolute confirmation of the identity of this novel metabolite. Another approach might be to use purified cystathionine-β-synthase for the synthesis of 3-ethylcystathionine on a semi-preparative scale. The product, 3-ethylcystathionine, should be isolated, purified and its structure subsequently confirmed by NMR and IR. For the purpose of the present study however, identification of 3-ethylcysteine from the EI mass spectra alone, as illustrated above, was deemed sufficient.

The *in vitro* inhibition of CBS by β-hydroxynorvaline may have been the result of a structural resemblance of HNV to L-serine. The observed inhibition may probably be due to the fact that HNV could be used as a "substrate" by CBS, with the resultant formation of the intermediary product, 3-ethylcystathionine. Cleavage of the latter compound by cystathionine-gamma-lyase may lead to 3-ethylcysteine as the transsulfuration product.

APPENDIX P

Quantification of S-adenosyl-L-methyionine and S-adenosyl-L-homocysteine in maternal and embryonic tissues

High performance liquid chromatography (HPLC) was employed in an attempt to quantify S-adenosylmethionine (SAM) and S-adenosylhomocysteine (SAH) in the livers of pregnant mice and their unborn offspring. A modified method of Wang *et al.* (2001) was used.

1. Reagents, materials, buffers and solutions:

(i) Reagents and materials

Sodium 1-Octanesulfonate was purchased from TCi, Tokyo. All the reagents used were of the highest purity and were obtained from Sigma Chemical Company.

(ii) Buffers and solutions

- Perchloric acid solution: 0.4 mol/l $HClO_4$
- S-Adenosyl-L-methionine stock solution: 50 µM prepared in 0.4 M $HClO_4$
- S-Adenosyl-L-homocysteine stock solution: 50 µM prepared in 0.4 M $HClO_4$
- Solvent A: 8 mM octanesulfonic acid; 50 mM NaH_2PO_4, pH adjusted to 3.0 with H_3PO_4
- Solvent B: 100 % Methanol

(iii) HPLC specifications

The chromatographic system consisted of a HPLC pump (Dionex model P580A HPG), equipped with an online degasser (Model DG-2410), an automated sample injector (ASI-100) and a Dionex UV/VIS detector (UVD 170S/340S). A Cosmosil 4.6 X 250 mm, 5C18-MSII column was used (Waters, code 38020-41) which was protected by a guard column (4 mm X 2 mm I.D.) containing a silica-based C18 sorbent packing.

2. Methods

(i) Sample preparation

Fresh mouse liver tissue and 10-day-old mouse embryos were used for the standardisation and validation of the analytical method. Samples of liver tissue (100 mg) were homogenised on ice in 4 volumes of 0.4 M $HClO_4$ in a Potter-Elvejham homogeniser (Glas-Col). After centrifugation for 15 minutes at 16 000 x *g* (4 °C), the supernatants were removed and frozen at –70 °C until they were used. Whole embryos (~50 µg) were homogenised in 4 volumes of 0.4 M $HClO_4$ in a Potter-Elvejham homogeniser (Glas-Col). Following centrifugation for 15 minutes at 16 000 x *g* (4 °C), the supernatants were removed and frozen at –70 °C until they could be analysed.

(ii) Method employed for the separation of SAM and SAH.

HPLC conditions and instrument settings

- Gradient protocol:
  - Initial conditions: Solvent A:Solvent B (80:20)
  - Ramp: After 8 minutes 80:20 to 60:40 within 30 seconds; maintain at 60:40 for 12.5 minutes and return to initial conditions within 30 seconds
  - Equilibrate at initial conditions for 10 minutes, prior to next run
- Column: Cosmosil 5C18-MSII column (150 mm x 4.6 mm)
- Volumetric flow rate 1.0 ml/min
- Auto sampler temperature: 25 °C
- Column oven temperature: 25 °C
- Upper pressure limit: 200 bar
- Ultraviolet detection: 254 nm
- Sample volume: 25 µl

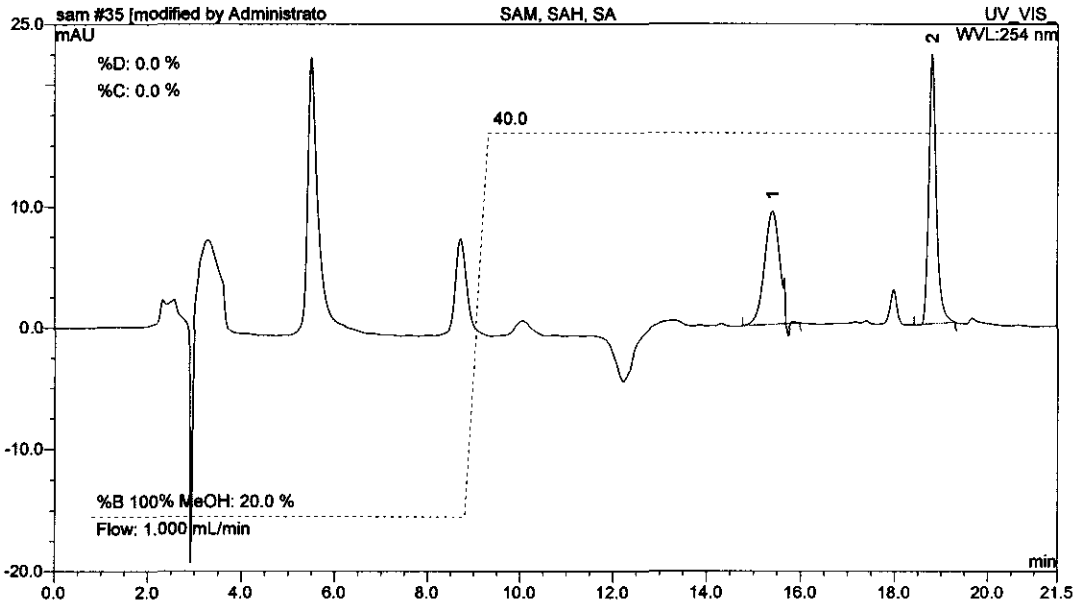

Figure P1. Separation of S-adenosyl-L-methionine and S-adenosyl-L-homocysteine standards (100 µM each). (1) SAH, (2) SAM.

(iii) Validation of the SAH/SAM assay

Calibration curves were obtained by analysing 5 standards, each in duplicate. All the samples were analysed with the method described in section P2 (ii).

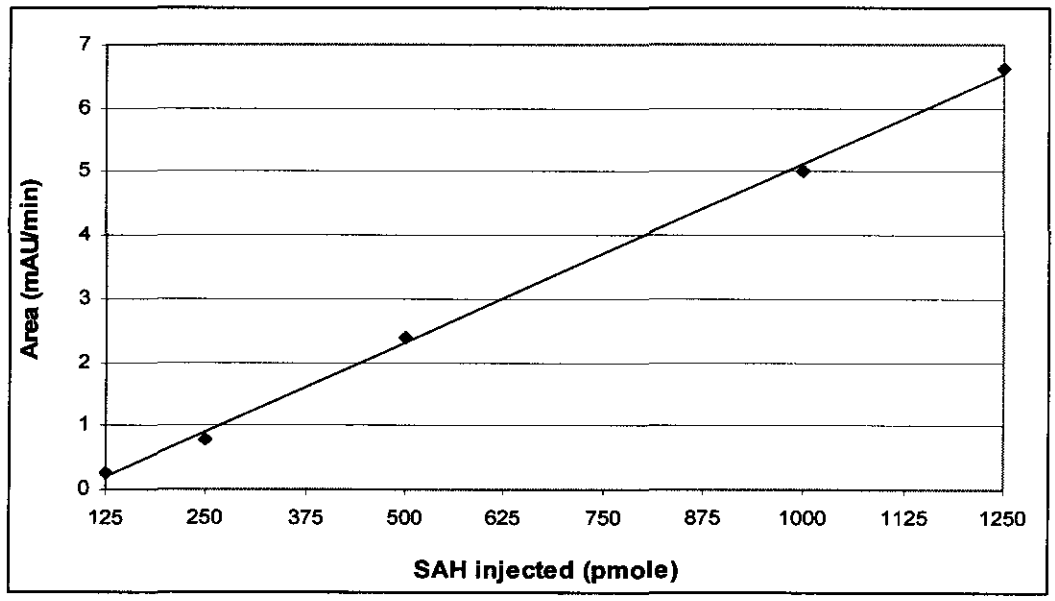

Figure P2. Calibration curve for S-adenosyl-L-homocysteine (SAH). (R^2 = 0.9983).

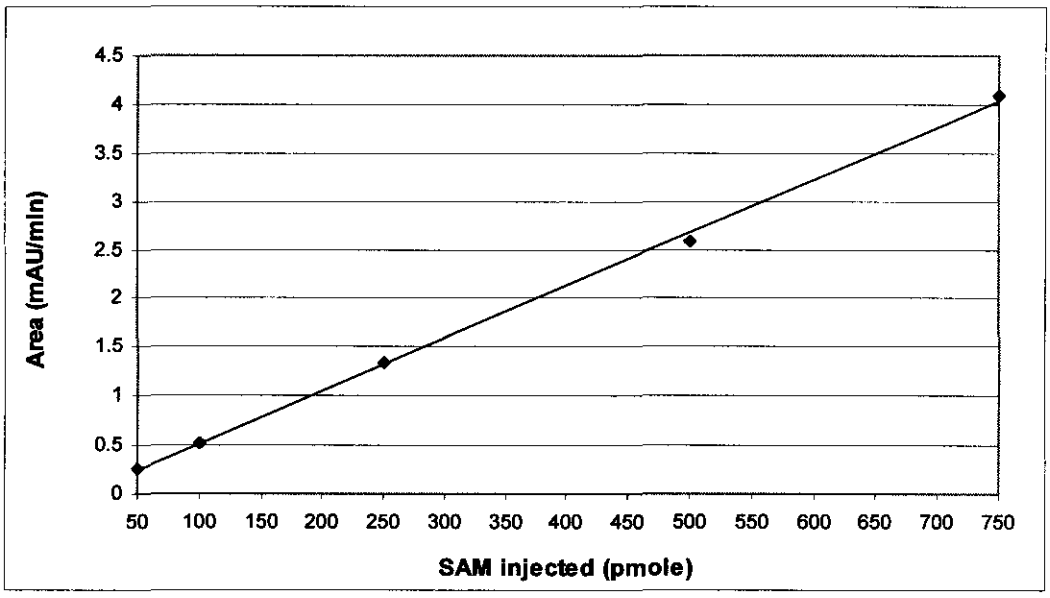

Figure P3. Calibration curve for S-adenosyl-L-methionine (SAM). (R^2 = 0.9987).

Good linearity was obtained for both SAH and SAM (R^2 > 0.9985) over the relevant concentration ranges.

(iv) Calculation of the SAH and SAM concentrations (Equation P1)

$$[\text{Metabolite}] = \frac{\text{pmole} \times \textit{Fraction}}{1000} \qquad \textit{(P1)}$$

Where:

[Metabolite] = is the concentration of the metabolite (SAH or SAM) in nmol/g tissue

pmole = the total pmoles measured in the sample (as calculated from the calibration curve for the specific metabolite (SAH or SAM)

Fraction = the fraction of the total sample injected into the HPLC

1000 = volume correction factor

(v) Measuring SAH and SAM concentrations in liver tissue.

Polyamine levels were measured in liver homogenates from pregnant Hanover-NMRI females. Freshly prepared sample supernatants were prepared as described in section P2 (ii) and analysed (in duplicate) with the described method.

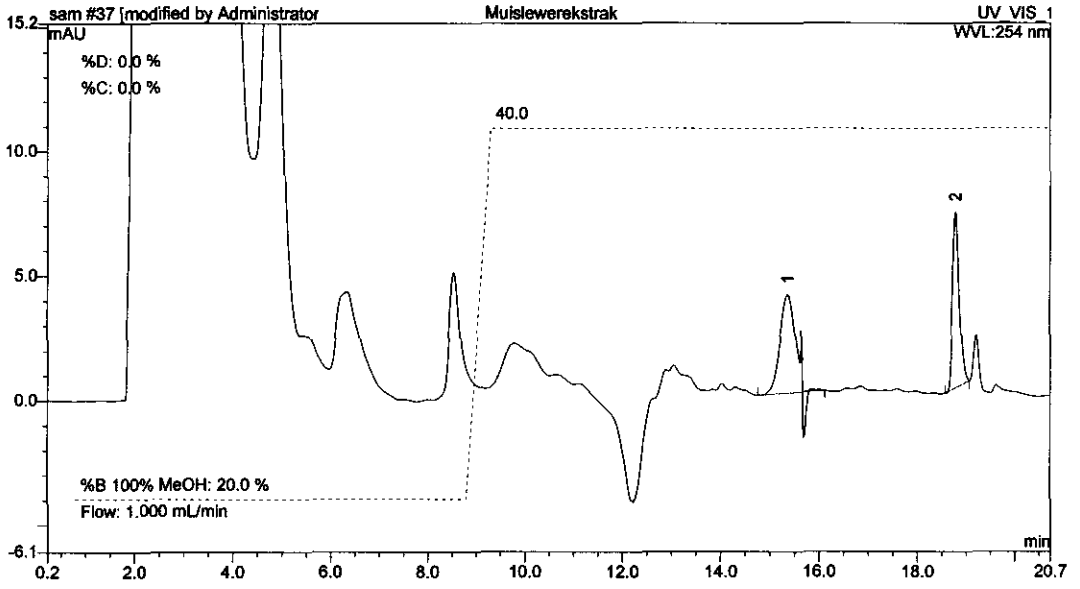

Figure P4. Quantification of SAH and SAM from a liver tissue sample.

TABLE P1. Quantification of SAM and SAH in liver homogenate.

Metabolite	Mean value (nmole/g)	Standard deviation	RSD
SAH	23.79	1.83	7.69
SAM	32.93	4.09	12.42

Mean of 2 replicates; RSD is the relative standard deviation (calculated as SD/Mean x 100)

Quantification of SAH and SAM in hepatic extracts from pregnant female mice proved to be problematic. Interference of unknown peaks in the chromatograms severely compromised quantification of the two metabolites.

(vi) Quantification of SAH and SAM in mouse embryos.

SAH and SAM levels were also measured in 10-day-old mouse embryos. Freshly prepared sample supernatants were prepared as described in section P2 (ii) and analysed (in duplicate) with the described method.

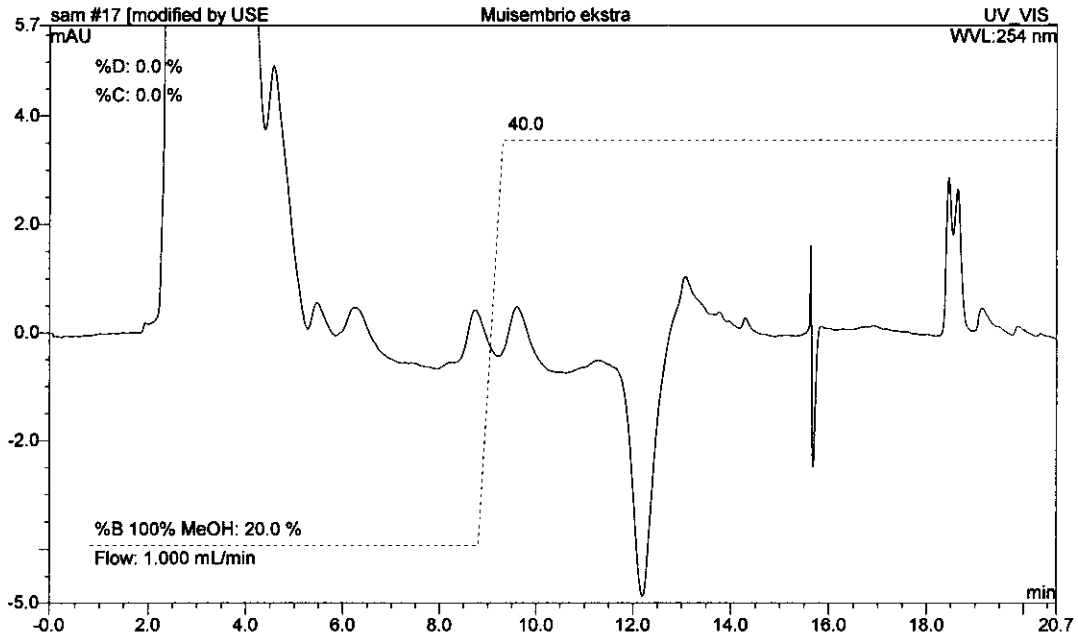

Figure P5. Quantification of SAH and SAM in whole mouse embryos.

The level of SAH in the 10-day-old mouse embryos appeared to have been below the detection capability of the employed analytical method. A peak was detected at 18.8 minutes, presumably that of SAM, but it could not be resolved from an unknown interfering peak, which caused problems with the quantification of the target analytes. With regard to the sensitivity problem, even by injecting a larger volume of the whole embryo tissue extract, SAH could still not be detected. A more sensitive method should be employed for the accurate quantification of SAH and SAM (i.e. fluorescence, electrochemical, mass spectrometry, etc.) in murine hepatic and whole embryo tissue.

APPENDIX Q

Quantification of homocystine and cystine with electrospray ionisation tandem mass spectrometry

Electrospray ionisation tandem mass spectrometry was used for the quantification of homocystine, since the technology as well as the expertise was available to this study.

1. Reagents, materials, buffers and solutions

(i) Reagents and materials

Homocystine and cystine were analysed with the isotope dilution method on a tandem mass spectrometer. The isotopes used, as well as their concentrations are given in Table Q1. All non-isotopically labelled compounds were purchased from Sigma Chemical Company, unless stated otherwise.

Table Q1. Isotopes and their concentration in the isotope mixture used as an internal standard for homocystine and cystine quantification.

Amino acids	Concentration
DL-Cystine (D4)	140.28 µmol/l
DL-Homocystine (D8)	39.82 µmol/l

Isotopes were purchased from Cambridge Isotope Laboratories, Inc.

(ii) Buffers and solutions

- Butanolic-HCl: HCl gas was passed through butanol until the desired concentration was reached (~5 mol/l).
- Water/acetonitrile/formic acid solution: (98:1:1; v/v).

2. Methods

(i) Derivatisation and ESI-MS-MS analysis of amino acids and carnitines

Liver homogenates from pregnant female mice and homogenates from their 10-day-old embryos (preparation described in 3.3.2) were diluted 10 times with distilled water. Amino acid isotope mixture (410 µl) was added to each sample (20 µl) in a plastic Eppendorf® reaction vial. Samples were

centrifuged for 30 minutes at 16 000 x *g* to remove any particles. The supernatant was recentrifuged at 16 000 x *g* for 20 minutes. The clear supernatant was dried under a nitrogen stream at 55 °C for 40 minutes. Butanolic-HCl was added (200 µl) to the samples and the samples incubated for 15 minutes at 55 °C. Prior to analysis by electrospray MS/MS, the excess derivatising reagent was removed by evaporation under a constant stream of dry nitrogen gas. The butylated samples were subsequently dissolved in 100 µl $H_2O/CH_3CN/HCOOH$ mixture and analysed. The concentrations of the amino acids and acylcarnites were calculated , employing Equation Q1 below:

$$[Metabolite] = \frac{Area\,(metabolite)}{Area\,(isotope)} \times \frac{Isotope\,(pmol)}{Creatinine\,(pmol)} \times CF \qquad \textbf{(Q1)}$$

Where: [Metabolite] = the metabolite concentration in mmol/mol creatinine

Area (metabolite) = the peak area obtained from the corresponding signal for the specific metabolite

Area (isotope) = the peak area of the corresponding isotope

Isotope = the amount of isotope in the sample measured in pmoles

creatinine = the amount of creatinine present in the sample measured in pmoles

CF = concentration correction factor

(ii) ESI-MS-MS analysis of butylated homocystine and cystine

Analyses were executed on a VG Quattro II triple quadropole instrument (Micromass, UK), equipped with a Hewlett Packard 1090 HPLC and a Hewlett Packard 1090 auto sampler (Waldbronn, Germany). Samples were separated on a Phenomenex Luna C18 (2) reverse phase column (250 x 2.00 mm, 5 micron), protected by a guard column (4 mm X 2 mm I.D.) which contained a silica-based C_{18} sorbent packing. A mobile phase gradient was used for the chromatographic separation of the amino acids and the carnitines. A flow rate of 0.2 ml/minute was maintained throughout the analysis. Initially the column was eluted with a mobile phase containing 99% water (containing 1% HCOOH) and 1% CH_3CN. The organic component of the mobile phase was gradually increased to 90% CH_3CN:10% H_2O over a 10-minute interval. The mobile phase composition was returned to the initial conditions over 5 minutes, where it was kept

constant for 20 minutes to re-equilibrate the column before the next sample was injected. The injection volume was 25 µl.

(iii) Conditions employed in the ESI-MS-MS analysis of amino acids and acylcarnitines

		Source (ES^+)		
Capillary		3.50 kVolts		
HV Lens		0.50 kVolts		
Cone		35 Volts		
Skimmer Offset		5 Volts		
Skimmer		1.5 Volts		
RF Lens		0.2 Volts		
Source Temperature		90 °C		
		MS1	**MS2**	
Ion Energy		1.0 Volts		1.0 Volts
Ion Energy Ramp		0.0 Volts		0.0 Volts
LM Resolution		14.0		13.5
HM Resolution		14.0		13.5
Lenses	(# 5)	100 Volts	(# 7)	250 Volts
	(# 6)	5 Volts	(# 8)	40 Volts
			(# 9)	5 Volts
Multiplier		750 Volts		

Nitrogen was used as drying and nebulizing gas. Flow rates for drying and nebulising were set at 350 and 20 $L.h^{-1}$, respectively.

Gradient protocol:

- Initial conditions: Acetonitrile:H_2O (70:30)
- Ramp: 70:30 to 100:0 within 4 minutes; maintain at 100:0 for 6 minutes and return to initial conditions within 30 seconds
- Equilibrate at initial conditions for 10 minutes, prior to next run

- Column: Cosmosil 5C18-MSII column (150 mm x 4.6 mm)
- Volumetric flow rate 1.0 ml/min
- Auto sampler temperature: 25 °C
- Column oven temperature: 25 °C
- Upper pressure limit: 200 bar

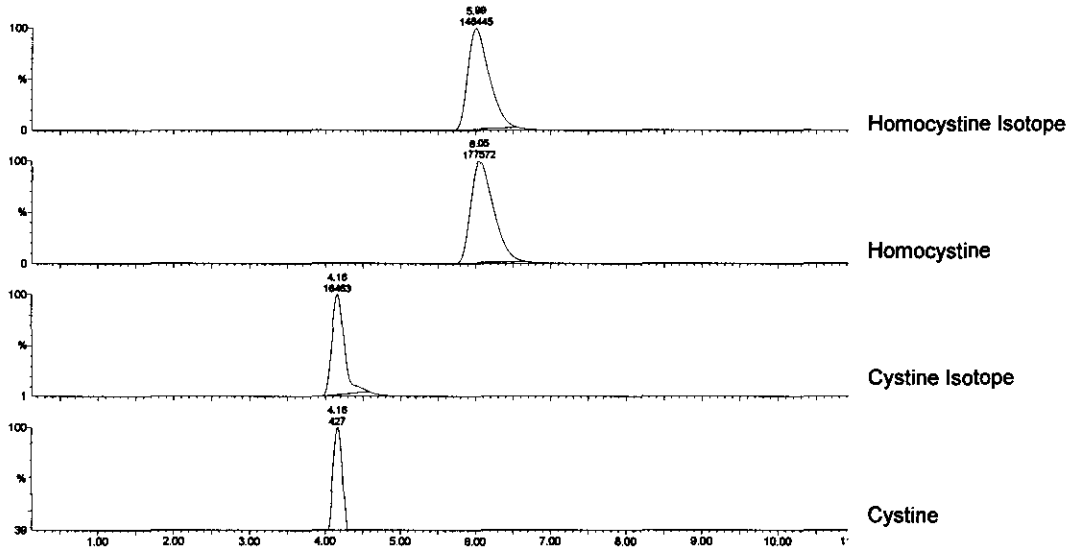

Figure Q1. Multiple Reaction Monitoring (MRM) chromatogram of homocystine and cystine standards with their corresponding isotopes.

Efficient separation and quantification of homocystine and cystine standards were achieved with the method described above. However, the concentration of homocystine in most mouse urine samples was below the detection limit of the analytical procedure employed. The method was therefore regarded as unsuitable for the accurate quantification of homocystine in mouse urine.

ABBREVIATIONS

5,10-CH_2-THF	5,10-methylene tetrahydrofolate
5-MeTHF	5-Methyltetrahydrofolate
Acyl-CoA	Acyl-coenzyme A
Asn	Asparagine
ATP	Adenosine triphosphate
BCHS	bis-Cyclohexyammonium sulphate
BHMT	Betaine-homocysteine methyltransferase
BSTFA	N,O-*bis*-(Trimethylsilyl)-trifluoroacetamide
CBS	Cystathionine-β-synthase
CDC	Centre for Disease Control
CEF	Chicken embryo fibroblasts
CGL	Cystathionine-γ-lyase
CHO	Chinese hamster ovary cells
CoA	Acetyl-coenzyme A
CpG	Cytosine-guanine dinucleotide
cSHMT	Cytoplasmic serine hydroxymethyltransferase
CTP	Cytosine triphosphate
CTPS	Cytosine triphosphate synthetase
dATP	Deoxyadenosine triphosphate
dCDP	Deoxycytidine diphosphate
dCMP	Deoxycytidine monophosphate
dCTP	Deoxycytidine triphosphate
DFMO	DL - α - Difluoromethylornithine
dGTP	Deoxyguanosine triphosphate
DHF	Dihydrofolate
DHPA	2,3-dihydroxypentanoic acid
DNA MTase	DNA methyltransferase
DNA	Deoxyribonucleic acid
DNApol	DNA polymerase
Dnmt1	DNA methyltransferase 1
dTMP	Deoxythymidine monophosphate
dTTP	Deoxythymidine triphosphate
dUMP	Deoxyuridine monophosphate
FPGS	Folylpolyglutamate synthetase
F-THF-S	10-formyl THF synthetase
GCS	Glycine cleavage system

GMK	Green monkey kidney cells
GTP	Guanosine triphosphate
H_4Pte	Tetrahydropteroate
$H_4PteGlu$	Tetrahydrofolate
$H_4PteGlu_6$	Tetrahydrofolate hexaglutamate
Hcy	L-homocysteine
HMGCoA	3-Hydroxy-3-methylglutaryl-CoA
HNV	β-Hydroxynorvaline
HSV	Herpes simplex virus
HTML	3-Hydroxytrimethyllysine
HTMLA	3-Hydroxytrimethyl aldolase
IMP	Inosine monophosphate
KHPA	2-keto-3-hydroxypentanoic acid
K_i	Inhibitor constant
K_m	Michaelis constant
LD_{50}	Lethal dose where 50 % of the experimental embryos die
M^5C-Mtases	N^5-methylcytosine methyltransferases
MAT	L-methionine-S-adenosyltransferase
MeCPs	Methyl-CpG-binding proteins
mg	Milligram
MGBG	Methylglyxal-*bis*-(guanylhydrazone)
ml	Millilitre
mm	Millimetre
MRC	Medical Research Council
MS	Methionine synthase
mSHMT	Mitochondrial serine hydroxymethyltransferase
MTHFD	Methylenetetrahydrofolate dehydrogenase
MTHFR	Methylenetetrahydrofolate reductase
MuLV	Murine leukaemia virus
N^1, N^{12}-Diacspm	N^1, N^{12}-diacetylspermine
N^1, N^8-Diacspd	N^1, N^8-diacetylspermidine
N^1-Acput	N^1-acetylputrecine
N^1-Acspd	N^1-acetylspermidine
N^1-Acspm	N^1-acetylspermine
N^8-Acspd	N^8-acetylspermidine
NAD^+	Nicotinamide adenine dinucleotide (oxidised)
NADH	Nicotinamide adenine dinucleotide (reduced)
$NADP^+$	Nicotinamide adenine dinucleotide, phosphate (oxidised)
NADPH	Nicotinamide adenine dinucleotide, phosphate (reduced)
NDPK	Nucleoside diphosphate kinase
NTD	Neural tube defect

ODC	Ornithine decarboxylase
OMP	Orotidine monophosphate
p.c.	Post coitus
PABA	*p*-aminobenzoic acid
PAO	Polyamine oxidase
PLP	Pyridoxal-5-phosphate
Put	Putrecine
Put/Spm	Putrescine/spermine ratio
RNA	Ribonucleic acid
RNR	Ribonucleotide reductase
RSA	Republic of South Africa
RT-PCR	Reverse transcriptase-polymerase chain reaction
SAH	S-adenosylhomocysteine
SAHase	Adenosyl homocysteinase
SAM	S-adenosylmetionine
SAM-DC	S-adenosyl-L-methionine decarboxylase
SEM	Standard error of the mean
Ser	Serine
SHMT	Serine hydroxymethyltransferase
Spd	Spermidine
Spm	Spermine
Tg_{50}	Concentration of teratogen that will induce 50 % NTD in exposed embryos
THF	Tetrahydrofolate
THF-CD	N^5-formimino THF cyclodeaminase
Thr	Threonine
TK	Thymidine kinase
TMABA	4-Trimethylaminobutyraldehyde
TMABA-DH	4-Trimethylaminobutyraldehyde dehydrogenase
TMCS	Trimethylchlorosilane
TML	N^6-trimethyllysine
TMLH	Trimethyllysine hydrolase
TS	Thymidine synthase
UDP	Uridine diphosphate
UMP	Uridine monophosphate
UTP	Uridine triphosphate
VPA	Valproic acid

REFERENCES

Adams, R.L.P. 1990. DNA methylation: The effect of minor bases on DNA-protein interactions. *Biochemical journal.* **265**, 309 – 320.

Alberts, M., Mamabolo, L., Potgieter, H.C., and Venter, P.A. 2004. Association between anthropometric measurements and growth in infants in the Northern Province. *(In preparation).*

Alonso-Aperte, E., Ubeda, N., Achon, M., Perez-Miguelsanz, J. and Varela-Moreiras, G. 1999. Impaired methionine synthesis and hypomethylation in rats exposed to valproate during gestation. *Neurology.* **52**, 750 – 756.

Athreya, B.H., and McCormick, M.C. 1987 Impact of chronic illness on families. *Rheumatic diseases clinics of North America.* **13**, 123 – 131.

Atkinson, I., Garrow, T., Brenner, A., and Shane, B. 1997. Human cytosolic folylpoly-γ-glutamate synthase. (*In* McCormick, D.B., Suttie, J.W., Wagner, C. Methods in Enzymology, Vol. 281. New York : Academic Press. pp 134 – 140).

Avila, M.A., García-Trevijano, E.R., Martínez-Chantar, M.L., Latasa, M.U., Pérez-Mato, I., Martínez-Cruz, L.A., Sánchez del Pino, M.M., Corrales, F.J., and Mato, J.M. 2002. S-Adenosylmethionine revisited: its essential role in the regulation of liver function. *Alcohol.* **27**, 163 – 167.

Bailey, L.B., and Gregory, J.F. 1999. Folate metabolism and requirements. *Recent advances in nutritional science.* **129**, 779 – 782.

Barile, F.A., Siddiqi, Z.E., Ripley-Rouzier, C., and Bienkowski, R.S. 1989. Effects of puromycin and hydroxynorvaline on the net production and intracellular degradation of collagen in human fetal lung fibroblasts. *Archives of biochemistry and biophysics.* **270**, 294 – 301.

Beck, F., Moffat, D.B., and Lloyd, J.B. 1973. Human Embryology and Genetics. Oxford : Blackwell Scientific Publications. p 196.

Bennett, M.J., Hosking, G.P., Smith, M.F., Grey, R.G., and Middleton, B. 1984. Biochemical investigations on a patient with a defect in cytosolic acetoacetyl-CoA thiolase, associated with mental retardation. *Journal of inherited metabolic disease.* **7**, 125 – 128.

Bester, M.J., Potgieter, H.C., and Vermaak, W.J. 1994. Cholate and pH reduce interference by sodium dodecyl sulphate in the determination of DNA with Hoechst. *Analytical biochemistry.* **223**, 299 – 305.

Bergmeyer, H.U., Hørder, M., and Markowetz, D. 1983. Reliability of laboratory results and practicability of procedures. (*In* Bergmeyer, H.U., Bergmeyer, J., and Grabl, M. *eds.* Methods of enzymatic analysis, Vol. 1. Weinheim : Verlag Chemie. pp 21 – 40).

Blough, H.A., Pauwels, R., De Clercq, E., Cogniaux, J., Sprecher-Goldberger, S., and Thiry, L. 1986. Glycosylation inhibitors block the expression of LAV/HTLV-III (HIV) glycoproteins. *Biochemical and biophysical research communications.* **26**, 33 – 38.

Botero-Ruiz, W., Biggers, W.J., and Sanyal, M.K. 1997. Augmentation of DNA synthesis in placental and fetal tissues *in utero* by maternal growth hormone treatment. *Early-Pregnancy: Biology and medicine.* **3**, 272 – 280.

Brits, M. 2004. Valproate induced metabolic perturbations in a mouse neural tube defect model. Potchefstroom : PU for CHE. (Thesis – M.Sc.).

Campbell, L.R., Dayton, D.H., and Sohal, G.S. 1986. Neural tube defects: a review of human and animal studies on the etiology of neural tube defects. *Teratology.* **34**, 171 – 187.

Caruso, A., Pellati, A., Bosi, P., Arena, N., and Stabellini, G. 1992. Effect of spermidine synthase inhibition in cultured chick embryo fibroblasts. *Cell biology international reports.* **16**, 349 – 358.

Cedar, H., and Razin, A. 1990. DNA methylation and development. *Biochemica et biophysica acta.* **1049**, 1 – 8.

Cetin, I., Fennessey, A.N., Quick, A.N.J., Marconi, A.M., Meschia, G., Battaglia, F.C., and Sparks, J.W. 1991. Glycine turnover and oxidation and hepatic serine synthesis form glycine in fetal lambs. *American journal of physiology - endocrinology and metabolism.* **260**, E371 – E378.

Cetin, I., Fennessey, P.V., Sparks, J.W., Meschia, G., and Battaglia, F.C. 1992. Fetal serine fluxes across fetal liver, hindlimb and placenta in late gestation: the role of fetal serine in placental glycine production. *American journal of physiology - endocrinology and metabolism.* **263**, E786 – E793.

Charmers, R.A., and Lawson, A.M. 1982. Organic acids in man. Analytical chemistry, biochemistry and diagnosis of organic aciduria. New York : Chapman and Hall. p 523.

Chasson, A.L., Grady, H.J., and Stanley, M.A. 1961. Determination of creatinine by means of automatic chemical analysis. *American journal of clinical pathology.* **35**, 83 – 88.

Chen, J., Hunter, D.J., Stampfer, M.J., Kyte, C., Chan, W., Wetmur, J.G., Mosig, R., Selhub, J., and Ma, J. 2003. Polymorphism in the Thymidylate Synthase Promoter Enhancer Region Modifies the Risk and Survival of Colorectal Cancer. *Cancer epidemiology, biomarkers & prevention.* **12**, 958 – 962.

Christensen, B., and Rosenblatt, D.S. 1995. Effects of folate deficiency on embryonic development. *Baillieres clinical haematology.* **8**, 617 – 637.

Christner, P., Carpousis, A., Harsch, M., and Rosenbloom, J. 1975. Inhibition of the assembly and secretion of procollagen by incorporation of a threonine analogue, hydroxynorvaline. *Journal of biological chemistry.* **250**, 7623 – 7630.

Cleland, W.W. 1967. The statistical analysis of enzyme kinetic data. (*In* Meister, A. Advances in enzymology, Vol. 29. New York : Wiley. pp 1 – 32).

Coakley, M.E., Rawlings, S.J., and Brown, N.A. 1986. Short-chain carboxylic acids, a new class of teratogens: studies of potential biochemical mechanisms. *Environmental health perspectives.* **70**, 105 – 111.

Coelho, C.N.D., and Klein, N.W. 1990. Methionine and neural tube closure in cultured rat embryos – Morphological and biochemical analyses. *Teratology.* **42**, 437 – 451.

Copp, A.J. 1997. The neural tube. (*In* Thorogood, P. Embryos, genes and birth defects. New York : Wiley. pp 133 – 152).

Czeizel, A.E., and Dudas, I. 1992. Prevention of the first occurrence of neural tube defects by periconceptional vitamin supplementation. *The New England journal of medicine.* **327**, 1832 – 1835.

Daum, R.S., Lamm, P.H., Mamer, O.A., and Scriver, C.R. 1971. A "new" disorder of isoleucine catabolism. *Lancet.* **2**, 1289 – 1290.

Davies, A.T., and Hoppel, C.L. 1986. Effect of starvation on the disposition of free and peptide-linked trimethyllysine in the rat. *Journal of nutrition.* **116**, 760 – 767.

De Groot, C.J., Haan, G.L., Hulstaert, C.E., and Hoomes, F.A. 1977. A patient with severe neurological symptoms and acetoacetyl-CoA thiolase deficiency. *Pediatric research.* **11**, 1112 – 1116.

Delport, S.D., Christianson, A.L., van der Berg, H.J.S., Wolmarans, L., and Gericke, G.S. 1995. Congenital anomalies in black South African liveborn neonates at an urban academic hospital. *South African medical journal.* **85**, 11 – 15.

Docherty, P.A., and Aronson, NN Jr. 1985. Effect of the threonine analog beta-hydroxynorvaline on the glycosylation and secretion of alpha 1-acid glycoproteins by rat hepatocytes. *Journal of biological chemistry.* **260**, 10847 – 10855.

Dodds, G.S. 1947. The essentials of human embryology, 3rd ed. New York : Wiley. pp 229 – 230.

Elmazar, M.M., and Nau, H. 1995. Ethanol potentiates valproic acid-induced neural tube defects (NTDs) in mice due to toxicokinetic interactions. *Reproductive toxicology.* **9**, 427 – 433.

Erasmus, E. 1987. Die gebruik van gaschromatografie, massaspektrometry en rekenaartegnologie in die identifisering van organise-suururië. Potchefstroom : PU for CHE. (Thesis – MSc) p 271.

Eskes, T.K. 2000. From anemia to spina bifida - the story of folic acid. A tribute to Professor Richard Smithells. *European journal of obstetrics, gynecology, and reproductive biology*. **90**, 119 – 123.

Fell, D., and Selhub, J. 1990. Disruption of thymidylate synthesis and glycine-serine interconversion by L-methionine and L-homocystine in Raji cells. *Biochimica et biophysica acta*. **1033**, 80 – 84.

Finnell, R.H., Bennett, G.D., Karras, S.B., and Mohl, V.K. 1988. Common hierarchies of susceptibility to the induction of neural tube defects by valproic acid and its 4-propyl-4-pentenoic acid metabolite. *Teratology*. **38**, 313 – 320.

Finnell, R.H., Wlodarczyk, B.C., Craig, J.C., Piedrahita, J.A., and Bennett, G.D. 1997. Strain-dependent alterations in the expression of folate pathway genes following teratogenic exposure to valproic acid in a mouse model. *American journal of medical genetics*. **70**, 303 – 311.

Finnell, R.H., Gould, A., and Spiegelstein, O. 2003. Pathobiology and genetics of neural tube defects. *Epilepsia*. **44**, 14 – 23.

Fisher, M.C., Zeisel, S.H., Mar, M.H., and Sadler, T.W. 2002. Perturbations in choline metabolism cause neural tube defects in mouse embryos in vitro. *FASEB Journal*. **16**, 619 – 621.

Fleming, A., and Copp, A.J. 1998. Embryonic folate metabolism and mouse neural tube defects. *Science*. **280**, 2107 – 2109.

Fontaine, M., Briand, G., Ser, N., Armelin, I., Rolland, M., Degand, P., and Vamecq, J. 1996. Metabolic studies in twin brothers with 2-methylacetoaetate-CoA thiolase deficiency. *Clinica Chimica acta*. **255**, 67 – 83.

Friso, S., Choi, S., Girelli, D., Mason, J.B., Dolnikowski, G.G., Bagley, P.J., Olivieri, O., Jacques, P.F., Rosenberg, I.H., Corrocher, R., and Selhub, J. 2002. A common mutation in the 5, 10-methylenetetrahydrofolate reductase gene affects genomic DNA methylation through an interaction with folate status. *Proceedings of the national academy of sciences USA*. **99**, 5606 – 5611.

Gebhardt, D.O.E. 1972. The use of the chick embryo in applied teratology. (*In* Wollam D.H.M., *ed*. Advances in teratology, 5th ed. London : Academic Press. pp 97 – 111).

Geller, A.M., and Kotb, M.Y. 1989. A binding assay for serine hydroxymethyltransferase. *Analytical biochemistry*. **180**, 120-125.

Gelderblom, W.C., Jaskiewicz, K., Marasas, W.F., Thiel, P.G., Horak, R.M., Vleggaar, R., and Kriek, N.P. 1988. Fumonisins – novel mycotoxins with cancer-

promoting activity produced by Fusarium moniliforme. *Applied and Environmental Microbiology.* **54**, 1806 – 1811.

George, T.M., and McLone, D.G. 1995. Mechanisms of mutant genes in spina bifida: a review of implications from animal models. *Pediatric neurosurgery.* **23**, 236 – 245.

George, T.M., and Fuh, E. 2003. Review of animal models of surgically induced spinal neural tube defects: implications for fetal surgery. *Pediatric neurosurgery.* **39**, 81 – 90.

Girgis, S., Suh, J.R., Jolivet, J., and Stover, P.J. 1997. 5-Formyltetrahydrofolate regulates homocysteine remethylation in human neuroblastoma. *Journal of biological chemistry.* **272**, 4729 – 4734.

Goyns, M.H. 1982. The role of polyamines in animal cell physiology. *Journal of theoretical biology.* **97**, 577 – 589.

Green, E.G., and Orme-Johnson, N.R. 1991. Inhibition of steroidogenesis in rat adrenal cortex cells by a threonine analogue. *Journal of steroid biochemistry and molecular biology.* **40**, 421 – 429.

Greene, N.D.E., Dunlevy, L.P.E., and Copp, A.J. 2003. Homocysteine is embryotoxic but does not cause neural tube defects in mouse embryos. *Anatomy and embryology.* **206**, 185 – 191.

Gregory, J.F., Cuskelly, G.J., Shane, B., Toth, J.P., Baumgartner, T.G., and Stacpoole, P.W. 2000. Primed, constant infusion with [$^2H_3$]serine allows in vivo kinetic measurement of serine turnover, homocysteine remethylation, and transsulfuration processes in human one-carbon metabolism. *American journal of clinical nutrition.* **72**, 1535 – 1541.

Hall, R.H. 1971. The modified nucleotides in nucleic acids. New York : Columbia University Press. pp 281 – 294.

Hamburger, V., and Hamilton, H.L. 1951. A series of normal stages in the development of the chick embryo. *Journal of morphology.* **88**, 49 – 92.

Hamosh, A., Johnston, M.V., and Valle, D. 1995. Nonketotic hyperglycinemia. (*In* Scriver, C.R., Beaudet, A.L., William, S.S., Valle, D., *eds.* The Metabolic and molecular basis of inherited disease, 7th ed. New York : McGraw-Hill. pp 1337 – 1348).

Harmon, D.L., Woodside, J.V., Yarnell, J.W., McMaster, D., Young, I.S., McCrum, E.E., Gey, K.F., Whitehead, A.S., and Evans, A.E. 1996. The common "thermolabile" variant of methylene tetrahydrofolate reductase is a major determinant of mild hyperhomocysteinaemia. *QJM.* **89**, 571 – 577.

Haukanes, K., Szajko, K., and Helland, D.E. 1990. Action of spermidine, N^1-acetylspermidine, and N^8-acetylspermidine at apurinic sites in DNA. *FEBS Letters.* **269**, 389 – 393.

Heby, O. 1981. Role of polyamines in the control of cell proliferation and differentiation. *Differentiation.* **19**, 1 – 20.

Heil, S.G., van der Put, N.M.J., Waas, E.T., den Heijer, M., Trijbels, F.J.M., and Blom, H.C. 2001. Is mutated serine hydroxymethyltransferase (SHMT) involved in the etiology of neural tube defects? *Molecular genetics and metabolism.* **73**, 164 – 172.

Henderson, L.M., Nelson, P.J., and Henderson, L. 1982. Mammalian enzymes of trimethyllysine conversion to trimethylaminobutyrate. *Federation proceedings.* **41**, 2843 – 2847.

Hendricks, K.A., Simpson, J.S., and Larsen, R.D. 1999 Neural tube defects along the Texas-Mexico border, 1993-1995. *American journal of epidemiology.* **149**, 1119 – 1127.

Herbig, K., Chiang, E., Lee, L., Hills, J., Shane, B., and Stover, P.J. 2002. Cytoplasmic serine hydroxymethyltransferase mediates competition between folate-dependent deoxyribonucleotide and S-adenosylmethionine biosyntheses. *Journal of biological chemistry.* **277**, 38381 – 38389.

Herman, J.G., Graff, J.R., Myöhänen, S., Nelkin, B.D., and Baylin, S.B. 1996. Methylation-specific PCR: A novel PCR assay for methylation status of CpG islands. *Proceedings of the national academy of science.* **93**, 9821 – 9826.

Hogan, B., Costantini, F., and Lacy, E. 1986. Manipulating the mouse embryo. A laboratory manual. New York : Cold Spring Harbour Laboratory. p 30.

Hortin, G., and Boime, I. 1981. Miscleavage at the presequence of rat preprolactin synthesized in pituitary cells incubated with a threonine analog. *Cell.* **24**, 453 – 461.

Inagaki, T., Wang, K., Higbee, R.G., McLone, D.G., and Knepper, P.A. 1996. Concanavalin-A-induced open neural tube defects in chick embryos. *Neurologia medico-chirurfica.* **36**, 691 – 697.

Jaffe, M. 1886. Ueber den Niederschlag, welchen Pikrinsaure in normalem Harn erzeugt and ueber eiene neue reaction des Kreatinins. *Zeitschrift fuer physiologische chemie.* **10**, 391 – 400.

Jhee, K., Niks, D., McPhie, P., Dunn, M.F., and Miles, E.W. 2002. Yeast cystathionine β-synthase reacts with L-allothreonine, a non-natural substrate, and L-homocysteine to form a new amino acid, 3-methyl-L-cystathionine. *Biochemistry.* **41**, 1828 – 1835.

Jordaan, J.H.L. 2000. Die sintese van derivate van Tetrasiklo[6.3.0.$0^{4,11}$.$0^{5,9}$]-undek-2-een-6-oon. Potchefstroom : PU for CHE. (Thesis – M.Sc).

Kafri, T., Ariel, M., Brandeis, M., Shemer, R., Urven, L., MaCarrey, J., Cedar, H., and Razin, A. 1992. Development pattern of gene-specific DNA methylation in the mouse embryo and germ line. *Genes and development.* **6**, 705 – 714.

Kalbag, S.S., and Palekar, A.G. 1990. Postnatal development of the glycine cleavage system in rat liver. *Biochemical medicine and metabolic biology.* **43**, 128 – 132.

Kang, SS., Wong, P.W., Susmano, A., Sora, J., Nurusis, M., and Ruggie, N. 1991. Thermolabile methylenetetrahydrofolate reductase: an inherited risk factor for coronary artery disease. *American journal of human genetics.* **48**, 536 – 545.

Khuhawar, M.Y., and Qureshi, G.A. 2001. Polyamines as cancer markers: applicable separation methods. *Journal of chromatography.* **764**, 385 – 407.

Kloeblen, A.S., and Batish, S.S. 1999. Understanding the intention to permanently follow a high folate diet among a sample of low-income pregnant women according to the Health Belief Model. *Health education research.* **14**, 327 – 338.

Kluijtmans, L.A.J., Broers, G.H.J., Stevens, E.M.B., Renier, W.O., Kraus, J.P., Trijbels, F.J.M., van der Heuvel, L.P.W.J., and Blom, H.J. 1996. Defective Cystathionine-β-synthase regulation by S-adenosylmethionine in a partially responsive homocystinuria patient. *Journal of clinical investigation.* **98**, 285 – 289.

Krähenbühl, S. 1996. Carnitine metabolism in chronic liver disease. *Life sciences.* **59**, 1579 – 1599.

Kraus, J.P. 1987. Cystathionine β-synthase (Human). (*In* Jacoby, W.B., and Griffith, O.W. Methods in Enzymology, Vol. 143. New York : Academic Press, Inc. pp 388 – 394).

Langman, J. 1975. Medical embryology, 3rd ed. Baltimore : The Williams and Wilkens Company. pp 60 – 63.

Leck, I. 1977. Correlation of malformation frequency with environmental and genetic attributes in man. (*In* Wilson, J.G., AND Fraser, F.C. Handbook of teratology, Vol 3. Comparative, maternal and epidemiologic aspects. New York : Plenum Press. pp 243 – 324).

Lee, M.E., and Wang, H. 1999. Homocysteine and hypomethylation. A novel link to vascular disease. *Trends in cardiovascular medicine.* **9**, 49 – 54.

Leech, R.W., and Payne, G.G. 1991 Neural tube defects: epidemiology. *Journal of child neurology.* **6**, 286 – 287.

Lei, H., Oh. S.P., Okano, M., Jüttermann, R., Kendrick, A.G., Jaenisch, R., and Li, E. 1996. De novo DNA cytosine methyltransferase activities in mouse embryonic stem cells. *Development.* **122**, 3195 – 3205.

Lemire, R.J. 1988. Neural tube defects. *JAMA.* **259**, 558 – 562.

Lertratanangkoon, K., Sevaraj, N., Scimeca, J.M., and Thomas, M.L. 1997. Glutathione depletion-induced thymidylate insufficiency for DNA repair synthesis. *Biochemical & biophysical research communications.* **234**, 470 – 475.

Lewis, D.P., Van Dyke, D.C., Stumbo, P.J., and Berg, M.J. 1998. Drug and environmental factors associated with adverse pregnancy outcomes. Part I: Antiepileptic drugs, contraceptives, smoking, and folate. *The annals of pharmacotherapy.* **32**, 802 – 817.

Li, E., Bears, C., and Jaenisch. R. 1993. Role of DNA methylation in genomic imprinting. *Nature.* **366**, 362 – 365.

Lin, S., and Guarente, L. 2003. Nicotinamide adenine dinucleotide, a metabolic regulator of transcription, longevity and disease. *Current opinion in cell biology.* **15**, 241 – 246.

Liquori, A.M., Costantino, L., Crescenzi, V., Elia, V., Giglio, E., Puliti, R., De Santis Savino, M., and Vitagliano, V. 1967. *Journal of molecular biology.* **24**, 113 – 122.

Locksmith, G.J., and Duff, P. 1998. Preventing neural tube defects: the importance of periconceptional folic acid supplements. *Obstetrics and gynecology.* **91**, 1027 – 1034.

Löwkvist, B., Emanuelsson, H., and Heby, O. 1985. Changes in polyamine synthesis and concentrations during chick embryo development. *Journal of experimental zoology.* **234**, 375 – 382.

Lucock, M.D., Daskalakis, I., Lumb, C.H., Schorah, C.J., and Levene, M.I. 1998. Impaired regeneration of monoglutamyl tetrahydrofolate leads to cellular folate depletion in mothers affected by a spina bifida pregnancy. *Molecular genetics and metabolism.* **65**, 18 – 30.

Luo, J., Nikolaey, A.Y., Imai, S., Chen, D., Su, F., Shiloh, A., Guarente, L., and Gu, W. 2001. Negative control of p53 by Sir2a promotes cell survival under stress. *Cell.* **107**, 137 – 148.

Marasas, W.F., Riley, R.T., Hendricks, K.A., Stevens, V.L., Sadler, T.W., Gelineau-van Waes, J., Missmer, S.A., Cabrera, J., Torres, O., Gelderblom, W.C., Allegood, J., Martinez, C., Maddox, J., Miller, J.D., Starr, L., Sullards, M.C., Roman, A.V., Voss, K.A., Wang, E., and Merrill, A.H. Jr. 2004. Fumonisins disrupt sphingolipid metabolism, folate transport, and neural tube development in embryo culture and in vivo: a potential risk factor for human neural tube defects among populations consuming fumonisin-contaminated maize. *Journal of Nutrition.* **134**, 711 – 716.

Marcé, M., Brown, D.S., Capell, T., Figueras, X., and Tiburcio, A.F. 1995. Rapid high-performance liquid chromatography method for the quantitation of polyamines as their dansyl derivatives: application to plant and animal tissues. *Journal of chromatography.* **666**, 329 – 335.

Makaula, N.A., Marasas, W.F., Badenhorst, C.J., Bradshaw, D., and Swanevelder, S. 1995. Oesophageal and other cancer patterns in four selected districts of Transkei, Southern Africa: 1985 – 1990. *African journal of health sciences.* **2**, 333 – 337.

Massare, M.J., and Blough. H.A. 1987. Inhibition of herpesvirus-induced thymidine kinase and DNA polymerase by β-hydroxynorvaline. *FEB.* **223**, 122 – 126.

Matsuda, M., and Keino, H. 1994. An open cephalic neural tube reproducibly induced by cytochalasin D in rat embryos *in vitro*. *Zoological science*. **11**, 547 – 553.

Mattson, M.P., and Shea, T.B. 2003. Folate and homocysteine metabolism in neural plasticity and neurodegenerative disorders. *Trends in neuroscience*. **26**, 137 – 146.

McDonnell R.J., Johnson, Z., Delaney, V., and Dack, P. 1999 East Ireland 1980-1994: epidemiology of neural tube defects. *Journal of epidemiology and community health*. **53**, 782 – 788.

Medical Research Council [MRC] Vitamin Study Research Group. 1991. Prevention of neural tube defects: results of the Medical Research Council vitamin study. *Lancet*. **338**, 131 – 137.

Meehan, R.R. 2003. DNA methylation in animal development. *Seminars in cell and development biology*. **14**, 53 – 65.

Metcalf, B.W., Bey, P., Danzin, C., Jung, M.J., Casara, P., and Vevert, J.P. 1987. Catalytic irreversible inhibition of mammalian ornithine decarboxilase by substrate and p roduct analogues. *Journal of the American chemical society*. **100**, 2551 – 2553.

Metz, J., Kelly, A., Swett, V.C., Waxman, S., and Herbert, V. 1986. Deranged DNA synthesis by bone marrow from vitamin B_{12}-deficient humans. *British journal of haematology*. **14**, 575 – 592.

Middleton, B. 1973. The oxoacyl-coenzyme A thiolases of animal tissues. *Biochemical journal*. **132**, 717 – 730.

Middleton, B., and Bartlett, K. 1983. The synthesis and characterisation of 2-methylacetoacetyl coenzyme A and its use in the identification of the site of the defect in 2-methylacetoacetic and 2-methyl-3-hydroxybutyric aciduria. *Clinica chimica acta*. **128**, 291 – 305.

Mienie, L.J. 1994. 'n Studie van geïnduseerde metaboliese weë weens 'n aangebore defek in propioniel-KoA-karboksilase. Potchefstroom : PU for CHE. (Thesis – Ph.D).

Mienie, L.J., Erasmus, E., and Knoll, D.P. 2004. Electrospray ionisation tandem mass spectrometry acylcarnitine analysis: Disease specific profiling and investigation of metabolite fragmentation reveals new information of glutamic acid interference. (In preparation)

Millington, D.S., Kodo, N., Norwood, D.L., and Roe, C.R. 1990. Tandem mass spectrometry: A new method for acylcarnitine profiling with potential neonatal

screening for inborn errors of metabolism. *Journal of inherited metabolic diseases.* **13**, 321 – 324.

Mills, J.L., McPartlin, J.M., Kirke, P.N., Lee, Y.J., Conley, M.R., Weir, D.G., and Scott, J.M. 1995. Homocysteine metabolism in pregnancies complicated by neural-tube defects. *Lancet.* **345**, 149 – 151.

Mills, J.L., Scott, J.M., Kirke, P.N., McPartlin, J.M., Conley, M.R., Weir, D.G., Molloy, A.M., and Lee, Y.J. 1996. Homocysteine and neural tube defects. *Journal of nutrition.* **126**, 756 – 760.

Miyazawa, S., Osumi, T., and Hashimoto, T. 1980. The presence of a new 3-oxoacyl-CoA thiolase in rat liver peroxisomes. *European journal of biochemistry.* **103**, 589 – 596.

Miyazawa, S., Furata, S., Osumi, T., Hashimoto, T., and Ui, N. 1981. Properties of peroxisomal 3-ketoacyl-CoA thiolase from rat liver. *Journal of biochemistry.* **90**, 511 – 519.

Modjadji, S.E.P., Alberts, M., and Potgieter, H.C. 2004 Pre- and post-fortification vitamin status of rural women in the Limpopo Province. *(In preparation).*

Monk, M., Boubelik, M., and Lehnert, S. 1987. Temporal and regional changes in DNA methylation in the embryonic and germ cell lineages during mouse embryo development. *Development.* **99**, 371 – 382.

Moore, C.A., Li, S., Li, Z., Hong, S.X., Gu, H.Q., Berry, R.J., Mulinare, J., and Erickson, J.D. 1997. Elevated rates of severe neural tube defects in a high-prevalence area in northern China. *American journal of medical genetics.* **73**, 113 – 118.

Mudd, S.H., Levy, H.L., and Skovby, F. 1995. Disorders of Transsulfuration. (*In* Scriver, C.R., Beaudet, A.L., William, S.S., Valle, D., *eds.* The Metabolic and molecular basis of inherited disease, 7th ed. New York : McGraw-Hill. pp 1279 – 1327).

Narkewicz, M.R., Sauls, S.D., Tjoa, S.S., Teng, C., and Fennessey, P.V. 1996a. Evidence for intracellular partitioning of serine and glycine metabolism in Chinese hamster ovary cells. *Biochemical journal.* **313**, 991 – 996.

Narkewicz, M.R., Thureen, P.J., Sauls, S.D., Tjoa. S., Nikolayevsky, N., and Fennessey, P.V. 1996b. Serine and glycine metabolism in hepatocytes from mid gestation fetal lambs. *Pediatric research.* **39**, 1085 – 1090.

Naruse, I., Collins, M.D., and Scott, W.J. 1988. Strain differences in the teratogenicity induced by sodium valproate in cultured mouse embryos. *Teratology.* **38**, 87 – 96.

Ncayiyna, D.J. 1986. Neural tube defects among rural blacks in the Transkei district. *South African medical journal.* **69**, 618 – 620.

Nevin, N.C., Johnston, W.P., and Merrett, J.D. 1981 Influence of social class on the risk of recurrence of anencephalus and spina bifida. *Developmental medicine and child neurology.* **23**, 155 – 159.

Oppenheim, E.W., Adelman, C., Liu, X., and Stover, P.J, 2001. Heavy chain ferritin enhances serine hydroxymethyltransferase expression and the *de novo* thymidine biosynthesis. *Journal of biological chemistry.* **276**, 19855 – 19861.

Op't Hoff, J. 1985. Genetic services for congenital and hereditary disorder. Pretoria : Eng Enterprises. pp 4.44 – 4.54.

Otsuka, H., and Kit, S. 1984. Nucleotide sequence of the marmoset herpesvirus thymidine kinase gene and predicted amino acid sequence of thymidine kinase polypeptide. *Virology.* **135**, 316 – 330.

Ou, C.Y., Stevenson, R.E., Brown, V.K., Schwartz, C.E., Allen, W.P., Khoury, M.J., Rozen, R., Oakley, G.P., and Adams, M.J. Jr. 1996. 5,10 Methylenetetrahydrofolate reductase genetic polymorphism as a risk factor for neural tube defects. *American journal of medical genetics.* **63**, 610 – 614.

Palmer, T. 1995. Understanding enzymes. London : Prentice Hall/Ellis Horwood. p 97.

Pelliniemi, T, and Beck, W.S. 1980. Biochemical mechanisms in the Killmann experiment: Critique of the deoxyuridine suppression test. *Journal of clinical investigation.* **65**, 449 – 460.

Persaud, T.V.N., and Kaplan, S. 1970. The effects of Hypoglycin-A, a leucine analogue, on the development of rat and chick embryos. *Life sciences.* **9**, 1305 – 1313.

Perry, D.K., and Hannum, Y.A. 1998. The role of ceramide in cell signalling. *Biochimica et Biophysica ACTA.* **1436**, 233 – 243.

Phelan, S.A., Ito, M., and Loeken, M.R. 1997. Neural tube defects in embryos of diabetic mice: role of the Pax-3 gene and apoptosis. *Diabetes.* **46**, 1189 – 1197.

Pillai, S.P., and Shankel, D.M. 1997. Polyamines and their potential to be antimutagens. *Mutation research.* **377**, 217 – 224.

Polonoff, E., Machida, C.A., and Kabat, D. 1982. Glycosylation and intracellular transport of membrane glycoproteins encoded by murine leukemia viruses. Inhibition by amino acid analogues and by tunicamycin. *Journal of biological chemistry.* **23**, 14023 – 14028.

Potgieter, H.C., Vermeulen, N.M.J. Potgieter, D.J.J., and Strauss, H.F. 1977. A toxic amino acid, 2(*S*)3(*R*)-2-amino-3-hydroxypent-4-ynoic acid from the fungus *Sclerotium Rolfsii. Photochemistry.* **16**, 1757 – 1759.

Ramsbottom, D., Scott, J.M., Molloy, A., Weir, D.G., Kirke, P.N., Mills, J.L., Gallagher, P.M., and Whitehead, A.S. Are common mutations of cystathionine β-

synthase involved in the aetiology of neural tube defects? *Clinical genetics.* **51**, 39 – 42.

Rao, N.A. 1991. Serine hydroxymethyltransferase: a target for cancer chemotherapy. *New trends in biological chemistry.* p 333 – 340.

Rebouche, C.J., Lehman, L.J., and Olson, L. 1986. *ε-N*-Trimethyllysine availability regulates the rate of carnitine biosynthesis in the growing rat. *Journal of nutrition.* **116**, 751 – 759.

Reddy, D.M., Crain, P.F., Edmonds, C.G., Gupta, R., Hashizume, T., Stetter, K.O., Widdel, F., and McCloseky, J.A. 1992. Structure determination of two new amino acid-containing derivatives of adenosine from tRNA of therophilic bacteria and archaea. *Nucleic acid research.* **20**, 5607 – 5615.

Renwick, S.B., Snell, K., and Baumann, U. 1998. The crystal structure of human cytosolic serine hydroxymethyltransferase: a target for cancer chemotherapy. *Structure.* **6**, 1105 – 1116.

Richter, B., Schultealbert, A.H., and Koch, M.C. 2002. Human *T* and risk for neural tube defects. *Journal of medical genetics.* **39**, e14 – e14.

Robinson, J. B., Brent, L.G., Sumegi, B., and Srere, P.A. 1987. An enzymatic approach to the study of the tricarboxylic acid cycle. (*In* Barley-Usmar, B.M., Rickwood, D., and Wilson, M.T. *eds.* Mitochondria – a practical approach. Oxford : IRL. pp 153 – 170).

Rosenblatt, D.S. 1995. Inherited disorders of folate transport and metabolism. (*In* Scriver, C.R., Beaudet, A.L., William, S.S., Valle, D., *eds.* The Metabolic and molecular basis of inherited disease, 7th ed. New York : McGraw-Hill. pp 3111 – 3128).

Rowe, P.B. 1983. Inherited disorders of folate metabolism. (*In* Stanbury, J.B., Wyngaarden, J.B., Fredrickson, D.S., Goldstein, J.L., Brown, M.S. The Metabolic and molecular basis of inherited disease, 5th ed. New York : McGraw-Hill. pp 498 – 521).

Salway, J.G. 1994. Metabolism at a glance. Guildford : Blackwell Science. pp 54 – 57.

Sadler, T.W., Merrill, A.H., Stevens, V.L., Sullards, M.C., Wang, E., and Wang, P. 2002. Prevention of fumonisin B1-induced neural tube defects by folic acid. *Teratology.* **66**, 169 – 176.

Schirch, L. 1982. Serine hydroxymethyltransferase. (*In* Meister, A. Advances in Enzymology, Vol. 53. New York : Wiley. pp 83 – 110).

Sega, G.A. 1974. Unscheduled DNA synthesis in the germ cells of male mice exposed *in vivo* to the chemical mutagen ethyl methanesulfonate. *Proceedings of the national academy of sciences of the United States of America.* **71**, 4955 – 4959.

Seiler, N. 1987. Functions of polyamine acetylation. *Canadian journal of physiology and pharmacology.* **65**, 2024 – 2035.

Selhub, J., and Miller, J.W. 1992. The pathogenesis of homocysteinemia: interruption of the coordinate regulation by S-adenosylmethionine of the remethylation and transsulfuration of homocysteine. *American journal of clinical nutrition.* **55**, 131 – 138.

Setoyama, C., Ding, S.H., Choudhury, B.K., Joh, T., Takeshima, H., Tsuzuki, T., and Shimada, K. 1990. Regulatory regions of the mitochondrial and cytosolic isoenzyme genes participating in the malate-aspartate shuttle. *Journal of biological chemistry.* **265**, 1293 – 1299.

Sim, K.G., Hammond, J., and Wilcken, B. 2002. Strategies for the diagnosis of mitochondrial fatty acid β-oxidation disorders. *Clinica chimica acta.* **323**, 37 – 58.

Singh, I. 1978. An introduction to human embryology for medical students, international ed. London : The MacMillan Press LTD. p 41.

Smith, P.K., Krohn, R.I., Hermanson, G.T., Mallia, A.K., Gartner, F.H., Provenzano, M.D., Goeke, N.M., Olsen, B.J., and Klenk, D.G. 1985. Measurement of protein using bicinchoninic acid. *Analytical biochemistry.* **150**, 76 – 85.

Somdyala, N.I., Marasas, W.F., Venter, F.S., Vismer, H.F., Gelderblom, W.C., and Swanevelder, S.A. 2003. Cancer patterns in four districts of the Transkei region--1991-1995. *South African medical journal.* **93**, 144 – 148.

Stack, M.E. 1998 Analysis of fumonisin B1 and its hydrolysis product in tortillas. *Journal of AOAC INTERNATIONAL.* **81**, 737 – 740.

Steegers-Theunissen, R.P., Boers, G.H., Trijbels, F.J., Finkelstein, J.D., Blom, H.C., Thomas, C.M., Borm, G.F., Wouters, M.G., and Eskes, T.K. 1994. Maternal hyperhomocysteinemia: a risk factor for neural-tube defects? *Metabolism: clinical and experimental.* **43**, 1475 – 1480.

Steegers-Theunissen, R.P. 1995. Folate metabolism and neural tube defects: a review. *European journal of obstetrics, gynecology, and reproductive biology.* **61**, 39 – 48.

Stevens, V.L., and Tang, J. 1997. Fumonisin B_1-induced sphingolipid depletion inhibits vitamin uptake via the glycosylphosphatidylinositol-anchored folate receptor. *Journal of biological chemistry.* **272**, 18020 – 18025.

Stover, P.J., Chen, L.H., Suh, J.R., Stover, D.M., Keyomarsi, K., and Shane, B. 1997. Molecular cloning, characterization, and regulation of the human mitochondrial serine hydroxymethyltransferase gene. *Journal of biological chemistry.* **272**, 1842 – 1848.

Strauss, W.M. 1987. Preparation of genomic DNA from mammalian tissue. (*In* Ausubel, F.M., eds. Current protocols in molecular biology, Vol 1. New York : Wiley. pp 2.2.1 – 2.2.3).

Sulik, K.K., and Sadler, T.W. 1993. Postulated mechanisms underlying the development of neural tube defects. Insights from in vitro and in vivo studies. *Annals of the New York academy of sciences.* **678**, 8 – 21.

Sunko, D.E., and Kisic, A. 1955. A synthesis of DL-α-Amino-β-hydroxy-valeric acid (Hydroxynorvaline). *Arhiv Kem.* **27**, 31.

Sweeney, L.J. 1998. Basic concepts in embryology. A student's survival guide. New York : McGraw-Hill. p 146; 184.

Sweetman, L., and Williams, J.C. 1995. Branched chain organic acidurias. (*In* Scriver, C.R., Beaudet, A.L., William, S.S., Valle, D., *eds.* The Metabolic and molecular basis of inherited disease, 7th ed. New York : McGraw-Hill. pp 1387 – 1422).

Sydenham, E.W., Thiel, P.G., Marasas, W.F.O., Shephard, G.S., Van Schalkwyk, D.J., and Koch, K.R. 1990. Natural occurrence of some *Fusarium* mycotoxins in corn from low and high esophageal cancer prevalence areas of the Transkei, southern Africa. *Journal of agricultural and food chemistry.* **38**, 1900 – 1903.

Tew, B. 1974. Spina bifida: family and social problems. *Special education: Forward trends.* **81**, 737 – 740.

Tipton, K.F. 1992. Principles of enzyme assay and kinetic studies. (*In* Eisenthal, R., and Danson, M.J. Enzyme assays – a practical approach. Oxford : IRL Press. pp 1 – 53).

Todd, W.J. 1986. Effects of specimen preparation on the apparent ultrastructure of microorgamisms. (*In* Aldrich, H.C. and Todd, W.J. Ultrastructure techniques for microorgamisms. New York : Plenum Press. p 87).

Ubbink, J.B., Christianson, A., Bester, M.J., van Allen, M.I., Venter, P.A., Delport, R., Blom, H.J., van der Merwe, A., Potgieter, H., and Vermaak, W.J.H. 1998. Folate status, Homocysteine metabolism, and methylene tetrahydrofolate reductase genotype in rural South African blacks with a history of pregnancy complicated by neural tube defects. *Metabolism.* **48**, 269 – 274.

Ushijima, T., Morimura, K., Hosoya, Y., Okonogi, H., Tatematsu, M., Sugimura, T., and Nagao, M. 1997. Establishment of methylation-sensitive-representational difference analysis and isolation of hypo- and hypermethylated genomic fragments in mouse liver tumors. *Proceedings of the national academy of science.* **94**, 2284 – 2289.

Van Aerts, L.A.G.J.M., Blom, H.J., De Abreu, R.A., Trijbels, F.J.M., Eskes, T.K.A.B., Copius Peereboom-Stegeman, J.M.J., and Noordhoek, J. 1994. Prevention of neural tube defects by and toxicity of L-homocysteine in cultured postimplantation rat embryos. *Teratology.* **50**, 348 – 360.

Van der Berg, G.A., Muskiet, F.A.J., Kingma, A.W., van der Slik, W., and Halie, M.R. 1986. Simultaneous gas-chromatographic determination o f ree and acetyl-conjugated polyamines in urine. *Clinical chemistry.* **32**, 1930 – 1937.

Van der Put, N.M., van der Heuvel, L.P., Steegers-Theunissen, R.P., Trijbels, F.J., Eskes, T.K., Mariman, E.C., den Heyer, M., and Blom, H.J. 1996a. Decreased methylene tetrahydrofolate reductase activity due to the C677T mutation in families with spina bifida offspring. *Journal of Molecular Medicine.* **74**, 691 – 694.

Van der Put, N.M., Trijbels, F.J.M., Hol, F., Eskes, T.K.A.B., Steegers-Theunissen, R.P., van den Heuvel, L.P.W.J., Mariman, E.C.M., and Blom, H.J. 1996b. Mutated methylenetetrahydrofolate reductase in sporadic and hereditary spina bifida offspring. (*In* Mato, J.M., and Caballero, A. eds. Proceedings of the 3rd workshop on methionine metabolism, molecular mechanism and clinical implications. 186 – 191).

Van der Put, N.M.J., van der Molen, E.F., Kluitmans, L.A.J., Heil, S.G., Trijbels, F.J.M., Eskes, T.K.A.B., van Oppenraaij-Emmerzaal, D., Banerjee, R., and Blom, H.J. 1997. Sequence analysis of the coding region of human methionine synthase: relevance to hyperhomocysteinaemia n neural-tube defects and vascular disease. *Quarterly journal of medicine.* **90**, 511 – 517.

Van der Put, N.M.J. 1999. Homocysteine, Folate and Neural tube defects – Biochemical and molecular genetic analysis. Nijmegen : Katholieke Universiteit. (Thesis - Ph.D.) pp 24 – 47.

Vaz, F.M., and Wanders, R.J.A. 2002. Carnitine biosynthesis in mammals. *Biochemical journal.* **361**, 417 – 429.

Vaziri, H., Dessain, S. K., Ng Eaton, E., Imai, S. I., Frye, R. A., Pandita, T. K., Guarente, L., and Weinberg, R. A. 2001. hSIR2(SIRT1) functions as an NAD-dependent p53 deacetylase. *Cell.* **107**, 149 – 159.

Venter, P.A., Christianson, A.L., Hutamo, C.M., Mekhwa, M.P., and Gericke, C.S. 1995. Congenital abnormalities in rural black South African neonates – a silent epidemic? *South African medical journal.* **85**, 15 – 20.

Voet, D., and Voet, J.G. 1995. Biochemistry, 2nd ed. New York : Wiley. pp 608 – 610; 1065 – 1070.

Vorster, W., Liebenberg, S.W., and Lizamore, D.J. 1995. The effect of diazepam on the development of *Gallus* embryos. *South African Journal of Science.* **91**, 538 – 541.

Wang, W., Kramer, P.M., Yang, S., Pereira, M.A., and Tao, L. 2001. Reversed-phase high-performance liquid chromatography procedure for the simultaneous determination of S-adenosyl-L-methionine and S-adenosyl-L-homocysteine in mouse liver and the effect of methionine on their concentrations. *Journal of chromatography.* **762**, 59 – 65.

Wasserman, C.R., Shaw, G.M., Selvin, S., Gould, J.B., and Syme, S.L. 1998. Socioeconomic status, neighborhood social conditions, and neural tube defects. *American journal of public health.* **88**, 1674 – 1680.

Warkany, J. 1971. Congenital Malformations: Notes and comments. Chicago : Year book medical publishers. p 189; pp 272 – 274.

Wegner, C., and Nau, H. 1992. Alteration of embryonic folate metabolism by valproic acid during organogenesis: implications for mechanism of teratogenesis. *Neurology.* **42**, 17 – 23.

Weir, D.G., and Scott, J.M. 1995. The biochemical basis of the neuropathy in cobalamin deficiency. *Baillliers clinical haematology.* **8**, 479 – 497.

Williamson, D.H., Lund, P., and Krebs, H.A. 1967. The redox state of free nicotinamide-adenine dinucleotide in the cytoplasm and mitochondria of rat liver. *Biochemical journal.* **103**, 514 – 527.

World Health Organization technical report series, no 438. 1970. Genetic factors in Congenital Malformations. Geneve : World Health Organization. pp 17 – 26.

Xue, H., Sakaguchi, T., Fujie, M., Ogawa, H., and Ichiyama, A. 1999. Flux of the L-serine metabolism in rabbit, human, and dog livers. *Journal of biological chemistry.* **274**, 16028 – 16033.

Yerby, M.S. 2003. Management issues for woman with epilepsy: neural tube defects and folic acid supplementation. *Neurology.* **61**, S23 – S26.

Yoshida, T., and Kikuchi, G. 1972. Comparative study on major pathways of glycine and serine catabolism in vertebrate livers. *Journal of biochemistry (Tokyo).* **72**, 1503 – 1516.

Zakataeva, N.P., Aleshin, V.V., Tokmakova, I.L., Troshin, P.V., and Livshits, V.A. 1999. A novel transmembrane *Escherichia coli* proteins involved in the amino acid efflux. *FEBS letters.* **452**, 228 – 232.

Zetterberg, H. 2004. Methylenetetrahydrofolate reductase and transcobalamin genetic polymorphisms in human spontaneous abortion: biological and clinical implications. *Reproductive biology and endocrinology.* **2**, 1 – 8.

Zittoun, J. 1995. Congenital errors of folate metabolism. *Baillieres clinical haematology.* **8**, 603 – 616.

Zwierzchowski, L., Czlonkowska, M., and Guszkiewich, A. 1986. Effect of polyamine limitation on DNA synthesis and development of mouse preimplantation embryos *in vitro*. *Journal of reproduction and fertility.* **76**, 115 – 121.

'N WOORD VAN DANK

Ek wil graag erkenning gee aan die volgende persone wat op verskeie maniere bygedra het tot hierdie studie :

- My promotor, Prof. Potgieter, vir sy leiding, ondersteuning en hulp die afgelope 6 jaar.
- Dr. Francois van der Westhuizen, my medepromotor vir sy ondersteuning.
- Die personeel van Biochemie, in besonder Prof. Japie Mienie en Mnr. Elardus Erasmus vir hul reuse bydrae tot hierdie projek.
- Dr. Willie Vorster, Mnr. Cor Bester en Me. Antionette Fick vir ondersteuning met die proefdierwerk.
- Dr. Megan Bester vir bystand met die selkultuurwerk.
- Johan, André en Daniël vir hulp met die KMR en IR.
- Dr Suria Ellis vir hulp met die statistiese ontleding van data.
- Die NRF vir finansiële ondersteuning.
- My ouers, Adunda, vriende en familie vir al die ondersteuning en liefde wat hulle so onbaatsugtig geskenk het deur al hierdie jare.
- Bo alles wil ek my Hemelse Vader bedank vir al die geleenthede wat ek ontvang het.